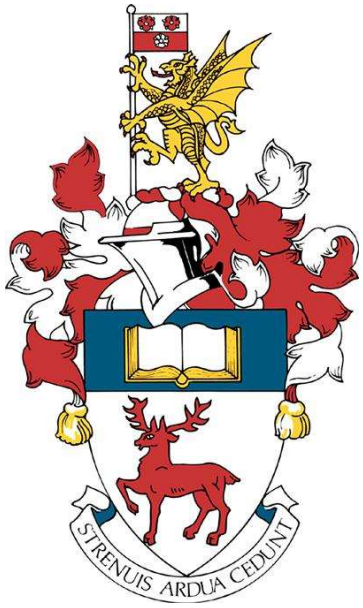

University of Southampton

Faculty of Medicine

Human Development & Health

Inflammatory responses of intestinal epithelial cells and their modulation by omega-3 polyunsaturated fatty acids.

DOI:

by

Luke Alexander Durkin

Thesis for the degree of Doctor of Philosophy

University of Southampton

Abstract

Faculty of Medicine

Human Development & Health

Thesis for the degree of Doctor of Philosophy

Inflammatory responses of intestinal epithelial cells and their modulation by omega-3 polyunsaturated fatty acids.

Luke Alexander Durkin

Long-chain ω-3 polyunsaturated fatty acids (PUFAs) are bioactive nutrients found in foods and supplements that have been attributed to a range of health benefits in a range of conditions, including arthritis, cardiovascular disease, and inflammatory bowel disease (IBD). Eicosapentaenoic acid (EPA) and docosahexaenoic acid (DHA) are two ω-3 PUFAs found in the flesh of fish, including salmon, mackerel, and herring, and in fish oil supplements. The essential ω-3 PUFA alpha-linolenic acid (ALA) is found mainly in plant-based dietary sources including walnuts, rapeseed oil, and flaxseeds. Due to poor cellular conversion, humans can only synthesise small amounts of EPA and DHA from ALA. Recently, interest has grown in alternative ω-3 PUFAs due to concerns over the sustainability of foods containing EPA and DHA, as well as diminishing concentrations of ω-3 PUFAs in these food sources. Docosapentaenoic acid (DPA) is an intermediate between EPA and DHA and is thought to possess similar bioactivity to EPA and DHA. Stearidonic acid (SDA) is an intermediate in the conversion of ALA to EPA. Documented benefits of ω-3 PUFA consumption are attributed to EPA and DHA, and to some extent ALA, whilst little is known about the effects of DPA and SDA.

Intestinal epithelial cells form part of the gut barrier and are responsible for maintaining regulated intestinal permeability and immune responses. Epithelial cell dysfunction during inflammation is part of the pathogenesis of chronic inflammatory conditions such as IBD. Pro-inflammatory cytokine release by intestinal immune cells can drive inflammatory processes leading to altered epithelial cell function. *In vitro* models of intestinal epithelial cells, including the

human adenocarcinoma cell line (Caco-2), have been utilised to assess changes to epithelial cells during inflammation. Experiments in this thesis aimed to describe the modulation of cytokine-induced inflammation in Caco-2 cells by different ω-3 PUFAs. Caco-2 cells were stimulated with a cocktail of inflammatory cytokines (TNF-α, IFN-γ, and IL-1β), with or without pre-treatment with EPA, DHA, DPA, ALA, or SDA. Cytokine stimulation induced hyper-permeability and increased inflammatory mediator production including intracellular adhesion molecule (ICAM)-1, vascular endothelial growth factor (VEGF), interleukin (IL)-6, CXCL8, and monokine-induced by γ-interferon (CXCL9). Cytokine stimulation also induced the nuclear factor kappa B (NF-κB) inflammatory pathway.

Exogenous ω-3 PUFAs were accumulated by Caco-2 cells after 48 hours treatment. EPA was converted to DPA, DPA to EPA retro-conversion was seen, and SDA was converted to EPA, unlike ALA. ω-3 PUFA pre-treatment had variable effects on cytokine-induced inflammation, although no ω-3 PUFA treatments affected cytokine-induced permeability. DHA had the most potent effects on inflammation, significantly reducing CXCL8 concentration in the culture medium and inhibiting the activation of the NF-κB. Other ω-3 PUFAs were ineffective at inhibiting NF-κB expression and activation, and did not affect inflammatory mediator production. Future work could further explore alternative inflammatory pathways regulated by ω-3 PUFAs to elucidate the anti-inflammatory potential of lesser studied ω-3 PUFAs, DPA and SDA. Furthermore, the production and action of pro-resolving lipid mediators from different ω-3 PUFAs in this model could be compared and contrasted. Overall, ω-3 PUFAs had different efficacies on cytokine-induced inflammation in a Caco-2 cell model. However, increased EPA content after SDA treatment suggests SDA could be an important source of EPA within the human epithelium.

Acknowledgements

Throughout my PhD experience, I was lucky enough to be whole-heartedly supported by my family and friends. Whether I was financially struggling (due to a ludicrous choice in accommodation), physically struggling (due to some completely preventable football injury), or mentally struggling (due to the turmoil of a global pandemic), I was lucky enough to have a support network that propelled me to the end.

First, I must thank my supervisors, Philip and Caroline, without you both I would have never had this opportunity. Your guidance and support have been invaluable in my completion of this PhD. I would also like to thank Ella, your high standards and no-nonsense attitude really aided my approach to everything in the lab and beyond.

Next, I would like to thank Alex, James, and Kalum. You boys were the heartbeat of my final stretch at university. Whether it was watching gardening programs, going to the gym, or stirring a cauldron or two, you all made this PhD experience a lot easier. I will always remember that Ranelagh Gardens house with utter fondness, thanks to you three.

Away from Southampton, I have always been lucky to have such supportive and caring parents. Mum and Mark, thank you for everything, you both inspire me so much. I've made it through this journey as your encouragement and belief in me spurred me on through the tough moments. You are my role models and I can't thank you enough for the platform you have given me.

Last, I would like to thank my love, Josie. I cannot thank you enough. You are my daily reminder that anything is possible.

Covid-19 Impact Statement

The Covid-19 pandemic has had a significant impact on the production of this PhD thesis. In March 2020, the university labs would close for nearly 3 months which directly restricted the time spent on generating original data for this thesis. Additionally, several ongoing experiments were discarded due to the sudden closure of all labs at the start of the pandemic. This severely impacted the conclusion of these experiments and restarting these experiments would later impact time spent on progressing and starting other experiments. During the reopening phase and subsequent months, government imposed restrictions limited access to resources, delayed incoming consumable orders, restricted access to lab space and prevented colleagues from cooperating with each other in the lab. Consequently, once the labs reopened starting new experiments and generating data was delayed further. Data and figures generated for this thesis were therefore affected by the impact of the Covid-19 pandemic.

Table of Contents

Table of Figures

Table of Tables

Research Thesis: Declaration of Authorship

Print name: Luke Alexander Durkin

Title of thesis: Inflammatory responses of intestinal epithelial cells and their modulation by omega-3 polyunsaturated fatty acids.

I declare that this thesis and the work presented in it is my own and has been generated by me as the result of my own original research.

I confirm that:

1. This work was done wholly or mainly while in candidature for a research degree at this University;

2. Where any part of this thesis has previously been submitted for a degree or any other qualification at this University or any other institution, this has been clearly stated;

3. Where I have consulted the published work of others, this is always clearly attributed;

4. Where I have quoted from the work of others, the source is always given. With the exception of such quotations, this thesis is entirely my own work;

5. I have acknowledged all main sources of help;

6. Where the thesis is based on work done by myself jointly with others, I have made clear exactly what was done by others and what I have contributed myself;

7. Parts of this work have been published as: [please list references below]:
Durkin LA, Childs CE, Calder PC. Omega-3 Polyunsaturated Fatty Acids and the Intestinal Epithelium—A Review. Foods. 2021;10(1):199.

Signature: Date

List of Abbreviations

AA – Arachidonic acid

ALA – alpha-linolenic acid

APS - ammonium persulphate

BB-12 - Bifidobacterium animalis subsp. lactis, BB-12

BCA – bicinchoninic acid

BIF – Bifidobacterium

BSA - bovine serum albumin

cAMP - cyclic-adenosine monophosphate

CCL2 – C-C motif chemokine ligand 2

CCL3 – C-C motif chemokine ligand 3

CCL4 – C-C motif chemokine ligand 4

CCL7 - C-C motif chemokine ligand 7

CCL9 – C-C motif chemokine ligand 9

CCL12 - C-C motif chemokine ligand 12

CCL19 - C-C motif chemokine ligand 19

CD - coeliac disease

CER – cereulide

COX – cyclooxygenase

CV – coefficient of variation

CXCL8 – C-X-C motif chemokine ligand 8

CXCL9 – C-X-C motif chemokine ligand 9

CYP450 - cytochrome P450

Cys2 - L-cystine dihydrochloride

DAPI - 4′,6-diamidino-2-phenylindole

DGLA - dihomo-gamma-linolenic acid

DHA – Docosahexaenoic acid

DMEM - Dulbecco's Modified Eagle Medium

DMF - 5,7-dimethoxyflavone

DMSO - dimethyl sulfoxide

DON – deoxynivalenol

DPA – docosapentaenoic acid

DSS – dextran sodium sulphate

EA – ellagic acid

EDA – eicosadienoic acid

EDTA - ethylenediaminetetraacetic acid

EET - epoxyeicosatrienoic acid

EPA – Eicosapentaenoic acid

ESA – eicosenoic acid

ETA - eicosatetraenoic acid

ETE - eicosatrienoic acid

FAK - focal adhesion kinase

FD4 – FITC-dextran 4 kDa

FFAR - free fatty acid receptors

FITC - fluorescein isothiocyanate

GIP - gastric inhibitory polypeptide

GLA – gamma-linolenic acid

GLP-1 - glucagon-like peptide-1

GPE - grape pomace extract

GPCR - G-protein coupled receptor

GSE - proanthocyanidin-rich grape seed extract

H_2SO_4 – sulphuric acid

HBSS - Hank's balanced sodium solution

HcC - high charge chenopodin

HETE - Hydroxyeicosatetraenoic acid

IBD - inflammatory bowel disease

ICAM-1 - intercellular adhesion molecule-1

IE-DAP - D-gamma-Glu-mDAP

IFN-γ – interferon-γ

IL-10 - interleukin-10

IL-12 - interleukin-12

IL-17 - interleukin-17

IL-18 - interleukin-18

IL-1α - interleukin-1α

IL-1β – interleukin-1β

IL-2 - interleukin-2

IL-4 - interleukin-4

IL-6 - interleukin-6

iNOS - inducible nitric oxide synthase

IP-10 - interferon gamma-induced protein-10

IRAK4 - interleukin-1 receptor-associated kinase 4

IκB - nuclear factor of kappa light polypeptide gene enhancer in B-cells inhibitor

IκK - IκB kinase

JAM - junction adhesion molecule

K_2CO_3 – potassium carbonate

$KHCO_3$ – potassium bicarbonate

LA – linoleic acid

LBP - Lycium barbarum polysaccharides

LcC - low charge chenopodin

LCG - *Lactobacillus casei* GG

LGG - *Lactobacillus rhamnosus* GG

LOX – lipoxygenase

LPS – lipopolysaccharides

LT – Leukotriene

LX – lipoxin

MAMP - microbe-associated molecular pattern

MAP - mitogen-activated protein

MAPK - mitogen-activated protein kinase

MDP - muramyl dipeptide

MLCK - myosin light-chain kinase

MPO – myeloperoxidase

MTT - 3-(4,5-dimethylthiazol-2-yl)-2,5-diphenyltetrazolium bromide

MΩ - megohm

NaCl – sodium chloride

NCGS - non-coeliac gluten sensitivity

NF-κB - nuclear factor-κB

OA – oleic acid

PA – palmitic acid

PBS - phosphate buffered saline

PDVF - polyvinylidene difluoride

PG - prostaglandin

pIκB – phosphorylated IκB

PKA – protein kinase A

PKC - protein kinase C

pMLC - phosphorylated-myosin light chain

PPAR - peroxisome proliferator-activated receptor

PRR - pattern recognition receptor

PUFA - polyunsaturated fatty acid

SA – stearic acid

SCFA - short-chain fatty acid

SDA – Stearidonic acid

SDS - sodium dodecyl sulphate

SDS-PAGE - sodium dodecyl sulphate-polyacrylamide gel electrophoresis

TB – theobromine

TEER - *trans*-epithelial electrical resistance

TEMED - N,N,N',N'-Tetramethylethylenediamine

TFF 3 – Trefoil factor 3

TGF-β1 - transforming growth factor-β1

TLR - toll-like receptor

TNBS - 2,4,6-trinitrobenzenesulfonic acid

TNF-α - tumour necrosis factor-α

TNS - tannase

Tris - tris(hydroxymethyl)aminomethane

Tris HCl - tris(hydroxymethyl)aminomethane hydrochloride

TRPM5 - transient receptor potential cation channel subfamily M member 5

TX – thromboxane

VCAM-1 - vascular cell adhesion molecule-1

VEGF - vascular endothelial growth factor

ZO-1 - zonula occludens-1

ω-3 – omega-3

ω-6 – omega-6

Chapter 1 - Literature Review

1.1. Gut epithelium and tight junctions

The human gut epithelium (*Figure 1.1*) is integral for the absorption of vital nutrients and as a barrier to potential toxins and pathogens. Composed largely of permeable enterocytes, as well as Paneth, goblet and enteroendocrine secretory cells, the structure of the gut epithelium is fundamental to maintaining normal absorptive and protective functions [1]. Gut epithelial cells are maintained in close proximity to one another through intercellular junctions consisting of cytoskeleton-associated tight junctions and adherens junctions, as well as intermediate-filament associated desmosomes [2]. Extensive exposure of the gut epithelium to the external environment is inevitable, and therefore the gut epithelium is under constant challenge by potential pathogens and their products, which could become inhibitory to the finely regulated and vital absorptive mechanisms. Intestinal epithelial cells or enterocytes form part of the mucosal barrier, and are integrated with intraepithelial lymphocytes, and located above the basement membrane and lamina propria. The epithelial layer forms part of the intestinal barrier that provides substantial protection from external stimuli and is a key component of the gut's role in innate and adaptive immunity [3].

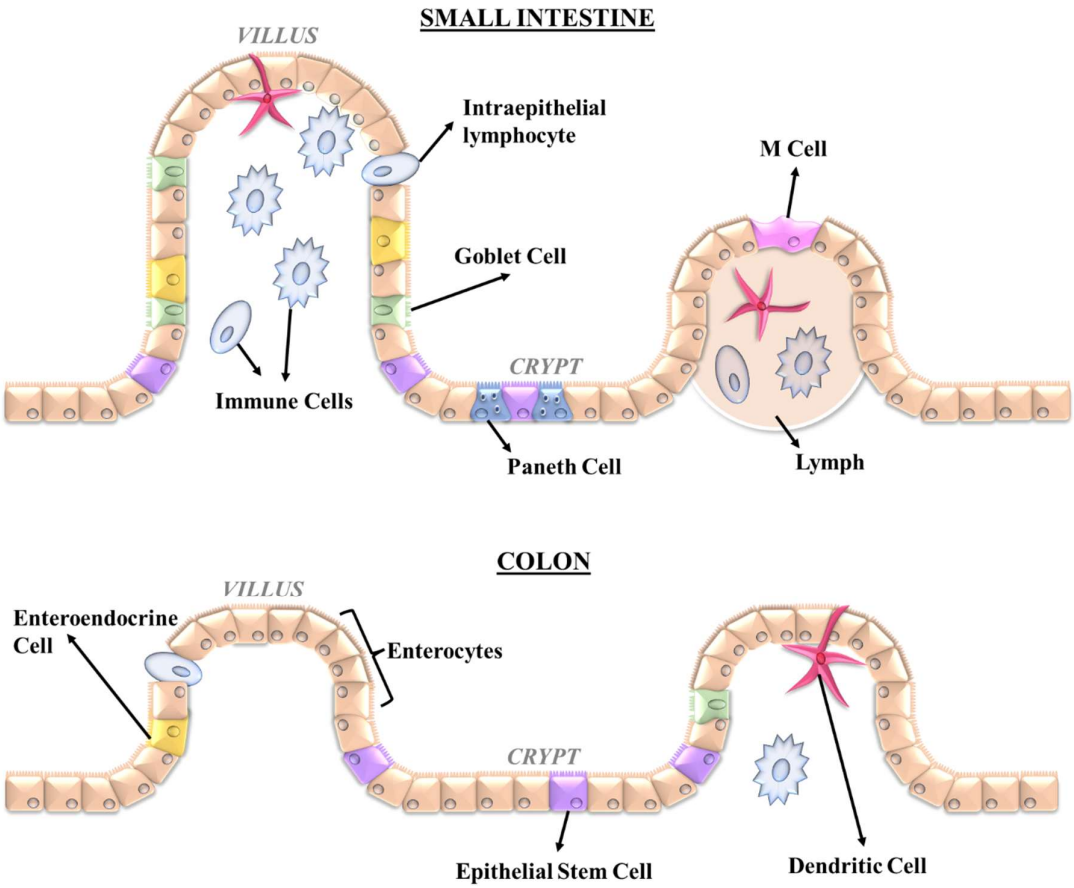

Figure 1.1: The structure of the human gut epithelium in the small intestine and colon. The various cell types in the gut epithelial layer form a protective barrier against potential toxins and pathogens, whilst regulating absorption of vital nutrients. Figure produced using Microsoft PowerPoint and adapted from [4].

Essential in gut epithelium function, tight junctions in the gut epithelial layer (*Figure 1.2*) consist of a range of transcellular proteins, including occludin, claudins, and tetraspanins, adhesion molecules, such as junction adhesion molecule (JAM), and scaffolding proteins, such as zonula occludens (ZO)-1 [5]. Tight junction permeability is modulated by a multitude of factors including pathways involving signalling molecules like protein kinase C (PKC) and mitogen-activated protein (MAP) kinase. Additionally, regulation of tight junction permeability is complemented by interactions with commensal and probiotic bacteria *in vivo* [6]. Tight junctions are susceptible to changes in the host's internal environment; heat- and exercise-induced hyperthermia is known to increase the permeability of the epithelial cell layer by inducing tight junction

dysfunction [7]. Endotoxin permeability and subsequent interaction with immune cells induces the release of proinflammatory cytokines, including tumour necrosis factor (TNF)-α, interferon (IFN)-γ, and interleukin (IL)-1β, which can alter the expression of ZO-1, occludin, and claudin proteins [8]. Low levels of persistent immune activation are thought to contribute to the increased epithelial transcellular and paracellular permeability seen in patients with inflammatory bowel disease (IBD), through redistribution of tight junction proteins, sodium-potassium ATPase disruption, and myosin light-chain kinase (MLCK)-induced contraction of enterocyte cytoskeletons [9].

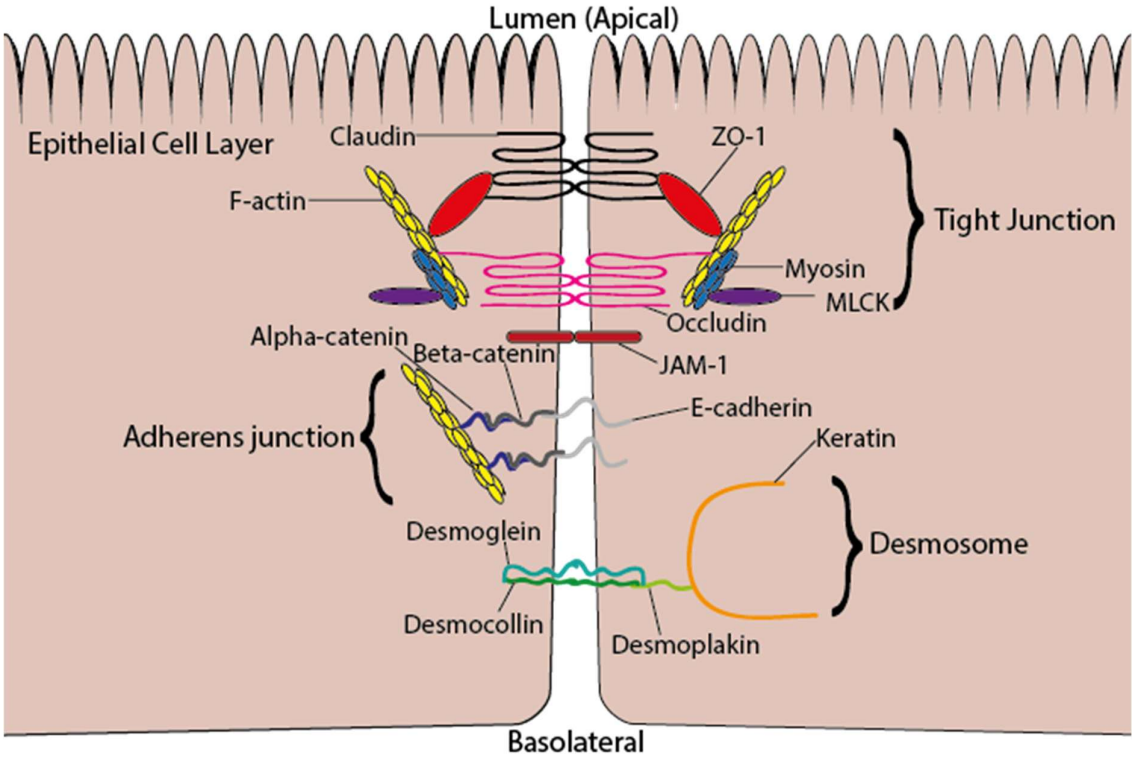

Figure 1.2: Structure of enterocyte tight junctions. Intracellular protein complex of zonula occludens (ZO) proteins, myosin and actin (perijunctional actin-myosin complex), interacts with extracellular proteins, occludins and claudins, which span the extracellular space to adjoining cells. Tight junction contraction can be modulated by myosin light-chain kinase (MLCK). The second intercellular junction type, adherens junctions, consist of a catenin-cadherin complex anchored to actin. Desmosomes, the final cell-cell junction, are formed of three proteins: desmogleins, desmocollins, and desmoplakin link the intracellular junction to the intermediate filament cytoskeleton. Junction adhesion molecule (JAM)-1 is associated with barrier function and tight junction assembly. Figure produced using Adobe Illustrator and adapted from [10].

1.2. Gut barrier – Microbiome, mucus layer, and epithelium

In healthy individuals, the epithelial cell layer is separated from the luminal contents of the gut by a bioactive layer of mucus and commensal bacteria. Commensal bacterial colonies in the gut are closely integrated with the human immune system from an early stage of development. These regulated interactions are established from pregnancy to birth and early development, where maternal nutrition and microbiota are influential in the development of a functioning immune system in the new-born [11]. Through downstream pathways, dietary and microbial metabolites induce effects on T-cells (TREG, TH17, and $CD4^+$) and B-cells [12], thereby interacting with both the innate and adaptive immune systems. Disruption of the diverse, homeostatic bacterial communities is attributed to the malabsorption of nutrients and the pathogenesis of intestinal inflammation, and influences the development of bowel cancer [13].

Commensal bacteria produce important signalling molecules, including lipopolysaccharides (LPS) and short-chain fatty acids (SCFAs), within the mucosal layer and act at the apical surface of the gut epithelium. LPS and SCFAs are integral in maintaining homeostasis in the gut, as well as altering signals from the epithelial layer to the immune system in response to pathogenic and dietary stimuli. Acetate, propionate, and butyrate are SCFAs produced by bacterial fermentation of dietary fibre, and can elicit anti-inflammatory signalling through G-protein coupled receptors (GPRs) on enterocytes and immune cells [14]. Free fatty acid receptors (FFARs) including FFAR2 and FFAR3, alongside GPR109A (aka hydroxycarboxylic acid receptor 2 and niacin receptor-1), are the principal GPRs located on the cell surface of enterocytes. FFAR2 signalling induces many downstream anti-inflammatory effects, including activation of neutrophils, differentiation of leukocytes, and release of peptide YY and 5-hydroxytryptamine, whilst FFAR3 signalling is important in leptin release in adipocytes [15]. SCFAs not utilised at surface-bound receptors can enter enterocytes through passive diffusion and more favourably through the solute transporters: monocarboxylate-transporter 1 and sodium-coupled monocarboxylate-transporter 1 [14]. SCFAs are used as the main source of energy for enterocyte proliferation, metabolism, and maintenance of the epithelial barrier, through the activation of hypoxia-inducible factor-1 and increased expression of barrier forming tight junction components [14]. Longer chain fatty acids act at different FFAR subtypes, FFAR1 and FFAR4, which elicit the release of intracellular Ca^{2+}, which subsequently induces the release of effector molecules, such as gastric inhibitory polypeptide (GIP) and

glucagon-like peptide (GLP)-1 [16]. GIP and GLP-1 elicit secretion of insulin after a meal [17] and as a consequence long-chain fatty acids are an important dietary regulator of glucose homeostasis[18].

Pattern recognition receptors (PRRs), alongside FFARs, modulate the immune response of enterocytes. PRRs include Toll-like receptors (TLRs) and an array of other receptors, including retinoic acid-inducible gene (Rig)-I-like helicases and nucleotide-binding oligomerisation domain 1/2 [19]. PRRs recognise structural motifs, known as microbe-associated molecular patterns (MAMPs), from bacteria located within the gut mucosal layer. PAMPs are highly conserved within both commensal and pathogenic bacteria, and are particularly linked to the regulation of inflammatory signalling molecule, nuclear factor-κB (NF-κB). NF-κB is important in an array of cellular responses within enterocytes and other cell types, including inflammation, proliferation, and apoptosis [20].

Many subtypes of TLRs are expressed on enterocytes, including TLR2 and TLR4, which are expressed on the apical surface membrane and are responsive to different components of commensal bacteria; TLR4 responds to LPS, whilst TLR2 (dimerised with TLR1 or TLR6) is responsive to bacterial cell wall lipoproteins. TLR5 is also expressed on enterocytes, but on the basolateral surface membrane, and is responsive to bacterial flagellin, whilst intracellular TLR9 responds to bacterial DNA motifs [21]. The innate activation of TLRs by commensal bacteria and metabolites elicits improved integrity of tight junctions in enterocytes, whilst also inducing the expression of cytoprotective heat-shock proteins and epidermal growth factor receptor ligands [22]. Furthermore, TLR signalling is integral in the production of antimicrobial peptides and the induction of epithelial cell proliferation and migration [23], and is therefore essential in maintaining gut epithelial barrier function. However, high dose LPS stimulation induces TLR4 signalling which activates localised focal adhesion kinase (FAK) adaptor proteins, which in turn, activate the innate immune signal transduction adaptor (MyD88) and interleukin-1 receptor-associated kinase 4 (IRAK4) pathway. MyD88 phosphorylation of IRAK4 leads to the opening of tight junctions and a rapid increase in epithelial paracellular permeability [24]. Consequently, TLR expression and activation must be tightly regulated to maintain the inflammatory state of the gut.

The regulated stimulation and expression of TLRs is governed by the mucus layer of the gut barrier. The four major commensal phyla in humans (*Firmicutes*, *Bacteroidetes*, *Actinobacteria*, and *Proteobacteria*) reside on the luminal surface of the looser, outer layer of mucus whilst a thicker, inner layer prevents direct interaction with the gut epithelial layer [25]. The gut mucus layers are integrated with mucins, charged polymeric glycoproteins, which are produced by goblet cells within the gut epithelial layer. Mucins act as adhesion sites for both commensal and pathogenic bacteria and therefore the presence and maintenance of commensal bacteria colonies is essential for resisting the colonisation of pathogenic bacteria. Additionally, mucin adhesion sites are targets for probiotics, which can protect against enterocyte tight junction damage by producing repair factors and nutrients [26]. The role of mucins is not exclusive to bacterial localisation, since they can also act as a substrate for SCFA production by commensal and probiotic bacteria [27]. Overall, the dynamic relationship between commensal bacteria, the gut luminal contents, the mucus layer, and the gut epithelial layer governs the effectiveness of the gut barrier in health and disease.

1.3. Gut barrier function in disease

Inflammatory bowel diseases (IBDs), such as ulcerative colitis and Crohn's disease, can drastically reduce the efficiency of nutrient absorption, whilst impairing gut barrier function and subsequently dysregulating the adaptive immune response in the gut, eventually leading to complete loss of regulated gut epithelial function. The symptomology associated with IBDs is often a consequence of a reduction in gut epithelial integrity, commonly known as a leaky gut [28]. Leaky gut refers to increased permeability through gut epithelial paracellular and transcellular pathways, permitting larger and potentially inflammatory molecules to pass through the gut barrier and subsequent interaction with the immunologically active sub-epithelial layer [29]. Intestinal permeability can be assessed *in vivo* using the non-invasive lactulose/mannitol test, and indicative of a leaky gut, is if lactulose, a large oligosaccharide which can only pass through a defective gut barrier, is excreted less efficiently [30]. The presence of endotoxins, such as bacterial LPS, in the blood stream is indicative of gut barrier dysfunction in IBDs, and is linked with hepatic, pancreatic and cardiac diseases [31]. Coinciding with decreased gut barrier integrity, dysbiosis of the gut microbiota in IBD is presented by alterations in commensal bacteria proportions,

with *Firmicutes* and *Bacteroidetes* colonies decreased and increased presence of *Proteobacteria* and *Actinobacteria* [32]. Furthermore, the severity of microbial dysbiosis compared to healthy individuals is dissimilar in the different IBDs, with decreased microbial variety seen more prominently in Crohn's disease than in ulcerative colitis [33].

Disruption of the intestinal microbiota in IBD alters the function of the epithelial barrier through tight junction dysfunction and altered TLR signalling. In Crohn's disease, downregulation of occludin, claudin-5, and claudin-8, as well as upregulation of claudin-2 (also seen in ulcerative colitis), induces tight junction dysfunction [34]. Increased presence of the inflammatory mediators TNF-α and IL-13 in IBD also alters tight junction function. TNF-α interacts with MLCK, a key regulator of tight junction permeability, leading to the endocytosis of occludin proteins and subsequent increased paracellular permeability. IL-13 alters claudin protein expression, notably the upregulation of claudin-2, whilst TNF-α-induced MLCK can also increase the transcription of claudin-2 [35]. Upregulated claudin-2 expression increases ion channel pores at epithelial tight junctions, which as a consequence induces an increase in epithelial paracellular permeability in IBD [36]. TLR signalling can influence the function of tight junctions and has complex effects on the production of pro-inflammatory mediators. TLR4 and TLR2 are upregulated on the epithelial cell surface in IBD, with TLR4 upregulation being responsible for epithelial cell hypersensitivity to LPS and TLR2 inducing the production of pro-inflammatory cytokine TNF-α [37]. Thus, dysbiosis of the gut induces alterations to epithelial inflammatory output and barrier integrity in IBD.

Significant intestinal immune responses are not exclusive to immunocompromised and genetically predisposed individuals, and inflammation can be present in otherwise healthy individuals according to specific lifestyle and dietary factors. Lifestyle factors, such as exercise, can alter gut homeostasis and gut barrier integrity through changes in gastrointestinal conditions, such as temperature and pH, which can increase the susceptibility to enteric inflammation. This is exemplified by the prevalence of gut inflammation in athletes as a consequence of exercise-induced changes in hormone release and alterations to the gut microbiota [38]. Dietary factors can also have a multitude of effects on the gut barrier, for example, a lack of fibre in the diet can markedly alter gut barrier function by increasing the presence of pathogenic and mucus-degrading bacteria [39]. Furthermore, obesity and diabetes driven hyperglycaemia

can also lead to barrier dysfunction through alterations in epithelial cell metabolism and in N-glycosylation pathways [40].

Inflammation caused by long-term barrier dysfunction can be exacerbated by bioactive components of the diet. Gluten, a structural group of proteins found in cereal grains, provides an antigenic challenge to the gut epithelium. In particular, the alcohol-soluble fraction of gluten, gliadins, can induce inflammatory effects in both healthy individuals and those predisposed to coeliac disease (CD). The autoimmune aspects of CD, including the presence of transglutaminase 2 autoantibodies and intraepithelial cytotoxic T-lymphocytes, are the drivers of the severe gluten reaction seen in those with CD [41]. Changes to the structure of the gut epithelium are also present in CD, which include villous atrophy, crypt hyperplasia, and tight junction dysfunction and these also increase the gut barrier susceptibility to gluten. Tight junction dysfunction induced by gliadins in CD alters the functionality of scaffolding protein ZO-1 and occludin, as well as downregulating barrier-forming claudins (claudin-3, claudin-5, and claudin-7) and upregulating channel-forming claudins (claudin-2 and claudin-15) [42].

In healthy individuals, gluten-induced gut inflammation has become more prominent in the population, indicated by the increasing presentation of non-coeliac gluten sensitivity (NCGS), whereby the consumption of gluten induces an innate immune response (without the adaptive immune response of CD) through alterations in TLR expression on gut epithelial cells [43]. Additionally, gliadins induce tight junction dysfunction in epithelial cells, increasing epithelial paracellular permeability, and inducing the production of pro-inflammatory cytokines (CXCL8 and TNF-α) through direct interaction with myeloid cells [44]. The importance of the gut barrier and, in particular, epithelium function is underlined by defective barrier function being attributed to an array of inflammatory diseases, including IBD, CD, and obesity. Epithelial barrier dysfunction is also implicated in healthy individuals upon changes to internal homeostasis and under substantial inflammatory challenge. Therefore, therapies targeted at protecting and repairing epithelial integrity have become pertinent in both healthy and diseased states.

1.4. Polyunsaturated fatty acids (PUFAs)

Susceptibility to intestinal inflammation may be influenced by increased consumption of fats and lower amounts of fibre, which are representative of a typical western diet. This dietary imbalance alters the composition of the gut microbiota, and the subsequent production of SCFAs, inducing inflammation, increasing gut barrier permeability, and inhibiting immune regulation [45]. Hence, changes to the diet can be essential in prevention and alleviation of gut inflammation and protecting the gut barrier through a variety of mechanisms. Consuming a wide variety of macronutrients, microbial dietary substrates, such as prebiotics, and bioactive compounds, such as polyphenols, improves gut microbial diversity and density, whilst maintaining intestinal epithelial barrier integrity and immune function. Short-term dietary intervention can drastically alter an individual's microbiome yet longer-term dietary changes are required to maintain changes within the gut microenvironment both in health and disease [46]. Dietary interventions aimed at altering the bacterial composition of the gut are currently utilised clinically, although optimal dietary strategies for inflammatory diseases are yet to be achieved [47]. Other dietary components, including calcium and vitamin D, involved in the maintenance of gut homeostasis are also believed to be important in preventing the development of IBD [48].

Long-chain omega-3 (ω-3) polyunsaturated fatty acids (PUFAs) are also believed to be favourably associated with the prevention of IBD and the general maintenance of long-term health. Consumption of ω-3 PUFAs has observable benefits in health and disease, especially in the development and function of the brain [49] and the anti-inflammatory roles of these fatty acids seem relevant in an array of diseases, including IBD, rheumatoid arthritis, asthma, and cardiovascular disease [50]. Despite the benefits of ω-3 PUFAs, currently consumption of omega-6 (ω-6) PUFAs is approximately 10 times the consumption of ω-3 PUFAs in the western diet, and whilst ω-6 PUFAs are essential, the large imbalance in ω-6 to ω-3 PUFA consumption has been associated with trends in increased body weight and obesity, as well as increased predisposition to inflammatory conditions [51].

The main dietary PUFAs are usually linoleic acid (LA; ω-6) and alpha-linolenic acid (ALA; ω-3). Through subsequent enzymatic processing, LA is predominantly converted into arachidonic acid (AA), and through further processing AA can be converted to docosapentaenoic acid (DPA; ω-6). As shown in Figure 1.3, ALA is primarily metabolised into eicosapentaenoic acid (EPA) and docosahexaenoic acid (DHA), as well as intermediate DPA (ω-3). EPA and DHA are available preformed in

the diet from eggs, meat, and fish and from omega-3 supplements. PUFAs interact with FFARs, especially FFAR1 and FFAR4, as well as specific ion channels, such as transient receptor potential cation channel subfamily M member 5 (TRPM5) channels, on the gut epithelial apical surface. Specifically, longer chain PUFAs, such EPA and DHA are known to promote FFAR4-induced β-arrestin recruitment which can have downstream anti-inflammatory effects [52]. Moreover, ω-3 PUFAs interact with the gut microbiota, promoting the diversity and proportion of SCFA-producing bacteria in humans [53], whilst also influencing gut barrier integrity and interactions with host immune cells [54], which are implicated in diseases including obesity, liver disease and IBDs [55].

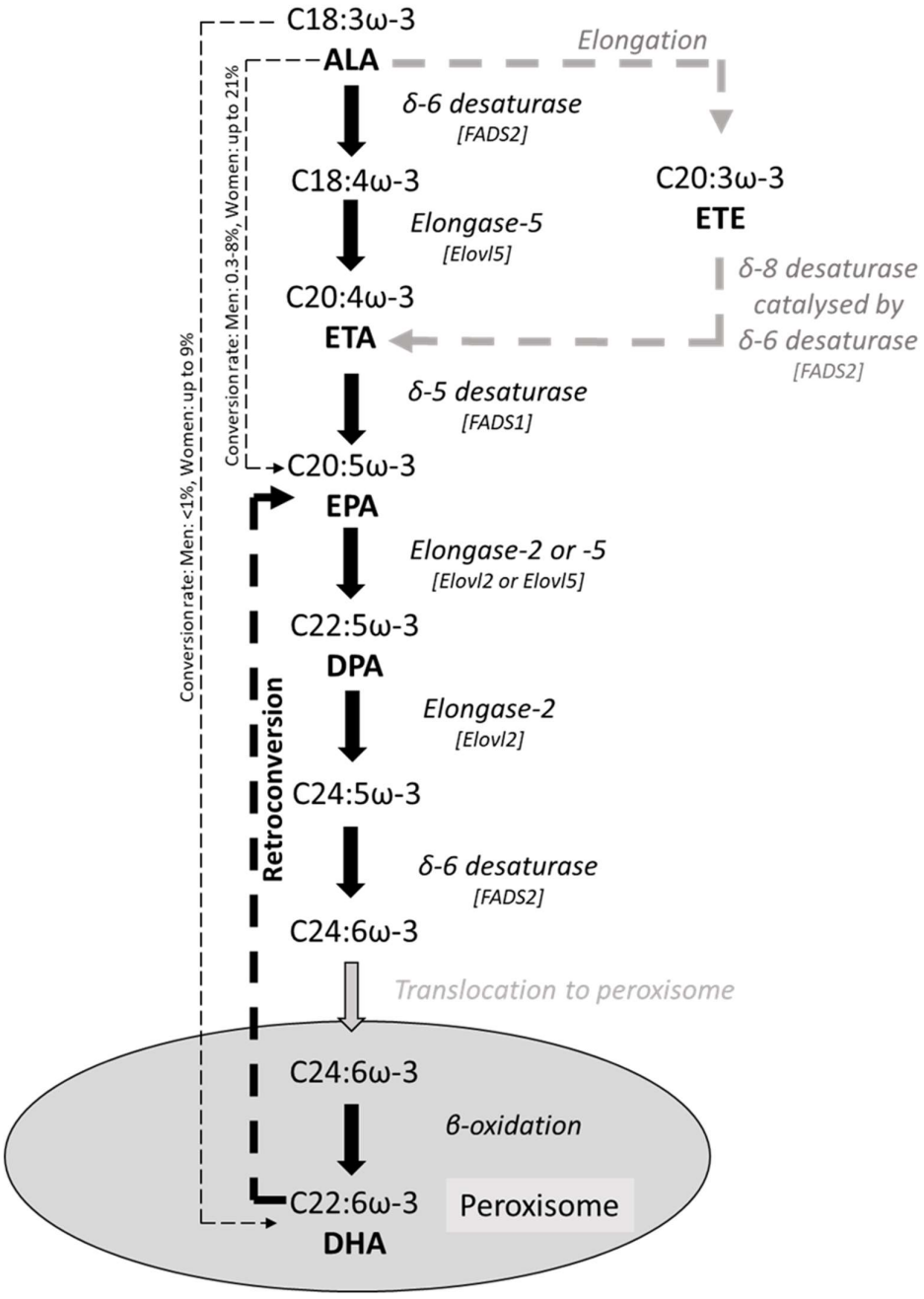

Figure 1.3: Metabolic conversion pathway from the essential ω-3 PUFA, ALA, to longer-chain ω-3 PUFAs, EPA, DPA and DHA.PUFA structure is represented as carbon atom number: double bond number and double bond type (ω-3 = omega-3). Figure produced using Microsoft PowerPoint and published in [10].

The processing of ω-3 PUFAs is integral in the production of anti-inflammatory mediators, which act upon an array of immune cells once released from the gut epithelium. PUFAs released from the phospholipid membrane are processed by enzymes including cyclooxygenases (COXs), lipoxygenases (LOXs), and

cytochrome P450 (CYP450) [56] (derivatives are shown in *Table 1.1*). Processing of PUFAs by these enzymes leads to the production of bioactive eicosanoids and docosanoids, which have an array of downstream physiological effects dependent on tissue expression, conditions, and cell type. Eicosanoids elicit cellular effects through a range of differentially expressed, tissue-specific GPRs on gut epithelial cells, which include the PGD_2 receptors, DP_1 and DP_2, PGE_2 receptors, EP_1-EP_4, $PGF_{2\alpha}$ receptor, FP, PGI_2 receptor, IP, and the TXA_2 receptor, TP. Eicosanoid receptor signalling constitutively enhances gut barrier function, nutrient absorption, regulated intestinal immune responses, and epithelial cell homeostasis [57]

Table 1.1: Mediators produced from ω-6 and ω-3 PUFAs. Derived from sources [58-68].

Messenger Type	**Converting Enzyme(s)**	**n-6 PUFA (AA) derivatives**	**Physiological Effect**	**n-3 PUFA (EPA, DHA) derivatives**	**Physiological Effect**
Prostaglandins	COX	PGD_2	Anti-inflammatory	PGD_3	Anti-inflammatory/Anti-thrombotic
		PGE_2	Pro-arrhythmic/Pro-inflammatory	PGE_3	Anti-arrhythmic/Anti-inflammatory
		PGF_2		PGF_3	
		PGI_2	Pro-arrhythmic/Pro-inflammatory/Platelet inhibitor	PGI_3	Anti-arrhythmic/Anti-inflammatory/Platelet inhibitor
Thromboxanes	COX	TXA_2	Platelet activator	TXA_3	Platelet activator
		TXB_2	Vasoconstriction	TXB_3	Vasodilation
Leukotrienes	5-LOX	Leukotriene (LT)A_4	Converted to LTB_4 and LTC_4	LTA_5	
		LTB_4	Pro-inflammatory	LTB_5	Anti-inflammatory
		LTC_4	Pro-inflammatory	LTC_5	Anti-inflammatory
		LTD_4	Pro-inflammatory	LTD_5	

		LTE_4	Pro-inflammatory	LTE_5	
Resolvins	COX-2 and 5-LOX/15-LOX and 5-LOX			RvE1 (EPA)	Anti-inflammatory
				RvD1 (DHA)	Anti-inflammatory
Protectins	15-LOX			PD1 (DHA)	Anti-inflammatory
Maresins	12-LOX			MaR1	Anti-inflammatory
Epoxyeicosatrienoic derivatives	CYP450	5,6- Epoxyeicosatrienoic acid (EET)	Anti-inflammatory (NF-kB inhibition)		
		8,9-EET	Anti-inflammatory		
		11,12-EET	Anti-inflammatory		
		14,15-EET	Anti-inflammatory		
Hydroxyleicosatetraenoic derivatives	5-LOX	5-Hydroxyeicosatetraenoic acid (HETE)	Pro-inflammatory		
	12-LOX	12-HETE	Vasodilation/Platelet aggregation		
	15-LOX	15-HETE	Anti-inflammatory		
Lipoxins	15-LOX	Lipoxin $(LX)A_4$	Anti-inflammatory		

COXs are responsible for the production of prostanoids, categorised into prostaglandins, prostacyclins and thromboxanes. The modulation of COX subtypes, COX-1 and COX-2, is important in regulating intestinal inflammation. COX-1 is a constituently present enzyme in most tissues and, specific to the gut, improves gut barrier integrity, whilst COX-2 is inducible and is seen overexpressed in inflamed tissues [69]. There are several different LOXs. These can have differential effects on ω-3 and ω-6 PUFAs: AA is converted into lipoxins and leukotrienes and EPA into leukotrienes while pro-resolving mediators (resolvins, protectins, and maresins) are produced from ω-3 PUFAs, including EPA, DHA, and DPA (ω-3) [56]. Resolvins, protectins, and maresins have all been shown to elicit anti-inflammatory and protective effects on the gut epithelium in models of IBD [70]. Like LOXs, COXs process ω-6 and ω-3 PUFAs differentially, AA is converted to 2-series prostaglandins, whereas EPA is converted into 3-series prostaglandins [71]. COX differential processing of PUFAs is important in maintaining gut homeostasis but during intestinal inflammation the levels of 2-series and 3-series becomes imbalanced. For example, EPA consumption reduces COX-derived prostaglandin E_2 (PGE_2) levels and increases PGE_3 during gastrointestinal inflammation [72]. Changes to 2-series prostaglandin sources and abundance rapidly alter 2-series prostaglandin physiological action. In particular, PGE_2 can have both pro-inflammatory and anti-inflammatory effects, and during intestinal inflammation PGE_2 levels are raised [73] which disrupts the normal regulated effect of low-level PGE_2 on T-cell signalling [74]. Furthermore, in an anti-inflammatory capacity, PGE_2 can induce 15-LOX activity and the subsequent production of anti-inflammatory lipoxins [58]. PUFA derived mediators also modulate tight junctions within the epithelial cell layer, altering the barrier paracellular permeability. COX-derived mediators from ω-3 PUFAs inhibit PGE_2-induced tight junction dysfunction, whilst LOX production of LTD_4 from AA increases paracellular permeability [57].

Overall, the differential processing of ω-3 and ω-6 PUFAs by COX and LOX can elicit complex effects in the pathogenesis of intestinal inflammation, carcinogenesis and a range of physiological functions.

1.5. Omega-3 PUFAs and the in vivo gut epithelium

The production of ω-3 PUFA-derived immunoregulatory lipid mediators can explain the anti-inflammatory potency of ω-3 PUFAs. However epithelial cells are likely to be exposed to ω-3 PUFAs directly and therefore direct interactions between ω-3 PUFAs and epithelial cells have been assessed *in vivo*, mainly using rodent models. Assessing the changes to the human intestinal epithelium provides challenges as obtaining biopsies from the intestine requires an invasive procedure. Two studies have assessed changes to human intestinal mucosa after short term [75] and long term [76] ω-3 PUFA-rich fish oil supplementation in patients with inflammatory bowel disease. Short-term fish oil supplementation increased colonic EPA and DHA concentrations and decreased colonic AA concentration as well as decreasing concentrations of AA-derived metabolites, PGE_2 and TXB_2 [75]. In a longer exposure study, increased rectal concentrations of EPA, but not DHA, were reported [76]. Several *in vitro* cell models and *in vivo* mouse models have shown alterations to gut epithelial cell membrane composition after ω-3 PUFA supplementation. Most rodent models reported on the effect of fish oil supplementation on intestinal tissue PUFA content with several studies reporting increased EPA and DHA content in colonic tissue [77-79] and one study reported increased EPA and DHA content in small intestine tissue [80]. Additionally, separate EPA and DHA supplementation has been shown to increase respective concentrations of those PUFAs in ileal tissue [81].

To observe effects of ω-3 PUFA supplementation in *in vivo* models, macroscopic histological changes have been monitored in rodent models of various intestinal inflammatory conditions. In particular, ω-3 PUFA supplementation has been assessed in various forms of experimental colitis with various results seen. Two studies indicated that DHA supplementation improved histological outcomes in necrotising enterocolitis models [82, 83]. Improved histological and pathological outcomes from EPA and DHA-rich diets (usually derived from fish oil) in colitis models have been reported [84-86]; however other studies reported no effect of EPA/DHA-rich diet on models of TNBS-induced colitis [79, 87] and one study reported worsened histological outcomes in a dextran sodium sulphate (DSS)-induced colitis model [79]. Fish oil supplementation had no effect on histological outcomes in a colitis model induced by adoptive transfer of naïve T-cells [78]. Yuceyar et al. reported opposing effects of fish oil supplementation provided through two different applications in a model of 2,4,6-trinitrobenzenesulfonic acid (TNBS)-induced colitis. Fish oil given in the diet improved disease pathology,

however application of fish oil by daily enema had no effect on pathological outcomes [88]. Studies of the effect of ALA on colitis have also reported mixed findings in models of colitis; Andoh et al. reported improved inflammatory damage scores in a TNBS colitis model [89], while Hassan et al. reported ALA supplementation decreased macroscopic lesions and mucosal neutrophil infiltration but had no effect on mucosal wall thickness and overall inflammatory score in a TNBS colitis model [90]. Additionally, Reifen et al. showed that ALA-rich sage oil had no effect on histological changes in DSS and TNBS-induced colitis and even increased mucosal inflammation in the DSS colitis model [79]. More recently, DPA was shown to have protective effects on histological changes induced by DSS colitis [91]. To establish a link between increased concentrations of ω-3 PUFAs in colonic tissue and improved pathological outcomes, Hudert et al. used a transgenic *fat-1* mouse model, in which the mice have constituently higher colonic concentrations of EPA, DPA, and DHA, to assess the effect on DSS-induced colitis. Histological improvements observed in the *fat-1* mice compared to wild type included increased colon length, decreased severity and thickness of inflammatory infiltrate, and decreased epithelial damage [92].

The effect of ω-3 PUFA supplementation on other experimental intestinal inflammatory conditions has not been explored as thoroughly as for experimental colitis. ω-3 PUFA supplementation improved histological outcomes in models of haemorrhagic shock [93], β-lactoglobulin-induced inflammation [94], and peritoneal dialysis [95]; additionally, DHA supplementation improved histological inflammation scores in an IL-10 deficiency model [96]. Fish oil supplementation had no effect on histological damage in rats chronically exposed to ethanol [97].

Several *in vivo* inflammatory models have explored the effect of ω-3 PUFAs on changes to intestinal permeability, using plasma endotoxin levels and changes to tight junction protein distribution and expression to indicate changes to epithelial function. EPA and DHA were separately shown to reduce intestinal permeability in a model of heatstroke, indicated through decreased plasma endotoxin and D-lactate levels, whilst increased tight junction protein distortion and decreased tight junction protein expression were attenuated [81]. DHA also reduced plasma endotoxin levels, indicating improved intestinal permeability, in a model of necrotising enterocolitis [82]. EPA-enriched fish oil was shown to protect ileal and colonic absorption in male Sprague-Dawley rats treated with acetic acid to induce colitis [98]. Fish oil supplementation also reduced plasma endotoxin levels and

improved tight junction protein, ZO-1, expression in epithelial tissue in male Wistar rats chronically exposed to ethanol [97]. In the transgenic *fat-1* mouse model, ZO-1 expression was maintained after induction colitis by DSS [92]. In a model of TNBS colitis, ω-3 PUFA supplementation had no effect on the expression of tight junction proteins, claudin-1 and occludin, and the expression of associated mucosal proteins, trefoil factor (TFF) 3 and MUC2 [87].

Inflammatory mediator production by epithelial cells allows for crosstalk between the intestinal epithelium and other cells that form and regulate the gut barrier, including immune cells and gut microbes, during both homeostasis and inflammation. In non-stimulated male Lewis rats, fish oil supplementation was shown to reduce intestinal mRNA expression of a range of inflammatory mediators, including TNF-α, IFN-γ, IL-4, IL-10, and IL-15, as well as IL-15 protein expression, but had no effect on IL-7 mRNA or protein expression [99]. During inflammation, epithelial cells alter inflammatory mediator production to mediate the intestinal immune response [100]. 8-week fish oil supplementation increased the production of IL-1β, IL-10, IL-12, TNF-α, and keratinocyte-derived chemokine in a model of adoptive transfer of naïve T-cell-induced colitis [78]. Additionally, ω-3 PUFA supplementation decreased the colonic expression of IL-2 and IL-4 mRNA [86], as well as colonic IL-6 production, but had no effect on TNF-α expression [87] in models of TNBS-induced colitis. 3-week EPA and DHA supplementation had no effect on cytokine production in a model of intestinal reperfusion and ischaemia [80]. DHA supplementation downregulated the production of TNF-α, IFN-γ, and IL-17 in mice deficient in IL-10 [96]. DPA supplementation, over a 4-week period, reduced the mRNA and protein expression of IL-1β, IL-6, and TNF-α, whilst increasing the production of IL-10 mRNA and protein [91]. Andoh et al. reported that dietary ALA supplementation over two weeks also attenuated mucosal IL-6 expression, but had no effect on mucosal TNF-α expression, in a TNBS colitis model [89].

Transgenic alteration of the colonic mucosa PUFA composition (increasing EPA, DPA, and DHA concentrations) influenced the expression of multiple inflammatory factors in the colonic mucosa of *fat-1* mice in response to DSS-induced colitis. Gene expression of inflammatory cytokines TNF-α and IL-1β was decreased, toll-interacting protein (toll-like receptor antagonist) gene expression was increased, and TFF3 gene expression was increased [92]. The changes in

these markers were associated with lower colonic activity of NF-κB and lower inducible nitric oxide synthase (iNOS) gene expression [92]. A further study using the *fat-1* mouse model compared the effect of increased long-chain PUFA concentrations in both acute and chronic DSS-induced colitis. In the colonic mucosa of *fat-1* mice, production of several inflammatory proteins including CCL2, CCL3, CCL7, CCL9, CCL12, CCL19, IL-1β, IL-7, IL-18, and TNF-α was attenuated in both acute and chronic colitis [101]. Additionally, increased production of CCL4, IL-1α, IL-4, IL-6, MMP-9, and MPO was attenuated in colonic mucosa of *fat-1* mice during acute colitis [101]. Increased production of anti-inflammatory cytokine, IL-10, was reported during chronic colitis, whilst IL-11 production was decreased during acute colitis [101]. Overall, it seems that increased presence of EPA, DPA, and DHA can regulate the expression of a plethora of inflammatory markers in colonic mucosa and exerts protective effects in both acute and chronic colitis.

The production of ω-3 PUFA-derived bioactive lipids and competitive inhibition of ω-6 PUFA-derived lipid mediators is another proposed mechanism underpinning the immunoregulatory properties of ω-3 PUFAs. In a human study, 12-week fish oil supplementation decreased colonic mucosal levels of AA-derived PGE_2 and TXB_2 in patients with inflammatory bowel disease [75]. However, rats fed EPA-enriched fish oil for 6 weeks had unexpectedly increased concentrations of PGE_2 and LTB_4 in colonic dialysates [98]. In a model of DSS-induced colitis, increased colonic concentrations of EPA, DPA, and DHA in transgenic *fat-1* mice had no effect on colonic expression of leukotriene (LT)B_4, PGE_2, and 15-hydroxyeicosatetraenoic acid, whilst levels of particular long-chain ω-3 PUFA-derived eicosanoids were significantly higher in colonic mucosa, including resolvin E1 and D3, protectin D1, prostaglandin E3, and LTB5 [92]. In a separate study using *fat-1* mice, increased presence of EPA, DPA, and DHA in colonic tissue attenuated increased PGE_2 levels in both acute and chronic DSS-induced colitis [101]. DPA supplementation also attenuated increased mucosal levels of PGE_2, as well as LTB_4, in a DSS-induced colitis model [91].

In a model of colitis, fish oil supplementation had no effect on mucosal expression of PGE_2, TXB_2, and LTB_4, but attenuated increased expression of AA-derived PGJ_2, 5,6-EET, 8,9-EET, and 14,15-EET [78]. Additionally, mucosal levels of EPA and DHA-derived metabolites PGE_3, TXB_3, LTB_5, 5-HEPE, and 17,18-EEP were increased [78]. Yuceyar et al. described that fish oil given by either daily enema

for 2 weeks or in the diet for 6 weeks, attenuated increased LTB_4 and LTC_4 levels in a model of TNBS colitis [88]. Further to this, in separate models of TNBS-induced colitis, 4 weeks dietary ω-3 PUFA supplementation and two weeks dietary ALA supplementation attenuated increased levels of leukotriene B_4 [87, 90]. In the ALA supplementation model, there was no effect on mucosal PGE_2 expression [90]. EPA and DHA supplementation increased the mucosal expression of TXB_3, 17,18-EEP, and 8-iso $PGF_{3\alpha}$ in a model of intestinal reperfusion and ischaemia [80].

ω-3 PUFAs interact with a variety of inflammatory mechanisms, including regulators of inflammatory mediator production, such as NF-κB and iNOS, and regulators of lipid mediators, including COX-2. In *fat-1* mice, increased presence of ω-3 PUFAs in colonic tissue reduced NF-κB activity and iNOS mRNA expression in DSS-induced colitis [92]. Furthermore, in a TNBS-induced colitis model, ALA supplementation reduced NF-κB activity, iNOS expression, and COX-2 expression, but had no effect on the phosphorylation of NF-κB inhibitory subunit, IκB, and mitogen-activated protein kinases (MAPKs), JNK and p38 [90]. Both fish oil and sage oil (providing ALA) decreased COX-2 mRNA expression in DSS and TNBS-induced colitis [79]. Fish oil given in the diet for 6 weeks reduced myeloperoxidase (MPO) activity in a TNBS-induced colitis model, whilst fish oil given by daily enema had no effect on MPO expression [88]. In TNBS colitis models, ω-3 PUFA supplementation suppressed COX-2 expression, iNOS expression [87], and colonic nuclear factor of activated T cells mRNA expression [86] but increased mRNA expression of IL-1α, MAPK kinase 3, TLR-2 [87], and peroxisome proliferator-activated receptor (PPAR)-γ [86]. In a model of necrotising enterocolitis, DHA supplementation had no effect on iNOS expression but downregulated phospholipase A_2 and platelet-activating factor receptor expression [82]. DPA supplementation reduced colonic COX and 5-LOX expression, and reduced MPO activity, in a model of DSS-induced colitis [91]. Overall, ω-3 PUFAs seem to influence numerous inflammatory pathways in different models of intestinal inflammation.

Using wild-type mice supplemented with EPA or DHA, de Vogel-van den Bosch *et al.*, produced a transcriptomic profile of cellular mechanisms altered by ω-3 PUFA supplementation to provide an overview of the pathways influenced by ω-3 PUFAs. Surprisingly, EPA and DHA supplementation had no effect on the mRNA

expression of ω-3 PUFA associated mechanisms, including long-chain fatty acid uptake, mitochondrial and peroxisomal β-oxidation, ω-oxidation, and metabolism of energy-yielding substrates, as well as oxidative stress mRNAs [102]. Both EPA and DHA downregulated mRNAs of cholesterol uptake transporter, Npc111, glucose uptake transporter, Sglt4, and serotonin transporter, Slc6a4 [102], whilst EPA singularly increased the expression of cholesterol efflux protein, Abca1, and dopamine transporter, Dat1, mRNAs [102].

Overall, it is therefore hard to draw a conclusion on the effects of ω-3 PUFAs supplementation on the gut epithelium. The varying results across the literature could be dependent on the variation between study design, including factors such as ω-3 PUFA(s) used, the source of each PUFA, supplementation dose and time, or delivery method of ω-3 PUFAs. However, the literature does indicate several proposed cellular processes that ω-3 PUFAs can target to alter the function of epithelial cells at rest and during inflammation; these are summarised in *Figure 1.4*.

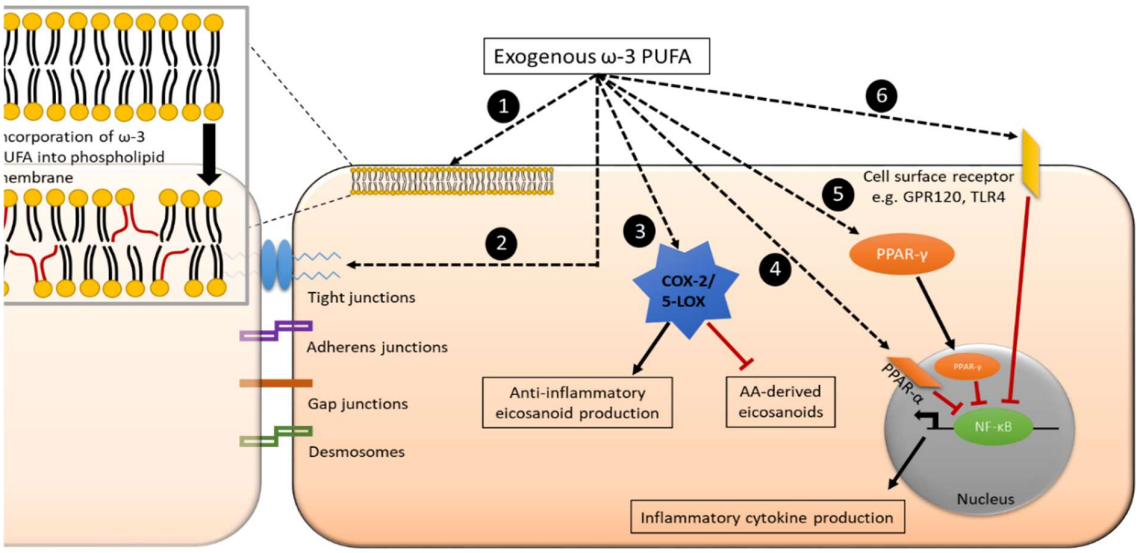

*Figure 1.4: Proposed mechanisms involved in ω-3 PUFA regulation of inflammation in intestinal epithelial cells. (**1**). Incorporation of ω-3 PUFA into phospholipid membrane/lipid rafts. (**2**). Modulation of tight junction protein expression and re-distribution. (**3**). Production of anti-inflammatory eicosanoids and inhibition of AA-derived eicosanoids catalysed by COX-2 or 5-LOX. (**4**). Activation of nuclear receptors, e.g., PPAR-α. (**5**). Translocation of transcription factors into nucleus, e.g., PPAR-γ. (**6**). Interaction with transmembrane/cell surface receptors, e.g., G-protein coupled receptor 120 (GPR120) and TLR4. Mechanisms 4, 5, and 6 lead to the inhibition of NF-κB and the subsequent reduced production of multiple inflammatory mediators. Figure produced using Microsoft PowerPoint and published in [10].*

1.6. Caco-2 cells – An in vitro model of the gut epithelium

Discovered and originally utilised in cancer research in the mid-1970s [103-105], the human adenocarcinoma cell line (Caco-2) has subsequently become a useful model in the study of human gut epithelial cell function. Caco-2 cells spontaneously differentiate and over a growth period of approximately 3 weeks will form polarised monolayers. Primarily, monolayers occur through adjacent cells forming tight junctions upon contact and the localisation of ZO-1 proteins to the cell-cell interface [106]. Tight junction assembly in Caco-2 cells is regulated by the expression of an array of genes, including genes for cytoskeletal and tight junction structural proteins, ZO-1, ZO-2, occludin, and β-actin, and several regulatory genes, including CD2-associated protein, cyclin-dependent kinase 4, and vascular endothelial growth factor A [107]. Several of these genes have been shown to be regulated by the SCFA butyrate [108] and by probiotic bacteria [107] during the formation of tight junctions in Caco-2 monolayers.

During cellular differentiation, Caco-2 cells form brush borders across the apical surface, with similar distribution to *in vivo* enterocytes [109]. Functional brush border formation with Caco-2 cells allows for similar transport properties to enterocytes, as well as supporting complementary signalling through transporters, such as Na^+/H^+ exchanger isoform 3, in the Caco-2 model [110]. Brush border presentation in Caco-2 cells is also important in the adhesion of bacteria to monolayers; *Lactobacillus acidophilus* species adhere favourably to fully differentiated (15 days post-seeding) brush border presenting Caco-2 cells compared to less differentiated cell monolayers (5, 7, 10 days post-seeding) [111]. Additionally, Caco-2 cells show similar receptor and transporter profiles to those of small intestinal cells [112], including the long-chain fatty acid receptor, FFAR4, although FFAR1, normally found on enterocytes, is not present [113].

The development and integrity of Caco-2 monolayers can be monitored by using the trans-epithelial electrical resistance (TEER) method. TEER values are indicative of permeability, a higher TEER value depicts a lower permeability. Usually, after 14-17 days Caco-2 monolayers will have a TEER value of 1400-2400 Ω per cm^2; TEER values will be altered by factors such as growth medium, passage number, and seeding density [114]. Appropriate growth conditions, including growth medium, seeding density, and cell confluence, are pertinent to achieving reliable

and repeatable Caco-2 monolayers. Low seeding densities ($3 \times 10^5/cm^2$) and confluence (50%) have been proposed as best practice for standardised, replicable monolayers, as well as a growth period of 21 days post-seeding to obtain fully-differentiated enterocyte-like cells [115]. A replicable Caco-2 model ensures that the changes in permeability, tight junction function, mediator secretion, and intracellular signalling can be assessed reliably when assessing specific inflammatory stimulants, mimicking *in vivo* gastrointestinal inflammation.

1.7. Caco-2 cells and modelling of gut inflammation

Caco-2 cell monolayers can be challenged with a multitude of inflammatory stimuli at different concentrations and times reflecting *in vivo* inflammatory conditions. Physiological inflammatory stimuli, including pro-inflammatory cytokines and bacterial LPS, have been used extensively as a challenge to Caco-2 cell monolayers. Cytokines, such as IFN-γ, TNF-α, and IL-1β all increase monolayer paracellular permeability, indicated by permeability measurements such as TEER, from concentrations as low as 10 ng/ml for TNF-α [116, 117] and IFN-γ [116], and 25 ng/ml for IL-1β [118]. Bacterial LPS from *E. coli* species increase Caco-2 monolayer permeability at higher concentrations (1 μg/ml) [119]. Cytokine-induced increases in monolayer permeability can be as a result of tight junction dysfunction, which can be induced through activation of NF-κB signalling pathways and by reducing localisation and expression of tight junction proteins [120]. Responses to inflammation are not limited to changes in permeability, as Caco-2 cells can produce an array of cytokines and chemokines, similar to gut epithelial cells, including IL-1β, CXCL8, IL-10, and transforming growth factor (TGF)β1, either constitutively or under inflammatory conditions [121]. Cytokines involved in the pathogenesis of IBD, such as TNF-α and IFN-γ, can be used to better understand the inflammatory disease-specific disruption to the gut epithelial layer, and to investigate potential therapies and preventative strategies.

Caco-2 monolayers can also be used to assess the impact of dietary components associated with changes in gut permeability, such as gliadin peptides from digested gluten [122] and probiotics [123]. This is pertinent as poor diet has been associated with the rise in gastrointestinal autoimmune diseases, which is attributed to an increase in gut epithelial permeability [124]. Using the Caco-2 model, apical α-gliadin stimulation (1 mg/ml) was shown to increase paracellular

permeability, indicated by both decreased TEER and increased FITC-dextran flux [125]. Additionally, expression of tight junction proteins ZO-1, claudin-1, claudin-3, claudin-4, and E-cadherin was significantly decreased after 4-hour gliadin stimulation. Fluorescent microscopy also showed a decrease in expression of claudins-3 and -4, and ZO-1, but not in claudin-1 and E-cadherin, as well as a reorganisation of F-actin [125]. In a separate model, it has been identified that α-gliadin acts at the chemokine receptor, CXCR3, which is present in both the Caco-2 model and in human intestinal epithelial cells [126]. Furthermore, α-gliadin peptide activation of CXCR3 increases the production of the inflammatory cytokine, TNF-α, through a cyclic-adenosine monophosphate (cAMP)-protein kinase A (PKA) pathway, as well as inducing the translocation of NF-κB into the nucleus [127].

Probiotics, live bacteria in food and supplements which have beneficial effects to the host [128], elicit beneficial anti-inflammatory effects through an array of mechanisms, including the production of inhibitory compounds and SCFAs, competition with pathogenic bacteria for nutrients and adhesion sites on the gut mucosal surface, and regulating enterocyte gene expression [129]. The Caco-2 cell model has been used to demonstrate the beneficial effects of probiotics on the gut epithelium *in vitro*. *Lactobacilli*, a genus of bacteria used in many probiotic products, have been shown to adhere to Caco-2 cells in a dose-dependent relationship between bacterial dose and adhesion rate [130]. The probiotic strain, *Lactobacillus casei GG* (LCG) can upregulate the expression of genes responsible for the expression of mucin in Caco-2 cells, which can prevent epithelial damage and bacterial translocation [131]. Furthermore, LCG and *Bifidobacterium animalis* MB5 are protective against the pathogenic enterotoxin-producing bacterium, *E. coli* K88, by inhibiting increases in CXCL8, IL-1β and TNF-α secretion in Caco-2 cells [132]. *Lactobacillus*, *Lactococcus,* and *Bifidobacterium* probiotic strains can increase epithelial integrity as well as preventing *Salmonella enteritidis* pathogenicity in the Caco-2 model [133].

The most pertinent issue with probiotics as a viable therapy for IBDs is the *in vivo* bacterial survival through gastrointestinal stress, as often large numbers of viable cells are lost or unable to adhere to the epithelial layer. However, the probiotic strains *Lactobacillus acidophilus* and *Lactobacillus delbrueckii* subjected to conditions representative of gastric emptying (low pH, bile salts, and pancreatic enzymes) *in vitro* remained viable, as well as maintaining the ability to adhere to

Caco-2 cells relatively well [134]. Encouragingly, more recently it has been shown increased adherence of *Lactobacillus paracasei* to mucin and Caco-2 cells when subjected to acid and bile stress [135]. Moreover, *Lactobacilli* have shown improved adherence and survival when epithelial cells were pre-treated with DHA [136], suggesting a contribution of a dietary component (DHA) to probiotic effectiveness *in vivo*. Overall, a strain that is optimal in both survival and adhesion *in vivo* remains elusive, and therefore, the Caco-2 model remains integral to developing an optimally effective probiotic therapy for IBDs.

The flexibility of the Caco-2 epithelial model means the model continues to be used to assess a diverse range of stimuli and treatments. Recent studies, summarised in *Table 1.2*, using the Caco-2 model have explored dietary treatments, such as polyphenols, specific polysaccharides and proteins against several inflammatory stimuli, including inflammatory cytokines, LPS, hydrogen peroxide, and oxysterol. Therefore despite the increased presence of gut epithelium 3-D models, such as gut-on-a-chip [137], the Caco-2 model remains a widely used tool in modelling enteric inflammatory conditions *in vitro* and is therefore essential in determining and assessing potential mechanisms implicating epithelial dysfunction for inflammatory conditions.

Table 1.2: Recent publications (since 2020) using Caco-2 cells as an inflammatory model.

Author (Year)	Treatment	Treatment concentration; time	Inflammatory stimulant	Stimulant concentration; time	Summary of results
Castro-Herrera et al. (2020) *[138]*	*Lactobacillus rhamnosus* GG (LGG) and/or *Bifidobacterium animalis subsp. lactis*, BB-12 (BB-12)	10:1 multiplicity of infection (Heat-inactivated); 22 hours	TNF-α, IFN-γ, and IL-1β	1 ng/ml, 10 ng/ml, and 1 ng/ml, respectively; 24 hours	No effect on increased permeability LGG, BB-12, and LGG+BB-12 reduced IL-6 and IL-18 secretion LGG reduced VEGF secretion No effect on CXCL8, ICAM-1, and IP-10 expression
Nallathambi et al. (2020) *[139]*	Proanthocyanidin-rich grape seed extract (GSE)	12.5 μg/ml; 24 hours	LPS	25 μg/ml; 24 hours	GSE reduced LPS-induced oxidative stress GSE increased oxidative stress enzyme mRNA expression GSE prevented increased tight junction permeability and loss of tight junction protein expression GSE increased anti-inflammatory cytokine mRNA expression GSE decreased pro-inflammatory cytokine mRNA expression
Iaia et al. (2020) *[140]*	Theobromine (TB)	10-30 μM; 24 hours	Oxysterol mixture (oxy-mix)	60 μM; 24 hours	TB attenuated oxy-mix-induced increases in CXCL8 and CCL2 expression

					TB attenuated oxy-mix-induced decreases in tight junction protein expression TB attenuated oxy-mix-induced MMP-2 and -9 secretion TB attenuated oxy-mix-induced apoptosis
Beisl et al. (2020) ***[141]***	Deoxynivalenol (DON) and/or cereulide (CER)	DON; 0.01-10 μg/ml; up to 72 hours CER; 0.1-100 ng/ml; up to 72 hours In combination; ratio (1:100) CER:DON	IL-1β	25 ng/ml; 3 hours	DON and CER induced cytotoxicity (synergistic effects were seen at 72 hours) DON increased CXCL8 mRNA and protein expression, more than combined DON/CER treatment CER increased TNF mRNA expression CER attenuated CXCL8 mRNA and protein expression
Capraro et al. (2020) ***[142]***	Low charge chenopodin (LcC) or high charge chenopodin (HcC)	0.5 mg/ml; 4 hours	IL-1β	10 ng/ml; 4 hours	LcC and HcC reduced NF-kB activation (LcC<HcC) LcC and HcC reduced CXCL8 expression LcC reduced CXCL8 expression when pre-incubated with IL-1β
Iglesias et al. (2020) ***[143]***	Ellagic acid (EA)	10-40 μM; up to 7 hours	IFN-γ and TNF-α	IFN-γ; 10 ng/ml; 24 hours (pre-incubation)	EA dose-dependently reduced IL-6 protein expression and CXCL8 mRNA and protein expression

				TNF-α; 10 ng/ml; up to 6 hours	EA inhibited ICAM-1 and NLRP3 expression EA prevented increased monolayer permeability EA prevented decreased occludin and ZO-1 expression EA inhibited increased oxidant production and NOX1 gene expression EA inhibited increased mitochondrial oxidant production and decreased membrane potential EA inhibited increased NF-kB and ERK1/2 activation EA inhibited increased MLCK gene expression and MLC phosphorylation
Nie et al. (2020) ***[144]***	Bifidobacterium (BIF)	10^8 CFU/ml; 24 hours	TNF-α	10 ng/ml; 24 hours	BIF attenuated cell apoptosis BIF attenuated increased IL-6 and CXCL8 protein expression Partially attenuated increased monolayer permeability BIF inhibited cell autophagy BIF attenuated activation of NF-kB and p38MAPK pathways

Martins et al. (2020) *[145]*	Grape pomace extract (GPE) with or without tannase (TNS)	100-500 μg/ml; up to 30 hours	IL-1β	1 or 20 ng/ml; 24 hours	High concentrations (500 μg/ml) GPE induced cell cytotoxicity GPE attenuated increased ROS production GPE attenuated the expression of NF-kB p65, CXCL8, and PGE2
Li et al. (2020) *[146]*	*Lycium barbarum* polysaccharides (LBP)	50-400 μg/ml; 24 or 48 hours	TNF-α	100 ng/ml; 24 hours	LBP partially prevented increased monolayer permeability (200 and 400 μg/ml) LBP partially attenuated the expression of IL-6, CXCL8, ICAM-1, and CCL2 LBP attenuated decreased expression of tight junction proteins LBP attenuated increased NF-kB expression and phosphorylation of IkBα LBP attenuated increased MLCK expression and phosphorylation of MLC
Hasegawa et al. (2021) *[147]*	L-cystine dihydrochloride (Cys2)	0.1-1 mM; 24 hours	Hydrogen peroxide	0.5 mM; 1-4 hours	Cys2 attenuated increased monolayer permeability Cys2 increased the ratio of claudin-4 in the detergent-insoluble fractions to soluble fractions

					Cys2 had no effect on tight junction protein expression Cys2 increased intracellular expression of glutathione Cys2 had no effect on oxidative stress markers Cys2 attenuated increased IL-1β mRNA expression (TNF-α tended to be attenuated)
Mayangsari et al. (2021) *[148]*	5,7-dimethoxyflavone (DMF)	50 μM; 48 hours	IL-1β	20 ng/ml; 48 hours	DMF reduced monolayer permeability DMF increased occludin and claudin-1 cytoskeletal association (decreased claudin-2 association) DMF decreased ZO-2, claudin-2, and claudin-3 expression (increased occludin expression) DMF increased mTOR phosphorylation DMF increased claudin-2 promoter plasmid activity and miR-16-5p expression DMF attenuated increased monolayer permeability DMF significantly attenuated decreased occludin expression (no effect on claudin-2)

1.8. Polyunsaturated fatty acids and gut epithelial cell models

Models of the gut epithelium, including Caco-2 cells, can be used to identify and characterise potential benefits of components of a healthy diet, including the effects of ω-3 PUFAs on intestinal epithelial cells. Caco-2 cells have the ability to take up exogenous PUFAs, with a 1:1 ratio of EPA:DHA being reported as favourable in this cell line [149]. The accumulation of fatty acids is differential in the phospholipid, neutral, and free fatty acid fractions of Caco-2 cells and seems to differ dependent on growth conditions, with EPA and DHA preferentially accumulating in the neutral fraction. Caco-2 cells possess PUFA processing capability with specific desaturase and elongase activity, with Caco-2 cells also exhibiting retroconversion of DHA to EPA [150]. Dietary relevant concentrations of EPA and DHA also show no effect on Caco-2 cell viability [151], and consequently, this ensures that Caco-2 cells are a suitable model for assessing the effects of ω-3 PUFAs on the gut epithelium. In T84 cell models, significant alterations in PUFA composition have been reported from time periods as short as 3 hours [152] and at concentrations from as low as 10 μM [153].

ω-3 PUFAs have been shown to both positively and negatively affect intestinal permeability *in vivo*. The effect of ω-3 PUFAs on permeability *in vitro* reflects this. Usami et al. reported that 24 hours supplementation with high concentrations (>50 μM) of ALA, EPA, or DHA dose-dependently increased Caco-2 cell permeability through a PKC-mediated pathway [154, 155]. However, a previous study had reported decreased permeability in Caco-2 cells supplemented with 100 μM EPA [156] and subsequently most *in vitro* studies have reported protective effects of ω-3 PUFAs on inflammatory stimulant-induced increases in permeability. In T84 cells, separately 100 μM EPA and DHA decreased IL-4-induced increased permeability [153], whilst in a separate T84 model, EPA and DHA were both shown to prevent increased permeability, changes to tight junction protein distribution and morphology, and the displacement of occludin and flotillin from lipid rafts in cells stimulated with TNF-α and IFN-γ [157]. Xiao et al. also described that separate EPA and DHA supplementation prevented deoxynivalenol-induced increased permeability and tight junction protein (ZO-1 and claudin) redistribution [158]. In a Caco-2 model of heat stress-induced inflammation, EPA and DHA were shown to have differing effects. EPA was able to attenuate increased permeability, altered tight junction protein distribution and morphology, and decreased ZO-1 and

occludin protein and mRNA expression [159]. DHA was also able to prevent decreased protein and mRNA levels of ZO-1 and occludin; however permeability was unaffected and there was no significant effect on tight junction protein distribution or morphology [159]. In a separate Caco-2 model, ALA and DHA were shown to attenuate the cytokine-induced loss of the tight junction component, occludin, without preventing increased paracellular permeability indicated by decreased TEER values [160]. Overall, variable results of ω-3 PUFA supplementation on epithelial permeability have been reported and little exploration has been done into the mechanisms of tight junction dysfunction affected by ω-3 PUFAs.

As well as influencing paracellular permeability and tight junction components, ω-3 PUFAs can influence inflammatory pathways and the subsequent production of inflammatory mediators. DHA potentiated the inhibition of NF-κB and secretion of GLP-1, through the activation of FFAR4, in Caco-2 cells [161]. EPA did not to induce NF-κB signalling and ICAM-1 release in unstimulated Caco-2 cells, but was shown to induce pro-inflammatory IL-6 and anti-inflammatory IL-10 expression after 16 hours exposure [162]. Long-term EPA supplementation (initial 3 hours, followed by 7 days) reduced stearoyl CoA desaturase and SREBP-1c mRNAs in unstimulated T84 and Caco-2 cells, but had no effect on PPAR-α mRNA expression [152]. EPA and DHA were shown to induce TGF-β1 mRNA expression in a HT29/HT29-MTX co-culture, but had no consistent effect on CXCL8 or heat shock protein 72 mRNAs [163]. EPA and DHA induced PPAR-α activity in Caco-2 cells, whilst DHA, not EPA, induced PPAR-γ activity and reduced triglyceride and apolipoprotein B secretion [164]. Neither EPA nor DHA had an effect on PPAR-δ activity in Caco-2 cells [164].

DHA also potentiated apoptosis in HT29 cells treated with TNF-α or anti-Fas monoclonal antibodies. In this model, DHA also slowed HT29 cell maturation, indicated by an increased presence of G_0/G_1 phase cells [165]. In platelet-activating factor-treated IEC-6 cells, DHA reduced TLR4 and platelet-activating factor receptor mRNAs [83]. DHA suppressed NF-κB activity and inhibited IkB degradation, which was coupled to a decrease in CXCL8 expression in HCT116 cells stimulated with either lauric acid, D-gamma-Glu-mDAP (IE-DAP; NOD1 ligand), or muramyl dipeptide (MDP; NOD2 ligand) [166]. EPA only reduced CXCL8 secretion in MDP-stimulated cells and had no effect on NF-κB activity or nuclear factor of kappa light polypeptide gene enhancer in B-cells inhibitor (IκB) degradation in any condition [166]. Vincentini et al. stimulated Caco-2 cells with α-gliadin peptides and were able to

show that DHA attenuated increased PGE_2 and CXCL8 secretion, increased phospholipase 2 activity, and increased COX-2 expression [167].

In IL-1β-stimulated Caco-2 cells, EPA and DHA attenuated increased PPAR-γ and iNOS expression, as well as increased IL-6 and CXCL8 production [168]. ALA, EPA, and DHA had no effect on IkB expression and additionally ALA had no effect on PPAR-γ or iNOS expression [168]. In a separate Caco-2 model of IL-1β-induced inflammation, ALA and sage oil reduced CXCL8 and COX-2 expression, whilst ALA supplementation also suppressed increased iNOS expression [79]. Wijendran et al. comparatively assessed the effects of EPA and DHA in three different epithelial cell lines: H4, NEC-IEC, and Caco-2 cells stimulated with IL-1β. EPA reduced CXCL8 and IL-6 mRNA and protein expression in H4 cells only, whilst DHA decreased CXCL8 mRNA and protein expression across all cell lines, IL-6 protein expression in NEC-IEC and H4 cells, and IL-6 mRNA in H4 cells only [169]. Altered CXCL8 and IL-6 expression by DHA, but not EPA, was associated to a decrease in NF-κB and IL-1R1 mRNAs in these cell lines [169].

Less is known about the anti-inflammatory properties of other ω-3 PUFAs, including the EPA-DHA intermediate DPA, although it is known that DPA elicits a similar production of anti-inflammatory mediators to EPA and DHA [170]. One model has shown that DPA had similar protective properties to EPA and DHA on cytokine-induced increases in tight junction permeability in Caco-2 cells [160]. The anti-inflammatory capacity of ω-3 DPA is yet to be fully elucidated and requires further assessment. The effects on epithelial barrier integrity, inflammatory mediator production, and regulatory inflammatory proteins by ω-3 PUFAs, including EPA, DHA, and ω-3 DPA, as well as plant-derived ω-3 PUFAs, in the Caco-2 model are yet to be fully understood and require further investigation.

1.9. Research gaps

The nutritional alleviation of inflammatory conditions is an extensively researched area, yet the optimal strategies for tackling intestinal inflammation remain elusive, although dietary intervention is considered a viable option [171]. There is evidence to suggest that ω-3 PUFAs, EPA and DHA, are inversely associated with the prevalence of IBD, through their competitive action with ω-6 PUFAs, namely AA [172]. Due to the large range of mediators that EPA, DHA, and other ω-3 PUFAs

produce and their varied actions, the overall mechanistic action of ω-3 PUFAs on the gut barrier during inflammation has not been fully elucidated. Consequently, models of the gut epithelium, including Caco-2 cells, provide a tool to assess the anti-inflammatory role of ω-3 PUFAs in intestinal inflammation. Pertinently, the model can be used to assess the effects of lesser-studied ω-3 PUFAs, such as DPA, and plant-derived ω-3 PUFAs, such as ALA and stearidonic acid (SDA) compared to the more defined action of EPA and DHA.

This lack of total clarity on the role of existing and emerging dietary ω-3 PUFAs in intestinal inflammation means that further elucidation via cell models is required. I will endeavour to develop a model of intestinal inflammation, using Caco-2 cells, which will allow me to assess the potential anti-inflammatory role of plant-derived ω-3 PUFAs and DPA compared to EPA and DHA.

1.10. Research Hypothesis

The known anti-inflammatory properties of EPA and DHA will be assessed against the lesser-known effects of DPA, and plant-derived ω-3 PUFAs, ALA and SDA in a model of cytokine-induced inflammation in Caco-2 cells. Overall, I expect to find that all ω-3 PUFAs will exhibit anti-inflammatory properties in this model of cytokine-induced inflammation. I hypothesise that EPA and DHA will exhibit anti-inflammatory properties in this model and that DPA will exhibit similar anti-inflammatory capacity. I hypothesise that plant-based ω-3 PUFAs will exhibit weaker anti-inflammatory properties to those of EPA, DHA, and DPA.

Chapter 2 Methods and Materials

2.1. Cell culture

2.1.1. Caco-2 cell culture and subculture

Caco-2 cells (1-3 million cells in 1 ml cryopreservation medium, see *2.1.3.*) stored in liquid nitrogen to maintain viability, were thawed in cold, unsupplemented DMEM and centrifuged for 5 minutes at 304 x *g* to produce a cell pellet. The supernatant was discarded, and the remaining cell pellet was resuspended in 12 ml warm (37°C) culture medium (*Table 2.1*, below) and transferred to a 75 cm^2 cell culture flask. Viable cells were incubated (37°C, 5% CO_2) for 2-3 days post-seeding to allow for attachment to the culture flask. Cells were then washed with Hank's balanced sodium solution (HBSS) to remove non-viable cells. Cells were disassociated from the culture flask by incubation with warm (37°C) trypsin solution (0.25% in HBSS, Merck, UK) for 6-8 minutes (37°C, 5% CO_2). Once cells were in suspension, culture medium was added to the flask (to inhibit trypsin) and the cells were centrifuged for 5 minutes at 304 x *g*. Trypsin/culture medium supernatant was discarded and the remaining cell pellet was resuspended in 24 ml culture medium (see *Table 2.1*), before being transferred to a 175 cm^2 cell culture flask for further incubation. Culture medium was replaced every 2-3 days and subculturing was performed at 70-80% confluence. Passages used in experiments were between 49 and 62.

Table 2.1: Constituents of Caco-2 culture medium. All components were purchased from Merck, UK.

Culture Medium Component	%Total Volume
Dulbecco's Modified Eagle Medium (DMEM)	86%
Foetal bovine serum	10%
L-glutamine	2% to give a final concentration of 4 mM
Penicillin and streptomycin	1% (50,000 IU penicillin, 50 mg streptomycin)
Non-essential amino acids	1% (4.45 mg L-Alanine, 7.50 mg L-Asparagine, 6.65 mg L-Aspartic Acid,

	7.35 mg L-Glutamic Acid, 3.75 mg Glycine, 5.75 mg L-Proline, 5.25 mg L-Serine)

2.1.2. Transwell preparation and culture

Transwell plates (12-well, 1.12 cm^2, 0.4 μm pore size) were pre-treated with 100 μl collagen solution (Type I solution from rat tail (Merck, UK), 0.5% in phosphate buffered saline (PBS)) on the apical surface of inserts. Plates were incubated for 5 hours at 37°C before collagen solution was removed. 200 μl and 1000 μl warm culture medium was added to the apical and basolateral compartments, respectively, overnight before transwells were seeded. Caco-2 cells grown to 70-80% confluence in culture flasks, were disassociated from the culture flask (see *2.1.1*) and were seeded onto the apical surface of transwell inserts at a density of 75,000 cells per cm^2, with 0.5 ml and 1.5 ml culture medium in the apical compartment and basolateral compartment, respectively. Cells were grown until differentiated (21 days) in transwells before use in experiments; culture medium was replaced every 2-3 days.

2.1.3. Caco-2 cell cryopreservation

Cells not used in experiments were suspended in 10% dimethyl sulfoxide (DMSO)/90% culture medium and transferred to internal-screw cryovials at a concentration of 1-3 million cells/ml. Cryovials containing Caco-2 cells were initially placed in a -80°C freezer, before being transferred to a liquid nitrogen store for long-term storage.

2.2. Cytokine stimulant preparation and storage

Lyophilised cytokines (PeproTech, UK) were resuspended in 1 ml culture medium to achieve diluted stocks of 10 μg/ml for TNF-α, 20 μg/ml for IFN-γ, and 2 μg/ml for IL-1β. Stocks were stored at -20°C. A cytokine cocktail of TNF-α, IL-1β, and IFN-γ (5 ng/ml, 5 ng/ml, and 50 ng/ml, respectively) was prepared in culture medium and used fresh on the day of each experiment. Cytokine concentrations to be used were determined in previous research to induce inflammation in Caco-2 cells.

2.3. PUFA storage and preparation

Stocks of ALA, EPA, DHA (Merck, UK), DPA, and SDA (Larodan, Sweden) were diluted in 100% ethanol and stored at -20°C until used. When being used for supplementation to cell cultures, PUFAs were diluted in warm culture medium to required concentrations (1 μM to 25 μM). Ethanol concentration was kept low at 0.1% total volume of the apical culture medium.

2.4. Caco-2 monolayer Permeability

2.4.1. Transepithelial Electrical Resistance (TEER)

The ionic permeability of Caco-2 monolayers was quantitatively monitored by TEER. Using an EVOM^2 voltohmeter and STX2 'chopstick' probes (World Precision Instruments), Caco-2 monolayers plated on 12-well transwell plates were measured up to every 2-3 days, prior to changing culture medium. Before measuring TEER, the voltohmeter was first calibrated using a test resistor, setting the resistance value to 1000 Ω. The probes were sequentially placed in distilled water, 75% isopropanol, and unsupplemented DMEM for up to 1 minute each, before taking readings. To take readings, probes were inserted into each transwell at a 90° angle to the plate (whilst ensuring the probes did not touch the monolayer – *Figure 2.1*) for 5-10 seconds to establish a stable TEER reading, which was then recorded. Between different treatments and plates, probes were washed by placing them in 75% isopropanol for up to 30 seconds, followed by distilled water and unsupplemented DMEM for 30 seconds each before taking the next set of readings. To maintain the temperature of transwell cultures, plates were placed on a constant temperature heat pad (Vet Tech) during TEER measurements.

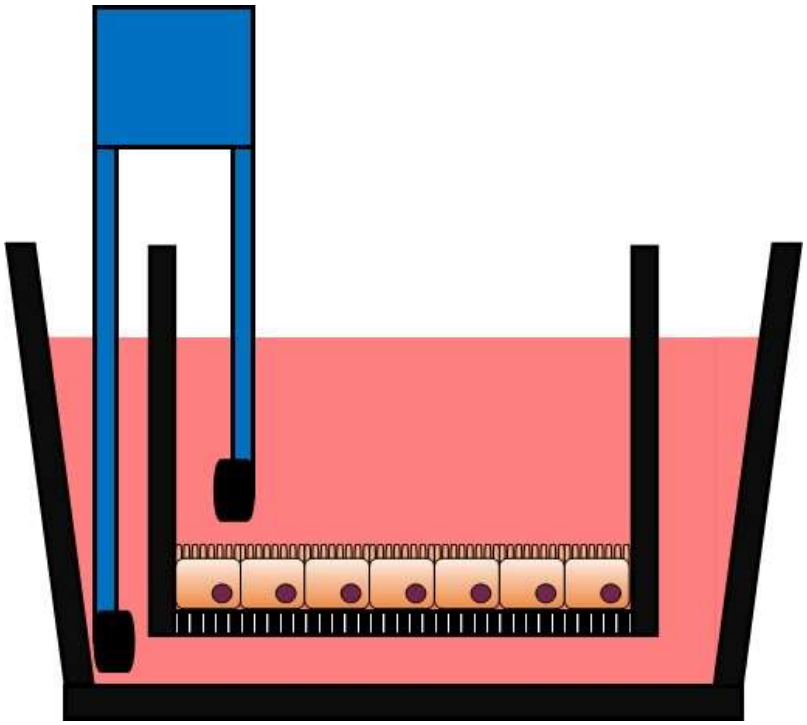

Figure 2.1: Transepithelial Electrical Resistance (TEER) measurements of Caco-2 cell monolayers were taken by the insertion of 'chopstick' probes at a 90o angle to the plate – avoiding contact with the cell monolayer. TEER readings were taken approximately 5-10 seconds after insertion of probes. Figure produced in Microsoft PowerPoint.

2.4.2. Fluorescein isothiocyanate (FITC)-dextran permeability

The macromolecular permeability of Caco-2 monolayers was quantitatively assessed by FITC-dextran permeability (average molecular weight 3,000-5,000, Merck, UK). 100 mg FITC-dextran powder was diluted in warmed HBSS (containing no phenol red) to a stock concentration of 10 mg/ml. After experimentation, Caco-2 monolayers were washed gently twice with warmed PBS in both the apical and basolateral compartments. After washing, FITC-dextran solution was further diluted to 1 mg/ml in HBSS (containing no phenol red) and 0.5 ml was added to each apical compartment. 1.5 ml HBSS (containing no phenol red) was added to each basolateral compartment. After 1 hour, triplicate 100 µl aliquots of the basolateral HBSS were transferred to black flat-bottomed plates. FITC-dextran fluorescence was quantified in the basolateral HBSS using a Glomax® Microplate reader (Promega, UK). Readings were taken at 475 nm excitation and 500-550 nm emission. FITC-dextran was quantified against a standard curve.

2.5. Analysis of inflammatory mediators using Luminex

Multi-analyte Luminex kits (R&D Systems, UK) were used to measure concentrations of cytokines and other inflammatory markers (see *Table 2.2*) in the medium taken from cultured Caco-2 cells. Cell supernatants were diluted prior to analysis where required. Following the manufacturer's instructions, briefly, standards and samples were suspended in microparticle solution and incubated for 2 hours at room temperature with gentle agitation. After incubation, microparticles were washed 4 times with wash buffer and biotin antibody solution was added for 1 hour at room temperature with gentle agitation. After incubation, microparticles were washed (as above) and streptavidin-phycoerythrin solution was added for 30 minutes at room temperature with gentle agitation. Microparticles were washed (as above) and resuspended in wash buffer. Plates were read on a Bio-Plex analyser (Bio-Rad, UK).

Table 2.2: Luminex analytes and detection limits. Values are approximate and can vary slightly between batches. Detection limits were specified per Luminex kit (R&D Systems).

Analyte	Upper Detection Limit	Lower Detection Limit
E-selectin	80,000 pg/ml	331 pg/ml
ICAM-1	1,690,000 pg/ml	2324 pg/ml
IL-6	1400 pg/ml	1.9 pg/ml
CXCL8	1050 pg/ml	1.4 pg/ml
IL-10	1000 pg/ml	4.1 pg/ml
IL-18	3020 pg/ml	4.1 pg/ml
IP-10	300 pg/ml	0.4 pg/ml
CXCL9	165,600 pg/ml	227 pg/ml
VCAM-1	2,150,000 pg/ml	8850 pg/ml
VEGF	2040 pg/ml	2.8 pg/ml

2.6. Confocal microscopy

Visualisation of tight junction proteins, ZO-1 and occludin, was performed by confocal microscopy. Caco-2 cells were grown on 12-well cell culture plates (3.8

cm^2) at a density of 70,000 cells/cm^2 for a total of 21 days. Culture medium was removed at day 21 and cells were then washed 3 times with cold PBS and fixed with 500 µl ice-cold methanol for 30 minutes (-20°C). 500 µl pre-block solution (2% bovine serum albumin (BSA) in PBS) was added to each well and cells were pre-blocked for 45 minutes (4°C). Anti-ZO-1 (FITC-conjugated mouse monoclonal; mAbcam 61357) and anti-occludin (rabbit monoclonal; ab216327) primary antibodies were diluted in PBS (1:100). Pre-block solution was removed, and samples were incubated in 500 µl primary antibody solution overnight (4°C) whilst control samples were similarly incubated but in PBS only. Donkey polyclonal anti-rabbit IgG (Alexa Fluor® 647) secondary antibody and 4′,6-diamidino-2-phenylindole (DAPI) were diluted in PBS (1:200 and 1:250, respectively). After primary antibody incubation, cells were washed in PBS three times and all wells were incubated in 500 µl secondary antibody/DAPI solution for 2 hours at room temperature. After 2 hours, cells were washed in PBS 3 times and after the final wash, 500 µl PBS was added to each well for imaging. Images were attained using a Leica SP8 microscope using a dry lens at x40 magnification. Lasers used to observe Caco-2 cells are summarised in *Table 2.3*.

Table 2.3: Antibodies used to visualise tight junction proteins, ZO-1 and occludin, in Caco-2 cells (all provided by abcam, UK).

Labelled Protein	Conjugate	Excitation	Emission	Laser
ZO-1	FITC	493 nm	528 nm	496 nm
Occludin	Alexa Fluor® 647	652 nm	668 nm	633 nm
Cell nuclei	DAPI	360 nm	460 nm	405 nm

2.7. Analysis of fatty acids by gas chromatography (GC)

2.7.1. Preparation of PUFA standards for GC

PUFA concentrations and fatty acid composition of Caco-2 cells were assessed by GC. PUFA standards (see section *2.3.*) were diluted to a concentration of 100 µM in

warm culture medium (0.1% ethanol in final volume). 800 µl of each diluted standard was transferred to screw-cap glass vials.

2.7.2. Preparation of Caco-2 cells for GC

Caco-2 cells were seeded onto 25 cm^2 flasks at a density 60,000 cells/cm^2 and grown for 21 days with growth media being replaced every 2-3 days. At day 21, Caco-2 cells were cultured in medium supplemented with 1 µM, 5 µM, 10 µM, or 25 µM EPA, DHA, DPA, ALA or SDA for 48 hours. After 48 hours, medium was removed, and cells were washed in HBSS 3 times. Cells were counted and resuspended to a concentration of 1.25 x 10^6 cells/ml, before 800 µl of cell suspension was transferred to screw-cap glass vials.

2.7.3. GC procedure

Following preparation, 30 µl internal standard (21:0 Non-esterified fatty acids; 1 mg/ml) was added to each cell sample vial which was subsequently thoroughly vortexed. 5 ml chloroform:methanol (2:1) solution with 50 mg/l BHT as antioxidant was added followed by 1 ml NaCl (1M), before thorough vortex mixing. Sample vials were centrifuged at 845 x *g* for 10 minutes. After centrifugation, the lower phase was collected by aspiration into fresh glass screw-cap vials. Standards and samples were dried under nitrogen at 40°C. Once dry, samples were resuspended by adding 500 µl dry toluene and thoroughly vortexing. 1 ml methylating agent (2% H_2SO_4 in methanol) was added, and each vial was gently mixed. Vials were capped and heated at 50°C for 2 hours. Vials were removed from the heat block and allowed to cool before 1 ml neutralising solution (0.25M $KHCO_3$, 0.5M K_2CO_3) and 1 ml dry hexane was added to each vial. Vials were then vortexed thoroughly and centrifuged at 211 x *g* for 2 minutes. The upper phase, containing fatty acid methyl esters, was then collected by aspiration into round bottom glass tube and dried under nitrogen at 40°C. Dry samples were twice resuspended in 75 µl dry hexane and transferred to autosampler vials.

2.7.4. GC run conditions

Fatty acid methyl esters (1 µl) were injected onto the column of an Agilent 6890 gas chromatograph. The column was an Agilent J&W resolution GC column with dimensions of 30 m x 0.22 mm x 0.25 µm. Fatty acid methyl esters were separated according to structure. Run conditions used for Caco-2 samples and PUFA standards were as follows: initial column temperature 115°C, held for 2 minutes, ramped

(10°C/minute) to 200°C, held for 11.5 minutes, ramped (60°C/minute) to 245°C, held for 4 minutes. The split ratio: 2:1 and a flame ionisation detector were used. Fatty acid methyl esters were identified by comparison of retention times with those of authentic standards. The use of 21:0 as an internal standard allowed quantification of Caco-2 fatty acids. An example of a chromatogram of a Caco-2 cell sample is shown in Figure 2.2.

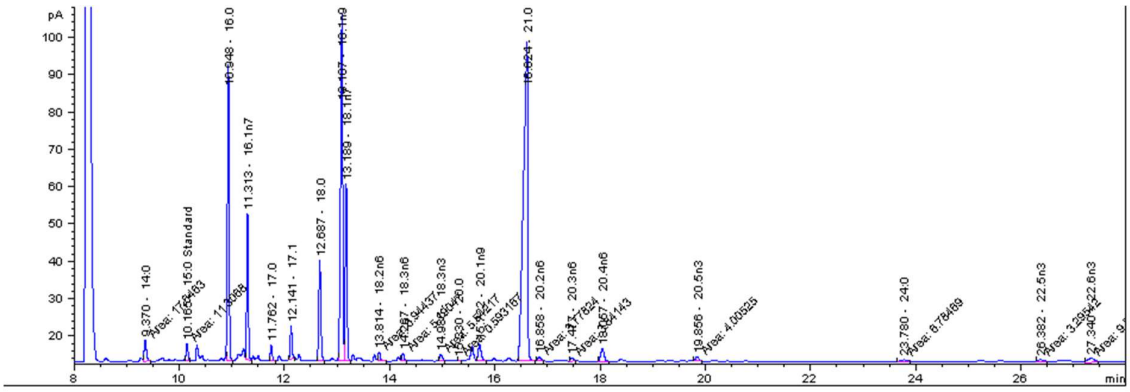

Figure 2.2: Example trace of Caco-2 cell fatty acid composition.

2.8. Western Blotting

2.8.1. Protein lysis and storage

After culture, Caco-2 cells were washed twice in ice-cold PBS. Lysis buffer containing 10 mM Tris(hydroxymethyl)aminomethane hydrochloride (Tris HCl), 1 mM Ethylenediaminetetraacetic acid (EDTA), 1% Triton™ X-100 solution (all purchased from Merck, UK), and 1% Halt™ protease and phosphatase inhibitor cocktail (ThermoFisher scientific, UK) was prepared on ice the day of cell collection. After washing, 200 µl of ice-cold lysis buffer was added to each well. Cells were dissociated from the bottom of each well by using a cell scraper and were left to lyse for 30 minutes. Cells in lysis buffer were transferred to Eppendorf tubes and centrifuged at 13,000 x *g* for 10 minutes. Supernatants containing lysed protein were collected and stored at -20°C until required.

2.8.2. Protein quantification

Protein was quantified using a bicinchoninic acid (BCA) assay. Following the manufacturer's instructions, 10 µl of protein solution (in duplicate) was added to a 96 well plate. BCA working reagent was prepared on the day of the BCA assay by

mixing BCA Reagent A and Reagent B (50:1). 200 µl of working reagent was added to each well containing protein samples. The plate was then wrapped in aluminium foil and placed on a plate shaker for 30 seconds to mix. The plate was then incubated at 37°C for 30 minutes. Absorbance was measured at 560 nm on a Glomax® Microplate reader (Promega, UK). Protein amounts were quantified against a series of BSA standards.

2.8.3. Sample preparation

On the day of blotting, 20-30 µg protein per sample was diluted with Laemmli Sample Buffer (4 to 1) and ultrapure 18.2 megohm (MΩ) water to achieve a final volume of 30 µl. Diluted samples were vortexed and centrifuged briefly, and then heated to 95°C for 5 minutes and allowed to cool before use.

2.8.4. Gel and buffer preparation

Mini-PROTEAN® Tetra Handcast Systems (BioRad, UK) were used to prepare gels for Western blotting. Gels were prepared up to 1 day prior to use and were kept at 4°C overnight. Gels were made using the components listed in *Table 2.4*.

Table 2.4: List of components for preparing 1 mm Western blot gels.

Gel	Component	Concentration	Volume/Mass
Separating gel (12%)	Tris(hydroxymethyl)aminomethane (Tris) buffer (pH 8.8)	1.5 M	2.5 ml
	Acrylamide/Bisacrylamide (37.5:1) solution	30%	4.0 ml
	Sodium dodecyl sulphate (SDS) solution	20%	50 µl
	Ammonium persulphate (APS)	10%	50 µl
	N,N,N',N'-Tetramethylethylenediamine (TEMED)	-	10 µl
	Ultrapure 18 MΩ water	-	3.4 ml
Stacking Gel (4%)	Tris buffer (pH 6.8)	0.5 M	2.5 ml
	Acrylamide/Bisacrylamide (37.5:1) solution	30%	4.0 ml

	SDS solution	20%	50 µl
	APS	10%	50 µl
	TEMED	-	10 µl
	Ultrapure 18 MΩ water	-	3.4 ml

Buffers used for Western blotting were prepared on the day of use. Buffers were prepared using components listed in *Table 2.5*.

Table 2.5: List of buffers and components used for Western blotting.

Buffer	Component	Volume/Mass	Final Concentration
Running Buffer (10x)	Tris(hydroxymethyl)aminomethane (Tris) base	30.3 g	250 mM
	Glycine	114.2 g	1.5 M
	Sodium dodecyl sulphate	10 g	35 mM
	Ultrapure 18 MΩ water	up to 1 litre	-
Running Buffer (1x)	Running Buffer (10x)	100 ml	10%
	Ultrapure 18 MΩ water	up to 1 litre	-
Transfer Buffer	Running Buffer (10x)	80 ml	8%
	Methanol	200 ml	20%
	Ultrapure 18 MΩ water	up to 1 litre	-
PBS+Tween	Polyoxyethylenesorbitan monooleate (Tween® 80)	500 µl	0.05%
	PBS	up to 1 litre	-
Blocking buffer	Skimmed milk powder	1 g	5%
	PBS+Tween	20 ml	-

2.8.5. Protein separation and transfer

Proteins were separated by sodium dodecyl sulphate-polyacrylamide gel electrophoresis (SDS-PAGE). 25 µl of prepared protein sample (see *2.8.3.*) was added to each well of prepared 1 mm gels (see *2.8.4.*) which was encased in a Mini-PROTEAN® vertical electrophoresis cell (BioRad, UK). Running buffer (1x, see *2.8.4.*) was added to the upper and lower chamber before connecting the electrodes to a

power supply. Samples and a pre-stained ladder (abcam, UK) were size fractioned through the stacking gel at 80 V (20-30 minutes), before being "run" through the separating gel at 180 V (up to 1.5 hours). Once the protein samples had been sufficiently separated (indicated by the pre-stained protein ladder), gels were removed from the electrophoresis cell. Proteins were transferred onto a polyvinylidene difluoride (PVDF) membrane using a Mini Trans-Blot® cell. Transfer stacks (cathode to anode) were formed in gel holder cassettes in the order: foam pad, filter paper, gel, PVDF membrane, filter paper, and foam pad. Before adding to the stack, foam pads, filter paper, and gels were soaked briefly in transfer buffer (see *2.8.4.*) and PVDF membranes were soaked briefly in pure methanol. Stacks were transferred to an electrode assembly and were then placed in the buffer tank. The upper and lower chambers of the buffer tank were filled with transfer buffer and an ice block was added to the lower chamber. The assembly was then connected to a power supply and run at 100 V for 1 hour at 4°C.

2.8.6. Western Blot blocking, antibody staining, and imaging

PVDF membranes with transferred proteins (see *2.8.5.*) were transferred to a sterile container and were blocked using blocking buffer (see *2.8.4.*) for 1 hour at room temperature. Primary antibodies (see *Table 2.6*) were added directly into the blocking buffer and were incubated at 4°C overnight. After primary antibody incubation, membranes were washed four times in PBS+Tween (see *2.8.4.*). Each membrane was then covered in blocking buffer containing secondary antibody (Goat Anti-Rabbit IgG H&L (HRP), ab205718, abcam) and was then incubated for 1 hour at room temperature. After secondary antibody incubation, membranes were washed four times in PBS+Tween before imaging. Imaging was performed on the GeneGnome XRQ chemiluminescence imager (Syngene, UK). Protein signals were enhanced using SuperSignal™ West Femto Maximum Sensitivity Substrate (ThermoFisher Scientific, UK).

Table 2.6: Primary antibodies used for Western Blotting.

Protein Target	Antibody	Dilution	Supplier	Product code
NF-κB p65	Recombinant Anti-NF-kB p65	1 in 10,000	abcam	ab32536

	antibody [E379]			
Phosphorylated NF-κB p65	Recombinant Anti-NF-kB p65 (phospho S536) antibody [EP2294Y]	1 in 1000	abcam	ab76302
IκBα	Recombinant Anti-IKB alpha antibody [EP697]	1 in 1000	abcam	ab76429
Phosphorylated IκBα	Phospho-IκBα (Ser32) (14D4) Rabbit mAb	1 in 1000	Cell Signalling Technology	2859S
MLCK	Recombinant Anti-Myosin light chain kinase/MLCK antibody [EP1458Y]	1 in 1000	abcam	ab76092
Phosphorylated MLC	Phospho-Myosin Light Chain 2 (Ser19) Antibody	1 in 1000	Cell Signalling Technology	3671S
GAPDH	Recombinant Anti-GAPDH antibody [EPR6256]	1 in 10,000	abcam	ab128915

2.9. MTT cell viability assay

Cell viability was assessed by 3-(4,5-dimethylthiazol-2-yl)-2,5-diphenyltetrazolium bromide (MTT) assay (abcam, UK) using Caco-2 cells seeded on 96-well flat bottom plates at 20,000 cells/well and grown for 21 days. After 21 days, ω-3 PUFA and cytokine treatments were performed. MTT powder was diluted in warmed PBS (37°C) to make a stock dilution at a concentration of 5 mg/ml. Stock MTT solution was then diluted 1:10 in warmed growth medium. Cell culture medium was removed and replaced with 100 µl diluted MTT solution and incubated (37°C) for 4 hours. After incubation, 75 µl of MTT solution was removed and replaced with 75 µl DMSO. Cells were then lysed by mixing. Plates were then wrapped in aluminium foil and placed on an orbital shaker for 10 minutes at 800 rpm. Plates were the incubated (37°C) for 10 minutes. Plates were then transferred to a Glomax® Microplate reader and absorbance readings were taken for each well at 550 nm (Promega, UK).

2.10. Statistical Analysis

Statistical analyses were performed on GraphPad Prism 9. Normality was determined using a Shapiro-Wilk normality test. Parametric, one-way ANOVA with Dunnett's multiple comparison tests, and non-parametric, Kruskal-Wallis test with Dunn's multiple comparisons tests, were used where appropriate. P values of <0.05 were considered to be statistically significant.

Chapter 3 - Caco-2 Cell Culture and Optimisation

3.1. Introduction

The intestinal epithelium along with the host microbiota and immune cells form the gut barrier, which acts as a moderator of intestinal permeability and immunity [173]. Under normal conditions, the gut barrier functions to prevent the uptake of commensal and pathogenic bacteria, luminal antigens, and undesirable solutes [174]. A combination of genetic and environmental factors underpins chronic intestinal inflammation and gut barrier dysfunction, which can lead to the development of chronic inflammatory conditions, including inflammatory bowel diseases (IBDs) and coeliac disease. Monocytic production of cytokines, including IL-1β and TNF-α, is believed to have a dual role in regulating intestinal homeostasis and inflammation [175]. During inflammation, inflammatory cytokines disrupt epithelial barrier function, through destabilisation of tight junctions between enterocytes [176]. Tight junction dysfunction and subsequent increased gut barrier permeability can be assessed *in vivo* through intestinal permeability assays, e.g. lactulose/mannitol excretion, and the increased presence of circulating and faecal biomarkers, such as zonula occludens, intestinal fatty acid binding protein, and secretory immunoglobulin A [177]. Furthermore, epithelial homeostatic mechanisms, including regulated chemokine/cytokine production and TLR signalling, normally maintained by crosstalk between the microbiota, epithelial cell layer, and immune cells are disrupted during intestinal inflammation [178]. Inflammation induces increased epithelial cell cytokine and chemokine production, which is responsible for the recruitment of monocytes [179].

Human epithelial cell models are important tools in modelling the *in vivo* gut barrier, as changes to epithelium integrity, uptake and transport of nutrients, and epithelial cell metabolism can all be assessed *in vitro*. The human adenocarcinoma cell line, Caco-2, spontaneously differentiates into heterogeneous monolayers of small intestinal-like enterocytes. Caco-2 cells form brush borders and tight junctions, and have similar gene, transporter, and receptor profiles to those of human epithelial cells [112] and are therefore a suitable model of *in vivo* gut epithelial cells, although these colorectal cells do have some differences in gene expression, including p53, APC, and β-catenin [180]. Cytokines involved in the pathogenesis of IBD, TNF-α, IFN-γ, and IL-1β, can all induce increased permeability in

Caco-2 monolayers [120] and consequently, this makes Caco-2 cells appropriate for modelling intestinal epithelial dysfunction during IBD-like inflammation and an important tool in assessing therapies in the prevention and alleviation of intestinal inflammation. Monitoring changes to the inflammatory state of Caco-2 cells, under cytokine-induced inflammation, can give further insight into inflammatory mechanisms and potential therapies to alleviate inflammation.

The aim of the research described in this chapter was to produce a replicable model of *in vitro* cytokine-induced inflammation using Caco-2 cells, which could later be used to assess proposed protective and anti-inflammatory effects of ω-3 PUFAs. Inflammation was assessed by changes to barrier function, through permeability measurements, and epithelial cell output, through the production of inflammatory cytokines. Subsequent chapters will delve further into the inflammatory mechanisms underpinning cytokine-induced inflammation and any regulatory effects of ω-3 PUFAs on these mechanisms.

3.2. Hypotheses and aims

3.2.1. Hypotheses

- Caco-2 cells can be consistently grown to form monolayers that show characteristics of an *in vivo* intestinal epithelium.
- IBD-associated cytokines will alter monolayer permeability and inflammatory mediator production in Caco-2 cells.

3.2.2. Aims

- To consistently grow Caco-2 monolayers.
- To observe tight junction proteins by confocal microscopy in Caco-2 cells.
- To observe changes in permeability and inflammatory mediator production induced by pro-inflammatory cytokines in Caco-2 cells.

3.3. Experimental Procedure

3.3.1. Caco-2 cell permeability

Caco-2 cells seeded on 12-well transwell plates (*Chapter 2.1.2*) were grown for a total of 21 days. TEER measurements (*Chapter 2.4.*) were taken every 2-3 days over the 21 days to establish the formation of differentiated monolayers.

3.3.2. Confocal imaging of tight junction proteins

Caco-2 cells were seeded onto 12-well cell culture plates and grown for 21 days at which point cells were fixed and stained for tight junction proteins, ZO-1 and occludin. Tight junction proteins were observed by confocal microscopy at appropriate wavelengths (*Chapter 2.6.*).

3.3.3. Cytokine-induced barrier dysfunction in Caco-2 cell monolayers

Caco-2 cells were grown for 21 days on transwell inserts (*Chapter 2.1.2*). After 21 days, pro-inflammatory cytokines TNF-α (5 ng/ml), IFN-γ (50 ng/ml) and IL-1β (5 ng/ml) were added to culture medium on the basolateral side for 4, 8, 12, 24 or 48 hours (*Chapter 2.2.*). Controls had basolateral medium replaced with growth medium containing no stimulant. TEER measurements (*Chapter 2.4.1.*) were taken prior to and after stimulation, at which point supernatants and cells were collected. FITC-dextran flux was assessed after cytokine stimulation (*Chapter 2.4.2.*).

3.3.4. Cytokine-induced inflammatory mediator production in Caco-2 cells

Inflammatory mediator production in stimulated and non-stimulated Caco-2 monolayers was assessed by Luminex assay (*Chapter 2.5.*). Apical and basolateral supernatants from cytokine-stimulated and control cells (*Chapter 3.3.3.*) were assessed for the presence of 9 mediators: interleukin (IL)-6, IL-10, IL-18, vascular endothelial growth factor (VEGF), interferon gamma-induced protein (IP)-10, monokine induced by gamma interferon (CXCL9), intercellular adhesion molecule (ICAM)-1, E-selectin, and vascular cell adhesion molecule (VCAM)-1.

3.3.5. Statistical analysis

Shapiro-Wilk normality tests were performed to assess Gaussian distribution of results. Statistical differences were identified using one-way ANOVA, if Gaussian distribution was determined, whereas Kruskal-Wallis test were used if significant skewness from normal distribution was detected. Normality tests are displayed in *Appendix*.

3.4. Chapter results

3.4.1 Caco-2 cells spontaneously form polarised monolayers

Caco-2 monolayer formation was assessed by TEER measurements taken over 21 days (*Chapter 3.3.1.*). As seen in *Figure 3.1*, initial TEER readings (day 3) were 427±142 Ω, and increased until day 5, where TEER reached 1286±252 Ω. Between days 5 and 10, TEER values slowly decreased with values dropping to 897±411 Ω at day 10. After day 10, TEER steadily increased until day 17 where it reached 2490±593 Ω. From day 17 to 21, TEER values remained relatively stable through to day 21 (day 19: 2621±474 Ω; day 21: 2556±409 Ω). Variability of measurements seemed to alter across the different time points with the highest variability seen on days 10 and 12 (coefficient of variation (CV) = 45.83% and 42.54%, respectively). Variability was lowest on days 19 and 21 (CV = 18.08% and 15.98%, respectively). All other measurements were moderately variable with CV values ranging from approximately 20-35%.

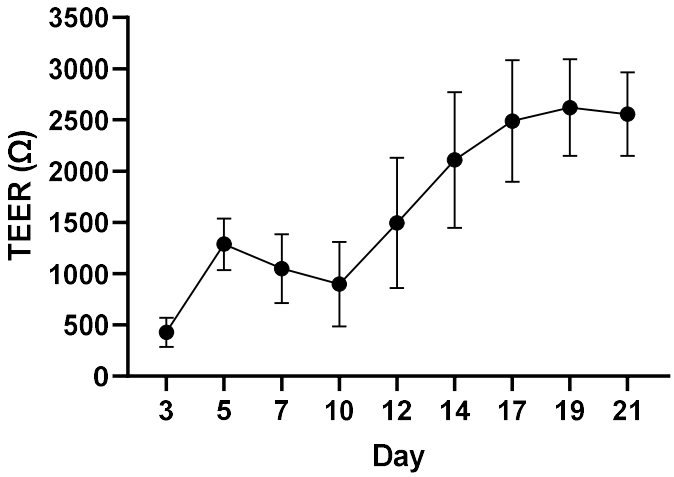

Figure 3.1: TEER measurements taken for 21 days (until differentiation) on 12-well transwell plates containing Caco-2 cell monolayers (grown in identical conditions) to assess subculture growth pattern and monolayer permeability variability. TEER measurements show a distinctive pattern across the time course: rapid increase in TEER between days 3 and 5, a slow and steady decrease between days 5-10, a near-linear increase between days 10-17, and a plateau in values between days 19-21. Data are displayed as mean±standard deviation. Data are from 2-3 technical replicates from 2-3 biological replicates from 30 independent experiments.

3.4.2. Caco-2 cells express localised tight junction proteins

Several images were taken from two distinct Z-locations of the cell monolayers to observe the distribution of ZO-1 and occludin (*Chapter 3.3.2.*). Both ZO-1 and occludin were observable at the selected loci: midway through the cell layer (*Figure 3.2.*) and closer to the apical surface (*Figure 3.3*). At the first locus (*Figure 3.2*), ZO-1 was expressed throughout and on the fringe of the cells adjacent to, but not spanning, the extracellular space. In contrast, occludin was localised at the apical surface of Caco-2 cells and spanning transcellular space between adjacent cells. This is especially clear in *Figure 3.3*, where occludin can be seen branching between adjacent cells. ZO-1 staining has also become dimmer at this higher position, indicating that it is localised lower in the cell than the transcellular occludin.

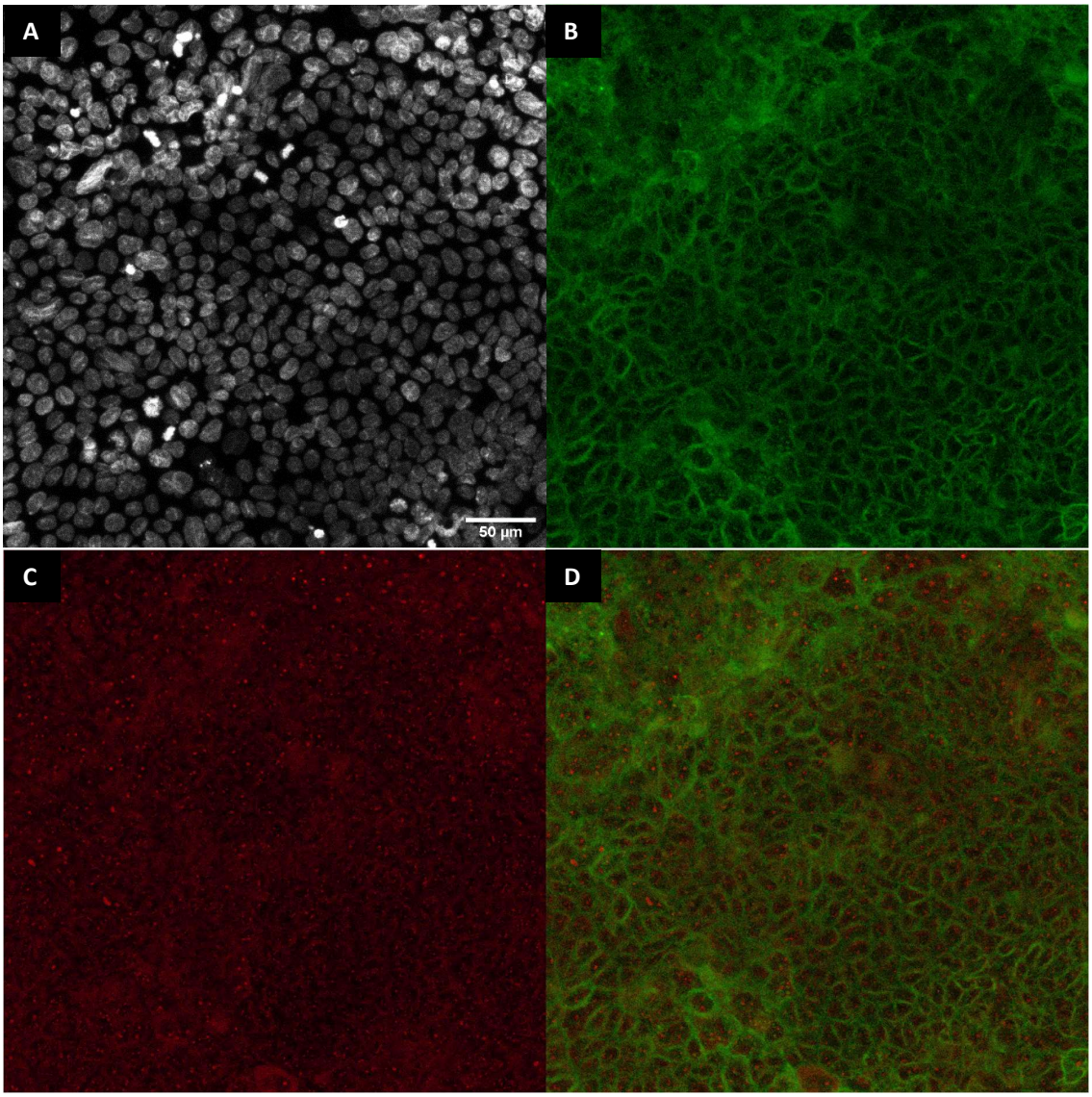

Figure 3.2: Confocal images (x40) of Caco-2 cells fluorescently labelled for tight junction proteins. Cell nuclei were stained using DAPI (A), transcellular spanning occludin with Alexa Fluor® 647 (B), and

anchoring protein ZO-1 with FITC (C). An overlay of ZO-1 and occludin staining is also shown (D). Images were taken from a single Z-location (24.4/48.8 μm). Images were taken from a single experiment.

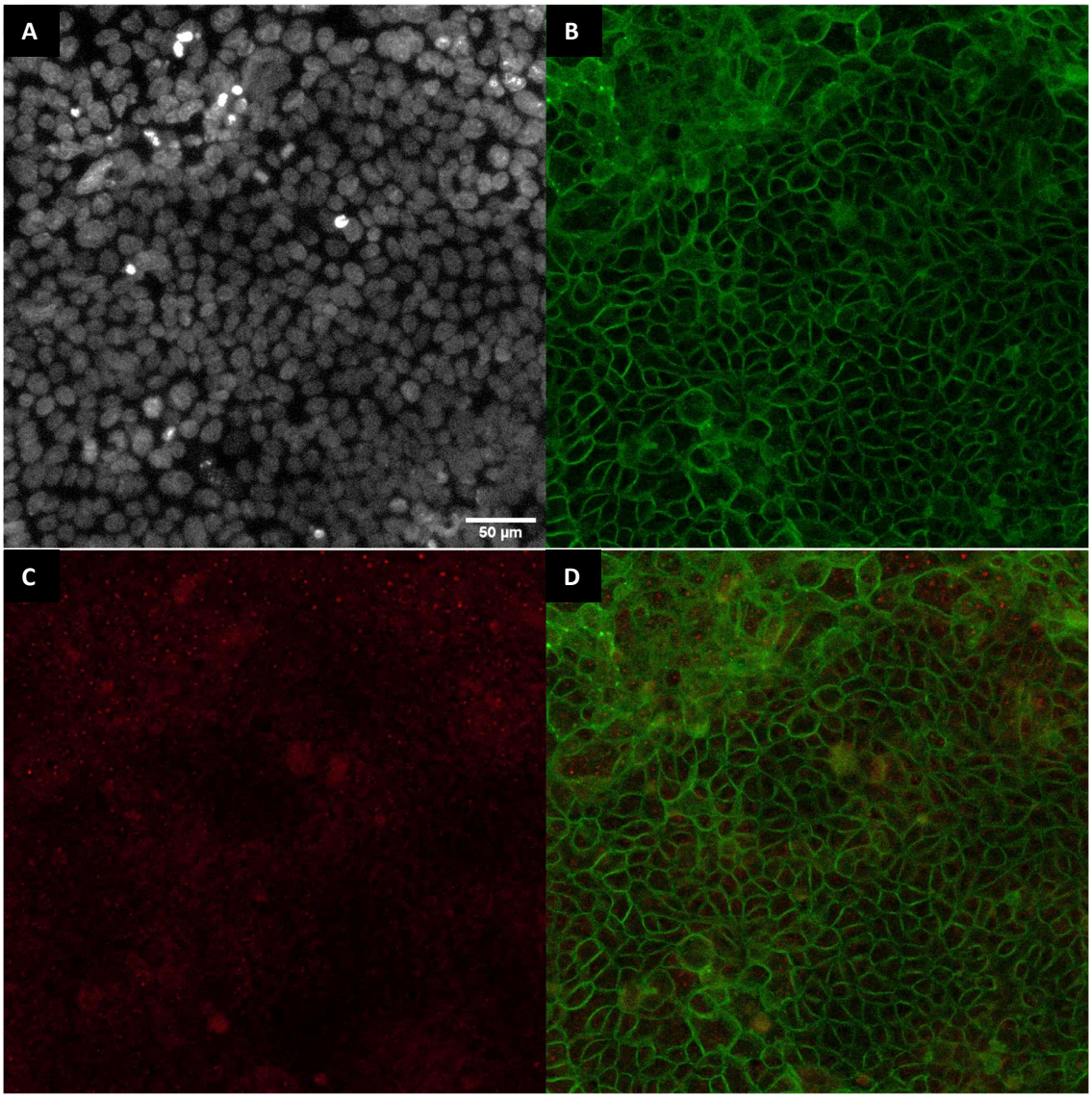

Figure 3.3: Confocal images (x40) of Caco-2 cells fluorescently labelled for tight junction proteins. Cell nuclei were stained using DAPI (A), transcellular spanning occludin with Alexa Fluor® 647 (B), and anchoring protein ZO-1 with FITC (C). An overlay of ZO-1 and occludin staining is also shown (D). Images were taken from a single Z-location (30.6/48.8 μm). Images were taken from a single experiment.

3.4.3. Pro-inflammatory cytokines increase Caco-2 cell monolayer permeability

Pro-inflammatory cytokines TNF-α, IFN-γ, and IL-1β were used to stimulate Caco-2 monolayers to induce barrier dysfunction (*Chapter 3.3.3.*). In *Figure 3.4*, it is shown that TEER values were decreased in comparison to non-stimulated controls, indicating an increase in monolayer permeability, at each time point (4-48 hours). Control TEER remained at similar values before and after the stimulation period (100.9±15.1%). 4, 8 and 12 hour readings showed similar decreases, approximately 10%, from initial readings after stimulation (91.1±4.1%, 91.4±3.6%, and 91.6±16.0%, respectively) and these were not significantly different from controls. 24 hour stimulation showed a more pronounced reduction in TEER (84.6±5.5%), and this was significant (p=0.0081) compared to controls. Evidently, 48 hours stimulation was markedly effective at decreasing TEER (43.0±24.8%) significantly compared to controls (p=0.0011).

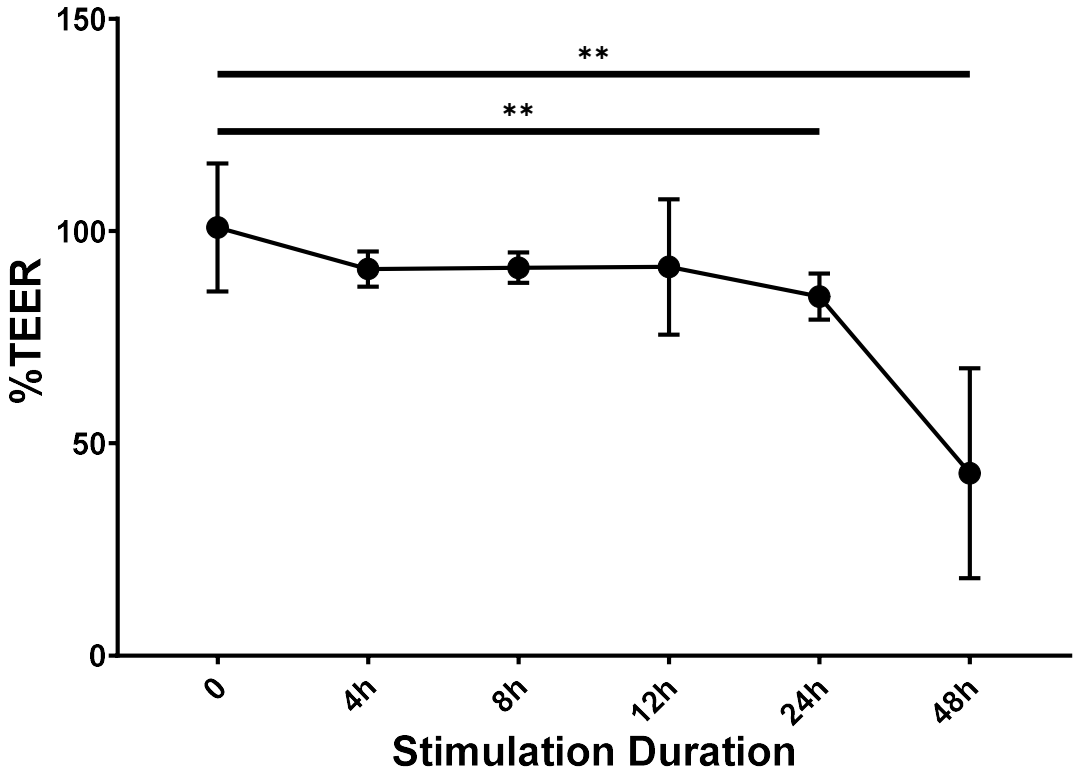

*Figure 3.4: Changes in TEER after combined TNF-α, IFN-γ, and IL-1β stimulation. Stimulation was performed using TNF-α (5ng/ml), IFN-γ (50ng/ml), and IL-1β (5ng/ml) applied to the basolateral side of monolayers. Controls were not stimulated). Cells were grown for 21 days (pre-PUFA) before measurements. TEER values are presented as %TEER, where: %TEER = (Final Reading/Initial Reading)*100. All data points are displayed as mean±standard deviation. Statistical significance was determined by non-parametric Kruskal-Wallis tests with Dunn's multiple comparisons tests, where ** p<0.01. Data are from 2 biological replicates from 3 independent experiments.*

Flux of FITC-dextran (FD4) across Caco-2 cell monolayers was used to assess changes to macromolecular permeability induced by pro-inflammatory cytokine stimulation (*Chapter 3.3.3.*). As shown in *Figure 3.5*, mean FD4 flux was higher in the stimulated group. However, some replicates within the cytokine-stimulated groups showed increased paracellular flux of FD4 with some replicates reaching 92 ng/ml/min. 8 replicates in the cytokine-stimulated group had FD4 flux greater than 20 ng/ml/min, whereas all replicates in the control exhibited flux below 10 ng/ml/min.

Correlation between changes to macromolecular permeability and ionic permeability was assessed by comparing FD4 flux with the corresponding change to TEER measurements (*Figure 3.6*). In the control group, changes to TEER were relatively consistent with no change above 10% reported (either up or down). This was consistent with the small changes in FD4 flux reported. Similar to the control measurements, TEER values were consistent within the stimulated group as all but one replicate were decreased by 20-40%. Despite consistent TEER readings, these readings were not proportional to the corresponding FD4 flux seen in these replicates suggesting changes to ionic permeability were not correlated with changes in macromolecular permeability.

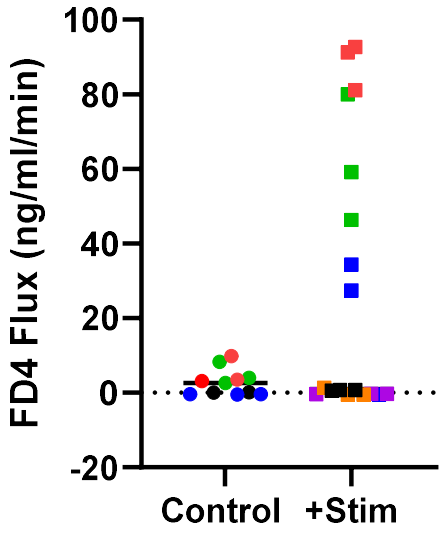

Figure 3.5: FITC-dextran (FD4) flux across Caco-2 monolayers with or without 24 hours combined TNF-α, IFN-γ, and IL-1β stimulation (5 ng/ml, 50 ng/ml, and 5 ng/ml, respectively). Controls were

unstimulated. FD4 in 0.5 ml HBSS was added to the apical compartment of the transwell plate after stimulation. After 1 hour, aliquots were taken from the basolateral compartment to determine FD4 flux. FD4 in aliquots was quantified by fluorescence readings on a microplate reader (Ex: 475 nm, Em: 500-550 nm). Control data were from 2-3 biological replicates from 4 independent experiments. +Stim data were from 3 biological replicates from 6 independent experiments. Each data point is a mean value of 3 technical replicates and separate colours indicate each separate independent experiment.

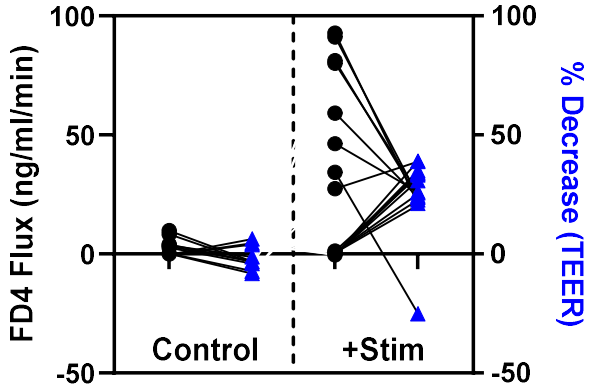

*Figure 3.6: FD4 flux across Caco-2 monolayers and corresponding changes to TEER with or without 24 hours combined TNF-α, IFN-γ, and IL-1β stimulation (5 ng/ml, 50 ng/ml, and 5 ng/ml, respectively). Controls were unstimulated. FD4 in 0.5 ml HBSS was added to the apical compartment of the transwell plate after stimulation. After 1 hour, aliquots were taken from the basolateral compartment to determine FD4 flux. FD4 in aliquots was quantified by fluorescence readings on a microplate reader (Ex: 475 nm, Em: 500-550 nm). TEER measurements were taken prior to and after stimulation. Changes in TEER are presented as %Decrease, where %Decrease = ((Initial reading – Post-stimulation reading)/Initial reading)*100. Control data were from 2-3 biological replicates from 4 independent experiments. +Stim data were from 3 biological replicates from 6 independent experiments. Each data point is a mean value of 3 technical replicates.*

3.4.4. Pro-inflammatory cytokines induce variable expression of inflammatory mediators in Caco-2 cell monolayers

Of the 9 inflammatory markers assessed (*Chapter 3.3.4.*), 6 were detectable within the range of the assays used. E-selectin and VCAM-1 were below the detection limit at each stimulation time point (4-48 hours) and in control monolayers and therefore it was not possible to determine any changes in these mediators. IP-10 was above the detection limit of the assay in stimulated monolayers and could be reassessed at a later date with diluted sample supernatants. Observations on the mediators within range are reported in this chapter.

ICAM-1 was released differentially in the apical and basolateral compartments for both control and stimulated monolayers, with higher release on the apical side from 8 to 24 hours stimulation by 2.0 to 8.7-fold (*Figure 3.7*). After 4 and 48 hours stimulation, ICAM-1 concentrations were similar in both compartments. Basolateral ICAM-1 release was significantly increased after 48-hour stimulation (p=0.0227) and apical release was significantly increased after 24- and 48-hour stimulation (p=0.0018 and <0.0001, respectively), when compared to control monolayers.

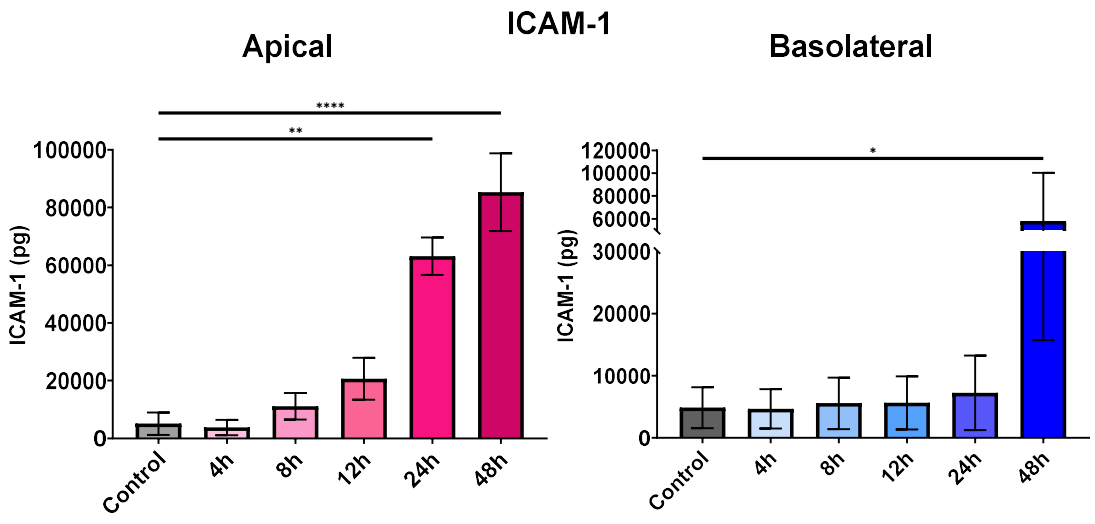

*Figure 3.7: ICAM-1 production by control and cytokine-stimulated Caco-2 monolayers. A mixture of TNF-α (5 ng/ml), IFN-γ (50 ng/ml), and IL-1β (5 ng/ml) was used as the stimulant and controls were not stimulated. Significant increase in ICAM-1 release was seen after 48 hours stimulation in the basolateral compartment and after 24- and 48-hours stimulation in the apical compartment, when compared to controls. Control cells showed some production of ICAM-1 in the absence of stimulation. Data are displayed as mean±standard deviation. Asterisks indicate significance compared to controls, where: * p<0.05, ** p<0.01, and **** p<0.0001. Control data were from 3-4 biological replicates from 3 independent experiments. Cytokine stimulated data were from 2 biological replicates from 3 independent experiments.*

Figure 3.8 shows that CXCL9 was released differentially in the apical and basolateral compartments in non-stimulated conditions (3.0-fold higher in the basolateral compartment). Basolateral CXCL9 levels were significantly different compared to controls after 24- and 48-hours stimulation (p=0.0007 and p<0.0001, respectively). Apical release was significantly increased at 12 (p=0.0497), 24 (p=0.0007), and 48 hours (p<0.0001) post-stimulation compared to controls. After 4- and 8-hours stimulation, basolateral CXCL9 concentrations exceeded apical concentrations by 3.8- and 4.4-fold, respectively. After 12- and 24-hours, differences in apical and

basolateral CXCL9 release were diminished (1.6 and 0.8 fold, respectively). After 48-hours stimulation, basolateral concentrations of CXCL9 greatly exceeded apical concentrations by 15.4-fold.

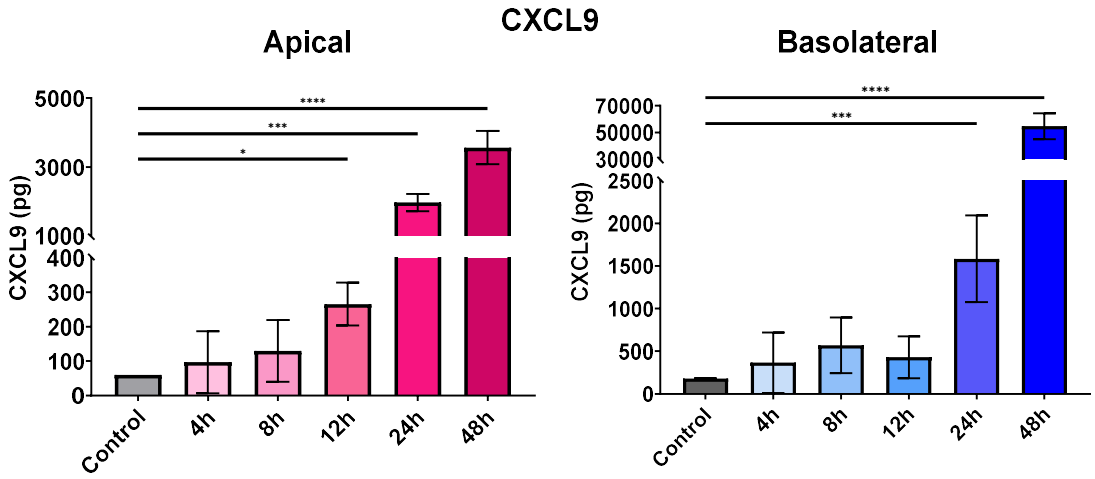

*Figure 3.8: CXCL9 production by control and cytokine-stimulated Caco-2 monolayers. A mixture of TNF-α (5 ng/ml), IFN-γ (50 ng/ml), and IL-1β (5 ng/ml) was used as the stimulant and controls were not stimulated. Significant increase in CXCL9 release was seen after 24- and 48-hours stimulation in the both the apical and basolateral compartment, when compared to controls. Additionally, apical production of CXCL9 was significantly increased after 12 hours stimulation. Control cells showed little production in the absence of stimulation. Data are displayed as mean±standard deviation. Asterisks indicate significance compared to controls, where: * p<0.05, *** p<0.001, and **** p<0.0001. Control data were from 3-4 biological replicates from 3 independent experiments. Cytokine stimulated data were from 2 biological replicates from 3 independent experiments.*

CXCL8 production (*Figure 3.9*) was significantly increased compared to controls in both the apical and basolateral compartments at 8 hours (p=0.0262 and p=0.0212, respectively), 12 hours (p=0.0004 and p=0.0012, respectively), and 24 hours (p<0.0001 for both) post-stimulation. 48 hours stimulation significantly increased CXCL8 release in the basolateral compartment (p=0.0003) with apical expression of CXCL8 appearing to diminish at 48 hours stimulation. CXCL8 release was comparably higher in the basolateral compartment than in the apical compartment from 4- to 24-hours stimulation (10.0- to 14.4-fold difference). After 48 hours stimulation, basolateral CXCL9 concentrations considerably exceeded apical concentrations (67.9-fold). Controls showed slightly larger amounts of CXCL8 (2.6-fold) in the apical compartment compared to the basolateral compartment, although control monolayer release was low in both compartments.

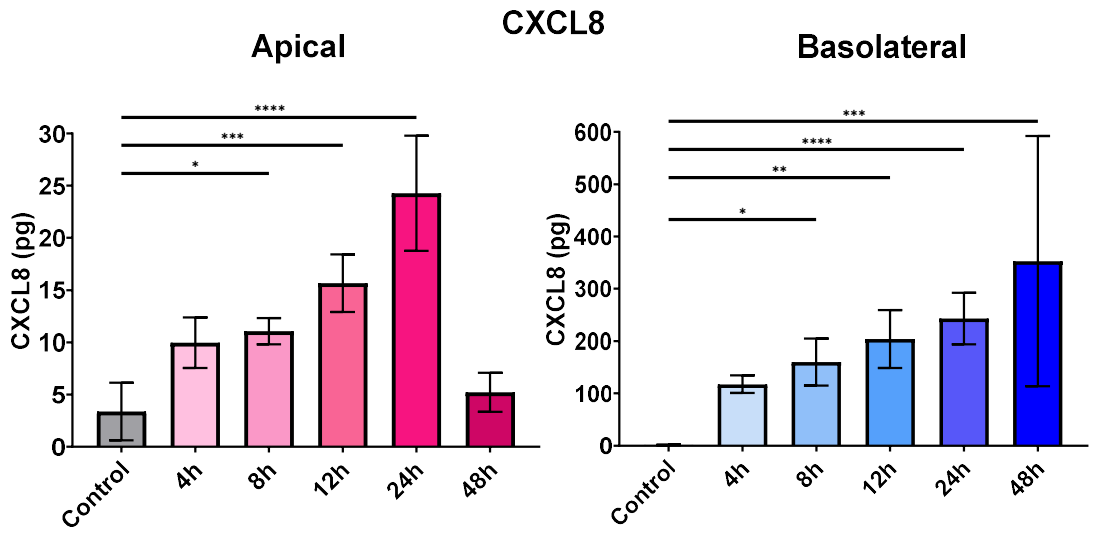

*Figure 3.9: CXCL8 production by control and cytokine-stimulated Caco-2 monolayers. A mixture of TNF-α (5 ng/ml), IFN-γ (50 ng/ml), and IL-1β (5 ng/ml) was used as the stimulant and controls were not stimulated. Significant increase in CXCL8 release was seen after 8-, 12-, and 24-hours stimulation in the both the apical and basolateral compartments, when compared to controls. Basolateral production of CXCL8 was also significantly increased after 48 hours stimulation. Control cells showed very little production in the absence of stimulation. Data are displayed as mean±standard deviation. Asterisks indicate significance compared to controls, where: * p<0.05, ** p<0.01, *** p<0.001, and **** p<0.0001. Control data were from 3-4 biological replicates from 3 independent experiments. Cytokine stimulated data were from 2 biological replicates from 3 independent experiments.*

In *Figure 3.10*, it is apparent that VEGF was released by non-stimulated controls in both the apical and basolateral compartments. VEGF concentrations were comparable in basolateral and apical supernatants in cells stimulated for 4 to 24 hours (0.6 to 1.6 fold differences). Basolateral VEGF concentrations were 5.5 fold higher in basolateral supernatants after 48 hours stimulation. VEGF release was significantly increased by cytokine-stimulation, compared to control levels, in the apical compartment after 24 hours ($p=0.0058$), as well as after 24 hours and 48 hours stimulation in the basolateral compartment ($p=0.002$ and $p<0.0001$, respectively).

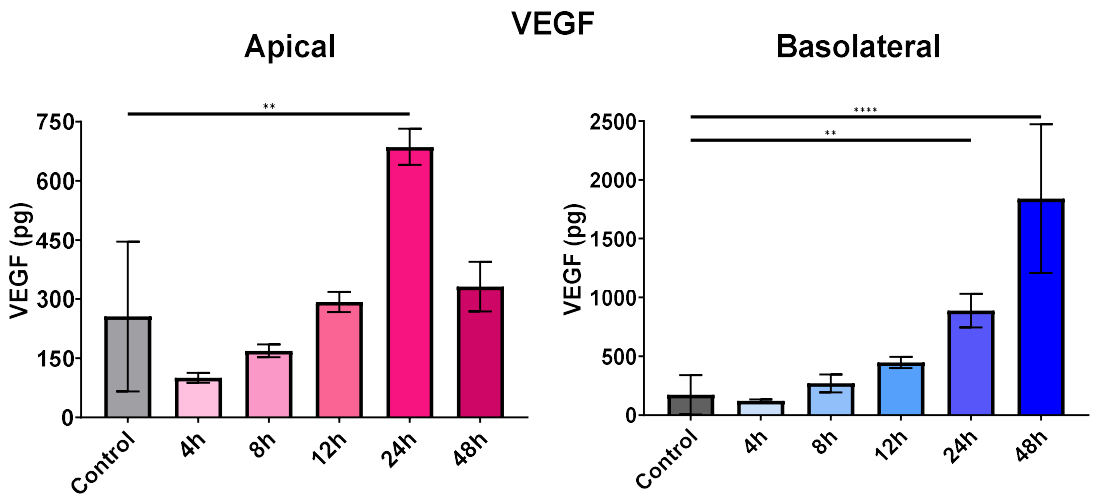

*Figure 3.10: VEGF production by control and cytokine-stimulated Caco-2 monolayers. A mixture of TNF-α (5 ng/ml), IFN-γ (50 ng/ml), and IL-1ß (5 ng/ml) was used as the stimulant and controls were not stimulated. Significant increase in VEGF release was seen after 24 hours stimulation in the both the apical and basolateral compartments, when compared to controls. Basolateral production of VEGF was also significantly increased after 48 hours stimulation. Control cells showed some production in the absence of stimulation, especially in the apical compartment, where VEGF release was more pronounced than after 4-, 8- and 12-hours stimulation. Data are displayed as mean±standard deviation. Asterisks indicate significance compared to controls, where: ** p<0.01 and **** p<0.0001. Control data were from 3-4 biological replicates from 3 independent experiments. Cytokine stimulated data were from 2 biological replicates from 3 independent experiments.*

IL-6 release was relatively low compared to other markers across controls and stimulations, particularly in the apical compartment where IL-6 levels were approximately 0.5-2.3 pg. Basolateral concentrations were slightly higher ranging between 1.6-26.4 pg (*Figure 3.11*). Stimulation did induce significant increases in the apical compartment at 24 hours and 48 hours (p=0.0042 and p=0.0055, respectively) and in the basolateral compartment at 4 hours and 24 hours (p=0.0011 and p<0.0001, respectively).

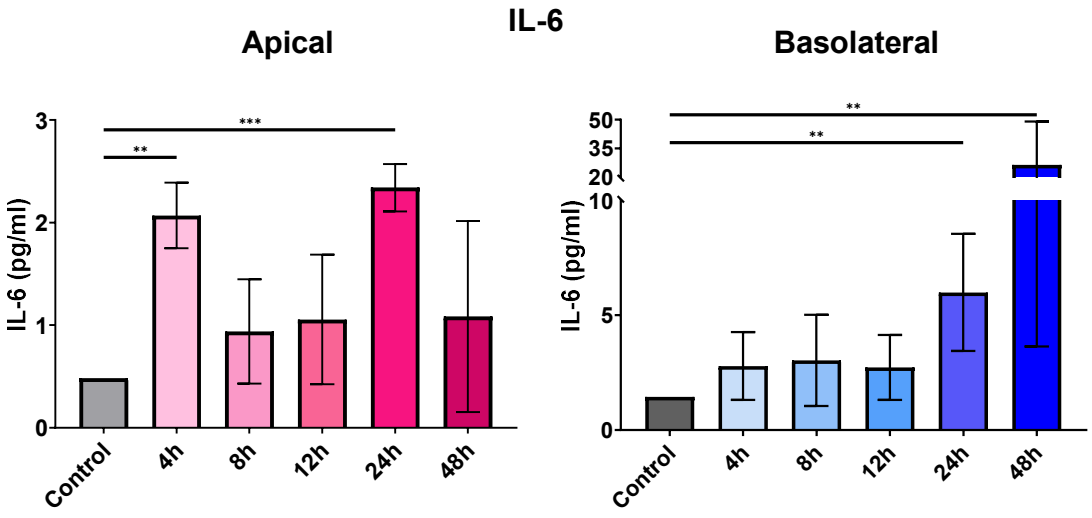

*Figure 3.11: IL-6 production by control and cytokine-stimulated Caco-2 monolayers. A mixture of TNF-α (5 ng/ml), IFN-γ (50 ng/ml), and IL-1ß (5 ng/ml) was used as the stimulant and controls were not stimulated. Significant increase in CXCL8 release was seen after 24- and 48-hours stimulation in the basolateral compartments, when compared to controls. Apical production of CXCL8 was also significantly increased after 4- and 24-hours stimulation, although this was at relatively low amounts (<3pg/ml). Control cells showed very little production in the absence of stimulation. Data are displayed as mean±standard deviation. Asterisks indicate significance compared to controls, where: ** p<0.01 and **** p<0.0001. Control data were from 3-4 biological replicates from 3 independent experiments. Cytokine stimulated data were from 2 biological replicates from 3 independent experiments.*

As shown in *Figure 3.12*, IL-18 release was consistently higher in the basolateral compartment compared to the apical compartment (3.2 to 4.7 fold). After 12-, 24-, and 48-hours stimulation, IL-18 release was significantly increased in both the apical ($p=0.0001$, $p<0.0001$, and $p=0.0006$, respectively) and basolateral compartments ($p=0.0007$, $p<0.0001$, and $p=0.0005$, respectively). IL-18 release was also significantly increased after 8 hours stimulation in the basolateral compartment ($p=0.0085$).

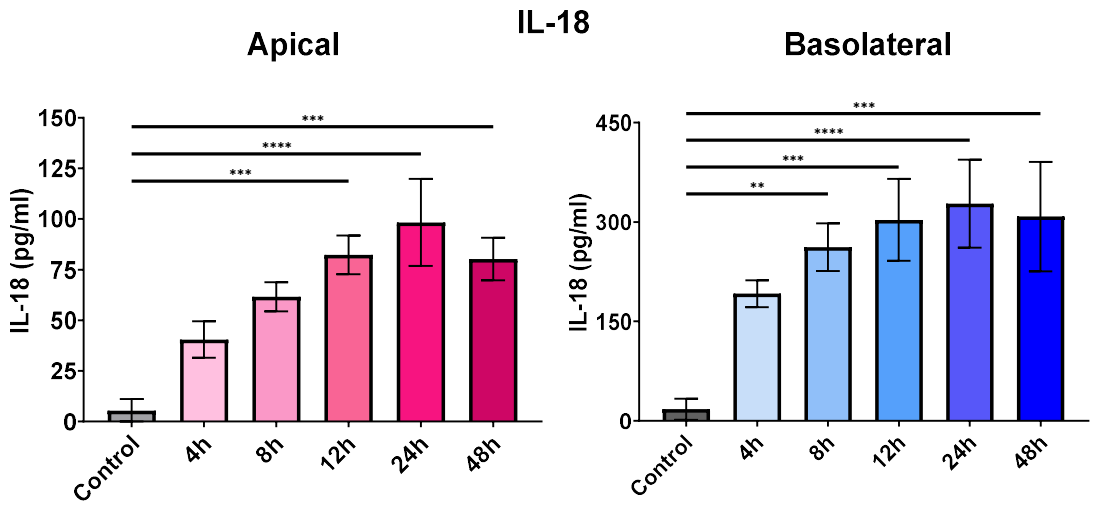

*Figure 3.12: IL-18 production by control and cytokine-stimulated Caco-2 monolayers. A mixture of TNF-α (5 ng/ml), IFN-γ (50 ng/ml), and IL-1ß (5 ng/ml) was used as the stimulant and controls were not stimulated. Significant increase in IL-18 release was seen after 12-, 24-, and 48-hours stimulation in the both the apical and basolateral compartments, when compared to controls. Additionally, basolateral production of IL-18 was also significantly increased after 8 hours stimulation. Control cells showed little production in the absence of stimulation. Data are displayed as mean±standard deviation. Asterisks indicate significance compared to controls, where: ** p<0.01, *** p<0.001, and **** p<0.0001. Control data were from 3-4 biological replicates from 3 independent experiments. Cytokine stimulated data were from 2 biological replicates from 3 independent experiments.*

Overall, co-stimulation treatment of TNF-α, IFN-γ, and IL-1β, induced a complex and differential release of inflammatory markers in Caco-2 cells over a 48-hour period. Basolateral production of all detectable markers was significantly increased by 24 hours stimulation, except ICAM-1 (significant at 48 hours). Apical release of all detectable markers was significantly increased at 24 hours post-stimulation. All other stimulation time points (4, 8, 12 and 48 hours) showed variable changes to mediator production in this Caco-2 model.

3.5. Chapter discussion and future work

The aim of this chapter was to optimise Caco-2 cells as an *in vitro* cell model of enteric inflammation. Firstly, I was able to show that Caco-2 cells spontaneously form polarised monolayers after 21 days growth. TEER measurements over 21 days showed a complex and yet consistent change to permeability in Caco-2 monolayers. Similar growth patterns have been shown previously [181], with TEER values showing increasing permeability which peaks between day 17-21. Notably in this set

of experiments, after an initial increase from day 3 to day 5, TEER decreased from day 5 to day 10. The cause of this drop is unknown, although, monolayers did recover between days 10 and 21 showing a steady increase in TEER, indicative of the monolayer forming tight junctions, which have been shown previously to be fully functional by day 19 at the earliest [182]. Interactions between Caco-2 cells and basement membrane proteins can influence the development and differentiation of cell monolayers. In this model, transwells were coated with type I collagen, which has been shown to induce rapid cell spreading compared to type IV collagen and laminin [183], which could explain the rapid increase in TEER between days 3 and 5. The drop between days 5 to 10 is hard to explain, although growth patterns can be distinct between specific cell subtypes and growth conditions, including culture medium and growth period [184]. It is accepted that a 15 days culture is enough for Caco-2 cells to exhibit barrier properties [184], although 21 days is more appropriate for Caco-2 cell differentiation and reliable permeability measurements [185].

The polarity and presentation of tight junctions in monolayers was assessed by confocal microscopy. In the intestinal epithelium, occludin spans the transcellular space and ZO-1 anchors transcellular proteins (such as occludin) to the actin cytoskeleton of epithelial cells [186]. I was able to demonstrate that Caco-2 monolayers had localised expression of ZO-1 and occludin at tight junctions on the apical surface, which has been shown previously in Caco-2 cells [187]. Expression of ZO-1 can be used as an indicator of enterocyte differentiation and has been shown in Caco-2 cells previously [188]. Occludin expression can impact intestinal epithelial differentiation as occludin deficiency has been shown to alter intestinal morphology and secretory function [189]. The close proximity and integration of these proteins is important in tight junction function, which has been demonstrated elsewhere, by disrupted localisation of ZO-1 and occludin being implicated in cytokine-induced tight junction dysfunction [190].

Increased presence of pathogenic bacteria [191], increased immune activation and the subsequent increased presence of inflammatory cytokines [192], or even heat stress [193] can all induce tight junction dysfunction through the reorganisation or downregulation of tight junction proteins. Subsequently, once Caco-2 monolayers could be reliably replicated, my next aim was to induce Caco-2 monolayer dysfunction using a mix of inflammatory cytokines (TNF-α, IFN-γ, and IL-1β). TNF-α, IFN-γ, and IL-1β, which are implicated in the pathogenesis of IBD, should loosely

replicate IBD-like gut barrier dysfunction and inflammatory mediator release. Using cell models it has been determined that TNF-α induces tight junction dysfunction through increases in MLCK and claudin-2 expression, IL-1β similarly upregulates MLCK expression and also redistributes occludin, and IFN-γ also redistributes cytoskeletal and tight junction proteins inducing increased epithelial permeability [186]. In accordance with these findings, I was able induce an increase in ionic monolayer permeability, indicated by a decrease in TEER, after 24- and 48-hours cytokine-stimulation (*Figure 3.4*). However, macromolecular permeability was not consistently affected by cytokine stimulation (*Figure 3.5* and *3.6*). Macromolecular permeability can be affected by cell type and concentrations of different tight junction proteins [194]. Occludin expression is associated with macromolecular permeability in Caco-2 cells, as occludin suppression by small-interfering RNA transfection induced increases in macromolecular permeability without affecting TEER [195]. Occludin was highly expressed in this cell model (*Figure 3.2* and *3.3*), which could contribute to the lack of cytokine-induced effect on macromolecular permeability shown in *Figure 3.5* and *3.6*.

Inflammatory mediator production was assessed in cytokine-stimulated Caco-2 monolayers. Epithelial cell cytokine production enacts an important role in intestinal mucosa homeostasis by signalling for cell injury and cell death, leading to the recruitment of immune cells [196]. Cytokine stimulation of Caco-2 monolayers induced an increase in release of several inflammatory mediators including ICAM-1, CXCL9, VEGF, CXCL8, IL-6, and IL-18, which have different roles in the inflammatory response of intestinal epithelial cells.

Firstly, intracellular adhesion molecule, ICAM-1, is important in leukocyte signalling during inflammation, with increased release indicative of inflammation. Both TNF-α and IL-1β are known to induce the increased release of ICAM-1 *in vivo* [197], which I was able to replicate in this model as significant ICAM-1 release was seen after 24 hours in the apical compartment and after 48 hours in both the apical and basolateral compartments. Additionally, VEGF release, which induces the expression of ICAM-1 and subsequent chemotaxis of monocytes and neutrophils, was also upregulated in this model of intestinal inflammation. The presence of VEGF was significantly increased in both compartments after 24 hours and in the basolateral compartment after 48 hours. It is apparent that cytokine stimulation of Caco-2 cells induces the release of leukocyte-recruiting mediators, suggesting an inflammatory

response is induced after stimulation for substantial periods of time (24 and 48 hours).

Interferon-induced inflammation was also seen in this Caco-2 model, indicated by an increased release of CXCL9 in the basolateral (12-, 24-, and 48-hour stimulation) and apical compartments (24- and 48-hour stimulation). CXCL9, also known as monokine-induced by γ-interferon (MIG), is involved in the recruitment and activation of T-lymphocytes through interactions with chemokine receptor, CXCR3, and local CXCL9 over-expression by enterocytes drives the accumulation of inflammatory cells on the mucosal surface in IBD [198]. Both CXCL9 and IP-10, also an activator of CXCR3, have been previously shown to be expressed by cytokine-stimulated Caco-2 cells [199]. I was not able to quantify the expression of IP-10, although further dilution of cell supernatants will make this possible. The expression was exceeding the detection limit, indicating a large increase of IP-10 production in stimulated cells, altogether suggesting that IFN-γ induces large releases of CXCL9 and IP-10 in this model.

Cytokines IL-6, CXCL8, and IL-18 are excessively produced and secreted in the gut mucosa of IBD sufferers. IL-6 is essential in T-cell survival and, similar to VEGF, increasing the presence of adhesion molecule ICAM-1 during intestinal inflammation [200]. CXCL8 is a neutrophil attractant in both forms of IBD [201], whilst IL-18 upregulation in IBD induces the release of inflammatory cytokines and chemokines [202]. Cytokine stimulation induced the release of IL-6, CXCL8, and IL-18 on the apical and basolateral side of Caco-2 cells. Basolaterally, significant release of CXCL8 and IL-18 was seen after 8 hours and remained significantly increased for both markers through 12, 24 and 48 hours, whereas IL-6 was significantly released after 24 and 48 hours in the basolateral compartment. Apically, release of these cytokines was more varied with IL-6 being significantly increased after 4 and 24 hours, CXCL8 at 8, 12, and 24 hours, and IL-18 at 12, 24, and 48 hours.

Overall, Caco-2 cells are highly responsive to co-stimulation with TNF-α, IFN-γ, and IL-1β, showing increased ionic permeability through monolayers and increased production of a range of inflammatory mediators. Persistent stimulation of the cells seemed to elicit the most pronounced effect, as at 24 and 48 hours the majority of mediators had significantly increased in production and there were significant increases in monolayer permeability. Using this inflammatory model will allow

evaluation of the proposed protective, anti-inflammatory effects of the long-chain ω-3 PUFAs EPA and DHA, which will be described in later chapters. Furthermore, the effects of the less well explored long-chain ω-3 PUFA, DPA, and plant-derived ω-3 PUFAs, ALA and SDA will be investigated.

Later chapters will investigate the effect of cytokines on inflammatory mechanisms and any protective effects of ω-3 PUFAs. The increased permeability seen in this model is most likely driven by cytokine-induced upregulation of MLCK activity and remodelling of tight junctions, through the downregulation of occludin, ZO-1, claudin-1, and claudin-4, which has been shown in the Caco-2 model previously [203]. The inflammatory mediator profile of cytokine-stimulated Caco-2 cells is similar to that of *in vivo* enterocytes in IBD, which supports the suggestion that the epithelium has an active role in the pathogenesis of IBD [204]. The induction of cytokine production in epithelial cells is attributed to the activation of NF-κB, which has an array of pro-inflammatory effects, when persistently activated during inflammation [205].

Subsequent chapters will focus on the inflammatory mechanisms driven by the cytokines used in this model, and in particular, the upregulation of MLCK and NF-κB and the modulation by ω-3 PUFAs. Quantification of NF-κB and MLCK, and associated markers of NF-κB/MLCK activation, will be compared in control and cytokine-stimulated cells, as well as cells pre-treated with ω-3 PUFAs. Additionally, cytokine-induced changes to the localisation of tight junction proteins will be observed using confocal microscopy

Chapter 4 - Analysis of incorporation and bioconversion of exogenous ω-3 PUFAs in Caco-2 cells

4.1. Introduction

The omega-3 (ω-3) PUFAs, eicosapentaenoic acid (EPA) and docosahexaenoic acid (DHA), are two of the main bioactive compounds derived from fatty fish and from fish oil supplements. EPA and DHA supplementation has reported benefits in a range of conditions, including obesity, arthritis, and cardiovascular disease [206]. EPA and DHA may also have benefits in intestinal inflammatory diseases, including IBDs, with some evidence suggesting anti-inflammatory effects of ω-3 PUFAs in animal models of IBD [207]. Specifically, cellular uptake, membrane incorporation and subsequent biochemical utilisation of EPA and DHA has exhibited benefits in cardiovascular disease [208], age-related health [209], and psychological conditions [210]. Increased incorporation of EPA and DHA into cell membranes is thought to increase membrane fluidity and modify lipid raft assembly, which can subsequently alter intracellular and extracellular signalling cascades and may be responsible for at least some of the EPA and DHA-elicited anti-inflammatory effects [211]. EPA and DHA can also be utilised by cells for the productions of specialised lipid mediators, including resolvins and protectins, which also contribute to the resolution of inflammation [212]. Further exploration into the mechanistic relationship between ω-3 PUFAs and intestinal epithelial cells could elucidate a role for ω-3 PUFAs in prevention and/or treatment of intestinal inflammation.

Less is known about the effects of the EPA-DHA intermediate, docosapentaenoic acid (DPA). DPA is the second most abundant ω-3 PUFA, after DHA, in brain tissue and increased presence of DPA has shown some improvements in cardiovascular, metabolic, and neurological conditions [213]. Like EPA and DHA, DPA drives the production of anti-inflammatory pro-resolving mediators, including DPA-derived resolvins, protectins, and maresins [214]. These lipid mediators are different in structure to those produced from EPA and DHA but they seem to have similar bioactivity [215]. ω-3 PUFA-derived lipid mediator production and signalling induces an array of effects on the gut including enhanced gut barrier function, nutrient absorption, regulated intestinal immune responses, and epithelial cell homeostasis [57]. Additionally, DPA may act as a reservoir for EPA and DHA since it

can be converted to both of these [216]. Further exploration into the utilisation of DPA in epithelial cells could provide insight into a direct role for DPA in regulating intestinal inflammation.

The importance of plant-derived ω-3 PUFAs has increased in recent years coinciding with the increased uptake of vegetarian and vegan diets, which limit the consumption of oily fish-derived EPA and DHA [217]. The main source of EPA and DHA for vegetarians and vegans is through the endogenous conversion of alpha-linolenic acid (ALA), as shown in Figure 3 (Chapter 1). ALA is considered an essential ω-3 PUFA, as it cannot be synthesised in animals. Hence it must be provided in the diet from sources such as green leafy vegetables, some vegetable oils (e.g. rapeseed oil), flaxseeds, and walnuts [218]. There is some evidence that ALA has cardioprotective and anti-inflammatory properties [219]. Research into other plant-derived ω-3 PUFAs, including stearidonic acid (SDA), is currently limited [220]. Recent evidence suggest that SDA can be more efficiently converted to EPA than ALA can, as it bypasses the rate limiting Δ6-desaturase step, and may have protective effects in inflammation, cardiovascular disease, and cancer [221]. Overall, increased presence of both oily fish-derived and plant-derived ω-3 PUFAs within the diet and subsequently in tissues has exhibited protective effects in a range of inflammatory conditions. The specific effects of lesser studied ω-3 PUFAs, in particular DPA and SDA, on epithelial cell function during inflammation have not been reported, whilst only a few effects of ALA have been reported.

The aim of the experiments described in this chapter is to assess the changes to Caco-2 cell fatty acid composition when exposed to a range of ω-3 PUFAs, including oily fish-derived EPA, DHA, and DPA, and plant-derived ALA and SDA. Providing Caco-2 cells with exogenous ω-3 PUFAs may increase the cellular proportion of the supplemented ω-3 PUFA and associated ω-3 PUFAs through enzymatic conversion, which could result in anti-inflammatory effects, which will be explored in further chapters.

4.2. Aims and Hypothesis

4.2.1. Aims

- To assess the accumulation of different ω-3 PUFAs by Caco-2 cells.
- To assess the interconversion between ω-3 PUFAs in Caco-2 cells.

- To compare the relative accumulation *vs* bioconversion of each ω-3 PUFA.

4.2.2. Hypotheses

- ω-3 PUFAs will be retained within Caco-2 cells.
- Interconversion between ω-3 PUFAs will favour elongation to long-chain ω-3 PUFAs, including EPA and DHA.
- ω-3 PUFA incorporation will displace ω-6 PUFAs, including arachidonic acid (AA).

4.3. Specific Experimental Procedure

4.3.1. Fatty acid supplementation

Caco-2 cells cultured until differentiation (21 days) were incubated for 48 hours with 4 concentrations of either EPA, DHA, DPA, ALA, or SDA (1, 5, 10 or 25 μM) prepared in growth medium (*Chapter 2.3.* and *2.7.2.*). Controls were incubated in growth medium only. Final ethanol concentration was maintained at 0.1% across all samples.

4.3.2. Gas chromatography

After 48 hours incubation, cells were washed twice with HBSS and then total lipid was extracted and cellular fatty acids analysed by gas chromatography (*Chapter 2.7.3.* and *2.7.4.*). In total, 24 fatty acids were quantified compared to a standard in order to quantify them (21:0 – see *Chapter 2.7.5.*).

4.3.3. Statistical analyses

Two-way ANOVA with Sidak's multiple comparisons tests were performed using GraphPad Prism 9 to determine significant differences between control and treatment groups.

4.4. Assessment of total lipid extracts of Caco-2 cells supplemented with different ω-3 PUFAs

4.4.1. EPA supplementation increases Caco-2 cell EPA and DPA content

Total lipid extracts from Caco-2 cells incubated with or without EPA for 48 hours, were assessed by gas chromatography (*Chapter 4.3.1*).

EPA supplemented at 10 μM and 25 μM significantly increased Caco-2 cell EPA and total omega-3 content (*Figure 4.1*). At 25 μM, EPA supplementation approximately doubled DPA content and quadrupled EPA content of Caco-2 cells (EPA: 25 μM 4.13±1.13 vs Control: 0.87±0.25; DPA: 25 μM 2.39±1.15 *vs* Control: 1.24±0.31). 25 μM EPA supplementation also significantly decreased oleic acid content (P<0.0001) and 10 μM EPA supplemented Caco-2 cells had significantly lower stearic acid content (P=0.0015). Lower concentrations (1 and 5 μM) of EPA had no significant effect on EPA content; however, cells had lower total omega-3 content (Figure 11). Caco-2 cells supplemented with 1 or 5 μM EPA had significantly higher concentrations of palmitic acid and palmitoleic acid (P<0.0001 for both concentrations and FAs). 5 μM EPA supplemented cells also had significantly lower stearic acid and oleic acid content (P=0.0015 and P=0.0036, respectively). All changes to quantified FAs by EPA supplementation are displayed in *Table 4.1*.

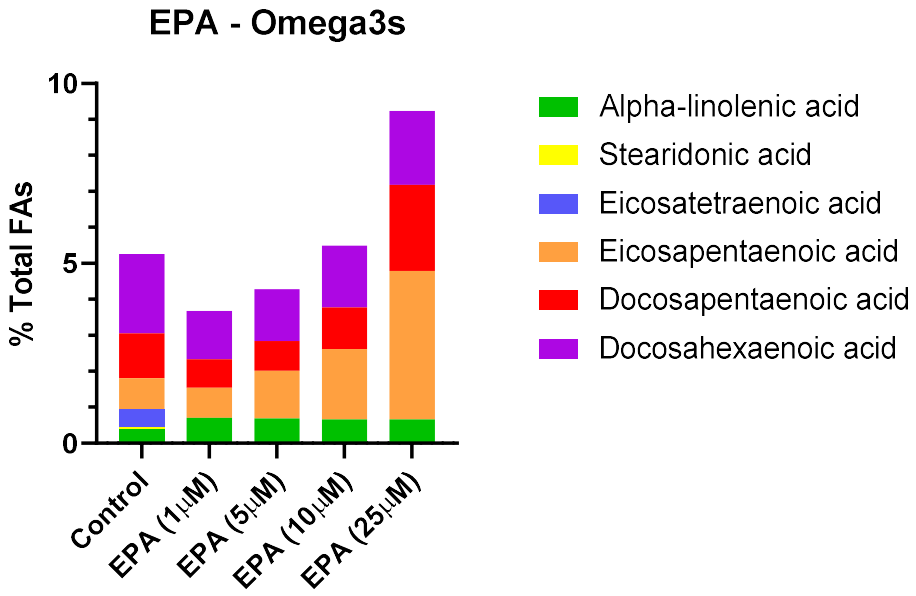

Figure 4.1: Total omega-3 content of Caco-2 cells supplemented with EPA assessed by gas chromatography. Caco-2 cells were incubated for 48 hours with EPA (1, 5, 10, or 25 μM) and control cells were incubated for 48 hours with no fatty acids. Low concentrations of EPA (1 and 5 μM) had lower total omega-3 content than control cells and significantly lower concentrations of DHA at 1 μM EPA (P=0.0473). Higher concentrations (10 and 25 μM) of EPA significantly increased Caco-2 cell EPA content compared to control (10 μM; P=0.001, 25 μM; P<0.0001). Additionally, 25 μM EPA supplementation significantly increased DPA content (P=0.0003). SDA and ETE were undetectable in

each of the EPA supplemented conditions. All omega-3 content values are expressed as a percentage of total fatty acids (% Total FAs) = (target FA (μg/1x10^6 cells)/total FA (μg/1x10^6 cells)) x100. P values were determined by two-way ANOVA with Sidak's multiple comparisons test. Control data was from 2 biological replicates from 9 independent experiments. EPA data (at each time point) was from 2 biological replicates from 4 independent experiments.

*Table 4.1: Fatty acid content of Caco-2 cells supplemented with EPA (1-25 μM) for 48 hours. Controls were incubated with growth medium only. All values are displayed as mean±standard deviation of total fatty acids (% Total FAs) = (target FA (μg/1x10^6 cells)/total FA (μg/1x10^6 cells)) x100. Statistical differences were determined by two-way ANOVA with Sidak's multiple comparison tests. Asterisks indicate statistical significance, where * p<0.05, ** p<0.01, *** p<0.001, and **** p<0.0001. Control data was from 2 biological replicates from 9 independent experiments. EPA data (at each time point) was from 2 biological replicates from 4 independent experiments.*

FA	Structure	Control	EPA			
			1 μM	5 μM	10 μM	25 μM
Myristic acid	14:0	1.37±0.16	1.53±0.35	1.53±0.25	1.32±0.03	1.22±0.11
Pentadecanoic acid	15:0	0.75±0.15	1.00±0.26	1.03±0.16	1.00±0.13	0.90±0.22
Palmitic acid (PA)	16:0	16.92±0.73	19.49±3.03****	18.84±2.09****	17.18±0.39	16.72±0.97
Palmitoleic acid	16:1ω7	6.85±0.68	8.32±1.79****	8.54±0.59****	7.69±0.05	6.44±0.71
Margaric acid	17:0	0.99±0.08	1.08±0.06	1.10±0.02	1.13±0.02	1.08±0.10
Heptadecenoic acid	17:1	2.15±0.30	2.47±0.21	2.62±0.10	2.62±0.10	2.29±0.25
Stearic acid (SA)	18:0	9.01±0.63	8.43±0.26	7.94±0.36**	7.94±0.16**	8.64±0.67
Oleic acid (OA)	18:1ω9	33.51±1.68	32.67±0.52	32.49±0.29**	32.67±1.02	31.01±1.62****
Vaccenic acid	18:1ω7	12.61±0.54	12.29±0.38	12.70±0.09	13.08±0.37	11.93±0.75
Linoleic acid (LA)	18:2ω6	1.41±0.20	1.17±0.44	1.01±0.11	1.17±0.07	1.31±0.15
Gamma-linolenic acid (GLA)	18:3ω6	0.70±0.06	0.69±0.13	0.69±0.11	0.79±0.01	0.76±0.06
Alpha-linolenic acid (ALA)	18:3ω3	0.41±0.33	0.70±0.04	0.69±0.07	0.66±0.03	0.66±0.04
Arachidic acid	20:0	1.24±0.49	1.44±0.30	1.52±0.12	1.62±0.02	1.57±0.03
Stearidonic acid (SDA)	18:4ω3	0.06±0.07	ND	ND	ND	ND
Eicosenoic acid (ESA)	20:1ω9	1.71±0.09	1.49±0.21	1.71±0.13	1.84±0.06	1.68±0.16
Eicosadienoic acid (EDA)	20:2ω6	0.49±0.09	0.40±0.14	0.52±0.11	0.47±0.11	0.44±0.05
Dihomo-gamma-linolenic acid (DGLA)	20:3ω6	0.78±0.10	0.77±0.14	0.74±0.08	0.70±0.04	0.82±0.19
Arachidonic acid (AA)	20:4ω6	2.77±0.51	1.99±1.11	2.02±0.75	2.39±0.35	2.65±0.37
Eicosatetraenoic acid (ETA)	20:4ω3	0.47±0.60	ND	ND	ND	ND
Eurcic acid	22:1ω9	0.66±0.69	0.48±0.57	0.17±0.17	0.21±0.21	0.62±0.78
Eicosapentaenoic acid (EPA)	20:5ω3	0.87±0.25	0.84±0.51	1.32±0.42	1.96±0.52**	4.13±1.13****
Tetracosa- acids	24:0	0.83±0.14	0.60±0.31	0.55±0.17	0.69±0.14	0.70±0.12
Docosapentaenoic acid (DPA)	22:5ω3	1.24±0.31	0.79±0.70	0.83±0.43	1.15±0.38	2.39±1.15***
Docosahexaenoic acid (DHA)	22:6ω3	2.21±0.64	1.35±1.25*	1.44±0.82	1.72±0.61	2.06±0.49
Total ω3	-	5.26±2.20	3.69±2.49	4.29±1.74	5.49±1.54	9.24±2.81
Total ω6	-	6.15±0.96	5.02±1.96	4.98±1.16	5.52±0.58	5.97±0.82
ω6/ω3 Ratio	-	1.17	1.36	1.16	1.00	0.65

4.4.2. DHA supplementation increases DHA content of Caco-2 cells

Total omega-3 content (*Figure 4.2*) and total FAs (*Table 4.2*) were assessed with or without pre-supplementation with DHA (1, 5, 10, or 25 μM). DHA supplementation (≥5 μM) increased Caco-2 DHA content compared to controls, with 25 μM DHA supplementation almost tripling Caco-2 cell DHA content (5 μM: 2.95±0.67; 10 μM: 3.92±0.64; 25 μM: 6.10±0.68 *vs* Control: 2.21±0.64). At all tested DHA concentrations, Caco-2 cell stearic acid and oleic acid contents were significantly decreased compared to controls (various P values, see *Table 4.2*). Cells supplemented with lower concentrations of DHA (1 and 5 μM) had significantly increased palmitic acid and palmitoleic acid (P<0.0001 for both concentrations and FAs) and 10 μM DHA supplemented Caco-2 cells had slightly higher palmitoleic acid (P=0.0152). All changes to quantified FAs by DHA supplementation are displayed in *Table 4.2*.

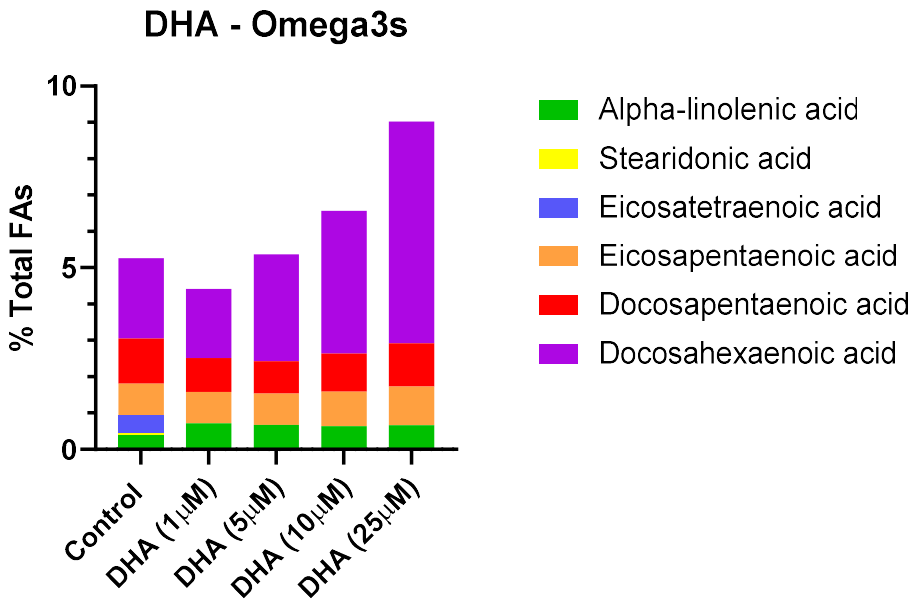

Figure 4.2: Total omega-3 content of Caco-2 cells supplemented with DHA assessed by gas chromatography. Caco-2 cells were incubated for 48 hours with DHA (1, 5, 10, or 25 μM) and control cells were incubated for 48 hours with no fatty acids. DHA content was significantly increased by DHA concentrations greater than 5 μM (5 μM; P=0.0185, 10 and 25 μM; P<0.0001). Total omega-3 content was higher than controls in cells supplemented with 10 or 25 μM. DHA supplementation at any concentration had no effect on other omega-3 PUFAs assessed. SDA and ETE were undetectable in each of the DHA supplemented cells. All omega-3 content values are expressed as a percentage of total fatty acids (% Total FAs) = (target FA (μg/1x10⁶ cells)/total FA (μg/1x10⁶ cells)) x100. P values were determined by two-way ANOVA with Sidak's multiple comparisons tests. Control data was from 2

biological replicates from 9 independent experiments. DHA data (at each time point) was from 2 biological replicates from 4 independent experiments.

*Table 4.2: Fatty acid content of Caco-2 cells supplemented with DHA (1-25 μM) for 48 hours. Controls were incubated with growth medium only. All values are displayed as mean±standard deviation of total fatty acids (% Total FAs) = (target FA (μg/1x10^6 cells)/total FA (μg/1x10^6 cells)) x100. Statistical differences were determined by two-way ANOVA with Sidak's multiple comparison tests. Asterisks indicate statistical significance, where * p<0.05, ** p<0.01, *** p<0.001, and **** p<0.0001. Control data was from 2 biological replicates from 9 independent experiments. DHA data (at each time point) was from 2 biological replicates from 4 independent experiments.*

FA	Structure	Control	DHA			
			1 μM	5 μM	10 μM	25 μM
Myristic acid	14:0	1.37±0.16	1.43±0.23	1.41±0.18	1.29±0.09	1.21±0.04
Pentadecanoic acid	15:0	0.75±0.15	0.91±0.17	0.99±0.16	0.93±0.06	0.85±0.13
Palmitic acid (PA)	16:0	16.92±0.73	18.61±2.07****	18.53±1.49****	16.89±0.13	16.30±0.55
Palmitoleic acid	16:1ω7	6.85±0.68	7.90±1.44****	8.24±0.29****	7.60±0.25*	6.76±0.66
Margaric acid	17:0	0.99±0.08	1.03±0.01	1.11±0.09	1.12±0.01	1.07±0.07
Heptadecenoic acid	17:1	2.15±0.30	2.36±0.11	2.49±0.11	2.60±0.06	2.39±0.26
Stearic acid (SA)	18:0	9.01±0.63	8.28±0.26*	7.94±0.14****	7.86±0.10****	8.10±0.47***
Oleic acid (OA)	18:1ω9	33.51±1.68	32.77±0.50*	31.99±0.19****	32.57±1.06***	32.08±1.13****
Vaccenic acid	18:1ω7	12.61±0.54	12.42±0.06	12.41±0.14	12.56±0.28	11.93±0.40
Linoleic acid (LA)	18:2ω6	1.41±0.20	1.33±0.21	1.11±0.03	1.18±0.09	1.30±0.15
Gamma-linolenic acid (GLA)	18:3ω6	0.70±0.06	0.78±0.15	0.72±0.05	0.76±0.01	0.78±0.05
Alpha-linolenic acid (ALA)	18:3ω3	0.41±0.33	0.71±0.05	0.67±0.03	0.64±0.02	0.66±0.06
Arachidic acid	20:0	1.24±0.49	1.61±0.14	1.59±0.04	1.60±0.03	1.62±0.02
Stearidonic acid (SDA)	18:4ω3	0.06±0.07	ND	ND	ND	ND
Eicosenoic acid (ESA)	20:1ω9	1.71±0.09	1.69±0.03	1.75±0.03	1.79±0.04	1.73±0.14
Eicosadienoic acid (EDA)	20:2ω6	0.49±0.09	0.46±0.06	0.50±0.09	0.49±0.09	0.44±0.05
Dihomo-gamma-linolenic acid (DGLA)	20:3ω6	0.78±0.10	0.68±0.15	0.70±0.07	0.73±0.06	0.75±0.06
Arachidonic acid (AA)	20:4ω6	2.77±0.51	2.38±0.71	2.31±0.45	2.54±0.14	2.62±0.34
Eicosatetraenoic acid (ETA)	20:4ω3	0.47±0.60	ND	ND	ND	ND
Eurcic acid	22:1ω9	0.66±0.69	0.24±0.25	0.22±0.22	0.20±0.21	0.28±0.28
Eicosapentaenoic acid (EPA)	20:5ω3	0.87±0.25	0.87±0.28	0.87±0.17	0.95±0.10	1.07±0.21
Tetracosa- acids	24:0	0.83±0.14	0.70±0.28	0.62±0.13	0.72±0.12	0.78±0.09
Docosapentaenoic acid (DPA)	22:5ω3	1.24±0.31	0.93±0.45	0.88±0.30	1.05±0.20	1.19±0.24
Docosahexaenoic acid (DHA)	22:6ω3	2.21±0.64	1.90±0.87	2.95±0.67*	3.92±0.64****	6.10±0.68****
Total ω3	-	5.26±2.20	4.40±1.65	5.37±1.17	6.56±0.96	9.02±1.19
Total ω6	-	6.15±0.96	5.64±1.29	5.34±0.69	5.70±0.39	5.90±0.65
ω6/ω3 Ratio	-	1.17	1.28	0.99	0.87	0.65

4.4.3. DPA supplementation increases the EPA and DPA content of Caco-2 cells

High concentrations of DPA (10 and 25 μM) induced a significant increase in both EPA and DPA content of Caco2 cells (*Figure 4.3*). At the highest concentration, DPA supplementation quadrupled DPA content compared to control cells (25 μM: 5.12±0.78 *vs* Control: 1.24±0.31) and doubled EPA content compared to controls (25 μM: 2.28±0.33 *vs* Control: 0.87±0.25). There were also significant decreases in palmitic acid, palmitoleic acid, oleic acid, and vaccenic acid (various P values, indicated in *Table 4.3*) at 25 μM DPA, but not at 10 μM. There was no significant effect on DPA or EPA content at 1 or 5 μM DPA, however there was significantly increased oleic acid content in cells supplemented with 1 μM DPA (*Table 4.3*).

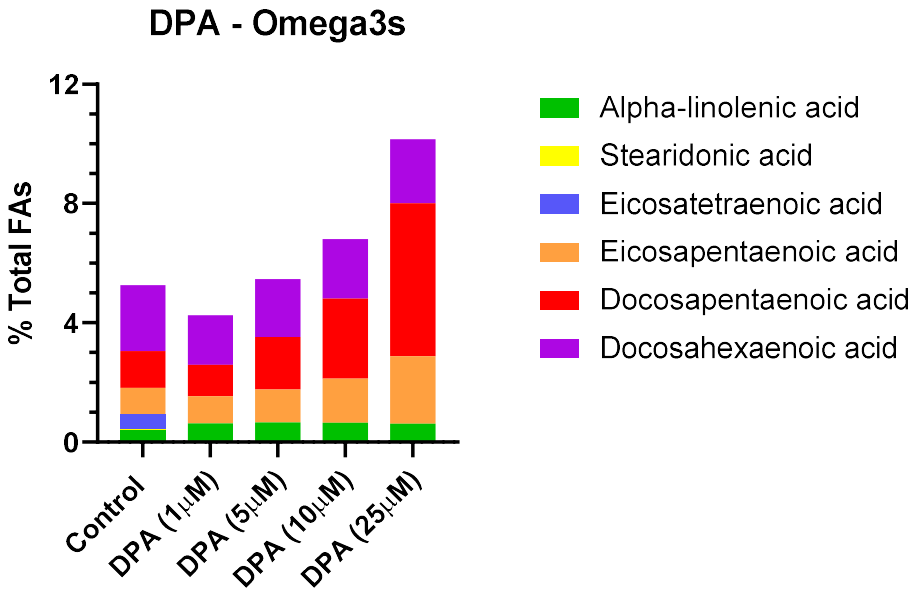

Figure 4.3: Total omega-3 content of Caco-2 cells supplemented with DPA assessed by gas chromatography. Caco-2 cells were incubated for 48 hours with DPA (1, 5, 10, or 25 μM) and control cells were incubated for 48 hours with no fatty acids. DPA content was significantly increased when cells were supplemented with higher DPA concentrations (10 and 25 μM; P<0.0001). EPA content was also significantly greater than controls in cells supplemented with 10 or 25 μM DPA (10 μM; P=0.0287, 25 μM; P<0.0001). Total omega-3 content was also higher at these concentrations. SDA and ETE were undetectable in each of the DPA supplemented cells. All omega-3 content values are expressed as a percentage of total fatty acids (% Total FAs) = (target FA (μg/1x10^6 cells)/total FA (μg/1x10^6 cells)) x100. P values were determined by two-way ANOVA with Sidak's multiple comparisons test. Control data was from 2 biological replicates from 9 independent experiments. DPA data (at each time point) was from 2 biological replicates from 5 independent experiments.

*Table 4.3: Fatty acid content of Caco-2 cells supplemented with DPA (1-25 μM) for 48 hours. Controls were incubated with growth medium only. All values are displayed as mean±standard deviation of total fatty acids (% Total FAs) = (target FA (μg/1x10^6 cells)/total FA (μg/1x10^6 cells)) x100. Statistical differences were determined by two-way ANOVA with Sidak's multiple comparison tests. Asterisks indicate statistical significance, where * p<0.05, ** p<0.01, *** p<0.001, and **** p<0.0001. Control data was from 2 biological replicates from 9 independent experiments. DPA data (at each time point) was from 2 biological replicates from 5 independent experiments.*

FA	Structure	Control	DPA			
			1 μM	5 μM	10 μM	25 μM
Myristic acid	14:0	1.37±0.16	1.28±0.13	1.23±0.06	1.21±0.11	1.12±0.06
Pentadecanoic acid	15:0	0.75±0.15	0.90±0.11	0.88±0.08	0.85±0.05	0.81±0.07
Palmitic acid (PA)	16:0	16.92±0.73	16.76±0.49	16.63±0.46	16.48±0.74	15.68±0.56****
Palmitoleic acid	16:1ω7	6.85±0.68	6.50±0.44	6.52±0.29	6.52±0.29	6.03±0.32***
Margaric acid	17:0	0.99±0.08	1.15±0.07	1.13±0.08	1.10±0.05	1.07±0.05
Heptadecenoic acid	17:1	2.15±0.30	2.51±0.28	2.50±0.20	2.44±0.17	2.31±0.22
Stearic acid (SA)	18:0	9.01±0.63	8.74±0.27	8.77±0.31	8.61±0.38	8.35±0.31**
Oleic acid (OA)	18:1ω9	33.51±1.68	34.74±1.03****	33.56±1.43	32.93±1.23	32.25±0.66****
Vaccenic acid	18:1ω7	12.61±0.54	12.83±0.55	12.55±0.35	12.36±0.36	11.82±0.42***
Linoleic acid (LA)	18:2ω6	1.41±0.20	1.54±0.17	1.52±0.15	1.48±0.14	1.51±0.11
Gamma-linolenic acid (GLA)	18:3ω6	0.70±0.06	0.78±0.12	0.84±0.16	0.75±0.11	0.72±0.09
Alpha-linolenic acid (ALA)	18:3ω3	0.41±0.33	0.62±0.04	0.65±0.07	0.64±0.07	0.61±0.02
Arachidic acid	20:0	1.24±0.49	1.63±0.13	1.61±0.14	1.60±0.14	1.54±0.12
Stearidonic acid (SDA)	18:4ω3	0.06±0.07	ND	ND	ND	ND
Eicosenoic acid (ESA)	20:1ω9	1.71±0.09	1.51±0.08	1.53±0.10	1.51±0.09	1.41±0.08
Eicosadienoic acid (EDA)	20:2ω6	0.49±0.09	0.46±0.09	0.54±0.07	0.52±0.05	0.46±0.03
Dihomo-gamma-linolenic acid (DGLA)	20:3ω6	0.78±0.10	0.70±0.14	0.74±0.06	0.75±0.05	0.78±0.07
Arachidonic acid (AA)	20:4ω6	2.77±0.51	2.57±0.69	2.74±0.23	2.75±0.18	2.85±0.23
Eicosatetraenoic acid (ETA)	20:4ω3	0.47±0.60	ND	ND	ND	ND
Eurcic acid	22:1ω9	0.66±0.69	0.44±0.41	0.56±0.53	0.56±0.52	0.37±0.33
Eicosapentaenoic acid (EPA)	20:5ω3	0.87±0.25	0.91±0.35	1.11±0.18	1.48±0.13*	2.28±0.33****
Tetracosa- acids	24:0	0.83±0.14	0.70±0.21	0.69±0.13	0.78±0.07	0.79±0.07
Docosapentaenoic acid (DPA)	22:5ω3	1.24±0.31	1.06±0.52	1.76±0.46	2.69±0.38****	5.12±0.78****
Docosahexaenoic acid (DHA)	22:6ω3	2.21±0.64	1.67±0.89	1.94±0.62	1.99±0.35	2.14±0.35
Total ω3	-	5.26±2.20	4.26±1.79	5.46±1.33	6.80±0.92	10.14±1.49
Total ω6	-	6.15±0.96	6.06±1.22	6.38±0.68	6.25±0.53	6.32±0.53
ω6/ω3 Ratio	-	1.17	1.42	1.17	0.92	0.62

4.4.4. ALA supplementation increases ALA content of Caco-2 cells

Total omega-3 content of Caco-2 cells dose-dependently increased with increasing concentrations of exogenous ALA (*Figure 4.4*). Caco-2 cells significantly accumulated ALA after 48 hours exposure to high concentrations of ALA. 10 μM ALA supplemented Caco-2 cells had 3 times higher ALA content than controls (10 μM: 1.28±0.08 *vs* Control: 0.41±0.33), whilst 25 μM ALA supplemented cells had approximately 8 times more ALA content than controls (25 μM: 3.20±0.28 vs Control: 0.41±0.33). As shown in *Figure 4.4*, ALA supplementation had no effect on any other ω-3 PUFA assessed. All ALA supplemented Caco-2 cells had increased oleic acid content compared to controls, whilst cells supplemented with ALA concentrations ≥5 μM had decreased levels of palmitic acid (*Table 4.4*). Interestingly, arachidonic acid was lower in all ALA supplemented cells when compared to control and this was significant at 1, 10, and 25 μM (*Table 4.4*).

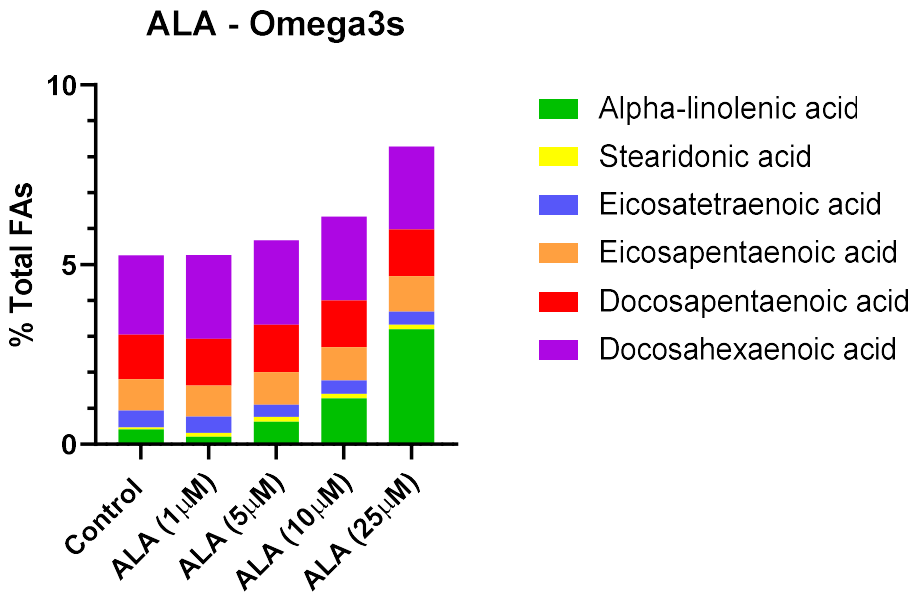

Figure 4.4: Total omega-3 content of Caco-2 cells supplemented with ALA assessed by gas chromatography. Caco-2 cells were incubated for 48 hours with ALA (1, 5, 10, or 25 μM) and control cells were incubated for 48 hours with no fatty acids. High concentrations of ALA (10 or 25 μM) significantly increased ALA content in Caco-2 cells (10 and 25 μM; P<0.0001). Lower concentrations of ALA (1 or 5 μM) had no effect on ALA content in Caco-2 cells. All concentrations of ALA had no effect on any of the other omega-3 PUFAs assessed but total omega-3 content seemed to increase with increased concentration of supplemented ALA. All omega-3 content values are expressed as a percentage of total fatty acids (% Total FAs) = (target FA (μg/1x10⁶ cells)/total FA (μg/1x10⁶ cells)) x100. P values were determined by two-way ANOVA with Sidak's multiple comparisons test. Control

data was from 2 biological replicates from 9 independent experiments. ALA data (at each time point) was from 2 biological replicates from 4 independent experiments.

*Table 4.4: Fatty acid content of Caco-2 cells supplemented with ALA (1-25 μM) for 48 hours. Controls were incubated with growth medium only. All values are displayed as mean±standard deviation of total fatty acids (% Total FAs) = (target FA (μg/1x10⁶ cells)/total FA (μg/1x10⁶ cells)) x100. Statistical differences were determined by two-way ANOVA with Sidak's multiple comparison tests. Asterisks indicate statistical significance, where * p<0.05, ** p<0.01, *** p<0.001, and **** p<0.0001. Control data was from 2 biological replicates from 9 independent experiments. ALA data (at each time point) was from 2 biological replicates from 4 independent experiments.*

FA	Structure	Control	ALA			
			1 μM	5 μM	10 μM	25 μM
Myristic acid	14:0	1.37±0.16	1.39±0.08	1.36±0.11	1.36±0.08	1.37±0.07
Pentadecanoic acid	15:0	0.75±0.15	0.68±0.05	0.67±0.03	0.66±0.05	0.65±0.04
Palmitic acid (PA)	16:0	16.92±0.73	16.40±0.56	16.27±0.66**	16.09±0.66****	15.78±0.59****
Palmitoleic acid	16:1ω7	6.85±0.68	6.64±0.34	6.60±0.46	6.47±0.28	6.35±0.39
Margaric acid	17:0	0.99±0.08	0.96±0.05	0.95±0.04	0.94±0.05	0.93±0.03
Heptadecenoic acid	17:1	2.15±0.30	2.01±0.22	1.95±0.17	1.94±0.20	1.88±0.16
Stearic acid (SA)	18:0	9.01±0.63	8.64±0.37	8.55±0.45	8.56±0.40	8.45±0.41
Oleic acid (OA)	18:1ω9	33.51±1.68	35.30±0.64****	35.20±0.63****	34.96±0.60****	34.13±0.62*
Vaccenic acid	18:1ω7	12.61±0.54	13.08±0.25	13.09±0.29	13.02±0.32	12.70±0.28
Linoleic acid (LA)	18:2ω6	1.41±0.20	1.41±0.15	1.40±0.15	1.42±0.12	1.37±0.15
Gamma-linolenic acid (GLA)	18:3ω6	0.70±0.06	0.75±0.13	0.72±0.14	0.77±0.14	0.67±0.10
Alpha-linolenic acid (ALA)	18:3ω3	0.41±0.33	0.21±0.03	0.63±0.07	1.28±0.08****	3.20±0.28****
Arachidic acid	20:0	1.24±0.49	0.67±0.04*	0.70±0.04	0.67±0.04*	0.67±0.04*
Stearidonic acid (SDA)	18:4ω3	0.06±0.07	0.11±0.07	0.13±0.08	0.12±0.07	0.13±0.08
Eicosenoic acid (ESA)	20:1ω9	1.71±0.09	1.71±0.10	1.74±0.13	1.72±0.13	1.69±0.10
Eicosadienoic acid (EDA)	20:2ω6	0.49±0.09	0.45±0.05	0.44±0.06	0.45±0.06	0.45±0.06
Dihomo-gamma-linolenic acid (DGLA)	20:3ω6	0.78±0.10	0.79±0.09	0.80±0.10	0.80±0.10	0.77±0.10
Arachidonic acid (AA)	20:4ω6	2.77±0.51	2.79±0.31	2.80±0.32	2.81±0.27	2.83±0.35
Eicosatetraenoic acid (ETA)	20:4ω3	0.47±0.60	0.45±0.32	0.34±0.21	0.38±0.25	0.36±0.23
Eurcic acid	22:1ω9	0.66±0.69	0.26±0.08	0.28±0.08	0.25±0.08	0.26±0.09
Eicosapentaenoic acid (EPA)	20:5ω3	0.87±0.25	0.87±0.19	0.90±0.18	0.92±0.16	0.99±0.18
Tetracosa- acids	24:0	0.83±0.14	0.82±0.15	0.80±0.15	0.77±0.10	0.75±0.10
Docosapentaenoic acid (DPA)	22:5ω3	1.24±0.31	1.30±0.10	1.33±0.09	1.30±0.08	1.30±0.15
Docosahexaenoic acid (DHA)	22:6ω3	2.21±0.64	2.33±0.23	2.35±0.26	2.34±0.24	2.31±0.31
Total ω3	-	5.26±2.20	5.26±0.93	5.68±0.89	6.33±0.88	8.29±1.22
Total ω6	-	6.15±0.96	6.19±0.73	6.15±0.77	6.25±0.70	6.09±0.77
ω6/ω3 Ratio	-	1.17	1.18	1.08	0.99	0.73

4.4.5. SDA supplementation increases SDA, ETE, and EPA content of Caco-2 cells

SDA supplementation, from 1 to 10 μM, had little effect on Caco-2 FA content with no significant effects observed except significantly higher oleic acid content in cells supplemented with 5 μM SDA, compared to controls (*Table 4.5*). However, 25 μM SDA supplemented cells had significantly increased SDA, ETE, and EPA contents compared to controls (*Figure 4.5*), whilst arachidonic acid content was slightly decreased (*Table 4.5*). After 48 hours supplementation with 25 μM SDA, Caco-2 cell SDA content was approximately 13 times higher than controls (25 μM: 0.77±0.09 *vs* Control: 0.06±0.07), whilst eicosatrienoic acid (ETE) and EPA content were over double that of controls (ETE: 25 μM: 1.42±0.82 *vs* Control: 0.47±0.60, EPA: 25 μM: 1.99±0.25 vs Control: 0.87±0.25). ALA content also seemed to be diminished across the SDA supplemented cells, as shown in Figure 15, although this was not statistically significant.

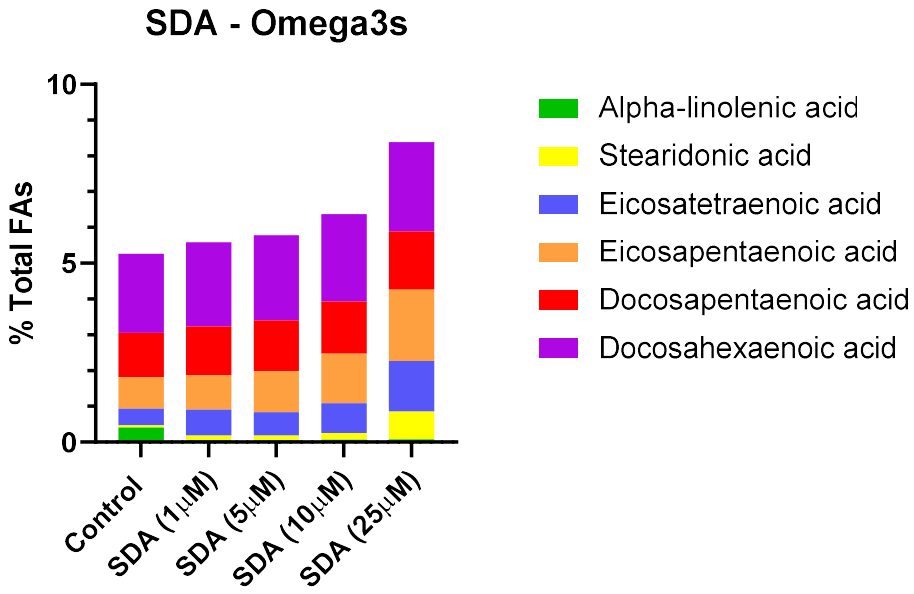

Figure 4.5: Total omega-3 content of Caco-2 cells supplemented with SDA assessed by gas chromatography. Caco-2 cells were incubated for 48 hours with SDA (1, 5, 10, or 25 μM) and control cells were incubated for 48 hours with no fatty acids. 25 μM SDA supplementation significantly increased SDA, ETE, and EPA content in Caco-2 cells (SDA; P=0.0075, ETE; P<0.0001, EPA; P<0.0001). Lower concentrations of SDA (1-10 μM) had no effect on SDA or any other omega-3 PUFA assessed in Caco-2 cells. Total omega-3 content seemed to increase with increased concentration of supplemented SDA. All omega-3 content values are expressed as a percentage of total fatty acids (% Total FAs) = (target FA (μg/1x10^6 cells)/total FA (μg/1x10^6 cells)) x100. P values were determined by two-way ANOVA with Sidak's multiple comparisons test. Control data was from 2 biological replicates from 9

independent experiments. SDA data (at each time point) was from 2 biological replicates from 4 independent experiments.

*Table 4.5: Fatty acid content of Caco-2 cells supplemented with SDA (1-25 μM) for 48 hours. Controls were incubated with growth medium only. All values are displayed as mean±standard deviation of total fatty acids (% Total FAs) = (target FA (μg/1x10^6 cells)/total FA (μg/1x10^6 cells)) x100. Statistical differences were determined by two-way ANOVA with Sidak's multiple comparison tests. Asterisks indicate statistical significance, where * p<0.05, ** p<0.01, *** p<0.001, and **** p<0.0001. Control data was from 2 biological replicates from 9 independent experiments. SDA data (at each time point) was from 2 biological replicates from 4 independent experiments.*

FA	Structure	Control	SDA			
			1 μM	5 μM	10 μM	25 μM
Myristic acid	14:0	1.37±0.16	1.36±0.18	1.31±0.14	1.38±0.19	1.25±0.11
Pentadecanoic acid	15:0	0.75±0.15	0.68±0.04	0.67±0.03	0.65±0.04	0.64±0.04
Palmitic acid (PA)	16:0	16.92±0.73	17.30±0.89	17.01±0.75	16.93±0.86	16.38±0.77
Palmitoleic acid	16:1ω7	6.85±0.68	6.64±0.45	6.71±0.53	6.52±0.42	6.32±0.36
Margaric acid	17:0	0.99±0.08	0.96±0.05	0.96±0.04	0.93±0.05	0.92±0.04
Heptadecenoic acid	17:1	2.15±0.30	1.90±0.23	1.90±0.20	1.90±0.21	1.91±0.17
Stearic acid (SA)	18:0	9.01±0.63	9.40±0.68	8.97±0.39	9.00±0.67	8.75±0.39
Oleic acid (OA)	18:1ω9	33.51±1.68	34.04±0.82	34.55±0.41****	33.98±0.65	33.16±0.49
Vaccenic acid	18:1ω7	12.61±0.54	12.40±0.65	12.45±0.43	12.41±0.43	12.05±0.11
Linoleic acid (LA)	18:2ω6	1.41±0.20	1.54±0.12	1.45±0.10	1.47±0.10	1.48±0.07
Gamma-linolenic acid (GLA)	18:3ω6	0.70±0.06	0.60±0.15	0.62±0.12	0.62±0.13	0.62±0.09
Alpha-linolenic acid (ALA)	18:3ω3	0.41±0.33	0.06±0.01	0.06±0.02	0.07±0.02	0.08±0.02
Arachidic acid	20:0	1.24±0.49	0.69±0.07	0.68±0.05	0.66±0.07	0.61±0.02*
Stearidonic acid (SDA)	18:4ω3	0.06±0.07	0.13±0.03	0.13±0.02	0.18±0.05	0.77±0.09**
Eicosenoic acid (ESA)	20:1ω9	1.71±0.09	1.59±0.12	1.63±0.08	1.61±0.06	1.52±0.11
Eicosadienoic acid (EDA)	20:2ω6	0.49±0.09	0.49±0.04	0.49±0.05	0.53±0.08	0.55±0.12
Dihomo-gamma-linolenic acid (DGLA)	20:3ω6	0.78±0.10	0.83±0.08	0.84±0.07	0.84±0.07	0.86±0.05
Arachidonic acid (AA)	20:4ω6	2.77±0.51	2.88±0.24	2.89±0.18	2.95±0.17	3.05±0.05
Eicosatetraenoic acid (ETA)	20:4ω3	0.47±0.60	0.72±0.58	0.65±0.41	0.84±0.54	1.42±0.82****
Eurcic acid	22:1ω9	0.66±0.69	0.30±0.09	0.27±0.10	0.46±0.43	0.80±0.98
Eicosapentaenoic acid (EPA)	20:5ω3	0.87±0.25	0.96±0.21	1.14±0.27	1.39±0.31	1.99±0.25****
Tetracosa- acids	24:0	0.83±0.14	0.83±0.12	0.79±0.12	0.78±0.15	0.76±0.09
Docosapentaenoic acid (DPA)	22:5ω3	1.24±0.31	1.37±0.18	1.42±0.22	1.45±0.19	1.63±0.28
Docosahexaenoic acid (DHA)	22:6ω3	2.21±0.64	2.35±0.26	2.38±0.28	2.44±0.19	2.50±0.18
Total ω3	-	5.26±2.20	5.59±1.28	5.79±1.22	6.38±1.31	8.39±1.65
Total ω6	-	6.15±0.96	6.34±0.63	6.30±0.53	6.40±0.55	6.55±0.37
ω6/ω3 Ratio	-	1.17	1.14	1.09	1.00	0.78

4.5. Discussion and future work

To determine the potential for functional effects of ω-3 PUFAs by Caco-2 cells, incorporation of different ω-3 PUFAs into Caco-2 cells was assessed by gas chromatography. Five different ω-3 PUFAs were used each at 4 different concentrations. The cell content of 24 fatty acids was determined. It was found that the ω-3 PUFAs were utilised differently by Caco-2 cells. In particular, ALA and DHA were accumulated by Caco-2 cells with apparently little or no conversion to other ω-3 PUFAs, whilst SDA, EPA and DPA appeared to be both accumulated and metabolised to other ω-3 PUFAs by Caco-2 cells.

It is thought that the accumulation of ω-3 PUFAs in cell membranes is through the displacement of ω-6 PUFAs, particularly AA, and a subsequent decrease in ω-6/ω-3 ratio [71]. In this model, increased concentrations of exogenous ω-3 PUFAs decreased ω-6/ω-3 ratio with all of the ω-3 PUFAs tested. However, in all the conditions the total amount of ω-6 PUFAs was not different from the controls. ω-3 PUFA supplementation, especially at the highest concentration (25 μM), instead seemed to significantly alter other fatty acids including stearic acid (EPA, DPA and DHA), oleic acid (EPA, DPA and DHA), vaccenic acid, palmitic acid, and palmitoleic acid (all DPA). Plant-derived ALA and SDA had the least effect on other fatty acids, as ALA supplementation decreased Caco-2 cell palmitic acid content, whilst both ALA and SDA supplementation decreased Caco-2 cell arachidonic acid content. EPA and DHA seemed to exhibit similar fatty acid displacement in this model, which has been previously shown in other cell types including endothelial cells [222] and mononuclear cells [223]. DPA induced changes in the greatest number of different fatty acids. DPA-induced changes to fatty acid composition in different cell types has not been thoroughly investigated. Short-term DPA supplementation in healthy individuals showed different DPA incorporation into red blood cells and plasma fractions, compared to EPA supplemented individuals [224]. Supplementation with DPA increased DPA content of plasma triacylglycerol and phospholipid fractions, as well as EPA content of triacylglycerol and cholesterol ester fractions and DHA content in the triacylglycerol fraction [224]. EPA supplementation did not affect the appearance of any other ω-3 PUFAs but increased EPA content in plasma phospholipid and cholesterol ester fractions and in red blood cell phospholipids [224]. Therefore, it seems that DPA and EPA have different fates in terms of which lipid fraction they are incorporated into and whether they are converted.

EPA appeared to be converted to DPA by Caco-2 cells; however, there was no subsequent conversion to DHA. In fact, low DHA content was observed in all EPA supplemented cells compared to controls (*Table 4.1*). Similar results have been shown in airway epithelial cells (Calu-3 cells), as exposure to increased concentrations of exogenous EPA dose-dependently increased cellular EPA and DPA content after 24 hours, whilst DHA content seemed to decrease with increased EPA exposure [225]. Beguin et al. also showed similar outcomes in intestinal T84 cells and Caco-2 cells after long-term exposure (7 day) to EPA [150]. Taken together these observations may suggest that not only is EPA not converted all the way to DHA in epithelial cells, but that EPA displaces DHA. It is not clear what happens to the displaced DHA, but it may be oxidised. In contrast to the findings of the current study and two literature reports [18,19], 48-hour exposure to 50 μM EPA in three different colonic cell lines, HT29, HT29-MTX, and Caco-2, significantly increased cellular EPA content, whilst DHA content seemed to slightly increase, although this was not significant [136].

Exogenous DHA was accumulated by Caco-2 cells from concentrations as low as 5 μM and the cell content of other ω-3 PUFAs were unaffected by DHA supplementation. This is different to what was shown in differentiating Caco-2 cells exposed to DHA for 7 days, as DHA was retro-converted to EPA [150]. Although this model used a similar concentration of DHA (30 μM) as the current model, this suggests that there could be a temporal factor in the retro-conversion of DHA to EPA, as 48-hour exposure to DHA did not increase Caco-2 cell EPA content (*Figure 4.2*). The differences could be attributed to the maturity of the cell line, as it has been reported elsewhere that differentiated and undifferentiated Caco-2 cells exhibit altered PUFA metabolism with differentiation lowering the activity of elongation, Δ5-desaturase, and retro-conversion pathways [226]. Additionally, the biochemical process of DHA to EPA retro-conversion has never totally been defined in humans; it could be attributed to two pathways, the ER-peroxisomal pathway and direct Δ4-desaturase pathway [227]. However, recent human evidence seems to suggest that increased EPA concentrations in red blood cells after DHA supplementation is due to the slowed metabolism and accumulation of EPA, rather than retro-conversion [228]. Therefore, this could explain why there is a lack of DHA to EPA conversion in Caco-2 cells seen in this model.

DPA supplementation induced an increase in both DPA and EPA content in this model suggesting some DPA retro-conversion capacity of Caco-2 cells. However,

DPA supplementation did not alter DHA content in this model (*Figure 4.3*). As EPA→DPA conversion was seen and not EPA/DPA→DHA, this indicates the steps between DPA→DHA are not operating so there is no endogenous production of DHA in Caco-2 cells. EPA→DPA bioconversion requires elongase-2 or elongase-5 activity, whilst DPA→DHA conversion has further processing through subsequent elongase-2, Δ6-desaturase, and peroxisomal β-oxidation [229]. It is therefore likely that the lack of DHA generation is due to the rate-limiting effects of Δ6-desaturase or peroxisomal β-oxidation. Other evidence of Δ6-desaturase rate-limiting present in this model is the lack of conversion of ALA→SDA (*Figure 4.4*). Despite a large incorporation of ALA over 48 hours, there was no significant increase in SDA or other longer-chain ω-3 PUFAs. Beguin et al. had also documented increased ALA content in differentiating Caco-2 cells after 7 days ALA exposure, but did not report on ALA→SDA conversion [150]. Additionally, 7-day ALA supplementation increased EPA content in differentiating Caco-2 cells [150], whereas SDA→EPA conversion, and not ALA→EPA conversion, was seen in the current model (Figure 4.5). These observations indicate a Δ6-desaturase-goverened rate-limiting step between ALA→SDA, making SDA a more effective substrate than ALA for the endogenous production of EPA in Caco-2 cells. SDA supplementation also increased EPA content in human red blood cells [230] and in rat liver tissue *in vivo* [231]. Thus, a lack of Δ6-desaturase activity in differentiated Caco-2 cells could explain the lack of appearance of SDA and EPA when cells were cultured with ALA and the lack of DHA appearance when the cells were cultured with EPA or DPA. However, the observations of Beguin et al. [19] suggest that less mature Caco-2 cells do possess Δ6-desaturase activity. Thus, the gene encoding the enzyme must be silenced or the enzyme itself inhibited once the cells become differentiated. The observed interconversion of ω-3 PUFAs and the potential limiting steps are summarised in *Figure 4.6*.

The research described in this chapter has explored the accumulation and bioconversion of ω-3 PUFAs in Caco-2 cells. Significant ω-3 PUFA accumulation has been described. This may result in altered cell function properties, and these are explored in the following chapters. The current results indicate the largest fatty acid composition changes when ω-3 PUFAs are used at a concentration of 25 μM. Hence experiments in subsequent chapters will mainly focus on the effect of ω-3 PUFAs at this concentration on cytokine-induced inflammation in Caco-2 cells (as defined in *Chapter 3*).

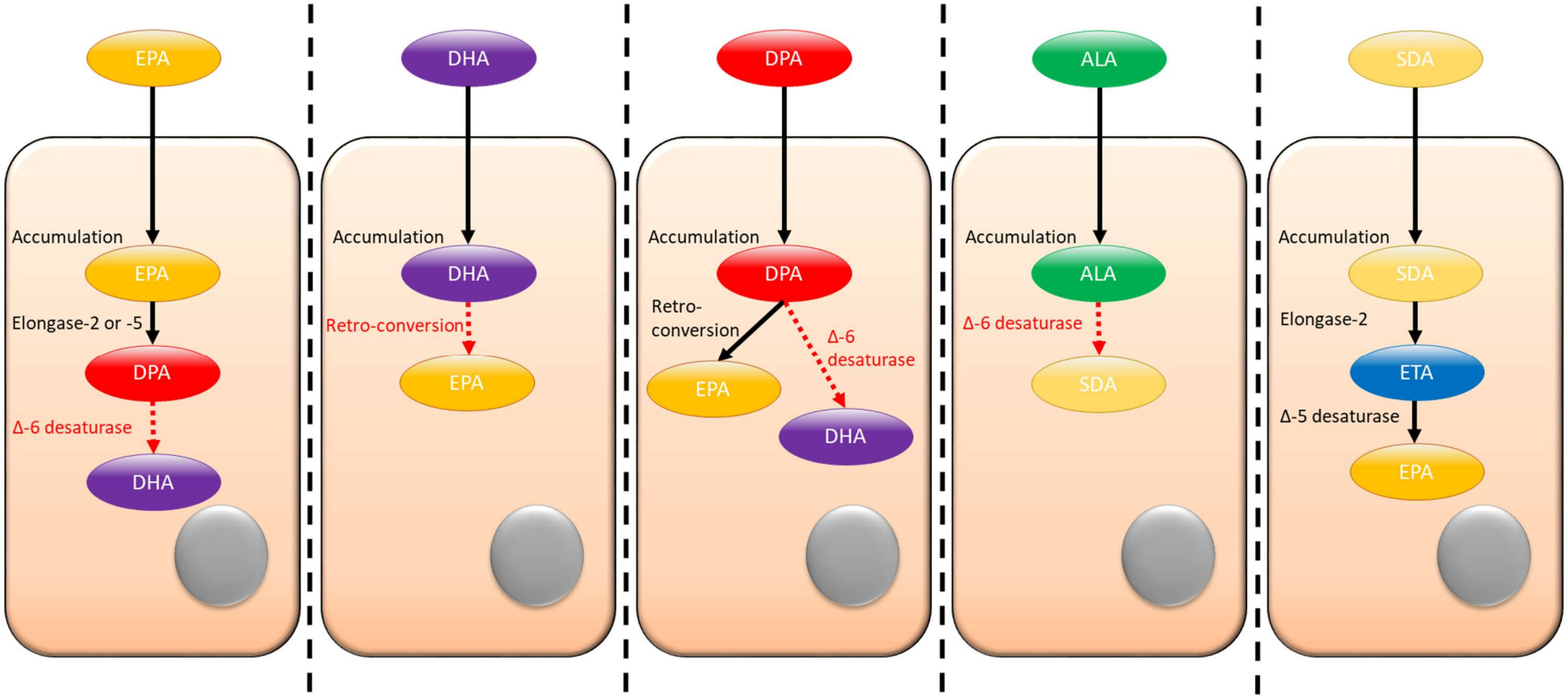

Figure 4.6: Proposed interconversion of ω-3 PUFAs in differentiated Caco-2 cells. From left to right, cells supplemented with EPA accumulated EPA and increased DPA content, likely through elongase-2 or elongase-5 activity, but no increase in DHA content was observed, indicating a lack of δ-6 desaturase activity. Cells supplemented with DHA accumulated DHA but no conversion to EPA, suggesting retro-conversion did not take place. Cells supplemented with DPA accumulated DPA and increased EPA content, presumably through a retro-conversion step, however no increase in DHA was reported, also indicating a lack of δ-6 desaturase activity. Cells supplemented with ALA accumulated ALA but no increases in SDA content were detected, another indication of a lack of δ-6 desaturase activity. Finally, cells supplemented with SDA accumulated SDA and increased ETA and EPA content, potentially through sequential elongation and desaturation by elongase-2 and δ-5 desaturase, respectively.

Chapter 5 - Can ω-3 PUFAs prevent cytokine-induced permeability of the Caco-2 cell monolayer?

5.1. Introduction

Epithelial cells form a major part of the intestinal barrier, which maintains intestinal permeability through regulated paracellular, transcellular, and transporter-mediated pathways, and is integral in controlling the intestinal immune response, as well as regulated absorption and secretion [232]. Increased intestinal permeability is associated to a range of factors, including gut dysbiosis, increased BMI, hyperglycaemia, inflammation (associated to a range of chronic inflammatory conditions), and poor diet [233]. The Western diet is often typified by being low in micronutrients and some other essential nutrients (including ω-3 PUFAs), coupled with excess energy (i.e. macronutrient), saturated fatty acids and sugar and in some people alcohol consumption, and is known to disrupt intestinal permeability [233]. In contrast, consumption of a varied, healthier diet can contribute to the maintenance of the intestinal barrier. Consumption of dietary fibre, and subsequent gut microbe produced short-chain fatty acids, vitamin D, and antioxidants, such as polyphenols and anthocyanin, have been shown to improve intestinal permeability [234].

Intracellular junctions, such as tight junctions (*Figure 1.2*, *Chapter 1.1.*), located at cell-cell adhesion points, can dynamically regulate epithelial permeability in response to a variety of stimuli [235]. Tight junctions consist of a range of intracellular proteins, including zonula occludens (ZO)-1, 2, and 3, and extracellular proteins, such as occludin and claudin proteins [192]. Tight junction protein expression and localisation can be disrupted rapidly and more slowly through the increased presence of TNF-α and IL-13, respectively [35]. Myosin light-chain kinase (MLCK) is the principal regulator of tight junction dysfunction induced by TNF-α; MLCK activation and subsequent MLC phosphorylation induces the internalisation of occludin and an increase in paracellular permeability [236]. Consequently, inhibiting MLCK activation has become a target in preventing cytokine-induced tight junction dysfunction. Dietary components, including curcumin [237] and puerarin [238], and sodium butyrate [239] have been shown to prevent tight junction dysfunction through the inhibition of MLCK.

ω-3 PUFAs are nutrients that exhibit anti-inflammatory properties, particularly through reductions in leucocyte chemotaxis and inflammatory cytokine and lipid

mediator production and increased production of ω-3 PUFA-derived lipid mediators that are anti-inflammatory and inflammation resolving [71]. However, a role for ω-3 PUFAs in the regulation of tight junctions in the intestinal epithelium has not been thoroughly explored. Evidence from rodent models mostly indicates a protective effect of dietary ω-3 PUFAs in models of intestinal inflammation including experimental colitis [84, 85, 88, 89], necrotising enterocolitis [82, 83], β-lactoglobulin-induced inflammation [94], and peritoneal dialysis [95]. Other rodent models do not support that ω-3 PUFAs have protective effects on intestinal inflammation [79, 87, 88, 97]. However, a lack of standardisation in application and dose may explain these variable results. Intestinal permeability factors, including tight junction protein expression, have also been shown to be protected by ω-3 PUFAs in various models of intestinal inflammation [82, 97, 98, 159]. Transgenic mice with increased colonic ω-3 PUFA content were also protected against macroscopic injury and changes to permeability induced by experimental colitis [92]. Consequently, supplementation of ω-3 PUFAs and increased cellular ω-3 PUFA content seems to have a protective effect on permeability *in vivo*. However, due to inconsistency of findings, this needs further exploration, whether all ω-3 PUFAs have the same effect and the mechanisms of action of ω-3 PUFAs in intestinal epithelial cells need to be identified.

To extrapolate on findings in rodent models, intestinal epithelial cell lines, including Caco-2 cells, have been used to define mechanistic changes induced by inflammatory stimuli such as cytokines, drugs and many nutrients including ω-3 PUFAs. Differentiated Caco-2 cells exhibit characteristics of mature enterocytes and form polarised monolayers cells with apical brush borders and tight junctions [180]. Caco-2 cells provide a simplified model of the *in vivo* intestinal barrier when cultured on permeable inserts, giving access to both apical and basolateral sides and providing an opportunity to assess molecular mechanisms of action which are sometimes difficult to assess *in vivo* [240]. In this chapter, a Caco-2 cell model will be used to assess changes to epithelial cell permeability when stimulated with inflammatory cytokines (TNF-α, IFN-γ, and IL-1β) with or without pre-treatment with a range of ω-3 PUFAs. There is some evidence that EPA and DHA can have protective effects on inflammation-induced changes to epithelial cell permeability [10]. However there has been little research on the effects of alternative ω-3 PUFAs. Hence, this chapter will assess the effects of well-studied EPA and DHA, as well as

EPA-DHA intermediate, DPA, and plant-derived ω-3 PUFAs, ALA and SDA, on permeability and permeability-associated mechanisms in cultured Caco-2 cells.

5.2. Hypotheses and aims

5.2.1. Hypotheses

- ω-3 PUFAs will attenuate the cytokine-induced increase in Caco-2 cell monolayer permeability
- ω-3 PUFAs will prevent the reorganisation and contraction of tight junction proteins
- Fish-derived ω-3 PUFAs will have more potent effects than plant-derived ω-3 PUFAs

5.2.2. Aims

- To observe changes to both ionic and macromolecular permeability after cytokine stimulation in Caco-2 cells supplemented with ω-3 PUFAs
- To visualise tight junction proteins after cytokine stimulation in Caco-2 cells supplemented with ω-3 PUFAs
- To determine alterations to tight junction-associated proteins after cytokine stimulation of Caco-2 cells supplemented with ω-3 PUFAs
- To compare the effects of individual ω-3 PUFAs and in particular, the effects of oily fish-derived ω-3 PUFAs *vs* plant-derived ω-3 PUFAs

5.3. Methods

5.3.1. ω-3 PUFA and cytokine treatments

Caco-2 cells were grown on transwell plates for 21 days until differentiation (*Chapter 2.1.2.*). After 21 days, cell culture medium in the apical compartment was supplemented with 25 μM EPA, DHA, DPA, ALA, or SDA. Control cultures were supplemented with culture medium only. Ethanol concentrations were maintained at 0.1% across all conditions including controls. To induce inflammation, pro-inflammatory cytokines TNF-α, IFN-γ, and IL-1β were added to culture medium at 5 ng/ml, 50 ng/ml, and 5 ng/ml, respectively.

5.3.2. Permeability measurements

As described in *Chapter 2.4.1.* and *2.4.2.*, permeability was assessed by TEER and FITC-dextran permeability. TEER measurements were taken prior to ω-3 PUFA supplementation, after 48 hours ω-3 PUFA supplementation, and after 24 hours cytokine stimulation. After cytokine stimulation, culture medium was replaced with HBSS containing FITC-dextran in the apical compartment of the transwells. After 1 hour, aliquots of medium were taken from the basolateral compartment to assess flux of FITC-dextran. These aliquots were added to wells of a 96-well plate and read on a plate reader at 475 nm excitation and 500-550 nm emission.

5.3.3. Confocal imaging of tight junction proteins

Confocal images were taken to observe changes to tight junction protein distribution. After differentiation, Caco-2 cells were treated with ω-3 PUFAs for 48 hours followed by 24 hours stimulation with pro-inflammatory cytokines (*Chapter 5.3.1.*). Cells were then fixed in ice-cold methanol and pre-blocked in 2% BSA in PBS (*Chapter 2.6.*). Tight junction proteins, ZO-1 and occludin, and cell nuclei were stained with primary antibodies and corresponding secondary antibodies (*Chapter 2.6.*). Images were taken at a single Z-location.

5.3.4. Quantification of permeability-associated proteins by Western blotting

Protein was extracted from Caco-2 cells treated with or without ω-3 PUFAs for 48 hours, followed by 24-hour incubation with or without pro-inflammatory cytokines (*Chapter 5.3.1*). After each treatment, cells were lysed, and protein was isolated (*Chapter 2.8.1.*). 20-30 μg protein per sample, as defined by the BCA assay (*Chapter 2.8.2.*), was size-fractionated against a pre-stained protein ladder and transferred onto a PDVF membrane for antibody staining (*Chapter 2.8.5.*). The staining procedure is described in *Chapter 2.8.6.*; in brief, blots were blocked for 1 hour before incubation with primary antibodies overnight. Blots were stained with primary antibodies for MLCK (abcam; ab76092), phosphorylated-myosin light chain (pMLC; Cell Signalling Technology; 3671S), or GAPDH (abcam; ab128915) overnight. After primary antibody incubation, blots were washed and then incubated with secondary antibody (abcam; ab205718) for 1 hour. Before imaging, blots were washed, and protein signals were enhanced using a chemiluminescent substrate. Proteins signals were quantified using ImageJ software.

5.3.5. Statistical analysis

Shapiro-Wilk normality tests were performed to assess Gaussian distribution of results. Statistical differences were identified using one-way ANOVA, if Gaussian distribution was determined, whereas Kruskal-Wallis test were used if significant skewness from normal distribution was detected. Normality tests are displayed in *Appendix*.

5.4. Results

5.4.1. ω-3 PUFA supplementation had no effect on cytokine-induced increased paracellular permeability

As shown in *Chapter 3.3.4.* a combination of inflammatory cytokines (TNF-α, IFN-γ, and IL-1β) induced a significant increase in permeability after 24 hours stimulation. In the current experiments, Caco-2 cells were pre-supplemented with ω-3 PUFAs for 48 hours prior to cytokine stimulation.

As shown in *Figure 5.1*, ω-3 PUFAs themselves had no effect on permeability. In addition, they were unable to prevent the cytokine-induced increase in paracellular permeability. TEER was not significantly affected after 48 hours supplementation with any ω-3 PUFA used. Control cell TEER values slightly decreased after 48 hours to approximately 95.8% and after cytokine stimulation TEER values were approximately 60.6% of pre-treatment values. EPA-treated cells were the most similar to control cells with TEER decreasing after the supplementation period (98.5%) and decreasing to 65.4% after cytokine stimulation. DHA and DPA seemed to slightly increase TEER after supplementation (DHA: 103.0%, DPA: 103.1%) and the TEER decreases seen after cytokine stimulation were similar in cells supplemented with these ω-3 PUFAs (DHA: 66.1%, DPA: 66.6%). Plant-derived PUFAs, ALA and SDA, had similar effects on TEER after supplementation and cytokine stimulation. Both these ω-3 PUFAs had little effect on TEER after supplementation (ALA: 99.6%, SDA: 100.1%) and had similar effects to other ω-3 PUFAs after cytokine stimulation (ALA: 66.2%, SDA: 67.0%). There were no significant differences between TEER values on day 21 and after PUFA treatments for all conditions. TEER was significantly reduced after cytokine stimulation compared to day 21 and post-PUFA treatment TEER in all conditions ($p<0.0001$).

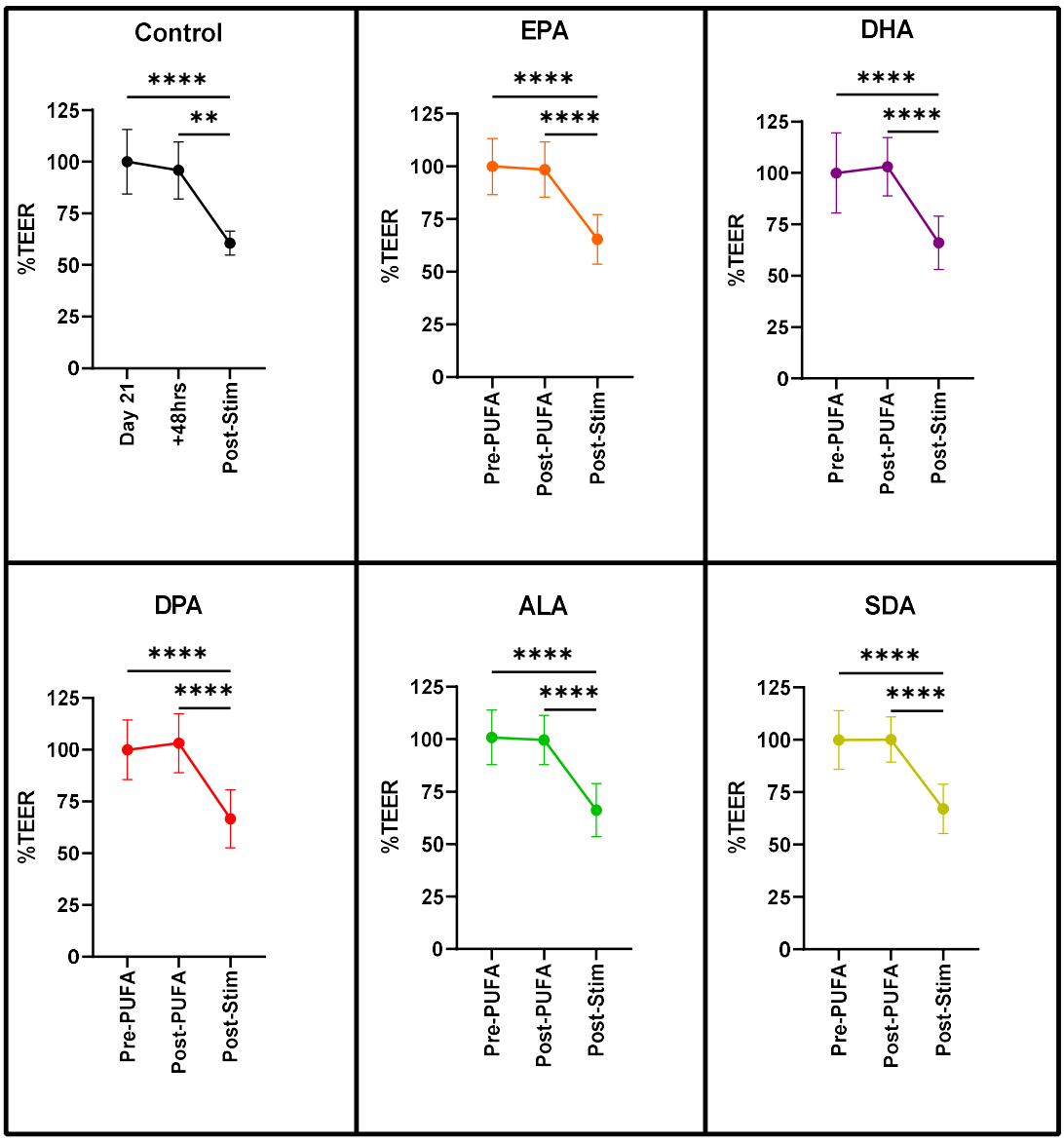

*Figure 5.1: Changes in TEER after 24 hours combined TNF-α, IFN-γ, and IL-1β stimulation with or without 48 hours pre-incubation with ω-3 PUFAs (25 μM; EPA, DHA, DPA, ALA, or DPA). Cells were grown for 21 days (pre-PUFA) before measurements. TEER values are presented as %TEER, where: %TEER = (Final Reading/Initial Reading)*100. Values were then normalised to Day 21/Pre-PUFA readings. Data are displayed as mean±standard deviation. Statistical comparisons were determined by non-parametric Kruskal-Wallis tests with Dunn's multiple comparisons tests, ** p<0.01 and **** p<0.0001. Data are from 2-3 biological replicates from 7 independent experiments for each condition.*

TEER was consistently changed by cytokine stimulation, regardless of pre-treatment with any ω-3 PUFA. FITC-dextran permeability was also unaffected by ω-3 PUFA pre-treatment, as shown in *Figure 5.2*. TEER decreases ranged from 28-45% across all samples and, in the majority of these samples, FITC-dextran flux remained low (<50

ng/ml/min). Overall, no effect of ω-3 PUFA treatment on macromolecular permeability was observed in cytokine-treated Caco-2 cells.

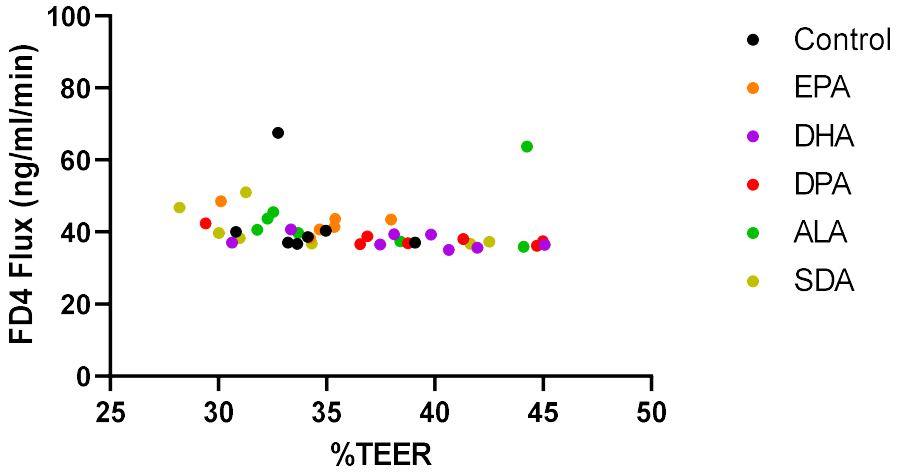

*Figure 5.2: Changes in TEER after 24 hours cytokine stimulation with or without ω-3 PUFA pre-treatment compared with FITC-dextran permeability 1 hour after cytokine treatment. Cells were treated with ω-3 PUFAs for 48 hours prior to cytokine stimulation. TEER values are presented as %TEER, where: %TEER = (Final Reading/Initial Reading)*100. Values were then normalised to Day 21/Pre-PUFA readings. Data are from 2-3 biological replicates from 3 independent experiments. Each data point is a mean value of 3 technical replicates.*

5.4.2. Observation of monolayers treated with ω-3 PUFAs and/or cytokines by confocal imagery

The results in *Chapter 5.4.1.* indicate that ω-3 PUFAs were not able to influence the changes in permeability induced by pro-inflammatory cytokines. To investigate the lack of effect seen for both cytokines and ω-3 PUFAs on macromolecular permeability, confocal images were taken of tight junction proteins ZO-1 and occludin in cells treated with ω-3 PUFAs and/or cytokines.

Confocal images were taken to compare control Caco-2 cells and cells stimulated with pro-inflammatory cytokines with or without prior treatment with ω-3 PUFAs. A single sample was observed for each condition and therefore tight junction proteins were not quantified. As shown in *Figures 5.3* and *5.4*, occludin staining was apparent in all conditions, whilst ZO-1 staining was not. There was little observable change in occludin expression between stimulated and unstimulated cells, except in cells treated with DHA. In DHA treated cells, stimulation seemed to dissociate

occludin from cellular junctions, as staining became less sharp at cell-cell adhesion points indicating dispersion of occludin proteins. The other notable observation is the appearance of 'ruffling' in stimulated EPA pre-treated cells, although this was not consistent across stimulated cells. No observable effects on occludin were seen in ALA, SDA, and DPA supplemented cells either in control or stimulated conditions (*Figure 5.4*).

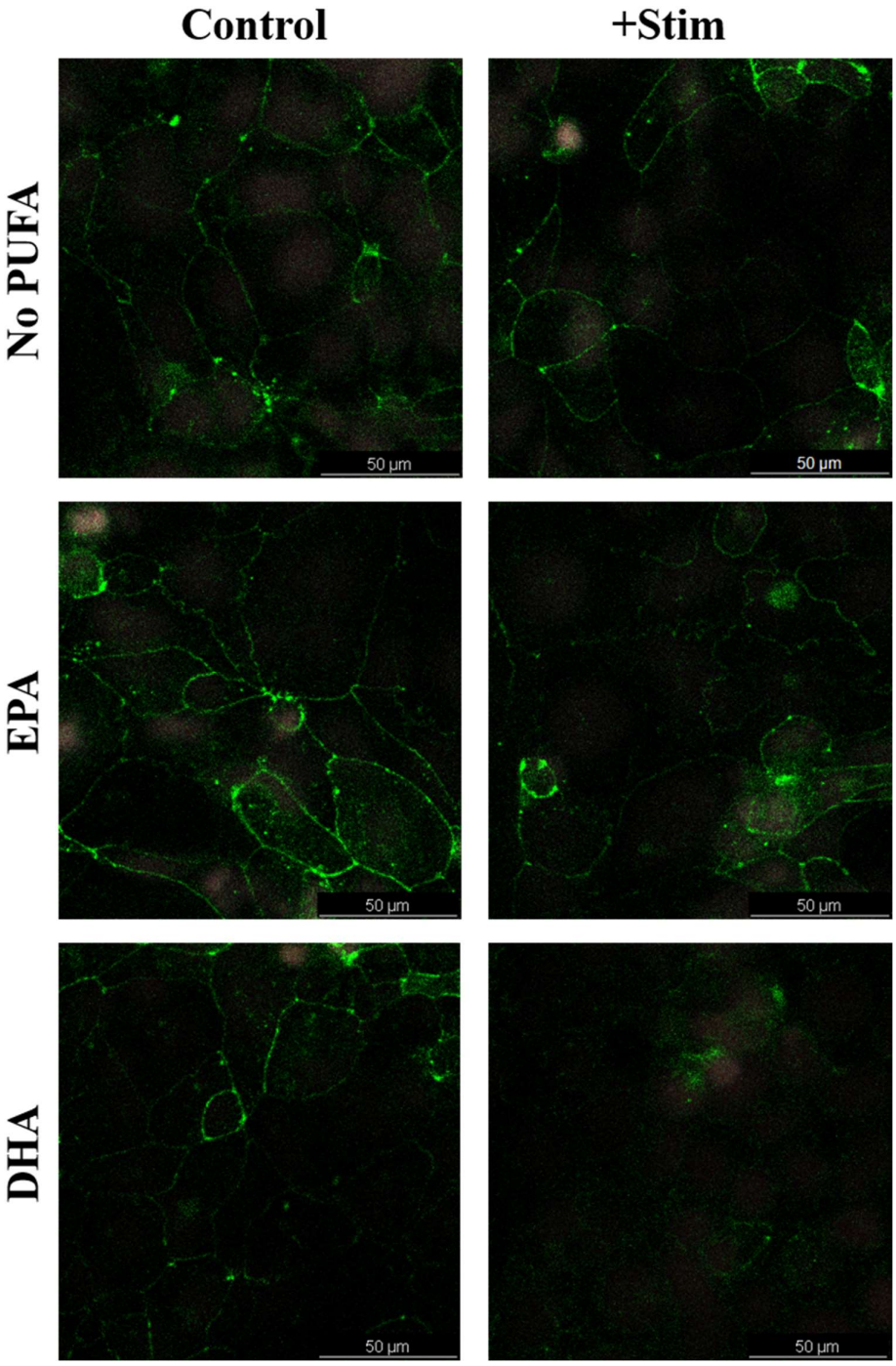

Figure 5.3: Confocal images of tight junctions in control Caco-2 cells or Caco-2 cells treated with pro-inflammatory cytokines (TNF-α, IFN-γ, and IL-1ß) for 24 hours with or without 48 hours pre-treatment

with EPA and DHA (25 uM). Occludin staining is shown in green, ZO-1 staining in red, and nuclei staining in white. Images were taken from a single experiment.

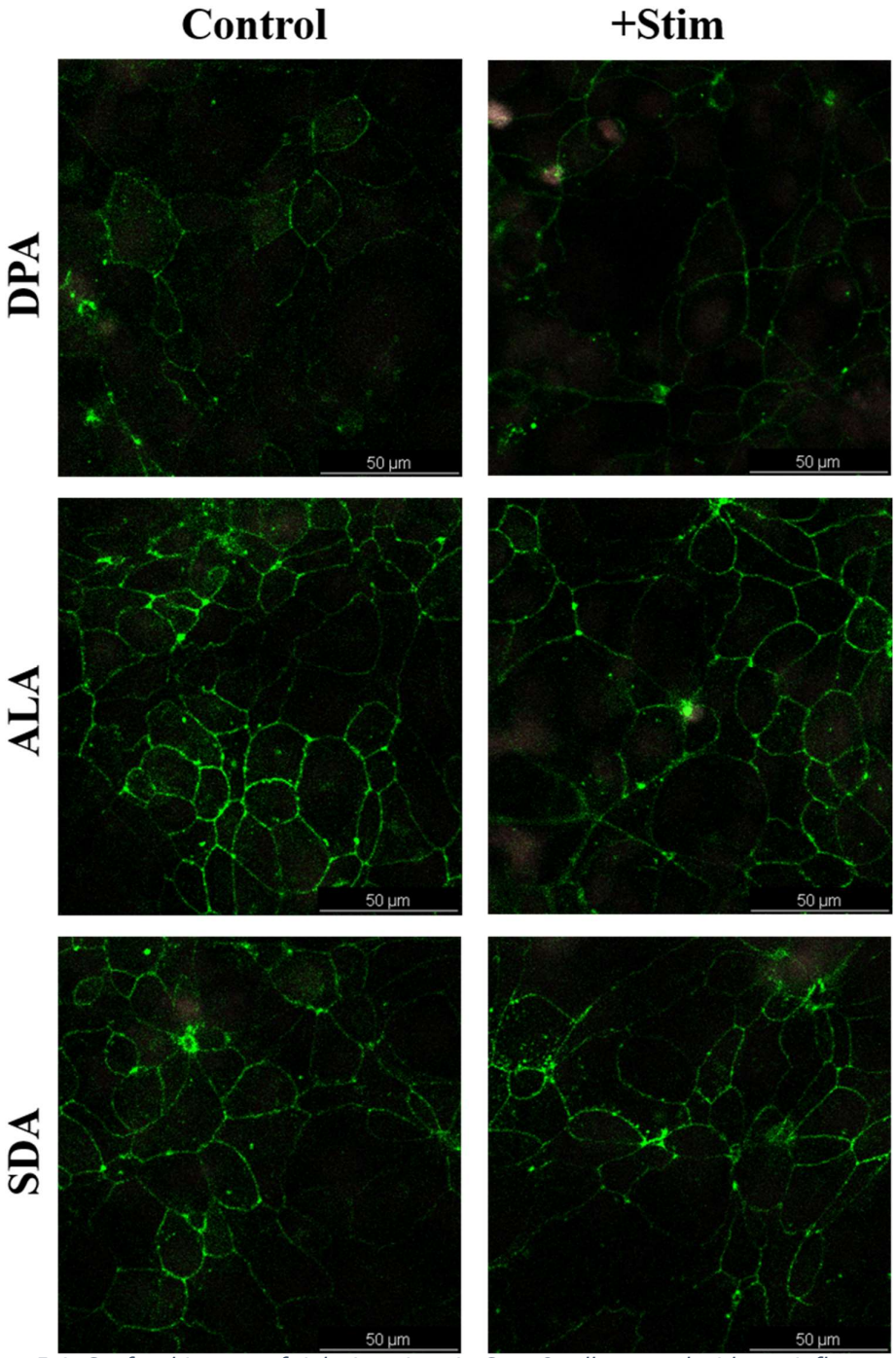

Figure 5.4: Confocal images of tight junctions in Caco-2 cells treated with pro-inflammatory cytokines (TNF-α, IFN-γ, and IL-1β) with or without 48 hours pre-treatment with DPA, ALA, or SDA (25 uM). Occludin staining is shown in green, ZO-1 staining in red, and nuclei staining in white. Images were taken from a single experiment.

5.4.3. Cytokines induce variable effects on tight junction-associated protein expression

As no effects of cytokines were observed in macromolecular permeability, indicated by both FITC-dextran measurements (*Chapter 5.4.1.*) and confocal imagery (*Chapter 5.4.2.*), increases in permeability associated with drops in TEER could be associated to contraction of tight junctions and the subsequent opening of ion channels. MLCK is an important regulator of epithelial cell tight junction contraction, through phosphorylation of actin-associated MLC. MLCK and pMLC protein expression were quantified by Western blotting to assess changes to MLCK expression and activity.

As shown in *Figure 5.5*, MLCK expression varied across the stimulation period. MLCK expression reduced by ≈35% after 15 minutes stimulation with cytokines and gradually increased back to non-stimulated (time 0) levels after stimulation for 1 hour. MLCK expression remained relatively stable after 1 hour until 6 hours. Although these trends were observed, statistical significance was not achieved.

To assess the activity of MLCK, the appearance of pMLC was assessed by Western blotting (*Figure 5.5*). pMLC expression was assessed at various time points, up to 6 hours after stimulation. The appearance of pMLC was not distinguishable from controls until 3 hours after stimulation. Both 3- and 6-hours stimulation seemed to induce increases in pMLC to levels approximately 5 times that of unstimulated cells (time 0), however, due to a low sample number, statistical differences could not be assessed.

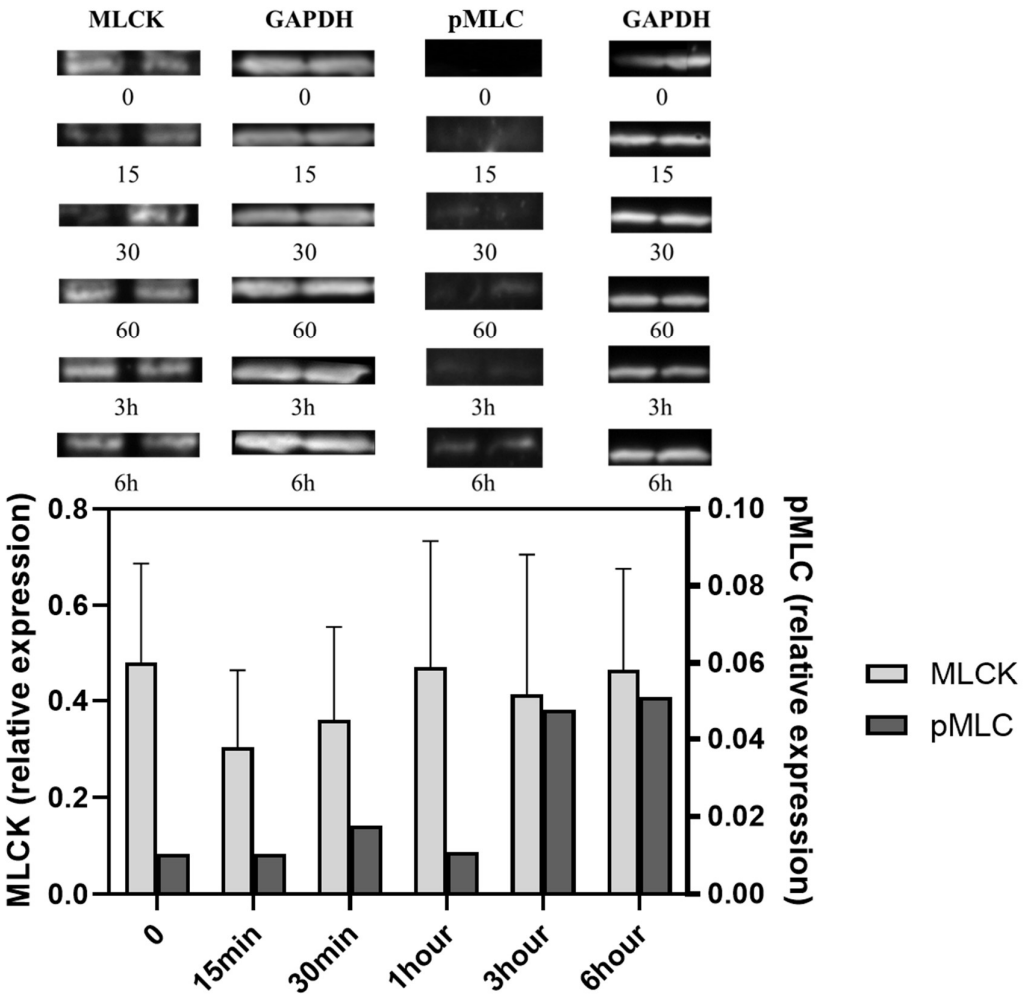

Figure 5.5: MLCK and phosphorylated(p)MLC protein expression quantified by Western Blot. Target proteins were quantified against reference protein, GAPDH. Caco-2 cells were stimulated for up to 6 hours with TNF-α, IFN-γ, and IL-1β (5 ng/ml, 50 ng/ml, and 5 ng/ml, respectively). MLCK data were from 2 biological replicates from 4 independent experiments. pMLC data were from 2 biological replicates from 2 independent experiments. Statistical differences were determined by non-parametric Kruskal-Wallis tests with Dunn's multiple comparisons tests.

5.4.4. ω-3 PUFAs had variable effects on tight junction-associated protein expression in control and cytokine-stimulated conditions

Cytokines drive changes to the regulator of tight junction contraction, MLCK, including expression and activation, through the phosphorylation of MLC. Whether ω-3 PUFAs have any effect on permeability under non-stimulated and stimulated conditions remains unclear.

MLCK expression appeared to be higher in cells treated with ω-3 PUFAs, in particular, cells treated with EPA and DPA (*Figure 5.6*). In control cells, significant changes in MLCK expression after cytokine stimulation could not be determined due to a lack of independent experiments. ω-3 PUFA treatment seemed to increase the expression of MLCK, although statistical differences could not be determined. After cytokine treatment, variable changes to MLCK expression were observed. In EPA-treated cells MLCK expression was lower after cytokine stimulation while in DHA-treated cells MLCK expression seemed to increase after cytokine stimulation, although neither of these differences was statistical significance could not be determined. DPA, ALA, and SDA pre-treatment had no observable effect on MLCK expression after cytokine treatment. A lack of significant effect of ω-3 PUFA treatment on MLCK expression corresponds with the lack of overall effect of these fatty acids on TEER and FITC-dextran (*Chapter 5.4.1.*).

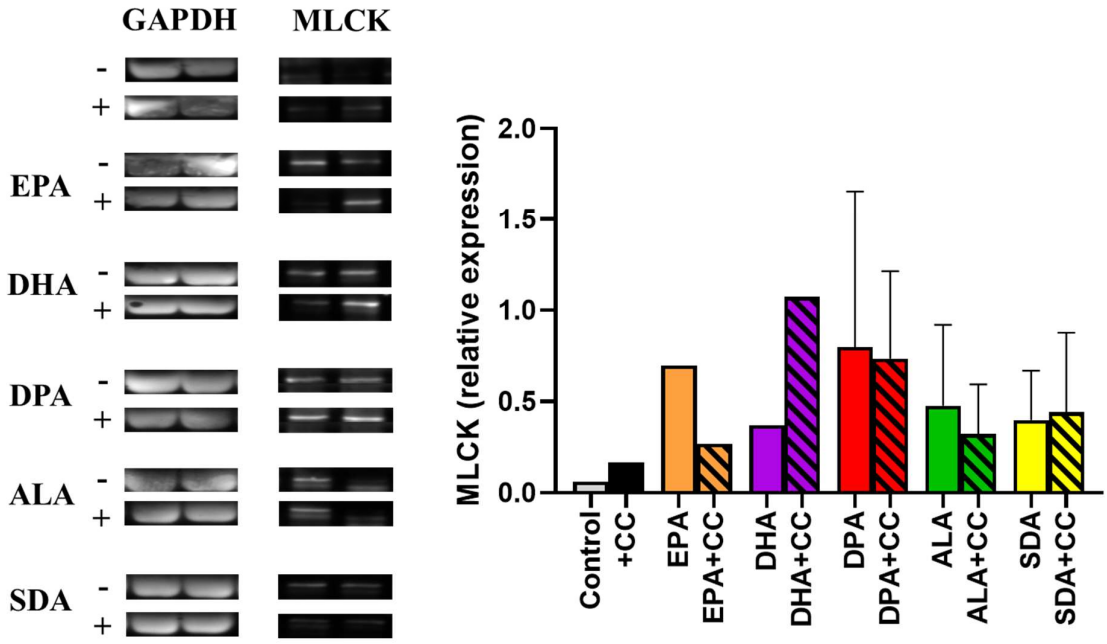

Figure 5.6: MLCK expression in cells treated with ω-3 PUFAs (EPA, DHA, DPA, ALA, or SDA) for 48 hours with (+) or without (-) an additional 1-hour cytokine treatment (CC). MLCK expression was relative to the expression of GAPDH. Control, EPA, and DHA data were from 2 biological replicates from 2 independent experiments. DPA, ALA, and SDA data were from 2 biological replicates from 3 independent experiments. Statistical comparisons in the DPA, ALA, and SDA groups were determined by Mann-Whitney test. Example blots are from 2 biological replicates from 1 independent experiment.

As shown in *Figure 5.7*, the activity of MLCK was affected differently by cytokine treatment and ω-3 PUFA treatment. In untreated cells, cytokine treatment increased pMLC expression, which corresponded to the increase in MLCK seen in *Figure 5.6*. EPA and DHA-treated cells had the highest pMLC expression, greater than both unstimulated and cytokine-stimulated control cells. ALA and SDA-treated cells expressed similar levels of pMLC to controls, whilst DPA-treated cells expressed lower levels of pMLC. Cytokine treatment reduced pMLC levels in EPA and DHA-treated cells, although pMLC expression remained higher than in control cytokine-stimulated cells. pMLC expression was also decreased in ALA and SDA-treated cells after cytokine stimulation. DPA-treated cells were the only cells to have increased expression of pMLC after cytokine stimulation; however, pMLC expression remained lower than in control cells. Due to the small sample size, these observed differences could not be statistically analysed.

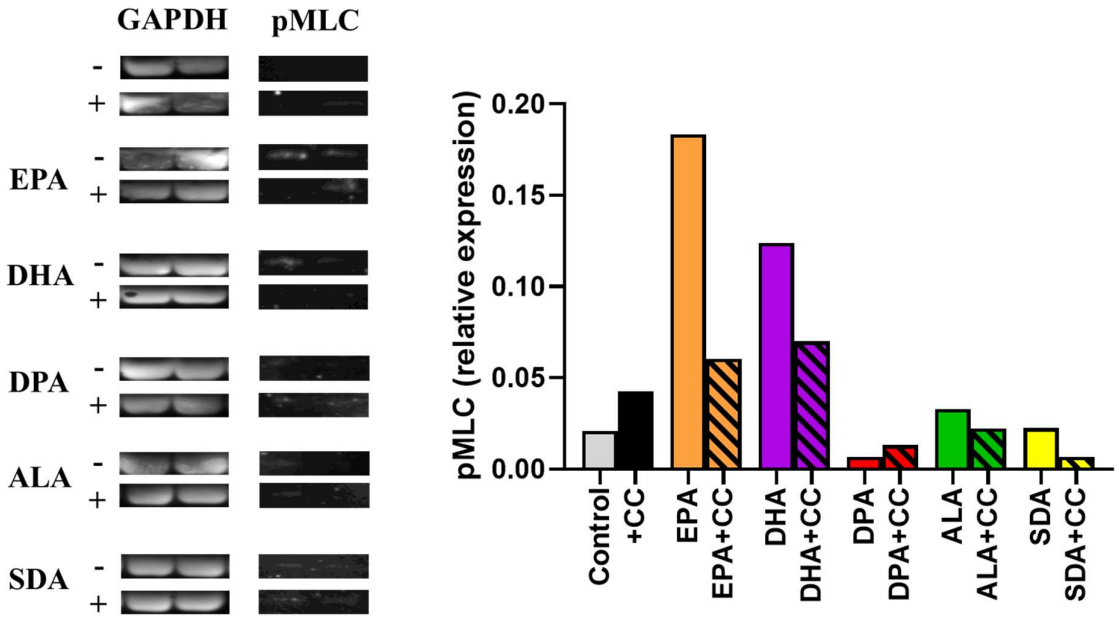

Figure 5.7: pMLC expression in cells treated with ω-3 PUFAs (EPA, DHA, DPA, ALA, or SDA) for 48 hours with (+) or without (-) an additional 1-hour cytokine treatment (CC). pMLC expression was relative to the expression of GAPDH. Data and example blots were from 2 biological replicates from 1 independent experiment.

5.5. Discussion

The aim of this chapter was to assess the effect of ω-3 PUFAs on intestinal epithelial cell permeability in control and cytokine-stimulated conditions. Overall, ω-3 PUFAs

seemed to have little effect on parameters of Caco-2 cell permeability. TEER results indicated that ω-3 PUFA-treated cells followed a similar pattern to control cells, after ω-3 PUFA treatment and cytokine stimulation (*Figure 5.1*). ω-3 PUFA supplementation also had no significant effect on FITC-dextran permeability. TEER decreased by between 25 to 45% after cytokine stimulation, which was not correlated with any treatment condition. FITC-dextran permeability remained low and was not correlated with lower TEER. In some cases, FITC-dextran measurements were drastically changed after ω-3 PUFA and cytokine treatment (greater than 100 ng/ml/min decrease), and these were excluded from the results (Control: N=2, EPA: N=3, DHA: N=1, DPA: N=2, ALA: N=2, SDA: N=2). Cytokine stimulation seemed to irreversibly disrupt Caco-2 monolayers, although as shown in the confocal imagery (*Figure 5.3* and *5.4*), tight junction protein distribution seemed relatively unaffected. Each of the cytokines used as a stimulant in these experiments, IFN-γ, TNF-α, and IL-1β, is known to regulate epithelial permeability during inflammation. IFN-γ induces disruption to tight junction protein distribution and expression, and can affect actin-myosin contractility [186]. TNF-α induces barrier dysfunction by inducing MLCK activity and increased expression of the pore-forming tight junction protein, claudin-2 [186]. IL-1β has also been shown to induce MLCK activity and can redistribute occludin during inflammation [186]. The increase in pMLC seen 3 and 6 hours after cytokine stimulation (*Figure 5.6*) is consistent with these known effects of TNF-α and IL-1β, although due to a lack of power significance was not achieved.

The variety of mechanisms implicated in the barrier dysfunction in this model may explain why ω-3 PUFAs had no effect on permeability. Previous evidence has suggested that EPA and DHA can prevent changes to permeability and associated tight junction protein redistribution induced by combined TNF-α and IFN-γ in the T84 epithelial cell model [157], using the same (25 μM) and higher concentrations (50 and 75 μM) of ω-3 PUFAs as used in this study. EPA and DHA at 100 μM were also shown to prevent IL-4-induced increases in permeability in T84 cells [153]. Previously, Usami et al. described that, at high doses, ALA, EPA, and DHA supplementation induced increases in permeability in Caco-2 cells [154, 155]. However, using up to 25 μM in these experiments, no effect on permeability was observed [154, 155]. In a separate model, Beguin et al. reported that 30 μM ALA, EPA, and DHA supplementation for 7 days did not affect Caco-2 cell permeability in non-stimulated conditions [160]. ALA and DHA, but not EPA, were able to attenuate combined cytokine and LPS-induced loss of occludin expression in Caco-2 cells, but

had no significant effect on TEER [160], which corresponds with the results presented in this chapter.

Cytokine induction of increased paracellular permeability seemed to be associated with an increase in MLCK expression and activity. The association between MLCK activity/expression and ω-3 PUFAs did not follow a particular pattern. MLCK expression was seemingly increased by all PUFAs to different extents with EPA and DPA increasing MLCK expression more so than ALA, SDA, and DHA. However, due to small sample size, it is hard to distinguish for certain the effect of ω-3 PUFAs on MLCK expression. Elsewhere, in the literature, evidence for an effect of ω-3 PUFAs on MLCK expression is scarce. One study described that fatty acid methyl esters from fish oil induced an increase in MLCK mRNA expression, but had no effect on permeability in Caco-2 cells [241]. Other nutrients, including glucose and medium chain fatty acids, can induce MLCK expression and activity and this is directly associated with hyper-permeability in epithelial cells [242]. However, some evidence suggests that increased MLCK expression may not always be associated with increased paracellular permeability. MLCK expression was increased in IL-18 stimulated Caco-2 cells, leading to IL-18-mediated disruption of occludin expression, although paracellular permeability remained unaffected [243]. After cytokine stimulation, MLCK expression varied according to ω-3 PUFA used. MLCK expression was relatively similar between cells treated with DPA, ALA, and SDA. Observable differences were seen in cells treated with EPA and DHA, although EPA-treated cells showed a decrease in MLCK after cytokine stimulation, whilst DHA-treated cells showed increased MLCK expression after cytokine stimulation. However, again these results must be interpreted with caution, and increasing the sample size may better identify the effect of different ω-3 PUFAs on MLCK expression in unstimulated and inflammatory conditions. The effects of ω-3 PUFA treatment or supplementation on MLCK expression have not been reported extensively elsewhere. MLCK expression can be associated with both increased contractility of tight junctions and epithelial cell shedding under inflammatory conditions [244]. MLCK hyper-expression is also attributed to alteration in cell morphology, through the contraction of the actin-myosin cytoskeleton [245]. Therefore, increased MLCK expression in ω-3 PUFA treated Caco-2 cells may alter cell morphology but does not subsequently affect monolayer permeability.

As shown in *5.4.1.*, cytokine stimulation consistently increased paracellular permeability regardless of ω-3 PUFA treatment. After cytokine stimulation, it is

expected that MLCK expression and subsequently MLCK activity will increase and, as shown in *Figures 5.3* and *5.4*, this pattern was seen in control cells, although statistical significance could not be determined. In ω-3 PUFA-treated cells, the pattern was less clear. MLCK expression was markedly increased by all ω-3 PUFAs, however, MLCK activity did not correspond to these increases for all ω-3 PUFA treatments. pMLC expression in EPA and DHA-treated cells decreased after cytokine stimulation, although pMLC expression exceeded that of both unstimulated and stimulated controls. Decreased pMLC expression was not associated with MLCK expression in DHA-treated cells, whilst decreased pMLC expression in EPA-treated cells seemed to correspond with decreases in MLCK expression. Li et al. reported that EPA and DHA prevented cytokine-induced changes in permeability attributed to tight junction disruption through changes in protein distribution and morphology [246]. Effects on MLCK were not reported in this study however and in the literature overall, the effect of ω-3 PUFAs on MLCK expression and activity are not reported. In a Caco-2 cell model, medium-chain fatty acids induce tight junction dysfunction by inducing MLCK activation [247], supporting the hypothesis that long-chain ω-3 PUFAs could induce MLCK activation. However, overexpression and activation of MLCK have been shown to increase paracellular permeability in Caco-2 cells [248], although MLCK expression and activation did not seem directly linked in this model.

Results from this chapter indicate that cytokine-induced changes to permeability are unaffected by ω-3 PUFA supplementation. Cytokine-induced disruption seemed to be independent from the tight junction contractility regulator, MLCK. Evidence elsewhere suggests ω-3 PUFAs, especially EPA and DHA, have protective effects on intestinal permeability through enhanced tight junction protein expression and suppression of inflammation-induced tight junction protein redistribution and distortion [249]. Confocal imagery of tight junction proteins in this chapter seemed to show that tight junction protein distribution remained unaffected by ω-3 PUFA supplementation and cytokine stimulation. As a result, further investigation into the effects of ω-3 PUFA supplementation on cytokine-induced inflammation is required as alteration in permeability is not the only facet of epithelial cell inflammation.

Chapter 6 - Can ω-3 PUFAs inhibit inflammatory mediator production by cytokine-stimulated Caco-2 cells?

6.1. Introduction

The role of the gut epithelium as a semi-permeable barrier responsible for regulated intestinal permeability is well documented. Soluble protein mediators, including cytokines and chemokines, support intestinal mucosal homeostasis through regulation of epithelial cell proliferation, cell death, and barrier permeability [179]. Regulated mediator production by epithelial cells has a role in the crosstalk between commensal bacteria and the intestinal immune system [250]. Intestinal epithelial cell mediator production can also condition other epithelial cell subtypes, such as dendritic cells, to maintain homeostatic mechanisms within the intestinal epithelium [251]. Microbial dysbiosis and cytokine production by intestinal immune cells drive the loss of epithelial cell function and generate pro-inflammatory processes within the gut epithelium [100]. Dietary habits, including the intake of a variety of foods and nutrients, can protect or impair regulated epithelial function. Some nutrients, including ω-3 PUFAs, have been shown to be protective in the intestinal epithelium, in terms of regulated permeability, regulated inflammatory mechanisms, and regulated interactions with other components of the intestinal barrier [10]. Crosstalk between intestinal microbes and intestinal immune cells is partly governed by cytokine output by epithelial cells. During inflammation or intestinal injury, epithelial cells increase production of chemotactic cytokines and chemokines to elicit processes in adjacent cells to re-establish a functional barrier [252]. Over-expression of mediators by epithelial cells is thought to contribute to barrier dysfunction, although due to the large quantity of inflammatory mediators produced by immune cells it is hard to distinguish mediators from those cells and from epithelial cells [173]. Epithelial cell models, such as Caco-2 cells, provide some insight into specific mediators produced by epithelial cells and the subsequent modulation by ω-3 PUFAs. Some ω-3 PUFAs are known to have regulatory effects on intestinal cell mediator production, both *in vitro* and *in vivo* [10].

Inflammatory mediator production is governed by a range of inflammatory processes including the transcription factor, NF-κB. NF-κB activation is controlled

by the phosphorylation of particular subunits by IκB kinase (IκK) induced by a variety of mechanisms including cellular responses to cytokine stimulation [253]. IκK phosphorylation of inhibitory subunit IκBα leads to the ubiquitination and subsequent degradation of this subunit allowing for nuclear translocation of NF-κB and transcription of NF-κB-associated genes [253]. Cytokine stimulation can increase phosphorylation of the NF-κB p65 subunit leading to activation through a conformational change [254]. The role of ω-3 PUFAs in the resolution of intestinal inflammation can be attributed to a variety of mechanisms and it is thought that suppression of NF-κB activation and subsequent down-regulated production of inflammatory mediators is one of these mechanisms. In transgenic mice with higher concentrations of ω-3 PUFAs, namely EPA, DPA, and DHA, colonic NF-κB activity was attenuated upon induction of colitis [92]. This suggests that higher concentrations of ω-3 PUFAs in intestinal tissue may suppress NF-κB activation. Consequently, this study will aim to establish a link between increased presence of a range of ω-3 PUFAs within epithelial (Caco-2) cells and regulation of NF-κB activity, as well as modulation of inflammatory mediators.

This chapter will aim to establish whether pre-treatment with ω-3 PUFAs can attenuate cytokine-induced inflammation in Caco-2 cells. Caco-2 cell inflammatory response will be quantified by measuring inflammatory cytokine and chemokine production, including the production of ICAM-1, CXCL9, CXCL8, VEGF, and IL-6 proteins, as well as the activation of and expression of proteins associated to the NF-κB signalling pathway.

6.2. Hypotheses and aims

6.2.1. Hypotheses

- ω-3 PUFAs will inhibit the production of inflammatory mediators by Caco-2 cells stimulated with pro-inflammatory cytokines.
- DHA will exhibit the most anti-inflammatory effects in cytokine-stimulated conditions compared to other ω-3 PUFAs.
- ω-3 PUFAs will decrease activation of NF-κB through effects on the signalling pathway leading to NF-κB activation.

6.2.2. Aims

- To assess Caco-2 cell production of pro-inflammatory and anti-inflammatory mediators by multiplex assay.

- To assess inflammatory mechanisms associated with cytokine expression by Western blot.
- To determine whether ω-3 PUFAs can suppress activation of inflammatory mediator production and associated inflammatory mechanisms.

6.3. Chapter-specific Methods

6.3.1. Multiplex analysis of Caco-2 cell supernatants

Multiple analytes associated with epithelial inflammation were measured using multiplex assays (Luminex). Supernatants were obtained from Caco-2 cells pre-treated with 25 μM EPA, DHA, DPA, ALA and SDA for 48 hours and then stimulated with pro-inflammatory cytokines for 24 hours (*Chapter 2.2.*). Controls were not pre-treated with ω-3 PUFAs and either stimulated or unstimulated. In brief, standards for ICAM-1, CXCL9, CXCL8, VEGF, and IL-6 and cell supernatants were suspended in microparticle solution and incubated for 2 hours at room temperature with gentle agitation. After incubation, microparticles were washed 4 times with wash buffer and biotin antibody solution was added for 1 hour at room temperature with gentle agitation. After incubation, microparticles were washed (as above) and streptavidin-phycoerythrin solution was added for 30 minutes at room temperature with gentle agitation. Microparticles were washed (as above) and resuspended in wash buffer. Plates were read on a Bio-Plex analyser (Bio-Rad, UK).

6.3.2 Western Blot of inflammation-associated proteins

Protein was obtained from Caco-2 cells treated with or without ω-3 PUFAs for 48 hours, followed by 24-hour incubation with or without pro-inflammatory cytokines (*Chapter 5.3.1*). After each treatment, cells were lysed, and protein was obtained (*Chapter 2.8.1.*). 20-30 μg protein per sample, as defined by BCA assay (*Chapter 2.8.2.*), was size-fractionated against a pre-stained protein ladder and transferred onto a PDVF membrane for antibody staining (*Chapter 2.8.5.*). The staining procedure is described in *Chapter 2.8.6.*; in brief, blots were blocked for 1 hour before incubation with primary antibodies overnight. Blots were then stained with primary antibodies for NF-κB p65 (abcam; ab32536), phospho-(p)NF-κB p65 (abcam; ab76302), IκBα (abcam; ab76429), phospho-IκBα (Cell Signalling Technology; 2895S) or GAPDH (abcam; ab128915) overnight. After primary

antibody incubation, blots were washed and were incubated with secondary antibody (abcam; ab205718) for 1 hour. Before imaging, blots were washed, and protein signals were enhanced using a chemiluminescent substrate. Proteins signals were quantified using ImageJ software.

6.3.3. Statistical analysis

Shapiro-Wilk normality tests were performed to assess Gaussian distribution of results. Statistical differences were identified using one-way ANOVA, if Gaussian distribution was determined, whereas Kruskal-Wallis test were used if significant skewness from normal distribution was detected. Normality tests are displayed in *Appendix*.

6.4. Results

6.4.1. ω-3 PUFAs and cytokine treatment had no effect on Caco-2 cell viability

Caco-2 cell viability after ω-3 PUFA treatment and subsequent cytokine stimulation was assessed by MTT assay (*Chapter 2.9.*). As shown in *Figure 6.1*, ω-3 PUFA treatments at 25 μM reduced cell viability by approximately 5-15%, although viability was not significantly different from control cells. Cytokine stimulation seemed to have little effect on cell viability with a ≈6% increase in viability seen, which was also not significantly different from unstimulated control cells. ω-3 PUFA treatment followed by cytokine stimulation also had no significant effect on Caco-2 cell viability.

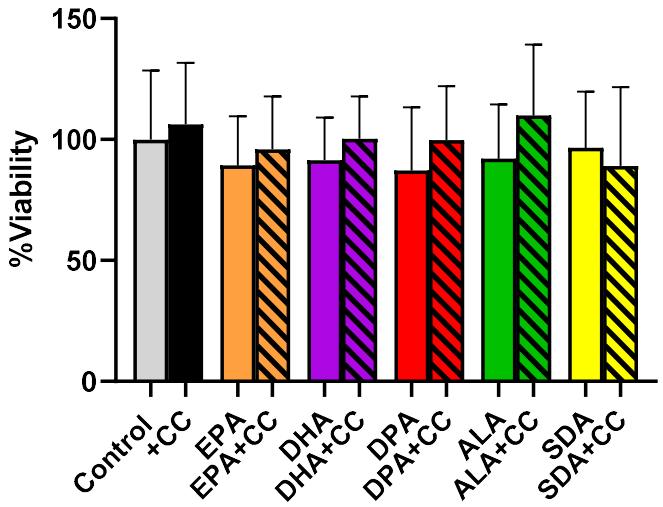

Figure 6.1: Viability of Caco-2 cells treated with ω-3 PUFAs (EPA, DHA, DPA, ALA, or SDA; 25 μM per ω-3 PUFA) for 48 hours and subsequently stimulated with pro-inflammatory cytokines (TNF-α, IFN-γ, IL-1β) for 24 hours. +CC indicates cells stimulated with cytokines. Control cells were cultured without ω-3 PUFAs and inflammatory cytokines. %Viability was determined by comparing MTT absorbance for each condition against the mean of unstimulated control cells, i.e. (sample MTT reading/average control MTT reading) x100 = %Viability. Data are displayed as mean±standard deviation. Statistical differences were determined using Brown-Forsythe and Welch ANOVA with Dunnett's multiple comparisons tests.

6.4.2. ω-3 PUFAs differentially alter Caco-2 cell cytokine production

Incubation with ω-3 PUFAs altered the fatty acid composition of Caco-2 cells (*Chapter 4*) but had no effect on cytokine-induced changes in permeability (*Chapter 5*). Caco-2 cells produce a range of mediators in response to an inflammatory stimulus and it is hypothesised that ω-3 PUFAs will regulate (decrease) mediator production during inflammation.

Figure 6.2 shows that ICAM-1 concentration on both apical and basolateral sides of cultured Caco-2 cells was markedly increased by cytokine stimulation, approximately 4.1-fold in apical supernatants and 5.9-fold in basolateral supernatants. ω-3 PUFA supplementation had no significant effect on the concentration of ICAM-1 on the apical side. The concentration of ICAM-1 in the basolateral media seemed to be affected by ω-3 PUFAs, although this was not statistically significant. EPA treatment resulted in 54% higher ICAM-1 concentration than seen in control stimulated cells, whilst DHA treatment resulted

in 48% higher ICAM-1 concentration than controls. Basolateral ICAM-1 concentration was not affected by DPA, or ALA. SDA treatment decreased ICAM-1 concentration by approximately 18% compared to controls, although again this was not statistically significant.

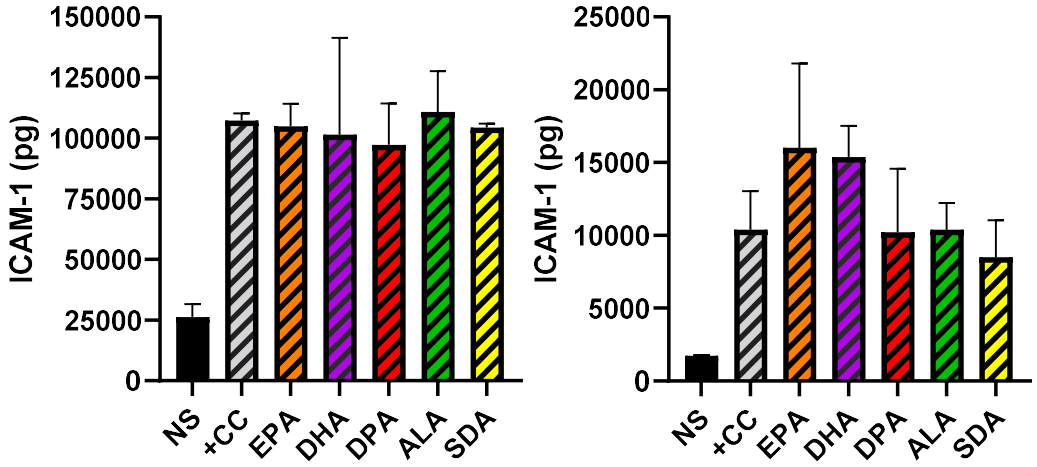

Figure 6.2: Concentration of ICAM-1 in the apical (left) and basolateral (right) medium of Caco-2 cells treated with ω-3 PUFAs (EPA, DHA, DPA, ALA, or SDA; 25 μM per ω-3 PUFA) for 48 hours and subsequently stimulated with pro-inflammatory cytokines (TNF-α, IFN-γ, IL-1β) for 24 hours. +CC indicates cells stimulated with cytokines without ω-3 PUFA pre-treatment. Unstimulated cells (NS) were cultured in culture medium only. NS data were from 3-4 biological replicates from 9 independent experiments, +CC data were from 3-4 biological replicates from 11 independent experiments, and ω-3 PUFA data were from 2-3 biological replicates from 3-4 independent experiments. Values are displayed as median±95% confidence intervals. Statistical comparisons were made using non-parametric Kruskal-Wallis tests with Dunn's multiple comparisons tests.

Cytokine stimulation induced a large increase in CXCL9 concentration, particularly in the apical compartment where stimulation increased CXCL9 concentration by approximately 14.6-fold, compared to 2.2-fold increase in the basolateral compartment (*Figure 6.3*). EPA and DHA-treated cells had slightly higher concentration of CXCL9 in both compartments, although this was not significantly different from control stimulated cells. DPA-treated cells had similar levels of CXCL9 to control stimulated cells in the apical compartment but had a lower concentration in the basolateral compartment; this was not significantly different to unstimulated cells but was also not significantly different from control stimulated cells. ALA and SDA-treated cells showed similarly lower CXCL9

concentration in the basolateral medium than stimulated control cells, although this was not statistically significant from either unstimulated or stimulated control cells. Apical concentration of CXCL9 was lower for SDA-treated cells, but not ALA-treated cells, compared to control stimulated cells, but was neither significant from non-stimulated controls nor stimulated controls.

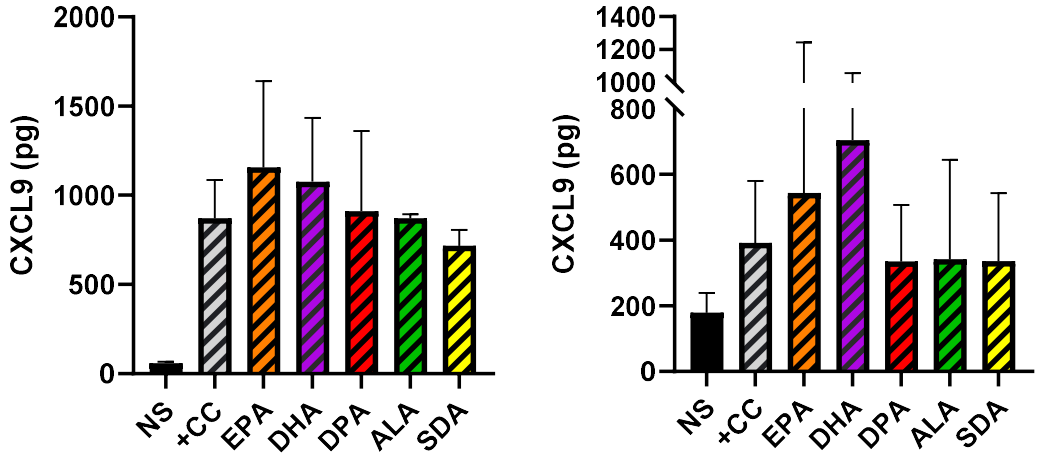

Figure 6.3: Concentration of CXCL9 in the apical (left) and basolateral (right) medium of Caco-2 cells treated with ω-3 PUFAs (EPA, DHA, DPA, ALA, or SDA; 25 μM per ω-3 PUFA) for 48 hours and subsequently stimulated with pro-inflammatory cytokines (TNF-α, IFN-γ, IL-1β) for 24 hours. +CC indicates cells stimulated with cytokines without ω-3 PUFA pre-treatment. Unstimulated cells (NS) were cultured in culture medium only. NS data were from 3-4 biological replicates from 9 independent experiments, +CC data were from 3-4 biological replicates from 11 independent experiments, and ω-3 PUFA data were from 2-3 biological replicates from 3-4 independent experiments. Values are displayed as median±95% confidence intervals. Statistical comparisons were made using non-parametric Kruskal-Wallis tests with Dunn's multiple comparisons tests.

The concentration of CXCL8 in both apical and basolateral compartments of unstimulated Caco-2 cells was relatively low (*Figure 6.4*). Cytokine stimulation induced a large increase in CXCL8 in both compartments (*Figure 6.4*), particularly in the basolateral compartment (81.5-fold increase) as non-stimulated concentrations CXCL8 were negligible. CXCL8 concentrations produced by ALA-, SDA-, and DPA-treated cells were significantly higher in comparison to non-stimulated control cells in both compartments. Although in both compartments SDA-treated cells seemed to produce higher concentrations of CXCL8, this was not statistically significant. ALA- and DPA-treated cells were also not significantly

different from control stimulated cells. In contrast, EPA and DHA-treated cells were not significantly different from non-stimulated cells in either compartment. Although CXCL8 concentrations produced by EPA pre-treated appeared lower than control stimulated cell, this was not statistically significant. DHA pre-treatment significantly decreased CXCL8 concentration in the apical compartment, but despite appearing to reduce CXCL8 concentrations in the basolateral compartment, this was not statistically significant.

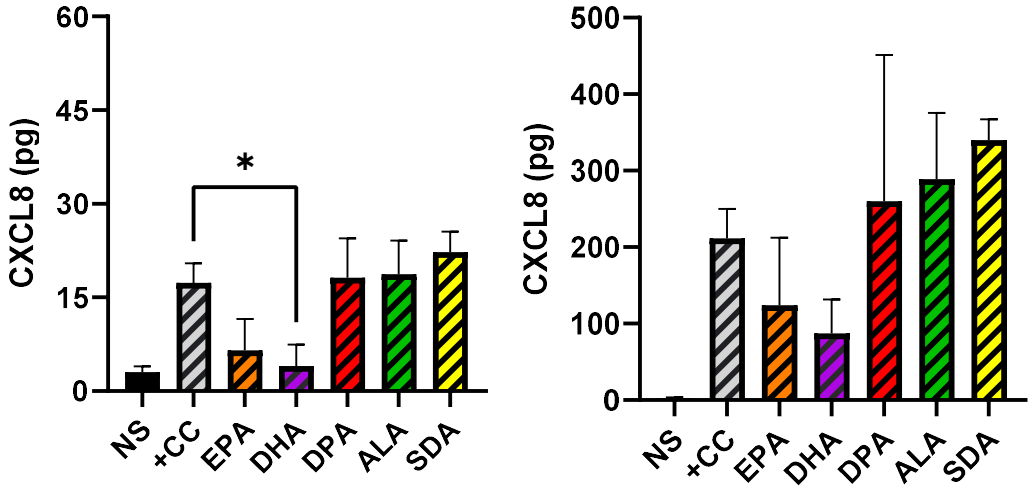

Figure 6.4: Concentration of CXCL8 in the apical (left) and basolateral (right) medium of Caco-2 cells treated with ω-3 PUFAs (EPA, DHA, DPA, ALA, or SDA; 25 μM per ω-3 PUFA) for 48 hours and subsequently stimulated with pro-inflammatory cytokines (TNF-α, IFN-γ, IL-1β) for 24 hours. +CC indicates cells stimulated with cytokines without ω-3 PUFA pre-treatment. Unstimulated cells (NS) were cultured in culture medium only. *NS data were from 3-4 biological replicates from 9 independent experiments, +CC data were from 3-4 biological replicates from 11 independent experiments, and ω-3 PUFA data were from 2-3 biological replicates from 3-4 independent experiments. Values are displayed as median±95% confidence intervals. Statistical comparisons were made using non-parametric Kruskal-Wallis tests with Dunn's multiple comparisons tests, where *p<0.05.*

Unlike for the other mediators, unstimulated Caco-2 cells had high concentrations of VEGF, particularly in the apical compartment (*Figure 6.5*). Cytokine stimulation did not significantly affect VEGF concentration in the apical compartment but significantly increased the concentration in the basolateral compartment. ω-3 PUFA supplementation had very little effect on VEGF concentration in the apical compartment with VEGF concentrations in all treatments reflecting that of stimulated controls cells. EPA pre-treated cells appeared to have higher levels of

VEGF in the basolateral compartment than control stimulated cells, although this was not statistically significant. ALA pre-treatment appeared to lower VEGF concentration in the basolateral compartment of cytokine stimulated cells but was neither significant from non-stimulated nor stimulated control cells.

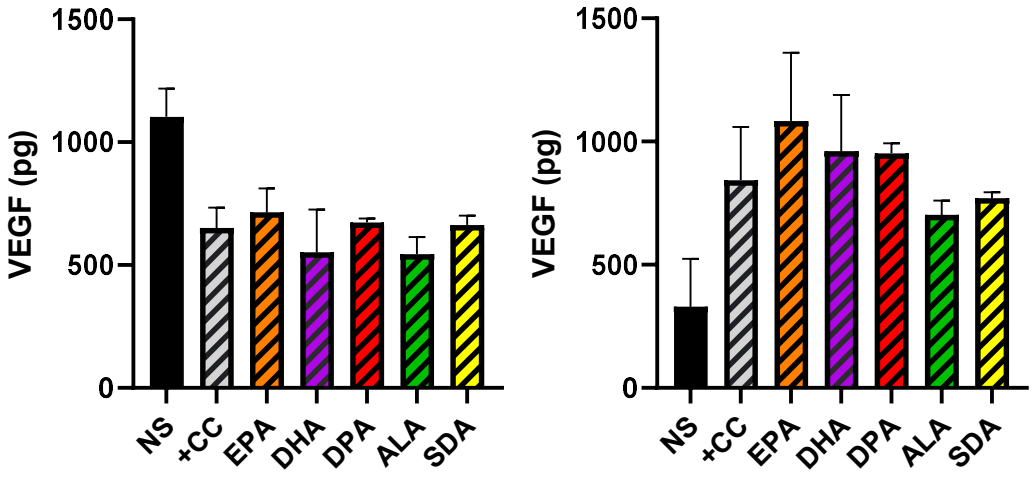

Figure 6.5: Concentration of VEGF in the apical (left) and basolateral (right) medium of Caco-2 cells treated with ω-3 PUFAs (EPA, DHA, DPA, ALA, or SDA; 25 μM per ω-3 PUFA) for 48 hours and subsequently stimulated with pro-inflammatory cytokines (TNF-α, IFN-γ, IL-1β) for 24 hours. +CC indicates cells stimulated with cytokines without ω-3 PUFA pre-treatment. Unstimulated cells (NS) were cultured in culture medium only. NS data were from 3-4 biological replicates from 9 independent experiments, +CC data were from 3-4 biological replicates from 11 independent experiments, and ω-3 PUFA data were from 2-3 biological replicates from 3-4 independent experiments. Values are displayed as median±95% confidence intervals. Statistical comparisons were made using non-parametric Kruskal-Wallis tests with Dunn's multiple comparisons tests.

Caco-2 cells expressed relatively modest levels of IL-6 compared to other mediators and cytokine stimulation induced a significant increase in IL-6 concentration in both apical and basolateral compartments (*Figure 6.6*). ω-3 PUFA supplementation had no significant effect on IL-6 concentration in either compartment.

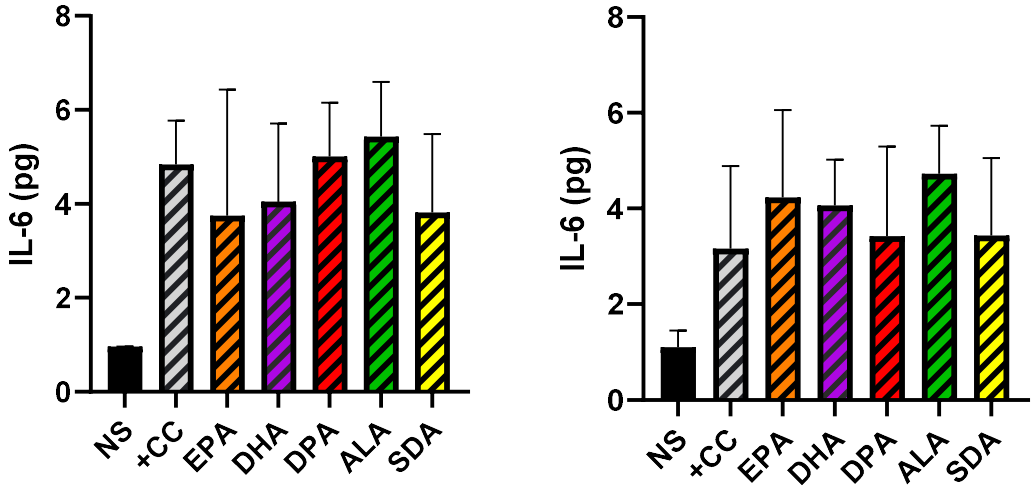

Figure 6.6: Concentration of IL-6 in the apical (left) and basolateral (right) medium of Caco-2 cells treated with ω-3 PUFAs (EPA, DHA, DPA, ALA, or SDA; 25 μM per ω-3 PUFA) for 48 hours and subsequently stimulated with pro-inflammatory cytokines (TNF-α, IFN-γ, IL-1β) for 24 hours. +CC indicates cells stimulated with cytokines without ω-3 PUFA pre-treatment. Unstimulated cells (NS) were cultured in culture medium only. NS data were from 3-4 biological replicates from 9 independent experiments, +CC data were from 3-4 biological replicates from 11 independent experiments, and ω-3 PUFA data were from 2-3 biological replicates from 3-4 independent experiments. Values are displayed as median±95% confidence intervals. Statistical comparisons were made using non-parametric Kruskal-Wallis tests with Dunn's multiple comparisons tests.

6.4.3. Cytokine stimulation activates NF-κB signalling cascade

Caco-2 cells produce a variety of inflammatory mediators in response to cytokine stimulation (see previous section) and some of these mediators are associated to the NF-κB signalling cascade. Western blot was used to quantify proteins associated to this inflammatory pathway.

Cytokine stimulation up to 6 hours did not significantly alter the amount of NF-κB or IκBα in Caco-2 cells (*Figure 6.7* and *6.8*). Nevertheless, NF-κB seemed to decrease upon cytokine stimulation (i.e. at 15 min) and to increase again later in the time course. IκBα tended to increase slightly up to 30 minutes stimulation and drop slowly up to 6 hours stimulation, although due to large variability in IκBα expression, significance was not achieved. In contrast, cytokine stimulation clearly increased phosphorylated (p)NF-κB and pIκBα (*Figure 6.7* and *6.8*). pNF-κB was increased at 15 and 30 min after stimulation (p=0.0011 and p=0.0038 vs

unstimulated cultures, respectively), and then returned towards basal levels. Likewise, pIκBα was significantly increased compared to unstimulated cells (time 0) at 15 minutes, 30 minutes, and 1 hour stimulation (p=0.0061, p=0.0499 and p=0.0026, respectively) before returning to basal levels.

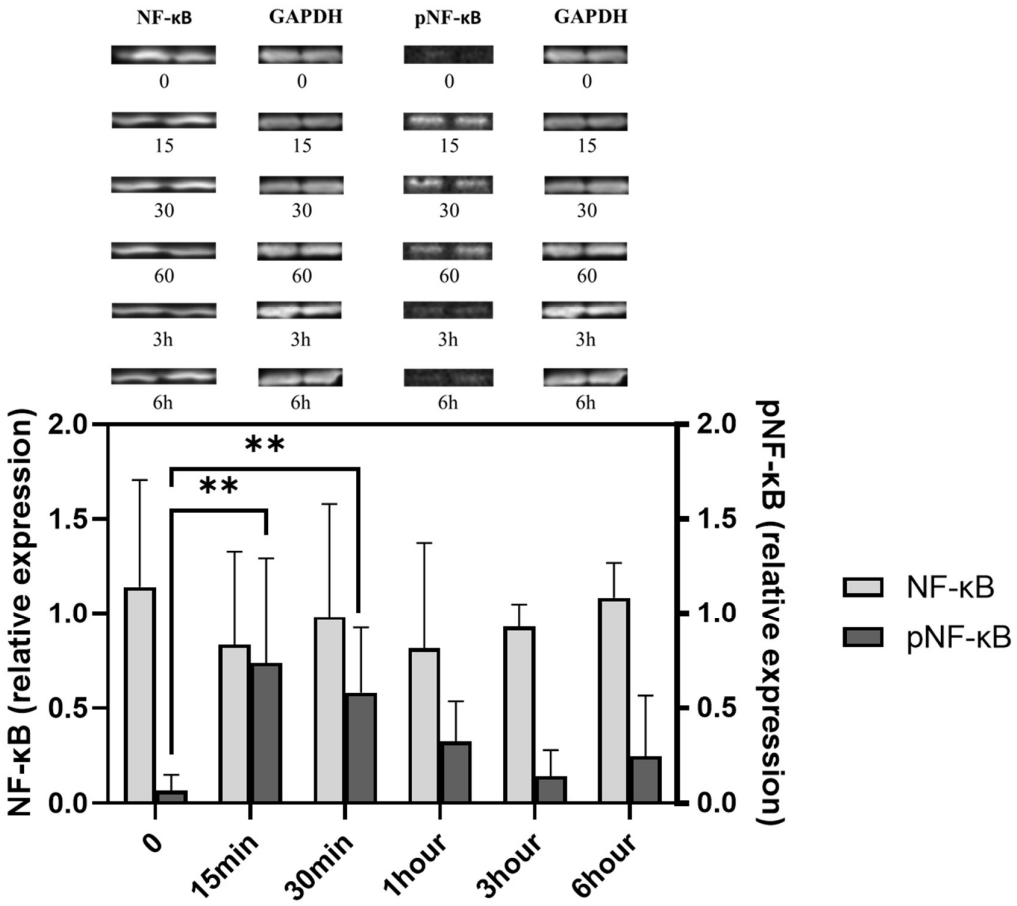

*Figure 6.7: NF-κB p65 subunit and phosphorylated(p)NF-κB p65 protein expression quantified by Western blot. Target proteins were quantified against reference protein, GAPDH. Caco-2 cells were stimulated with TNF-α, IFN-γ, and IL-1β (5 ng/ml, 50 ng/ml, 5 ng/ml, respectively) for up to 6 hours. NF-κB p65 subunit data were from 2 biological replicates from 6 independent experiments. pNF-κB p65 subunit data were from 2 biological replicates from 4 independent experiments. Data are displayed as mean±standard deviation. Statistical differences were determined by non-parametric Kruskal-Wallis tests with Dunn's multiple comparisons tests, where ** p<0.01.*

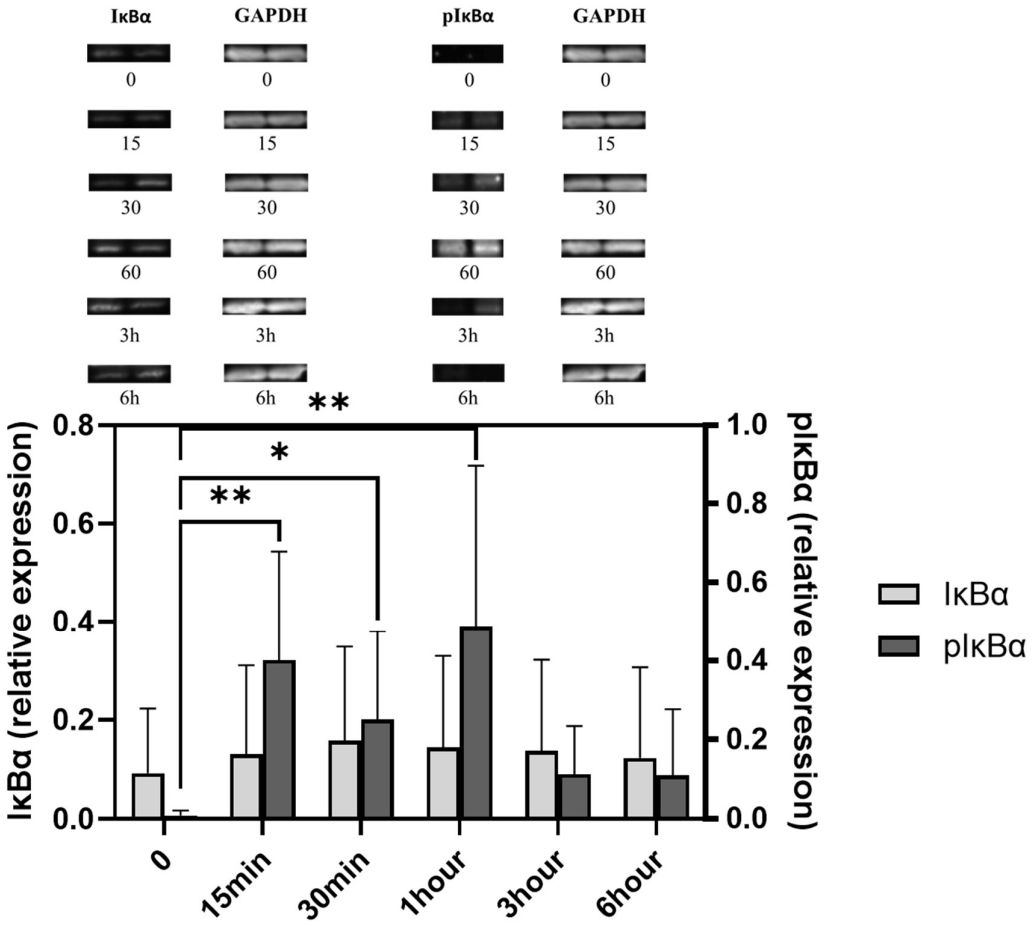

*Figure 6.8: NF-κB p65 inhibitory subunit, IκBα, and phosphorylated(p)IκBα protein expression quantified by Western blot. Target proteins were quantified against reference protein, GAPDH. Caco-2 cells were stimulated with TNF-α, IFN-γ, and IL-1β (5 ng/ml, 50 ng/ml, 5 ng/ml, respectively) for up to 6 hours. IκBα data were from 2 biological replicates from 9 independent experiments. pIκBα data were from 2 biological replicates from 3 independent experiments. Data are displayed as mean±standard deviation. Statistical differences were determined by non-parametric Kruskal-Wallis tests with Dunn's multiple comparisons tests, where * p<0.05 and ** p<0.01.*

6.4.3. ω-3 PUFAs alter NF-κB-associated protein expression

Cytokine stimulation induced activation of NF-κB indicated by an increase in phosphorylated NF-κB and pIκBα expression. Proteins associated with the NF-κB signalling pathway were quantified in cells pre-treated with different ω-3 PUFAs (EPA, DHA, DPA, ALA, and SDA; 25 μM) in comparison to untreated cells in either control or stimulated conditions.

As shown in *Table 6.1*, trends in the data suggest 30 minutes cytokine stimulation was able to induce an increase in the expression of pNF-κB and pIκBα,

although due to variability of the data this was not significant (p=0.1143 and p=0.3939, respectively). Trends also suggest DPA, ALA, and SDA-treated cells showed the largest relative increase in pNF-κB expression after cytokine stimulation, with pNF-κB exceeding NF-κB in these conditions. However, statistical differences between NF-κB and pNF-κB in all conditions could not be determined due to a lack of experimental data for pNF-κB expression (2 independent experiments). In DHA treated cells, cytokine stimulation seemed to have the least effect on NF-κB and pNF-κB expression. EPA supplemented cells exhibited significantly higher levels of NF-κB compared to unstimulated control cells (p=0.0361). Cytokine stimulation reduced NF-κB expression in EPA supplemented cells, although this did not meet the statistical significance threshold (p=0.0792). IκBα expression was relatively low and was largely unchanged by cytokine stimulation in all conditions. After cytokine stimulation, the appearance of pIκBα was increased; however, this was not statistically significant (p=0.3939). Higher levels of pIκBα were seen in EPA, DPA, ALA, and SDA-treated cells after cytokine stimulation, whereas there was no difference in pIκBα expression post-stimulation in DHA-treated cells. However, all ω-3 PUFA treated cells expressed lower levels of IκBα compared to controls before and after stimulation. Example blots for NF-κB-associated protein are shown in *Figure 6.9*.

*Table 6.1: Relative expression of NF-κB, phosphorylated (p)NF-κB, IκBα, and pIκBα in Caco-2 cells pre-treated with ω-3 PUFAs (EPA, DHA, DPA, ALA, and SDA; 25 μM) with or without subsequent stimulation with pro-inflammatory cytokines (TNF-α, IFN-γ, and IL-1β; 5 ng/ml, 50 ng/ml, 5 ng/ml, respectively) for 24 hours. NF-κB data were from 2 biological replicates from 6 independent experiments. pNF-κB data were from 2 biological replicates from 2 independent experiments. IκBα data were from 2 biological replicates from 4 independent experiments. pIκBα data were from 2 biological replicates from 4 independent experiments. All data, except pNF-κB data, are displayed as mean ± standard deviation. pNF-κB data are displayed as median (lower 95% CI, upper 95% CI). Statistical differences between protein expression were determined by non-parametric Kruskal-Wallis tests with multiple comparisons and Mann-Whitney t-tests, where appropriate. Asterisks indicate significant differences between treatment groups, where * =p<0.05. Superscript lettering indicates significant differences between treatment groups, where [a]=p<0.05.*

PUFA	*Cytokine stimulation (+/-)*	*NF-κB*	*pNF-κB*	*IκBα*	*pIκBα*
None	-	0.36±0.25	0.01 (0.001, 0.23)	0.10±0.15	0.16±0.20
	+	0.69±0.96	0.23 (0.05, 0.50)	0.02±0.02	0.38±0.44

EPA	-	**1.04±0.69***	0.03 (0.01, 0.06)	0.004±0.008	0.0002±0.02
	+	0.56±0.45	0.22 (0.04, 0.41)	0.02±0.02	0.20±0.18
DHA	-	0.44±0.31	0.03 (0.00, 0.44)	0.01±0.01	0.04±0.04
	+	0.43±0.36	0.08 (0.07, 0.29)	0.02±0.01	0.13±0.16
DPA	-	0.43±0.41	0.04 (0.01, 0.07)	0.03±0.05	0.04±0.05
	+	0.34±0.25	0.32 (0.01, 1.08)	0.04±0.06	0.24±0.19
ALA	-	0.53±0.55	0.10 (0.03, 0.21)	0.03±0.04	0.01±0.01
	+	0.22±0.18	0.45 (0.01, 1.20)	0.02±0.02	0.21±0.24
SDA	-	0.36±0.31	0.09 (0.01, 0.17)	0.03±0.04	0.02±0.03
	+	0.26±0.24	0.76 (0.21, 1.33)	0.02±0.02	0.29±0.33

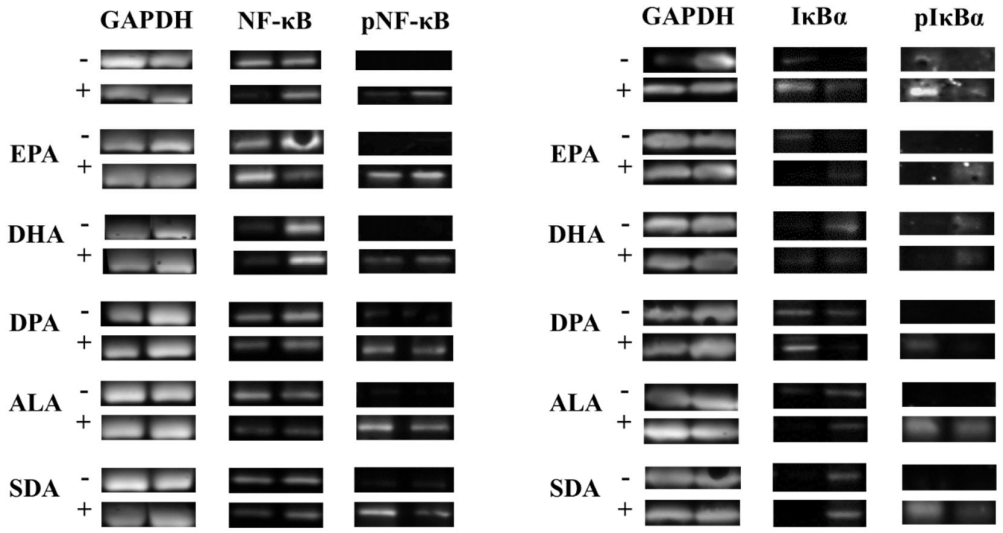

Figure 6.9: Example Western blots for NF-κB, phosphorylated (p)NF-κB, IκBα, and pIκBα against reference protein GAPDH in Caco-2 cells pre-treated with ω-3 PUFAs (EPA, DHA, DPA, ALA, and SDA; 25 μM) with (+) or without (-) subsequent stimulation with pro-inflammatory cytokines (TNF-α, IFN-γ, and IL-1β; 5 ng/ml, 50 ng/ml, 5 ng/ml, respectively) for 24 hours. NF-κB/pNF-κB and IκBα/pIκBα blots are from independent experiments.

6.5. Discussion

Stimulation of Caco-2 cells with a cocktail of inflammatory cytokines increased pNF-κB and pIκBα and increased the concentrations of several inflammatory mediators on both the apical and basolateral sides. Inflammatory mediator concentrations and the NF-κB signalling pathway were variably effected by pre-

treatment with ω-3 PUFAs. EPA-treated cells seemed to express higher basal levels of NF-κB than control cells, whilst levels of pIκBα were increased after cytokine stimulation in EPA-treated cells. DPA and ALA pre-treatment had no significant effect on NF-κB or pNF-κB expression, but pIκBα levels were significantly increased after cytokine stimulation in cells with those treatments. SDA-treated cells were the only cells to express higher levels of pNF-κB, as well as increased pIκBα, after cytokine stimulation. DHA treatment showed no significant increase on any of the NF-κB-associated proteins when comparing non-stimulated and stimulated cells. Previously, ω-3 PUFAs were shown to have no significant effect on cytokine-induced alterations to Caco-2 permeability (*Chapter 5*) and consequently there is a disparity between the effects of ω-3 PUFAs on epithelial cell permeability and epithelial cell inflammatory response. The mediators assessed are all considered to be involved in epithelial cell proliferation and inflammatory regulation. Firstly, intracellular adhesion molecule, ICAM-1, is important in leukocyte signalling during epithelial inflammation and injury, with increased release indicative of inflammation. Both TNF-α and IL-1β are known to induce the increased release of ICAM-1 from epithelial cells *in vivo* [197] and 24 hour stimulation in the Caco-2 cell model increased ICAM-1 concentration in both apical and basolateral compartments (*Figure 6.2*). EPA and DHA were shown to attenuate increased ICAM-1 expression induced by TNF-α in an endothelial cell model [255] but in unstimulated Caco-2 cells EPA was shown to have no effect on ICAM-1 expression [162]. In the current study EPA and DHA tended to increase ICAM-1 in the basolateral compartment, although not significantly. It is not known whether cell surface ICAM-1 was affected by ω-3 PUFA treatment in this model; elsewhere it was shown that DHA, EPA, and SDA reduced cell surface expression of ICAM-1 in endothelial cells [256]. Increased concentrations of ICAM-1 in cell supernatants could be indicative of cleavage of cell surface ICAM-1 to initiate wound healing processes in response to inflammation [257].

VEGF-A release, which induces the expression of ICAM-1 and subsequent chemotaxis of monocytes and neutrophils, was also upregulated in this model of intestinal inflammation. VEGF secretion has also been shown to play a role in intestinal cell migration and wound healing in epithelial cell models [258]. The concentration of VEGF was also relatively high compared to other mediators, particularly in the apical compartment, which could be attributed to the cancer cell properties of the Caco-2 cell line, as VEGF secretion has been related to

colonic tumour proliferation in intestinal tissue [259]. In this model, VEGF was markedly increased in the basolateral compartment by cytokine stimulation but decreased in the apical compartment (*Figure 6.5*) which could suggest a shift in phenotype from cell proliferation to cell healing. DHA, DPA, and SDA pre-treatment had no significant effect on VEGF concentration in either compartment. EPA pre-treatment seemed to increase VEGF concentrations in the basolateral compartment compared to stimulated controls (*Figure 6.5*). EPA has been shown to increase VEGF expression through GPR120 and PPAR-γ activation in adipocytes [260] but has been shown to decrease VEGF expression in fibroblasts [261] and HT-29 colon cancer cells [262]. In this model, ALA supplementation seemed to lower VEGF concentration in both apical and basolateral compartments (*Figure 6.5*). ALA has been shown to attenuate VEGF secretion in TNF-α stimulated EA.hy926 endothelial cells [263] and choroid-retinal endothelial cells stimulated with high levels of glucose [264]. Data from these experiments suggests that ALA may also suppress VEGF expression in intestinal epithelial cells, although further replicates are required to confirm this finding.

CXCL9, also known as chemokine ligand 9, is involved in the recruitment and activation of T-lymphocytes through interactions with chemokine receptor, CXCR3, and local CXCL9 over-expression by enterocytes drives the accumulation of inflammatory cells on the mucosal surface in IBD [198]. CXCL9 concentration was increased by cytokine stimulation in this model and this has been previously shown in another model of cytokine-stimulated Caco-2 cells [199]. Evidence for effects of ω-3 PUFAs on IFN-γ-induced inflammation is limited. In this model, other ω-3 PUFAs had no significant effect on CXCL9 concentration (*Figure 6.3*) and elsewhere in the literature there is little evidence for effects of ω-3 PUFAs on CXCL9 expression. Ramakers et al. described that EPA had no effect on CXCL9 secretion in unstimulated Caco-2 cells [162]. Evidence from this model suggests that other ω-3 PUFAs, as well as EPA, have no effect on CXCL9 expression under inflammatory conditions.

The cytokines IL-6 and CXCL8 are excessively produced and secreted in the gut mucosa of those with IBD [265]. IL-6 is essential in T-cell survival and, similar to VEGF-A, increases the presence of adhesion molecule ICAM-1 during intestinal inflammation [200]. CXCL8 is secreted by epithelial cells during onset of intestinal inflammation in both forms of IBD [266] and acts as a neutrophil attractant [201]. Supernatant IL-6 concentrations in this model were relatively low

but were increased by cytokine stimulation. Unexpectedly, there was no effect of ω-3 PUFAs on IL-6 concentration. In contrast, EPA and DHA treatments have been shown to attenuate IL-6 expression in cytokine stimulated endothelial cells [256] and macrophages [267], as well as in IL-1β stimulated Caco-2 cells [168]. In the current model, CXCL8 concentration in the apical compartment was significantly decreased by DHA pre-treatment. CXCL8 concentrations in the basolateral compartment and in both compartments also appeared to be lower than control stimulated cells in DHA and EPA-treated cells, respectively (*Figure 6.4*). However, this was not statistically significant due to a lack of power. Modest EPA supplementation (10 μM) has been shown to significantly attenuate CXCL8 expression in an IL-1β stimulated Caco-2 model [168] but had no effect on CXCL8 expression when used at 100 μM in a different IL-1β stimulated Caco-2 cell model [169]. DHA has been shown to be effective at reducing CXCL8 expression at a range of concentrations (10 μM to 100 μM) in Caco-2 cell models of IL-1β-induced inflammation [168, 169]. DHA used at 2 μM also reduced CXCL8 expression in a model of α-gliadin-induced inflammation in Caco-2 cells [167]. It seems that DHA is able to attenuate CXCL8 production across a range of Caco-2 models.

DPA and ALA had no significant effect on CXCL8 concentration in either compartment. However in a previous model, ALA was shown to reduce CXCL8 secretion by Caco-2 cells stimulated with IL-1β [79]. In a corneal epithelial cell model, HCE, ALA also significantly attenuated LPS-induced CXCL8 expression [268]. Anti-inflammatory effects of ALA are often attributed to conversion to longer-chain ω-3 PUFAs, although Reifen et al. suggest that, due to only modest conversion of ALA to EPA, ALA must exhibit its own anti-inflammatory effects in intestinal inflammation [79]. As was shown in *Chapter 4*, there was no conversion of ALA to EPA during the 48-hour supplementation period in this model and therefore the lack of effect of ALA seen might be partly associated to this lack of conversion. However, unlike ALA, SDA was converted to EPA after 48 hours supplementation (*Chapter 4*) and in this model SDA treatment appeared to slightly increase CXCL8 concentration in both compartments, although not significantly so (*Figure 6.4*). Little is known about the anti-inflammatory effects of SDA; however, this is the opposite to the effects of EPA, suggesting that SDA may have effects independent of its conversion to EPA.

The selected mediators in this model are associated to the important inflammatory regulator, NF-κB; transcription of ICAM-1 [269], CXCL9 [270], CXCL8 [271], VEGF [272], and IL-6 [273] is regulated by NF-κB. Levels of NF-κB and IκBα, as well as phosphorylated versions of these proteins, were used to assess NF-κB activity. Increased levels of phosphorylated IκBα were detected after 15 minutes, 30 minutes, and 1 hour stimulation in this model (*Figure 6.8*). Phosphorylated NF-κB was significantly increased 15 and 30 minutes after cytokine stimulation in this model (*Figure 6.7*). These effects and their timing are consistent with the cascade of the response to inflammatory stimulation that leads to NF-κB activation and translocation to the nucleus. In this study, it appeared that ω-3 PUFAs influenced the NF-κB pathway differently (*Table 6.1*). Phosphorylated proteins appeared to be the most affected by ω-3 PUFA treatment, with all ω-3 PUFA treatments, except DHA, exhibiting higher levels of pIκBα after stimulation. The effect on NF-κB p65 phosphorylation was more varied with DPA-, ALA- and SDA-treated cells expressing more pNF-κB after stimulation but EPA- and DHA-treated cells did not significantly increase pNF-κB expression. EPA-treated cells had similar expression to controls, whereas DHA-treated cells appeared to express lower levels of pNF-κB compared to controls.

Evidence in the literature also suggests variable effects of ω-3 PUFAs on NF-κB expression and activation. Marion-Letellier et al. compared the effects of modest (10 μM) levels of EPA, DHA, and ALA on IκBα expression in Caco-2 cells stimulated with IL-1β and no effect was reported [168]. In a HCT116 epithelial cell model, DHA supplemented at 20 μM, attenuated increased NF-κB activation induced by a variety of inflammatory stimuli, whilst EPA used at the same concentration had no effect [166]. Wijendran et al. also described that DHA, but not EPA, supplemented at high concentrations (100 μM) was able attenuate NF-κB mRNA expression in Caco-2, H4, and NEC-IEC epithelial cell models [169]. Overall, evidence from epithelial cell models suggests that DHA may have a more potent effect on NF-κB activation, in line with what was seen in this study.

Less is known about the effect of DPA and plant-derived ω-3 PUFAs, ALA and SDA on the NF-κB pathway. Effects of DPA have often been attributed to bioconversion to EPA and DHA, as well as the production of unique specialised resolving mediators [274]. In this model, after 48 hours supplementation with DPA, DPA was converted to EPA, but not DHA (*Chapter 4*). However, in a macrophage model

(RAW264.7) stimulated with LPS, DPA treatment was shown to downregulate IL-6 and IL-1β mRNA expression, independent of conversion to DHA [275]. Evidence to suggest that DPA impacts the NF-κB pathway is limited; however, recently DPA pre-treatment has been shown to inhibit NF-κB activation in microglial BV2 cells [276] and human bronchial explants [277]. Subsequently, DPA seems to exhibit anti-inflammatory properties akin to EPA and DHA in these *in vitro* models. DPA supplementation in this model had no effect on the NF-κB-associated proteins compared to control cells after stimulation (*Table 6.1*). Overall, DPA had no effect on NF-κB activation and signalling as mediator production was unaffected also.

Plant-derived ω-3 PUFAs, ALA and SDA also induced variable effects on NF-κB expression and activity. ALA and SDA increased pNF-κB expression after stimulation but appeared to decrease IκBα expression compared to controls (*Table 6.1*). ALA has been reported to have an inhibitory effect on the NF-κB signalling cascade in both an *in vivo* colitis model [90] and an *in vitro* corneal epithelial cell model [268]. However, limited evidence has been reported on the effect of ALA directly on intestinal epithelial cells with *in vivo* models of colitis the only indicator of ALA-associated effects on intestinal tissue. SDA is the least studied of the ω-3 PUFAs used in these experiments and the knowledge of the role of SDA in health is limited. It is thought that exogenous SDA can be used as a source of EPA, avoiding the rate limiting Δ6-desaturase step in the conversion of ALA to SDA and consequently any beneficial effect of SDA has been attributed to the conversion of SDA to longer-chain ω-3 PUFAs [221]. However, in LPS-stimulated RAW 264.7 macrophages, SDA was shown to attenuate NF-κB activity suggesting SDA may have its own anti-inflammatory properties [278]. In this model, SDA expressed higher levels of pNF-kB and may have slightly increased CXCL8 expression. Further investigation is required to establish a role for SDA in cytokine-induced inflammation.

This chapter aimed to assess the effects of the different ω-3 PUFAs on cytokine-induced inflammation in a Caco-2 cell model. DHA exhibited anti-inflammatory properties in reducing the activation of NF-κB and production of CXCL8. EPA also appeared to reduce CXCL8 concentrations, although significance could not be attained, and had less effect on the activation of NF-κB compared to DHA. The intermediate in conversion of EPA to DHA, DPA, had no significant effect on inflammatory mediator concentrations or NF-κB activation. The plant-derived ω-3

PUFAs, ALA and SDA, had variable effects on Caco-2 cell cytokine production. ALA had little effect on mediator concentrations and NF-κB activity and expression, whilst SDA appeared to slightly increase CXCL8 concentration in both compartments, coupled with a significant increase in pNF-κB expression after cytokine stimulation, suggesting SDA may in fact be pro-inflammatory in this model. All ω-3 PUFA pre-treatments, except DHA, resulted in higher expression of pIκBα after cytokine stimulation, although levels of IκBα appeared to be lower than control cells in all ω-3 PUFA treatments,

In conclusion, this model suggests that DHA exhibits anti-inflammatory properties by inhibiting the induction of NF-κB signalling and the subsequent production of CXCL8. Other ω-3 PUFAs had little to no effect on NF-κB signalling and subsequent mediator production. The finding that DHA is effective but that other ω-3 PUFAs are not (at the concentration tested) agrees with the view that DHA is a potent bioactive lipid in comparison to other ω-3 PUFAs [256]. I had hypothesised that the less-studied ω-3 PUFAs, namely DPA and SDA, would potentiate their own ant-inflammatory effects, but this was not seen. Further exploration into the actions of these ω-3 PUFAs in epithelial cells is required to determine whether they can promote anti-inflammatory actions, as seen in other cell types such as monocytes, macrophages and endothelial cells.

Chapter 7 - Discussion

7.1. Caco-2 cells as a model of intestinal enterocytes

The cells used in these experiments were the long-established human adenocarcinoma cell line, Caco-2. Lea described that after differentiation for 14-21 days, the Caco-2 cell line expresses similar morphological and functional properties to small intestinal enterocytes [240]. These properties include similar membrane-associated receptors and transporters, production of inflammatory mediators, and morphologically polarised cells with apical brush borders and tight junctions [240]. Subsequently, Caco-2 cells maintained in transwell systems have been utilised as a model for the study of epithelial cell transport, interactions between epithelial cells and intestinal microbes, and interactions of bioactive molecules with epithelial cells [240]. However, extrapolation of effects on Caco-2 cells to the *in vivo* epithelium must be made with caution. Although Caco-2 cell models provide insight into changes to epithelial cell function in isolation, they lack the variety of cell types present in the *in vivo* epithelium, as well as factors such as the presence of mucus and unstirred water layer [240].

In this model, Caco-2 cells were cultured following recommendations by Natoli et al. to produce optimally differentiated monolayers to assess the effects of ω-3 PUFAs on cytokine-induced inflammation [115]. Maintaining low seeding density of Caco-2 cells is important in restricting the development of differently differentiated colonies [279] and helped promote replicability across experiments. Careful standardisation of growth conditions, including strict differentiation periods (21 days total) and maintaining components of growth medium, was implemented to improve replicability of the model. Additionally, cells were fixed to transwell inserts using a type I collagen solution which has been shown previously to promote efficient cell spreading and proliferation [183]. As shown in Chapter 3, Caco-2 cells followed a replicable growth pattern, establishing monolayers showing high TEER values and tight junction protein expression. Growing cells in this way allowed supplementation with a range of ω-3 PUFA on cytokine-induced inflammation to be tested.

Once a replicable Caco-2 cell model was established, TNF-α, IFN-γ, and IL-1β were used as stimulants to induce inflammation. TNF-α, IFN-γ, and IL-1β are all produced excessively by intestinal immune cells during the onset of intestinal inflammation [280], interacting with receptors on the basolateral membrane of

epithelial cells and hence the cytokine stimuli in these experiments were added to the basolateral compartment of the transwell system. Chapter 3 described the effect of 24 hours stimulation of Caco-2 cells with cytokines, which induced increases in paracellular permeability and increased the production of several inflammatory markers, including IL-6, CXCL8, IL-18, VEGF, CXCL9, and ICAM-1, all of which are associated to the intestinal epithelial cell inflammasome. IL-6 and CXCL8 are pro-inflammatory cytokines attributed to increased NF-κB activity in epithelial cells [281]. IL-6 is thought have a pleiotropic role in intestinal inflammation as it can prevent apoptosis and promote cell healing [282]. CXCL8 secretion by epithelial cells is a response to cell injury and promotes neutrophil recruitment [283]. Like IL-6, IL-18 production by epithelial cells has a dual role in the intestinal epithelium with constitutive IL-18 production maintaining normal barrier function while during inflammation, IL-18 is thought to exacerbate inflammation through promoting mononuclear cell IFN-γ production [284]. CXCL9 is a potent chemokine attractant, contributing to the recruitment of IFN-γ producing monocytes, and is itself directly linked to IFN-γ-induced inflammation in epithelial cells, suggesting part of a positive feedback loop in the intestinal epithelium [285]. VEGF and ICAM-1 secretion is associated with wound healing and epithelial cell migration in the intestinal barrier [257, 258]. These markers were measured to give insight into the variety of pathways induced by the cytokines used in this model.

7.2. ω-3 PUFAs – Sources, application, and current evidence

Ω-3 polyunsaturated fatty acids are nutritional fatty acids derived from a variety of sources, including oily fish, some red meat, eggs, nuts and seeds. Experimental studies suggest that ω-3 PUFAs possess anti-inflammatory properties within different cell types. However, studies conducted in humans have often reported little or no effect of ω-3 PUFAs on the pathogenesis of IBDs, which is partly attributed to chronic dysfunction and eventual loss of a functional intestinal epithelium [286]. ω-3 PUFA supplementation trials in humans are often focused on the curative repair or management of the intestinal barrier after the onset of the disease; however some evidence suggest that ω-3 PUFA supplementation may increase the risk of IBD diagnosis [287]. Exploration of ω-3 PUFA pre-treatment in this Caco-2 cell model provides some insight into the contribution of ω-3 PUFAs

during the onset of immunogenic inflammation. Effects of well-studied EPA and DHA were compared to the lesser studied EPA-DHA intermediate, DPA, and the plant-derived ω-3 PUFAs, ALA and SDA.

7.2.1. EPA & DHA

Long-chain ω-3 PUFAs, eicosapentaenoic acid (EPA) and docosahexaenoic acid (DHA), are two of the main bioactive compounds derived from fatty fish and from fish oil. Concentrations used in these experiments did not exceed 25 μM, which is modest to blood concentrations that can be achieved through modest consumptions of oily fish; with plasma concentrations of EPA and DHA averaging 182 μM and 33 μM, respectively, in healthy people consuming oily fish once to twice a month [288]. Marine sources of ω-3 PUFAs includes salmon, which provides 0.32 g EPA and 1.11 g DHA per 100 g, mackerel, which provides 0.90 g EPA and 1.40 g DHA per 100 g, and cod, which provides 0.08 g EPA and 0.14 g DHA per 100 g [289]. Through assessment of the opinions of expert scientific and authoritative bodies, The Global Organization for EPA and DHA (GOED) currently recommends adults should consume 500 to 1000 mg per day of EPA and DHA [290]; however average global consumption of EPA and DHA does not exceed 100 mg per day in adults [291]. Although fish are the main dietary source of EPA and DHA, fish stocks are finite and this has driven the development of alternate sources of EPA and DHA, such as genetically modified plants and microalgae [291].

EPA and DHA have an array of beneficial effects in a multitude of diseases, including obesity, arthritis, and cardiovascular disease [206]. EPA and DHA may also have benefits in other inflammatory diseases, including IBD, with some evidence supporting anti-inflammatory effects of ω-3 PUFAs in models of IBD [207]. At a cellular level, benefits of ω-3 PUFAs in IBD can be attributed to enzymatic processing of EPA and DHA driving the production of anti-inflammatory mediators, such as eicosanoids. ω-3 PUFA-derived eicosanoid production and signalling induces an array of effects on the gut including enhanced gut barrier function, nutrient absorption, regulated intestinal immune responses, and epithelial cell homeostasis [57].

The effects of ω-3 PUFAs are not exclusive to bioactive mediator production, and it is thought that incorporation of ω-3 PUFAs into cells can potentiate anti-inflammatory effects. Increasing the proportion of long-chain ω-3 PUFAs in cell membranes can elicit a multitude of effects including altering membrane fluidity and structure, eicosanoid production, induction of signalling pathways and gene expression [292]. Evidence from *in vivo* murine models has shown fish oil supplementation increases EPA and DHA in small intestinal [80] and colonic tissue [77-79]. 12 weeks fish oil supplementation in humans has also shown that dietary EPA and DHA is incorporated into colonic tissue [75]. Increased incorporation of EPA and DHA can translate into protective effects on the intestinal epithelium *in vivo*. Transgenic fat-1 mice with higher colonic concentrations of long-chain ω-3 PUFAs (EPA, DPA, and DHA) had lower iNOS expression and NF-κB activity [92]. Exogenous sources of long-chain ω-3 PUFAs, particularly fish oil, have been shown to modulate inflammatory pathways in models of colitis including COX-2 mRNA and protein expression [79, 87], iNOS protein expression [87], myeloperoxidase activity [88] and mRNA expression of other inflammation-associated pathways including PPAR-γ [86], mitogen-activated protein kinase kinase 3, and TLR-2 [87]. These effects on intestinal tissue provide insight into ω-3 PUFA-derived effects on intestinal tissue; however, this may not be representative of the effects of these fatty acids directly on intestinal epithelial cells.

Epithelial cell models are used to elucidate mechanisms that may be implicated in the anti-inflammatory capacity of different ω-3 PUFAs. Caco-2 cells are one of several models used to assess the effects of ω-3 PUFAs on the intestinal barrier. Other epithelial cell lines, including T84 and HT-29, have been utilised to assess alterations in enterocyte function during differentiation and inflammation, although all these models including Caco-2 cells, have the caveat that they may not represent the complete characteristics of human intestinal epithelial cells [293]. Despite this, these long-established models have been used to assess possible effects of ω-3 PUFAs on intestinal epithelial cells. Kimura et al. described the effect of separate EPA and DHA supplementation for 24 hours on unstimulated Caco-2 cells, using the same concentration as in the current experiments (25 μM). DHA upregulated PPAR-α and PPAR-γ activity, as well as triglyceride and apolipoprotein B secretion, but had no effect on PPAR-δ activity,

whilst EPA supplementation upregulated PPAR-α activity but did not effect PPAR-γ or PPAR-δ activity [164].

7.2.2. DPA

DPA is an intermediate in the conversion of EPA to DHA. The effects of DPA have garnered interest recently as it is found in not insignificant amounts in some foods. Dietary sources of DPA include fish of the *Clupidae* family (including sardines and herring), red meat (including beef liver and lamb), and it is particularly rich in seal meat and fat [213]. DPA is also more abundant than EPA in human milk suggesting it may have a role in infant development [213]. In fact, the biological effects of DPA reported in the literature include greater stimulation of endothelial cell migration and accumulation in plasma and red blood cell lipids than EPA, and greater inhibition of platelet aggregation than both EPA and DHA [294]. Like EPA and DHA, effects of DPA on inflammation have been elucidated in cardiovascular models and it has been shown to inhibit angiogenesis and inflammatory gene expression in endothelial cells [294]. Research on DPA in epithelial cells and intestinal tissue is limited. Zheng et al. described that 300 mg/kg body weight DPA given by gavage for 28 days improved inflammation and tissue morphology in C57 mice treated with DSS to induce colitis [91]. Colonic inflammatory markers including IL-1β, IL-6, TNF-α, LTB_4, and PGE_2 were down-regulated, whilst IL-10 expression was upregulated, in DPA supplemented mice [91]. *In vivo* pro-resolving effects of DPA in the intestine can be attributed to the production of DPA-derived mediators including protectin $D1_{n\text{-}3\ DPA}$ and resolvin $D5_{n\text{-}3\ DPA}$ which regulate the recruitment of neutrophils and production of inflammatory mediators in DSS-induced colitis [295]. The overall anti-inflammatory mechanisms of DPA in the intestinal epithelium or epithelial cells are unknown. Evidence from microglia suggests that DPA exhibits anti-inflammatory effects through the inhibition of MAPK p38 and NF-κB p65 [276]. However, as shown in Chapter 6, DPA didn't inhibit cytokine-induced NF-κB activation and subsequent production of mediators in this current Caco-2 cell model.

7.2.3. ALA & SDA

Due to concerns of over-fishing and decreasing availability of EPA and DHA in fish stock, as well as increasing numbers of people choosing to consume a plant-based diet, interest has risen on the effects of plant-derived ω-3 PUFAs, ALA and SDA. ALA is an essential ω-3 PUFA, which can only be obtained in the diet from sources such as vegetable oils, including flaxseed oil, and some nuts and seeds, including chia seeds [296]. SDA is structurally very similar to ALA as it is one step down the bioconversion pathway of ALA to EPA and is naturally found in echium and hemp oils [221]. Interest has grown in the effects of SDA as it is significantly more readily converted to EPA, compared to ALA, and subsequently transgenic plant oils containing higher levels of SDA have been produced [221]. In this study, Caco-2 cells treated with 25 μM SDA for 48 hours had significantly higher concentrations of EPA, whilst the same supplementation conditions with ALA did not significantly alter EPA concentrations. This is the first study to report the likely conversion of exogenous SDA to EPA in an epithelial cell model. This suggests that SDA may be a pre-cursor for EPA synthesis in the human epithelium. Based upon analysis of red blood cells, evidence from human trials has suggested that *in vivo* SDA to EPA conversion is approximately 17 to 30%, compared to 0.1 to 9% conversion of ALA to EPA [297]. Little is known about whether SDA has anti-inflammatory effects like other ω-3 PUFAs. Preliminary findings from a RAW 264.7 macrophage model how that SDA inhibits LPS activation of NF-κB, iNOS, and MAPK pathways [278]. SDA supplementation in the current research induced NF-κB activation after cytokine stimulation, with SDA significantly increasing pNF-κB expression after cytokine-stimulated cells. This increase in pNF-κB was coupled with slightly elevated CXCL8 concentrations in both apical and basolateral media, although this was not statistically significant. However, CXCL9 secretion after cytokine stimulation appeared lower in SDA-treated cells. These preliminary findings suggest that, although SDA is readily converted to EPA, it may not possess the same anti-inflammatory capacity as EPA and DHA during cytokine-induced inflammation.

As the major essential ω-3 PUFA derived from plant sources, the potential anti-inflammatory effects of ALA have been explored in a number of previous studies. Reflected in the current model, bioconversion of ALA to long-chain ω-3 PUFAs is low; however, ALA is readily accumulated in cells and so it is possible that ALA may act in a way other than conversion through to EPA and DHA. *In vivo* evidence suggests that ALA supplementation has beneficial effects including cardiovascular

protective effects, anti-oxidant activity, and anti-inflammatory properties [298]. Hassan et al. described effects of ALA supplementation on TNBS-induced colitis in Sprague-Dawley rats. 2 weeks supplementation with ALA reduced mRNA and protein levels of TNF-α and AA-derived LTB_4, as well as decreasing activation of NF-κB and the expression of COX-2 and iNOS, indicating ALA supplementation may supress inflammation in intestinal tissue [90]. Subsequently, studies have tried to replicate effects of ALA in epithelial cell models. Caco-2 cells supplemented with 10 μM ALA for 48 hours had decreased COX-2, iNOS, and CXCL8 expression after stimulation with IL-1β [79]. In the same model, ALA provided as sage oil to the same molar concentration, also reduced the expression of COX-2 and CXCL8 in IL-1β stimulated Caco-2 cells [79]. However, in another model 10 μM ALA supplementation for 18 hours did not inhibit IL-1β-induced expression of PPAR-γ and iNOS in Caco-2 cells, although supplementation with EPA and DHA were effective in the same model [168]. In this Caco-2 cell model, 48 hours supplementation with 25 μM ALA seemed to induce NF-κB activation, although except for a slight decrease in VEGF expression, mediator production was relatively unaffected by ALA supplementation. Purported effects of ALA in colonic tissue may not be associated to effects within epithelial cells.

7.3. Discussion of findings

7.3.1. Caco-2 cells accumulate and convert ω-3 PUFAs

Chapter 4 reported the accumulation and conversion of ω-3 PUFAs in Caco-2 cells. Across a range of concentrations, 48 hours supplementation with a range of ω-3 PUFAs altered the composition of Caco-2 cells. Each supplemented ω-3 PUFA was accumulated in cells at 25 μM. Bioconversion was evident in cells treated with EPA, DPA, and SDA particularly with EPA being elongated to DPA, DPA retro-converted to EPA, and SDA converted to EPA. Interconversion of ω-3 PUFAs has been reported in Caco-2 cells previously. Beguin et al. described that supplementation with 30 μM ALA, EPA, or DHA for 7 days significantly increased total ω-3 PUFA content in Caco-2 cells [150]. Beguin et al. reported a modest conversion of ALA to EPA, with approximately 34% higher EPA content in ALA treated cells after 7 days treatment [150], in comparison to 48 hours supplementation with 25 μM ALA increasing EPA content by approximately 12%,

which was not significantly different from control cells. This suggests rate-limited ALA conversion to EPA in these cells, which is a well-documented limitation of the biosynthesis of long-chain PUFAs from ALA in humans [299]. Both models report a large accumulation of ALA in Caco-2 cells with 48 hours supplementation increasing ALA content by ≈680% and 7 days supplementation increasing ALA content by ≈1090%. SDA is thought to be more readily converted to EPA and this was reported in this model. 25 μM SDA supplementation increased EPA content by ≈130%, far exceeding the conversion seen with 30 μM ALA supplementation for 7 days [150].

30 μM EPA supplementation for 7 days lead to a large accumulation of EPA, increasing Caco-2 cell EPA content by ≈1570% [150], compared to ≈375% increase in this model. EPA supplementation also increased DPA content in both Caco-2 cell models by ≈690% in a 7 day supplementation model [150] and by ≈93% in the current model. Neither model showed a significant increase in DHA content after EPA supplementation, in fact DHA was marginally lower in cells supplemented with EPA for 7 days (≈9%) [150] and 48 hours (≈7%). After 7 days treatment, DHA supplementation for 7 days and 48 hours lead to significant accumulation of DHA in Caco-2 cells, increasing DHA content by ≈1190% [150] and ≈176%, respectively. DHA supplementation significantly increased EPA content after 7 days (≈110%) [150], which was not seen after 48 hours supplementation suggesting that rate-limited retro-conversion between DHA to EPA can occur in Caco-2 cells. Interestingly, DPA content was not significantly increased after DHA supplementation in either model. 25 μM DPA supplementation led to a large accumulation of DPA in Caco-2 cells (≈313%), as well as DPA to EPA retro-conversion indicated by a 162% increase in EPA content. *In vivo* evidence for ω-3 PUFA conversion in epithelial cells is also limited, largely due to ω-3 PUFAs being provided as fish oil (providing both EPA and DHA) and low ω-3 PUFA conversion rates which could mask any endogenous conversion. In Wistar rats supplemented with pure EPA and DHA for 3 weeks, no endogenous conversion was reported but EPA and DHA were accumulated in ileal tissue phospholipids [81]. The relative rate of ω-3 PUFAs being utilised for the production of eicosanoids is also not known [300] and this could also contribute to masking the interconversion between ω-3 PUFAs.

7.3.2. Disparity between ω-3 PUFA-derived effects on cytokine-induced inflammation

The effects of ω-3 PUFAs were assessed in two facets of cytokine-induced inflammation in Caco-2 cells, permeability and production of inflammatory mediators. As described in Chapter 5, fish-derived ω-3 PUFAs (EPA, DHA, and DPA) and plant-derived ω-3 PUFAs (ALA and SDA) had no effect on the cytokine-induced increase in paracellular permeability. However as described in Chapter 6, ω-3 PUFAs were shown to have variable effects on inflammatory mediator production and activation of the NF-κB pathway. Thus, there seems to be a disconnect between the effects of ω-3 PUFAs on permeability and on inflammatory mediator production. Inflammation in this model was induced using a 'cocktail' of pro-inflammatory cytokines, namely TNF-α, IFN-γ, and IL-1β. Differentiated Caco-2 cells were stimulated with this cocktail for 24 hours which seemed to induce inflammation indicated by an increase in permeability and increased secretion of inflammatory markers. TNF-α and IFN-γ contribute to intestinal barrier dysfunction through the contraction of tight junctions, through the activation of MLCK, and through the internalisation of tight junction proteins, including occludin [280]. TNF-α has also been shown to drive epithelial barrier dysfunction through a NF-κB-dependent down-regulation of PKC expression and upregulation of myosin II heavy chain proteins, a complementary pathway to MLCK induced barrier dysfunction [301]. IFN-γ also induces multiple pathways in intestinal epithelial cells, activating β-catenin through protein kinase B (AKT) and phosphoinositide-3 kinase (PI3K) [302]. Prolonged exposure to IFN-γ in intestinal epithelial cells can induce the inhibition of Wnt-β-catenin homeostatic pathway leading to increased apoptosis and reduced cell proliferation [303]. IL-1β has been shown to induce epithelial cell dysfunction through NF-κB and MLCK activation and suppression of occludin protein expression [286]. IL-1β also induces MyD88 signalling within epithelial cells [304]. Thus, there are a multitude of pathways stimulated by TNF-α, IFN-γ, and IL-1β in epithelial cells and the divergence of effects of ω-3 PUFAs on permeability and on inflammatory mediator production, suggests that only some pathways are sensitive to these fatty acids.

Studies assessing the effects of ω-3 PUFAs on epithelial permeability have reported mixed outcomes. Usami et al. reported that 24-hour ALA and EPA supplementation induced dose-dependent (50 to 200 μM) increases in

permeability in Caco-2 cells, whilst DHA induced dose-dependent increases in Caco-2 monolayer permeability at lower concentrations (10 to 100 μM) [154, 155]. However, cells used in these models were supplemented with ω-3 PUFAs 4 days post-seeding and may not reflect the effects of ω-3 PUFAs on differentiated Caco-2 cells. As shown in Chapter 5, each of these ω-3 PUFAs, along with DPA and SDA, had no effect on permeability after 48 hours supplementation in differentiated Caco-2 cells when used at 25 μM. 48 hours supplementation with EPA and DHA at 100 μM, but not 10 μM, partially inhibited IL-4-induced increased permeability [153]. EPA and DHA also inhibited TNF-α and IFN-γ-induced increased permeability in T84 cells at 25 to 75 μM, through the maintenance of tight junction morphology and tight junction protein distribution [157]. There was no obvious effect on tight junction protein distribution and morphology, observed by confocal microscopy, by cytokine stimulation or ω-3 PUFA treatment in this Caco-2 model. Additionally, Caco-2 monolayers seemed to remain relatively impermeable to FITC-dextran, but TEER consistently dropped after cytokine stimulation. This led to the hypothesis that tight junctions are contracting to increasing paracellular permeability, which is controlled by the upregulation and activation of MLCK. Cytokine stimulation appeared to induce an increase MLCK activation after 3 hours stimulation in this model. ω-3 PUFA treatments induced variable effects on the expression and activation of MLCK, without altering increases in Caco-2 monolayer permeability. Fish oil supplementation has been previously shown to increase MLCK mRNA expression in Caco-2 cells [241], although the effects on MLCK protein expression have not been reported. DHA supplementation has been linked to the internalisation of occludin through the activation of PKC and MLCK pathways increasing Caco-2 cell monolayer permeability [305], although DHA supplementation in this Caco-2 model upregulated MLCK expression and activation, with no increase in paracellular permeability being observed. EPA, DPA, ALA, and SDA supplemented cells also showed increased expression of MLCK in both stimulated and unstimulated conditions. Phosphorylation of MLC was more variable as EPA and DHA-treated cells expressed higher levels of pMLC when unstimulated compared to after cytokine stimulation. The same pattern was seen in ALA and SDA-treated cells, although pMLC expression was lower than control cells in unstimulated and stimulated conditions. DPA supplemented cells had the lowest expression of pMLC showing a slight increase after cytokine stimulation. These variable effects

on MLCK and pMLC expression, but lack of effect on permeability measurements, indicate that increased monolayer permeability seem to be independent of MLCK activation; other pathways implicated in tight junction dysfunction, such as threonine kinase and tyrosine kinase [306], might be associated with the increased permeability seen in this model.

Although no effect on permeability was reported, ω-3 PUFA supplementation variably affected inflammatory mediator production and the activation of the upstream NF-κB pathway. Some *in vivo* evidence suggests that increased concentrations of long-chain ω-3 PUFAs in colonic tissue downregulate NF-κB activity [92] and consequently the specific role of ω-3 PUFA modulation of NF-κB in intestinal epithelial cells has been assessed *in vitro* previously. Marion-Letellier et al. compared the efficacy of co-incubation of ω-3 PUFAs and an inflammatory stimulant, IL-1β, on the expression of NF-κB inhibitory subunit, IκBα, in Caco-2 cells [168]. ALA, EPA, and DHA supplementation had no significant effect on IκBα, although trends seemed to indicate EPA and DHA increased IκBα expression, whilst ALA decreased IκBα expression. Results from the current study did not indicate that any of these PUFAs significantly alter IκBα expression, although levels of phosphorylated IκBα seemed to be attenuated by ω-3 PUFA supplementation after cytokine stimulation. Phosphorylation of IκBα during inflammation induces ubiquitination and degradation of the inhibitory subunit, leading to increased activation of NF-κB [253]. Subsequently, inhibiting IκBα phosphorylation should indicate a lower activity of NF-κB. DHA used at 20 μM, comparable to this study, has been shown to attenuate NF-κB activation and degradation of IκBα in HCT116 epithelial cells treated with Nod2 agonists, whilst EPA supplementation had no significant effect [166]. These results along with the results from the current study indicate that DHA is more potent than EPA in inhibiting the activation of NF-κB. Overall, in comparison to DHA, the other ω-3 PUFAs tested were less potent with regard to the ability to dampen the production of inflammatory mediators. However, all ω-3 PUFAs, including DHA, were ineffective at modulating mechanisms linked to cytokine-induced permeability.

7.3.3. Limitations

Studies described in this thesis probe into the effects of ω-3 PUFAs from different sources on two major components of cytokine-induced inflammation in a Caco-2 epithelial cell model. Caco-2 cells were co-stimulated with TNF-α, IFN-γ, and IL-1β, all of which are attributed to the onset and pathogenesis of intestinal barrier dysfunction. The multitude of inflammatory processes induced by the co-stimulation provides a challenge as assessing all of these pathways would be implausible. Hence, the major effector pathways for alterations in epithelial cell permeability and cytokine production, NF-κB and MLCK, respectively, were assessed. Although the Caco-2 model provides some insight into the effects of ω-3 PUFAs on enterocytes, it is unclear how this translates to the *in vivo* epithelium. Firstly, although Caco-2 cells are a well-established model of intestinal epithelial cells, it is clear there are differences between the carcinoma-derived cell line and human enterocytes. Secondly, epithelial cells do not exist in isolation, with a multitude of cells present in the cell layer, including mucus-expressing goblet cells and intraepithelial lymphocytes. Epithelial cells are also in a constant state of dynamic homeostasis, responding to signals from both the host's microbiome and milieu of cells in the lamina propia. Caco-2 cells are only representative of one component in a large, dynamic system; however, as a simplistic model to assess possible mechanisms of nutrient interactions with epithelial cells, in terms of permeability and mediator production, Caco-2 cells are a useful tool. Nevertheless, co-culture models would be a useful extension of this research. Thirdly, the Caco-2 cells were cultured in a static system, which is unlike the dynamic environment of the intestine. Recent advances in *in vitro* technology have led to the development of fluidic 3D models called 'gut-on-a-chip' [307]. These systems are developed to better represent the conditions of an *in vivo* gut environment, through dynamic fluidics and cell co-cultures, addressing some of the issues of static *in vitro* models [307]. Assessing ω-3 PUFAs in this type of model could give a better representation of *in vivo* interactions between ω-3 PUFAs and *in vivo* epithelial cells.

Caco-2 cells were supplemented with pure ω-3 PUFAs, provided as free-fatty acids, to assess the direct effects of each ω-3 PUFA on epithelial inflammation. However, humans do not consume pure ω-3 PUFAs; we consume ω-3 PUFAs present within foods and supplements in combination with other fatty acids and other types of nutrients. The presence of other nutrients is likely to impact the functionality of ω-3 PUFAs as bioactive nutrients. In particular, the presence of ω-

6 PUFAs within the diet is thought to competitively inhibit the effects of ω-3 PUFAs, through utilisation of receptors and enzymes that will process both ω-3 and ω-6 PUFAs [308]. Additionally, many factors can influence the bioavailability of ω-3 PUFAs *in vivo* including the form of ω-3 PUFAs provided (ethyl-ester, triglycerols, phospholipids, or free fatty acids) and the source of ω-3 PUFAs [309]. Therefore, it is important to recognise that this model represents idealistic conditions allowing for assessment of potential effects of each ω-3 PUFA individually.

7.4. Assessment of hypotheses and future areas of research

The aim of this work was to establish an epithelial cell model of cytokine-induced inflammation and then compare the modulatory effects of different ω-3 PUFAs using this model. This aim was achieved, and Caco-2 cells stimulated with pro-inflammatory cytokines TNF-α, IFN-γ, and IL-1β responded consistently in terms of increased paracellular permeability, increased inflammatory mediator secretion, and the induction of the MLCK and NF-κB pathways. Although activation of these pathways was explored, it would also be of interest to inhibit these particular pathways to help determine the direct contribution of each to the outcomes of cytokine stimulation seen.

It was hypothesised that EPA and DHA would have the most potent anti-inflammatory activity opposing the pro-inflammatory stimulation, in comparison to the EPA-DHA intermediate, DPA, and the plant-derived ω-3 PUFAs, ALA and SDA. It was expected that DPA would exhibit similar anti-inflammatory properties to EPA and DHA, which was not the case. I also hypothesised that ALA and SDA will exhibit different properties in comparison to the marine-derived ω-3 PUFAs. This was apparent as results indicated that ALA and SDA modulated different mediators to EPA and DHA. Future work can be targeted to delve further into alternate mechanisms influenced by plant-derived ω-3 PUFAs, such as effects on oxidative damage, receptor activation or cell surface protein expression. Exploration of the regulatory actions of plant-derived ω-3 PUFAs is particularly important as food sources rich in both EPA and DHA become more scarce and depleted in ω-3 PUFA content. Trends suggest that ω-3 PUFA concentrations in farmed fish have reduced considerably in recent years [310].

Although the aims and hypotheses of this thesis were achieved, there are many more potential pathways affected and interactions between ω-3 PUFAs and intestinal epithelial cells during cytokine-induced inflammation. Future work should compare the production of ω-3 PUFAs-derived eicosanoids in unstimulated and cytokine-stimulated epithelial cells. ω-3 PUFA supplementation has been shown to regulate the expression of enzymes, including COX-2, which are responsible for the generation of bioactive lipids in colonic tissue *in vivo* [79]. ω-3 PUFA supplementation also has been shown to regulate the expression of AA-derived mediators and increase the expression of specialised ω-3 PUFA-derived mediators in colonic tissue *in vivo* [78]. Changes in AA content were not observed after supplementation with any of the tested ω-3 PUFAs in the current model, although assessing comparative effects of different ω-3 PUFAs on the utilisation of AA could be assessed in future work. The production of eicosanoids could be assessed through ELISA and the expression of processing enzymes, including COX and LOX, could be assessed by Western blot. Caco-2 cells have been shown to possess COX and LOX activity [311] and this may give further insights into the processing and utilisation of ω-3 PUFAs within epithelial cells.

As well as COX and LOX activity, defining the pathways for bioconversion of ω-3 PUFAs and the ω-3 PUFA concentrations in different lipid fractions would also provide new information on the destination for each ω-3 PUFA within epithelial cells. In particular, assessing the activity and expression of converting enzymes, such as delta-5 and delta-6 desaturase, or use of radiolabelled ω-3 PUFAs could be used to elucidate the metabolic fates of each ω-3 PUFA. Lastly, establishing the interactions between ω-3 PUFAs and cell surface receptors may explain effects seen in this model. Each of the mechanisms studied and potential mechanisms for future studies are summarised in *Figure 7.1*.

In conclusion, the findings from this thesis have confirmed previous findings, in particular, that DHA is the most potent ω-3 PUFA in attenuating inflammation against a wider range of comparator n-3 PUFA than those previously studied. Novel findings from this thesis, show that DPA and SDA are important potential sources of EPA within Caco-2 cells. In particular, the increased presence of EPA after SDA supplementation, and not after ALA supplementation, further indicates that SDA is a source of EPA in epithelial cells. Whether the conversion seen in the current model would be translational to the *in vivo* epithelium is unknown. Further exploration of

SDA as a source of EPA in human cells and tissue should be considered in future research.

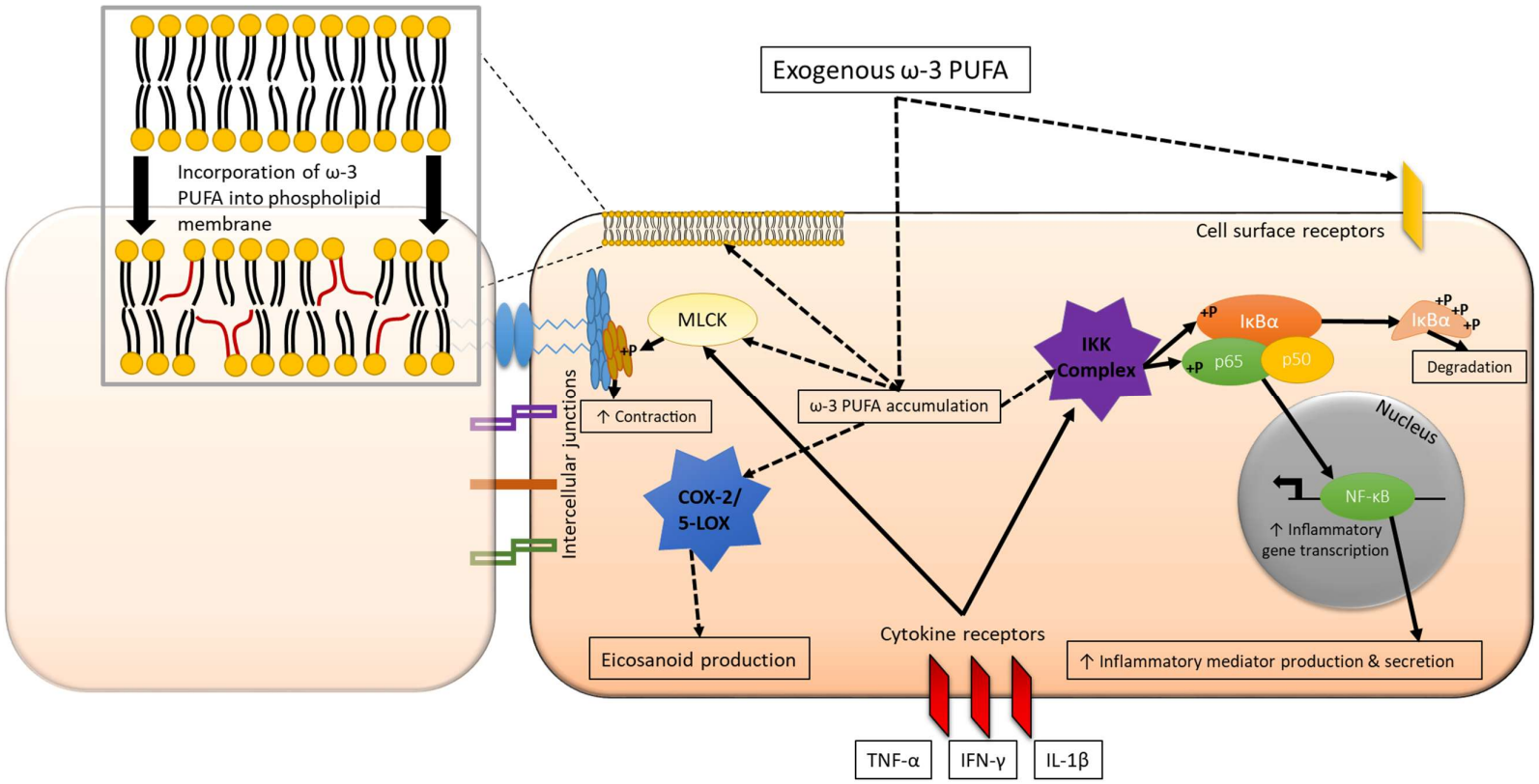

Figure 7.1: Summary of mechanisms associated with epithelial cell-ω-3 PUFA interactions during cytokine-induced inflammation. Pro-inflammatory cytokines (TNF-α, IFN-γ, and IL-1ß) interact with cytokine receptors on the basolateral membrane leading to signalling cascades which induce MLCK and NF-κB activity leading to increased paracellular permeability and inflammatory mediator production, respectively. MLCK activation leads to the phosphorylation of MLC which can contract tight junctions and lead to tight junction protein redistribution. NF-κB activation is instigated by the IKK complex which phosphorylates both the inhibitory subunit, marking it for degradation, and the p65 subunit, leading to nuclear translocation and the subsequent transcription of inflammatory genes. ω-3 PUFAs accumulated in epithelial cells seem to induce variable effects on MLCK expression without affecting cytokine-induced changes to paracellular permeability. ω-3 PUFAs also variably effect the phosphorylation of NF-κB p65 and IκBα subunits which significantly altered inflammatory mediator secretion.

Although not assessed in this model, accumulated ω-3 PUFAs are likely processed by COX and LOX enzymes leading to the production of ω-3 PUFA-derived eicosanoids. Additionally, ω-3 PUFAs are also likely incorporated into phospholipids, leading to increased cell membrane fluidity.

.

Appendix

Chapter 3 Normality (Shapiro-Wilk) tests

Figure	Outcome	Apical/Basolateral	Condition	W	Passed?	P value
4	%TEER	N/A	Control	0.7596	No	**0.007**
			4 hours	0.8769	Yes	0.2551
			8 hours	0.9094	Yes	0.4322
			12 hours	0.675	No	**0.0033**
			24 hours	0.8707	Yes	0.229
			48 hours	0.8757	Yes	0.312
7	ICAM-1	Basolateral	Control	0.7521	No	**0.0038**
			4 hours	0.704	No	**0.0068**
			8 hours	0.7301	No	**0.0126**
			12 hours	0.7765	No	**0.0358**
			24 hours	0.7198	No	**0.0099**
			48 hours	0.9149	Yes	0.4691
7	ICAM-1	Apical	Control	0.9265	Yes	0.4145
			4 hours	0.8246	Yes	0.0968
			8 hours	0.8005	Yes	0.0594
			12 hours	0.8027	Yes	0.0622
			24 hours	0.8692	Yes	0.2231
			48 hours	0.7419	No	**0.0166**
8	CXCL9	Basolateral	Control	0.3657	No	**<0.0001**
			4 hours	0.6444	No	**0.0015**
			8 hours	0.7736	No	**0.0336**
			12 hours	0.8837	Yes	0.2866
			24 hours	0.9443	Yes	0.6939
			48 hours	0.9868	Yes	0.9798
8	CXCL9	Apical	Control	0.3657	No	**<0.0001**
			4 hours	0.4961	No	**<0.0001**
			8 hours	0.8324	Yes	0.1127
			12 hours	0.8743	Yes	0.244
			24 hours	0.8491	Yes	0.1548
			48 hours	0.841	Yes	0.1328

9	CXCL8	Basolateral	Control	0.3657	No	**<0.0001**
			4 hours	0.7872	No	**0.0449**
			8 hours	0.8721	Yes	0.2346
			12 hours	0.9734	Yes	0.9147
			24 hours	0.8341	Yes	0.1165
			48 hours	0.8091	Yes	0.0709
9	CXCL8	Apical	Control	0.9027	Yes	0.2346
			4 hours	0.8591	Yes	0.1861
			8 hours	0.9257	Yes	0.5475
			12 hours	0.9617	Yes	0.8325
			24 hours	0.9548	Yes	0.7793
			48 hours	0.8573	Yes	0.18
10	VEGF	Basolateral	Control	0.7835	No	**0.0091**
			4 hours	0.8337	Yes	0.1155
			8 hours	0.9033	Yes	0.3938
			12 hours	0.8936	Yes	0.3376
			24 hours	0.7901	No	**0.0477**
			48 hours	0.9203	Yes	0.5076
10	VEGF	Apical	Control	0.892	Yes	0.1787
			4 hours	0.9417	Yes	0.6725
			8 hours	0.9864	Yes	0.9785
			12 hours	0.8909	Yes	0.3229
			24 hours	0.8843	Yes	0.2895
			48 hours	0.9185	Yes	0.4944
11	IL-6	Basolateral	Control	0.3657	No	**<0.0001**
			4 hours	0.7577	No	**0.0237**
			8 hours	0.8381	Yes	0.1257
			12 hours	0.7673	No	**0.0293**
			24 hours	0.9138	Yes	0.4619
			48 hours	0.8709	Yes	0.2298
11	IL-6	Apical	Control	0.3657	No	**<0.0001**
			4 hours	0.9218	Yes	0.5183
			8 hours	0.7677	No	**0.0295**
			12 hours	0.736	No	**0.0145**

			24 hours	0.9147	Yes	0.4677
			48 hours	0.658	No	**0.0022**
12	IL-18	N/A	Control	0.7771	No	**0.0076**
			4 hours	0.9009	Yes	0.3794
			8 hours	0.964	Yes	0.8503
			12 hours	0.832	Yes	0.1119
			24 hours	0.8929	Yes	0.3337
			48 hours	0.9125	Yes	0.4529
12	IL-18	N/A	Control	0.7198	No	**0.0015**
			4 hours	0.8576	Yes	0.1811
			8 hours	0.9916	Yes	0.9928
			12 hours	0.8497	Yes	0.1566
			24 hours	0.85	Yes	0.1575
			48 hours	0.819	Yes	0.0865

Chapter 5 Normality (Shapiro-Wilk) tests

Figure	Outcome	PUFA	Condition	W	Passed?	P value
1	%TEER	N/A	Day 21	0.8059	No	**0.0112**
			+48 hours	0.7738	No	**0.0043**
			Post-Stim	0.8907	Yes	0.142
		EPA	Day 21	0.9087	Yes	0.0815
			Post-PUFA	0.8631	No	**0.0137**
			Post-Stim	0.898	Yes	0.053
		DHA	Day 21	0.9793	Yes	0.9151
			Post-PUFA	0.8605	No	**0.0065**
			Post-Stim	0.9301	Yes	0.1386
		DPA	Day 21	0.95	Yes	0.3408
			Post-PUFA	0.8472	No	**0.0038**
			Post-Stim	0.9261	Yes	0.1149
		ALA	Day 21	0.9205	Yes	0.1014
			Post-PUFA	0.8517	No	**0.0057**
			Post-Stim	0.9462	Yes	0.3133
		SDA	Day 21	0.9217	Yes	0.1218
			Post-PUFA	0.8463	Yes	**0.0058**

			Post-Stim	0.9586	No	0.5442
5	MLCK	N/A	0 minutes	0.9694	Yes	0.8932
			15 minutes	0.8211	No	**0.0479**
			30 minutes	0.8491	Yes	0.1205
			60 minutes	0.8682	Yes	0.1447
			3 hours	0.931	Yes	0.5596
			6 hours	0.9036	Yes	0.3534
6	pMLC	N/A	0 minutes	0.9335	Yes	0.6152
			15 minutes	0.9379	Yes	0.6414
			30 minutes	0.8269	Yes	0.1599
			60 minutes	0.9899	Yes	0.9571
			3 hours	0.8984	Yes	0.4233
			6 hours	0.8821	Yes	0.3476
7	MLCK	N/A	NS	0.9382	Yes	0.6436
			+CC	0.9492	Yes	0.711
		EPA	NS	0.8932	Yes	0.3979
			+CC	0.8235	Yes	0.1514
		DHA	NS	0.9547	Yes	0.7454
			+CC	0.687	No	**0.0081**
		DPA	NS	0.9044	Yes	0.4004
			+CC	0.9735	Yes	0.9148
		ALA	NS	0.7964	Yes	0.0546
			+CC	0.8921	Yes	0.3295
		SDA	NS	0.9566	Yes	0.793
			+CC	0.8548	Yes	0.1719
7	MLCK	N/A	NS	N too small	No	N too small
			+CC	N too small	No	N too small

		EPA	NS	N too small	No	N too small
			+CC	N too small	No	N too small
		DHA	NS	N too small	No	N too small
			+CC	N too small	No	N too small
		DPA	NS	0.8421	Yes	0.2017
			+CC	0.8752	Yes	0.3187
		ALA	NS	0.681	No	**0.0068**
			+CC	0.9229	Yes	0.5533
		SDA	NS	0.7886	Yes	0.0832
			+CC	0.7527	No	**0.0409**

Chapter 6 Normality (Shapiro-Wilk) tests

Figure	Outcome	Apical/Basolateral	Condition	W	Passed?	P value
1	Viability	N/A	Control	0.8854	Yes	0.2714
			Control+CC	0.9634	Yes	0.1318
			EPA	0.9206	Yes	0.6986
			EPA+CC	0.7802	Yes	0.4137
			DHA	0.7664	Yes	0.2099
			DHA+CC	0.9043	Yes	0.7274
			DPA	0.9524	Yes	0.1024
			DPA+CC	0.7103	Yes	0.0818
			ALA	0.9586	Yes	0.6874
			ALA+CC	0.9365	Yes	0.2369
			SDA	0.7702	Yes	0.1328
			SDA+CC	0.8331	Yes	0.2419
2	ICAM-1	Apical	NS	0.8854	No	**0.0053**

			+CC	0.9634	Yes	0.2880
			EPA+CC	0.9206	Yes	0.4742
			DHA+CC	0.7802	No	**0.0259**
			DPA+CC	0.7664	No	**0.0040**
			ALA+CC	0.9043	Yes	0.2777
			SDA+CC	0.9524	Yes	0.7168
2	ICAM-1	Basolateral	NS	0.7103	No	**<0.0001**
			+CC	0.9586	Yes	0.1408
			EPA+CC	0.9365	Yes	0.6074
			DHA+CC	0.7702	No	**0.0205**
			DPA+CC	0.8331	No	**0.0228**
			ALA+CC	0.9158	Yes	0.3587
			SDA+CC	0.9133	Yes	0.3393
3	CXCL9	Apical	NS	0.7174	No	**<0.0001**
			+CC	0.8702	No	**0.0007**
			EPA+CC	0.8809	Yes	0.2304
			DHA+CC	0.9456	Yes	0.6897
			DPA+CC	0.8841	Yes	0.0988
			ALA+CC	0.8611	Yes	0.0986
			SDA+CC	0.9406	Yes	0.5887
3	CXCL9	Basolateral	NS	0.8854	No	**0.0004**
			+CC	0.9634	No	**0.0008**
			EPA+CC	0.9206	Yes	0.179
			DHA+CC	0.7802	Yes	0.8324
			DPA+CC	0.7664	Yes	0.0687

			ALA+CC	0.9043	Yes	0.2185
			SDA+CC	0.9524	No	**0.0165**
4	CXCL8	Apical	NS	0.9414	Yes	0.1201
			+CC	0.9073	No	**0.0063**
			EPA+CC	0.8982	Yes	0.3202
			DHA+CC	0.9595	Yes	0.8141
			DPA+CC	0.5835	No	**<0.0001**
			ALA+CC	0.7453	No	**0.0048**
			SDA+CC	0.9081	Yes	0.3028
4	CXCL8	Basolateral	NS	0.8477	No	**0.0031**
			+CC	0.9561	Yes	0.1628
			EPA+CC	0.7833	No	**0.0279**
			DHA+CC	0.9434	Yes	0.6692
			DPA+CC	0.8422	No	**0.0294**
			ALA+CC	0.8895	Yes	0.1972
			SDA+CC	0.9376	Yes	0.5564
5	VEGF	Apical	NS	0.9098	No	**0.0196**
			+CC	0.9285	No	**0.0253**
			EPA+CC	0.9266	Yes	0.5224
			DHA+CC	0.8815	Yes	0.2332
			DPA+CC	0.8764	Yes	0.0787
			ALA+CC	0.9113	Yes	0.3248
			SDA+CC	0.9249	Yes	0.4343
5	VEGF	Basolateral	NS	0.8621	No	**0.0056**
			+CC	0.9495	Yes	0.1008
			EPA+CC	0.9183	Yes	0.4564
			DHA+CC	0.9351	Yes	0.595
			DPA+CC	0.9339	Yes	0.4232
			ALA+CC	0.9199	Yes	0.3913
			SDA+CC	0.8856	Yes	0.1795
6	IL-6	Apical	NS	0.9237	No	**0.0429**
			+CC	0.8024	No	**<0.0001**
			EPA+CC	0.8825	Yes	0.2378
			DHA+CC	0.9647	Yes	0.8582

			DPA+CC	0.9407	Yes	0.5071
			ALA+CC	0.8832	Yes	0.1696
			SDA+CC	0.6878	No	**0.001**
6	IL-6	Basolateral	NS	0.7767	No	**0.0002**
			+CC	0.8225	No	**<0.0001**
			EPA+CC	0.9938	Yes	0.9983
			DHA+CC	0.9043	Yes	0.3578
			DPA+CC	0.8021	No	**0.0099**
			ALA+CC	0.8681	Yes	0.1173
			SDA+CC	0.894	Yes	0.219
7	NF-kB	N/A	0 minutes	0.9426	Yes	0.5323
			15 minutes	0.9385	Yes	0.4786
			30 minutes	0.9297	Yes	0.3764
			60 minutes	0.9197	Yes	0.2832
			3 hours	0.936	Yes	0.63
			6 hours	0.984	Yes	0.9252
8	pNF-kB	N/A	0 minutes	0.8261	Yes	0.054
			15 minutes	0.8744	Yes	0.1664
			30 minutes	0.8973	Yes	0.2731
			60 minutes	0.9335	Yes	0.5483
			3 hours	0.828	Yes	0.0566
			6 hours	0.8019	No	**0.03**
9	IkBa	N/A	0 minutes	0.723	No	**0.0001**
			15 minutes	0.7474	No	**0.0003**
			30 minutes	0.8143	No	**0.0024**
			60 minutes	0.7804	No	**0.0008**
			3 hours	0.7517	No	**0.0003**
			6 hours	0.6558	No	**<0.0001**
10	pIkBa	N/A	0 minutes	0.767	No	**0.0291**
			15 minutes	0.9197	Yes	0.5036
			30 minutes	0.8935	Yes	0.3368
			60 minutes	0.9145	Yes	0.4663
			3 hours	0.855	Yes	0.1727
			6 hours	0.6605	No	**0.0023**

Table 1	NF-kB	N/A	Control	0.9275	Yes	0.3543
			Control+CC	0.6645	No	**0.0004**
			EPA	0.9161	Yes	0.2875
			EPA+CC	0.8982	Yes	0.1505
			DHA	0.8923	Yes	0.1261
			DHA+CC	0.8339	No	**0.0234**
			DPA	0.8251	No	**0.0183**
			DPA+CC	0.8771	Yes	0.0806
			ALA	0.7894	No	**0.0068**
			ALA+CC	0.847	No	**0.0337**
			SDA	0.8814	Yes	0.0914
			SDA+CC	0.8539	No	**0.041**
Table 1	IkBa	N/A	Control	0.6587	No	**0.0034**
			Control+CC	0.9515	Yes	0.7255
			EPA	0.7845	Yes	0.0773
			EPA+CC	0.9966	Yes	0.9882
			DHA	0.7169	No	**0.0179**
			DHA+CC	0.6625	No	**0.0039**
			DPA	0.9487	Yes	0.7083
			DPA+CC	0.8809	Yes	0.3424
			ALA	0.9657	Yes	0.8146
			ALA+CC	0.848	Yes	0.2197
			SDA	0.8176	Yes	0.1377
			SDA+CC	0.9976	Yes	0.9922
Table 1	pNF-kB	N/A	Control	0.7179	No	**0.0036**
			Control+CC	0.9131	Yes	0.3767
			EPA	0.9194	Yes	0.4251
			EPA+CC	0.8985	Yes	0.28
			DHA	0.935	Yes	0.5627
			DHA+CC	0.8674	Yes	0.1422
			DPA	0.5306	No	**<0.0001**
			DPA+CC	0.655	No	**0.0007**
			ALA	0.7319	No	**0.0051**
			ALA+CC	0.8064	No	**0.0335**

			SDA	0.7461	No	**0.0074**
			SDA+CC	0.7773	No	**0.0163**
Table 1	pIkBa	N/A	Control	0.8166	Yes	0.0825
			Control+CC	0.8079	Yes	0.0691
			EPA	0.7864	No	**0.0442**
			EPA+CC	0.7795	No	**0.0382**
			DHA	0.7782	No	**0.0371**
			DHA+CC	0.807	Yes	0.0679
			DPA	0.7599	No	**0.0249**
			DPA+CC	0.9301	Yes	0.5812
			ALA	0.8514	Yes	0.1616
			ALA+CC	0.8485	Yes	0.1531
			SDA	0.7678	No	**0.0296**
			SDA+CC	0.7869	No	**0.0446**

List of References

1. Henderson P, van Limbergen JE, Schwarze J, Wilson DC. Function of the intestinal epithelium and its dysregulation in inflammatory bowel disease. Inflammatory bowel diseases. 2010;17(1):382-95.
2. Luissint A-C, Parkos CA, Nusrat A. Inflammation and the intestinal barrier: leukocyte–epithelial cell interactions, cell junction remodeling, and mucosal repair. Gastroenterology. 2016;151(4):616-32.
3. Turner JR. Intestinal mucosal barrier function in health and disease. Nature Reviews Immunology. 2009;9:799.
4. Mittal R, Coopersmith CM. Redefining the gut as the motor of critical illness. Trends in Molecular Medicine. 2014;20(4):214-23.
5. González-Mariscal L, Betanzos A, Nava P, Jaramillo BE. Tight junction proteins. Progress in Biophysics and Molecular Biology. 2003;81(1):1-44.
6. Ulluwishewa D, Anderson RC, McNabb WC, Moughan PJ, Wells JM, Roy NC. Regulation of Tight Junction Permeability by Intestinal Bacteria and Dietary Components. The Journal of Nutrition. 2011;141(5):769-76.
7. Pires W, Veneroso CE, Wanner SP, Pacheco DA, Vaz GC, Amorim FT, et al. Association between exercise-induced hyperthermia and intestinal permeability: a systematic review. Sports Medicine. 2017;47(7):1389-403.
8. Dokladny K, Zuhl MN, Moseley PL. Intestinal epithelial barrier function and tight junction proteins with heat and exercise. Journal of Applied Physiology. 2015;120(6):692-701.
9. Piche T. Tight junctions and IBS-the link between epithelial permeability, low-grade inflammation, and symptom generation? Neurogastroenterology & Motility. 2014;26(3):296-302.
10. Durkin LA, Childs CE, Calder PC. Omega-3 Polyunsaturated Fatty Acids and the Intestinal Epithelium—A Review. Foods. 2021;10(1):199.
11. Macpherson AJ, de Agüero MG, Ganal-Vonarburg SC. How nutrition and the maternal microbiota shape the neonatal immune system. Nature Reviews Immunology. 2017;17:508.
12. Fung TC, Olson CA, Hsiao EY. Interactions between the microbiota, immune and nervous systems in health and disease. Nature Neuroscience. 2017;20:145.

13. Sommer F, Bäckhed F. Know your neighbor: Microbiota and host epithelial cells interact locally to control intestinal function and physiology. BioEssays. 2016;38(5):455-64.
14. Parada Venegas D, De la Fuente MK, Landskron G, González MJ, Quera R, Dijkstra G, et al. Short chain fatty acids (SCFAs)-mediated gut epithelial and immune regulation and its relevance for inflammatory bowel diseases. Frontiers in immunology. 2019;10:277.
15. Ichimura A, Hirasawa A, Hara T, Tsujimoto G. Free fatty acid receptors act as nutrient sensors to regulate energy homeostasis. Prostaglandins & other lipid mediators. 2009;89(3-4):82-8.
16. Hara T, Kashihara D, Ichimura A, Kimura I, Tsujimoto G, Hirasawa A. Role of free fatty acid receptors in the regulation of energy metabolism. Biochimica et Biophysica Acta (BBA) - Molecular and Cell Biology of Lipids. 2014;1841(9):1292-300.
17. Hansen L, Holst JJ. The effects of duodenal peptides on glucagon-like peptide-1 secretion from the ileum: a duodeno–ileal loop? Regulatory peptides. 2002;110(1):39-45.
18. Flachs P, Rossmeisl M, Kopecky J. The effect of n-3 fatty acids on glucose homeostasis and insulin sensitivity. Physiological research. 2014;63:S93.
19. Zhang K, Hornef MW, Dupont A. The intestinal epithelium as guardian of gut barrier integrity. Cellular Microbiology. 2015;17(11):1561-9.
20. Oeckinghaus A, Ghosh S. The NF-kappaB family of transcription factors and its regulation. Cold Spring Harb Perspect Biol. 2009;1(4):a000034.
21. De Kivit S, Tobin MC, Forsyth CB, Keshavarzian A, Landay AL. Regulation of intestinal immune responses through TLR activation: implications for pro-and prebiotics. Frontiers in immunology. 2014;5:60.
22. Peterson LW, Artis D. Intestinal epithelial cells: regulators of barrier function and immune homeostasis. Nature Reviews Immunology. 2014;14(3):141.
23. Abreu MT. Toll-like receptor signalling in the intestinal epithelium: how bacterial recognition shapes intestinal function. Nature Reviews Immunology. 2010;10(2):131.
24. Guo S, Nighot M, Al-Sadi R, Alhmoud T, Nighot P, Ma TY. Lipopolysaccharide regulation of intestinal tight junction permeability is mediated by TLR4 signal transduction pathway activation of FAK and MyD88. The Journal of Immunology. 2015:1402598.

25. Spiljar M, Merkler D, Trajkovski M. The immune system bridges the gut microbiota with systemic energy homeostasis: focus on TLRs, mucosal barrier, and SCFAs. Frontiers in immunology. 2017;8:1353.
26. Collado MC, Isolauri E, Salminen S, Sanz Y. The impact of probiotic on gut health. Current drug metabolism. 2009;10(1):68-78.
27. Montagne L, Piel C, Lalles J. Effect of diet on mucin kinetics and composition: nutrition and health implications. Nutrition Reviews. 2004;62(3):105-14.
28. Salim SaY, Söderholm JD. Importance of disrupted intestinal barrier in inflammatory bowel diseases. Inflammatory bowel diseases. 2010;17(1):362-81.
29. Bischoff SC, Barbara G, Buurman W, Ockhuizen T, Schulzke J-D, Serino M, et al. Intestinal permeability – a new target for disease prevention and therapy. BMC Gastroenterology. 2014;14(1):189.
30. Michielan A, #x, Inc, #xe0, R. Intestinal Permeability in Inflammatory Bowel Disease: Pathogenesis, Clinical Evaluation, and Therapy of Leaky Gut. Mediators of Inflammation. 2015;2015:10.
31. Fukui H. Endotoxin and other microbial translocation markers in the blood: A clue to understand leaky gut syndrome. Cellular & Molecular Medicine: Open access. 2016;2(3).
32. Frank DN, St. Amand AL, Feldman RA, Boedeker EC, Harpaz N, Pace NR. Molecular-phylogenetic characterization of microbial community imbalances in human inflammatory bowel diseases. Proceedings of the National Academy of Sciences. 2007;104(34):13780-5.
33. Ananthakrishnan AN. Epidemiology and risk factors for IBD. Nature Reviews Gastroenterology &Amp; Hepatology. 2015;12:205.
34. Schulzke JD, Ploeger S, Amasheh M, Fromm A, Zeissig S, Troeger H, et al. Epithelial tight junctions in intestinal inflammation. Annals of the New York Academy of Sciences. 2009;1165(1):294-300.
35. Buckley A, Turner JR. Cell biology of tight junction barrier regulation and mucosal disease. Cold Spring Harbor perspectives in biology. 2018;10(1):a029314.
36. Van Itallie CM, Holmes J, Bridges A, Gookin JL, Coccaro MR, Proctor W, et al. The density of small tight junction pores varies among cell types and is increased by expression of claudin-2. Journal of cell science. 2008;121(3):298-305.
37. Fawkner-Corbett D, Simmons A, Parikh K. Microbiome, pattern recognition receptor function in health and inflammation. Best Practice & Research Clinical Gastroenterology. 2017;31(6):683-91.

38. Clark A, Mach N. Exercise-induced stress behavior, gut-microbiota-brain axis and diet: a systematic review for athletes. Journal of the International Society of Sports Nutrition. 2016;13(1):43.
39. Desai MS, Seekatz AM, Koropatkin NM, Kamada N, Hickey CA, Wolter M, et al. A Dietary Fiber-Deprived Gut Microbiota Degrades the Colonic Mucus Barrier and Enhances Pathogen Susceptibility. Cell. 2016;167(5):1339-53.e21.
40. Thaiss CA, Levy M, Grosheva I, Zheng D, Soffer E, Blacher E, et al. Hyperglycemia drives intestinal barrier dysfunction and risk for enteric infection. Science. 2018;359(6382):1376.
41. Sollid LM, Jabri B. Triggers and drivers of autoimmunity: lessons from coeliac disease. Nature Reviews Immunology. 2013;13:294.
42. Schumann M, Siegmund B, Schulzke JD, Fromm M. Celiac Disease: Role of the Epithelial Barrier. Cellular and Molecular Gastroenterology and Hepatology. 2017;3(2):150-62.
43. Volta U, Caio G, Tovoli F, De Giorgio R. Non-celiac gluten sensitivity: questions still to be answered despite increasing awareness. Cellular & molecular immunology. 2013;10(5):383.
44. Rotondi Aufiero V, Fasano A, Mazzarella G. Non-Celiac Gluten Sensitivity: How Its Gut Immune Activation and Potential Dietary Management Differ from Celiac Disease. Molecular Nutrition & Food Research. 2018;62(9):1700854.
45. Richards JL, Yap YA, McLeod KH, Mackay CR, Mariño E. Dietary metabolites and the gut microbiota: an alternative approach to control inflammatory and autoimmune diseases. Clinical & Translational Immunology. 2016;5(5):e82.
46. Conlon M, Bird A. The impact of diet and lifestyle on gut microbiota and human health. Nutrients. 2015;7(1):17-44.
47. Barbara G, Feinle-Bisset C, Ghoshal UC, Santos J, Vanner SJ, Vergnolle N, et al. The Intestinal Microenvironment and Functional Gastrointestinal Disorders. Gastroenterology. 2016;150(6):1305-18.e8.
48. Lee D, Albenberg L, Compher C, Baldassano R, Piccoli D, Lewis JD, et al. Diet in the Pathogenesis and Treatment of Inflammatory Bowel Diseases. Gastroenterology. 2015;148(6):1087-106.
49. Ruxton C, Reed SC, Simpson M, Millington K. The health benefits of omega-3 polyunsaturated fatty acids: a review of the evidence. Journal of Human Nutrition and Dietetics. 2004;17(5):449-59.

50. Yates CM, Calder PC, Rainger GE. Pharmacology and therapeutics of omega-3 polyunsaturated fatty acids in chronic inflammatory disease. Pharmacology & therapeutics. 2014;141(3):272-82.
51. Simopoulos AP. An increase in the omega-6/omega-3 fatty acid ratio increases the risk for obesity. Nutrients. 2016;8(3):128.
52. Ulven T, Christiansen E. Dietary fatty acids and their potential for controlling metabolic diseases through activation of FFA4/GPR120. Annual review of nutrition. 2015;35:239-63.
53. Watson H, Mitra S, Croden FC, Taylor M, Wood HM, Perry SL, et al. A randomised trial of the effect of omega-3 polyunsaturated fatty acid supplements on the human intestinal microbiota. Gut. 2017.
54. Costantini L, Molinari R, Farinon B, Merendino N. Impact of Omega-3 Fatty Acids on the Gut Microbiota. International Journal of Molecular Sciences. 2017;18(12):2645.
55. Marchesi JR, Adams DH, Fava F, Hermes GD, Hirschfield GM, Hold G, et al. The gut microbiota and host health: a new clinical frontier. Gut. 2016;65(2):330-9.
56. Michalak A, Mosińska P, Fichna J. Polyunsaturated Fatty Acids and Their Derivatives: Therapeutic Value for Inflammatory, Functional Gastrointestinal Disorders, and Colorectal Cancer. Frontiers in Pharmacology. 2016;7(459).
57. Moreno JJ. Eicosanoid receptors: Targets for the treatment of disrupted intestinal epithelial homeostasis. European Journal of Pharmacology. 2017;796:7-19.
58. Schmitz G, Ecker J. The opposing effects of n− 3 and n− 6 fatty acids. Progress in lipid research. 2008;47(2):147-55.
59. Spector AA, Kim H-Y. Cytochrome P450 epoxygenase pathway of polyunsaturated fatty acid metabolism. Biochimica et Biophysica Acta (BBA) - Molecular and Cell Biology of Lipids. 2015;1851(4):356-65.
60. Pilkington SM, Murphy SA, Kudva S, Nicolaou A, Rhodes LE. COX inhibition reduces vasodilator PGE2 but is shown to increase levels of chemoattractant 12-HETE in vivo in human sunburn. Experimental dermatology. 2015;24(10):790-1.
61. Rådmark O, Werz O, Steinhilber D, Samuelsson B. 5-Lipoxygenase, a key enzyme for leukotriene biosynthesis in health and disease. Biochimica et Biophysica Acta (BBA) - Molecular and Cell Biology of Lipids. 2015;1851(4):331-9.
62. Bankova LG, Boyce JA. A new spin on mast cells and cysteinyl leukotrienes: Leukotriene E₄ activates mast cells in vivo. Journal of Allergy and Clinical Immunology. 2018;142(4):1056-7.

63. Bader A, Martini F, Schinella GR, Rios JL, Prieto JM. Modulation of Cox-1, 5-, 12- and 15-Lox by Popular Herbal Remedies Used in Southern Italy Against Psoriasis and Other Skin Diseases. Phytotherapy Research. 2015;29(1):108-13.
64. Adili R, Tourdot BE, Mast K, Yeung J, Freedman JC, Green A, et al. First selective 12-LOX inhibitor, ML355, impairs thrombus formation and vessel occlusion in vivo with minimal effects on hemostasis. Arteriosclerosis, thrombosis, and vascular biology. 2017;37(10):1828-39.
65. Kong D, Shen Y, Liu G, Zuo S, Ji Y, Lu A, et al. PKA regulatory IIα subunit is essential for PGD₂-mediated resolution of inflammation. The Journal of Experimental Medicine. 2016;213(10):2209-26.
66. Schwab JM, Serhan CN. Lipoxins and new lipid mediators in the resolution of inflammation. Current opinion in pharmacology. 2006;6(4):414-20.
67. Kumar A, Mastana SS, Lindley MR. n-3 Fatty acids and asthma. Nutrition research reviews. 2016;29(1):1-16.
68. Dyerberg J, Bang H. All cis-5, 8, 11, 14, 17 eicosapentaenoic acid and triene prostaglandins: potential anti-thrombotic agents. Taylor & Francis; 1980.
69. Nurmi JT, Puolakkainen PA, Rautonen NE. Bifidobacterium Lactis sp. 420 Up-Regulates Cyclooxygenase (Cox)-1 and Down-Regulates Cox-2 Gene Expression in a Caco-2 Cell Culture Model. Nutrition and Cancer. 2005;51(1):83-92.
70. Schwanke RC, Marcon R, Bento AF, Calixto JB. EPA- and DHA-derived resolvins' actions in inflammatory bowel disease. European Journal of Pharmacology. 2016;785:156-64.
71. Calder PC. Marine omega-3 fatty acids and inflammatory processes: Effects, mechanisms and clinical relevance. Biochimica et Biophysica Acta (BBA) - Molecular and Cell Biology of Lipids. 2015;1851(4):469-84.
72. Djuric Z, Turgeon DK, Sen A, Ren J, Herman K, Ramaswamy D, et al. The Anti-inflammatory Effect of Personalized Omega-3 Fatty Acid Dosing for Reducing Prostaglandin E₂ in the Colonic Mucosa Is Attenuated in Obesity. Cancer Prevention Research. 2017;10(12):729.
73. Montrose DC, Nakanishi M, Murphy RC, Zarini S, McAleer JP, Vella AT, et al. The role of PGE2 in intestinal inflammation and tumorigenesis. Prostaglandins & Other Lipid Mediators. 2015;116-117:26-36.
74. Maseda D, Banerjee A, Johnson EM, Washington MK, Kim H, Lau KS, et al. mPGES-1-Mediated Production of PGE(2) and EP4 Receptor Sensing Regulate T Cell Colonic Inflammation. Frontiers in immunology. 2018;9:2954-.

75. Hillier K, Jewell R, Dorrell L, Smith C. Incorporation of fatty acids from fish oil and olive oil into colonic mucosal lipids and effects upon eicosanoid synthesis in inflammatory bowel disease. Gut. 1991;32(10):1151-5.
76. Hawthorne A, Daneshmend T, Hawkey C, Belluzzi A, Everitt S, Holmes G, et al. Treatment of ulcerative colitis with fish oil supplementation: a prospective 12 month randomised controlled trial. Gut. 1992;33(7):922-8.
77. Nieto N, Torres MI, Ríos A, Gil A. Dietary Polyunsaturated Fatty Acids Improve Histological and Biochemical Alterations in Rats with Experimental Ulcerative Colitis. The Journal of Nutrition. 2002;132(1):11-9.
78. Bosco N, Brahmbhatt V, Oliveira M, Martin F-P, Lichti P, Raymond F, et al. Effects of increase in fish oil intake on intestinal eicosanoids and inflammation in a mouse model of colitis. Lipids in Health and Disease. 2013;12(1):81.
79. Reifen R, Karlinsky A, Stark AH, Berkovich Z, Nyska A. α-Linolenic acid (ALA) is an anti-inflammatory agent in inflammatory bowel disease. The Journal of Nutritional Biochemistry. 2015;26(12):1632-40.
80. Brahmbhatt V, Oliveira M, Briand M, Perrisseau G, Schmid VB, Destaillats F, et al. Protective effects of dietary EPA and DHA on ischemia–reperfusion-induced intestinal stress. The Journal of nutritional biochemistry. 2013;24(1):104-11.
81. Xiao G, Yuan F, Geng Y, Qiu X, Liu Z, Lu J, et al. Eicosapentaenoic acid enhances heatstroke-impaired intestinal epithelial barrier function in rats. Shock. 2015;44(4):348-56.
82. Caplan MS, Russell T, Xiao Y, Amer M, Kaup S, Jilling T. Effect of polyunsaturated fatty acid (PUFA) supplementation on intestinal inflammation and necrotizing enterocolitis (NEC) in a neonatal rat model. Pediatric research. 2001;49(5):647-52.
83. Lu J, Jilling T, Li D, Caplan MS. Polyunsaturated fatty acid supplementation alters proinflammatory gene expression and reduces the incidence of necrotizing enterocolitis in a neonatal rat model. Pediatric research. 2007;61(4):427-32.
84. Vilaseca J, Salas A, Guarner F, Rodriguez R, Martinez M, Malagelada J. Dietary fish oil reduces progression of chronic inflammatory lesions in a rat model of granulomatous colitis. Gut. 1990;31(5):539-44.
85. Shoda R, Matsueda K, Yamato S, Umeda N. Therapeutic efficacy of N-3 polyunsaturated fatty acid in experimental Crohn's disease. Journal of gastroenterology. 1995;30:98-101.

86. Yao J, Lu Y, Zhi M, Hu P, Wu W, Gao X. Dietary n-3 polyunsaturated fatty acids ameliorate Crohn's disease in rats by modulating the expression of PPAR-γ/NFAT. Molecular Medicine Reports. 2017;16(6):8315-22.
87. Charpentier C, Chan R, Salameh E, Mbodji K, Ueno A, Coëffier M, et al. Dietary n-3 PUFA may attenuate experimental colitis. Mediators of inflammation. 2018;2018.
88. Yuceyar H, Ozutemiz O, Huseyinov A, Saruc M, Alkanat M, Bor S, et al. Is administration of n-3 fatty acids by mucosal enema protective against trinitrobenzene-induced colitis in rats? Prostaglandins Leukotrienes and Essential Fatty Acids. 1999;61(6):339-46.
89. Andoh A, Tsujikawa T, Ishizuka I, Araki Y, Sasaki M, Koyama S, et al. N-3 fatty acid-rich diet prevents early response of interleukin-6 elevation in trinitrobenzene sulfonic acid-induced enteritis. International journal of molecular medicine. 2003;12(5):721-5.
90. Hassan A, Ibrahim A, Mbodji K, Coëffier M, Ziegler F, Bounoure F, et al. An α-linolenic acid-rich formula reduces oxidative stress and inflammation by regulating NF-κB in rats with TNBS-induced colitis. The Journal of nutrition. 2010;140(10):1714-21.
91. Zheng Z, Dai Z, Cao Y, Shen Q, Zhang Y. Docosapentaenoic acid (DPA, 22: 5n-3) ameliorates inflammation in an ulcerative colitis model. Food & function. 2019;10(7):4199-209.
92. Hudert CA, Weylandt KH, Lu Y, Wang J, Hong S, Dignass A, et al. Transgenic mice rich in endogenous omega-3 fatty acids are protected from colitis. Proceedings of the National Academy of Sciences. 2006;103(30):11276-81.
93. Li Y, Wang X, Li N, Li J. The study of n-3PUFAs protecting the intestinal barrier in rat HS/R model. Lipids in Health and Disease. 2014;13(1):146.
94. Haddi A, Guendouz M, Tabet SA, Mehedi N, Kheroua O, Saidi D. Polyunsaturated fatty acids affect intestinal anaphylactic response in BALB/c mice sensitized with β-lactoglobulin. Revue Française d'Allergologie. 2018;58(6):437-43.
95. Tang H, Zhu X, Gong C, Liu H, Liu F. Protective effects and mechanisms of omega-3 polyunsaturated fatty acid on intestinal injury and macrophage polarization in peritoneal dialysis rats. Nephrology. 2019;24(10):1081-9.
96. Zhao J, Shi P, Sun Y, Sun J, Dong JN, Wang HG, et al. DHA protects against experimental colitis in IL-10-deficient mice associated with the modulation of intestinal epithelial barrier function. The British journal of nutrition. 2015;114(2):181-8.

97. Chien Y-W, Peng H-C, Chen Y-L, Pai M-H, Wang H-Y, Chuang H-L, et al. Different Dietary Proportions of Fish Oil Regulate Inflammatory Factors but Do Not Change Intestinal Tight Junction ZO-1 Expression in Ethanol-Fed Rats. Mediators of Inflammation. 2017;2017:5801768.
98. Empey LR, Jewell LD, Garg ML, Thomson AB, Clandinin MT, Fedorak RN. Fish oil-enriched diet is mucosal protective against acetic acid-induced colitis in rats. Canadian journal of physiology and pharmacology. 1991;69(4):480-7.
99. Wang J, Zhang H, Ma H, Lu B, Wang J, Li Y, et al. Inhibitory effect of dietary n-3 polyunsaturated fatty acids to intestinal IL-15 expression is associated with reduction of TCRαβ+ CD8α+ CD8β− intestinal intraepithelial lymphocytes. The Journal of nutritional biochemistry. 2008;19(7):475-81.
100. Okumura R, Takeda K. Roles of intestinal epithelial cells in the maintenance of gut homeostasis. Experimental & molecular medicine. 2017;49(5):e338-e.
101. Gravaghi C, La Perle KM, Ogrodwski P, Kang JX, Quimby F, Lipkin M, et al. Cox-2 expression, PGE2 and cytokines production are inhibited by endogenously synthesized n-3 PUFAs in inflamed colon of fat-1 mice. The Journal of nutritional biochemistry. 2011;22(4):360-5.
102. de Vogel-van den Bosch HM, Bünger M, de Groot PJ, Bosch-Vermeulen H, Hooiveld GJ, Müller M. PPARalpha-mediated effects of dietary lipids on intestinal barrier gene expression. BMC genomics. 2008;9(1):231.
103. Tom BH, Rutzky LP, Jakstys MM, Oyasu R, Kaye CI, Kahan BD. Human colonic adenocarcinoma cells. In vitro. 1976;12(3):180-91.
104. Leibovitz A, Stinson JC, McCombs WB, McCoy CE, Mazur KC, Mabry ND. Classification of human colorectal adenocarcinoma cell lines. Cancer research. 1976;36(12):4562-9.
105. Fogh J, Fogh JM, Orfeo T. One hundred and twenty-seven cultured human tumor cell lines producing tumors in nude mice. Journal of the National Cancer Institute. 1977;59(1):221-6.
106. Anderson JM, Van Itallie CM, Peterson MD, Stevenson BR, Carew EA, Mooseker MS. ZO-1 mRNA and protein expression during tight junction assembly in Caco-2 cells. The Journal of cell biology. 1989;109(3):1047-56.
107. Anderson RC, Cookson AL, McNabb WC, Park Z, McCann MJ, Kelly WJ, et al. Lactobacillus plantarum MB452 enhances the function of the intestinal barrier by increasing the expression levels of genes involved in tight junction formation. BMC Microbiology. 2010;10(1):316.

108. Peng L, Li Z-R, Green RS, Holzman IR, Lin J. Butyrate Enhances the Intestinal Barrier by Facilitating Tight Junction Assembly via Activation of AMP-Activated Protein Kinase in Caco-2 Cell Monolayers. The Journal of Nutrition. 2009;139(9):1619-25.
109. Hidalgo IJ, Raub TJ, Borchardt RT. Characterization of the human colon carcinoma cell line (Caco-2) as a model system for intestinal epithelial permeability. Gastroenterology. 1989;96(3):736-49.
110. Janecki AJ, Montrose MH, Zimniak P, Zweibaum A, Tse CM, Khurana S, et al. Subcellular Redistribution Is Involved in Acute Regulation of the Brush Border Na+/H+ Exchanger Isoform 3 in Human Colon Adenocarcinoma Cell Line Caco-2 PROTEIN KINASE C-MEDIATED INHIBITION OF THE EXCHANGER. Journal of Biological Chemistry. 1998;273(15):8790-8.
111. Chauviere G, COCONNIER M-H, KERNéIS S, FOURNIAT J, SERVIN AL. Adhesion of human Lactobacillus acidophilus strain LB to human enterocyte-like Caco-2 cells. Microbiology. 1992;138(8):1689-96.
112. Delie F, Rubas W. A Human Colonic Cell Line Sharing Similar-ities With Enterocytes as a Model to Exam-ine Oral Absorption: Advantages and Limi. Critical Reviews" in Therapeutic Drug Carrier Systems. 1997;14(3):221-86.
113. Mobraten K, Haug TM, Kleiveland CR, Lea T. Omega-3 and omega-6 PUFAs induce the same GPR120-mediated signalling events, but with different kinetics and intensity in Caco-2 cells. Lipids in Health and Disease. 2013;12.
114. Hilgendorf C. The Intestinal Epithelial Barrier in Vitro: Carrier Mediated and Passive Transport in Normal and Genetically Modified Caco-2-cells and Other Intestinal Cell Lines: Das Intestinale Epithel in Vitro 1999.
115. Natoli M, Leoni BD, D'Agnano I, D'Onofrio M, Brandi R, Arisi I, et al. Cell growing density affects the structural and functional properties of Caco-2 differentiated monolayer. Journal of cellular physiology. 2011;226(6):1531-43.
116. Cao M, Wang P, Sun C, He W, Wang F. Amelioration of IFN-γ and TNF-α-induced intestinal epithelial barrier dysfunction by berberine via suppression of MLCK-MLC phosphorylation signaling pathway. PloS one. 2013;8(5):e61944.
117. Nahidi L, Leach ST, Lemberg DA, Day AS. Osteoprotegerin exerts its pro-inflammatory effects through nuclear factor-κB activation. Digestive diseases and sciences. 2013;58(11):3144-55.
118. Tesoriere L, Attanzio A, Allegra M, Gentile C, Livrea M. Indicaxanthin inhibits NADPH oxidase (NOX)-1 activation and NF-κB-dependent release of inflammatory

mediators and prevents the increase of epithelial permeability in IL-1β-exposed Caco-2 cells. British Journal of Nutrition. 2014;111(3):415-23.
119. Ling X, Linglong P, Weixia D, Hong W. Protective effects of bifidobacterium on intestinal barrier function in LPS-induced enterocyte barrier injury of Caco-2 monolayers and in a rat NEC model. PloS one. 2016;11(8):e0161635.
120. Capaldo CT, Nusrat A. Cytokine regulation of tight junctions. Biochimica et Biophysica Acta (BBA) - Biomembranes. 2009;1788(4):864-71.
121. Eckmann L, Jung HC, Schürer-Maly C, Panja A, Morzycka-Wroblewska E, Kagnoff MF. Differential cytokine expression by human intestinal epithelial cell lines: Regulated expression of interleukin 8. Gastroenterology. 1993;105(6):1689-97.
122. Lindfors K, Blomqvist T, Juuti-Uusitalo K, Stenman S, Venäläinen J, Mäki M, et al. Live probiotic Bifidobacterium lactis bacteria inhibit the toxic effects induced by wheat gliadin in epithelial cell culture. Clinical & Experimental Immunology. 2008;152(3):552-8.
123. Isolauri E, Kirjavainen P, Salminen S. Probiotics: a role in the treatment of intestinal infection and inflammation? Gut. 2002;50(suppl 3):iii54-iii9.
124. Lerner A, Matthias T. Changes in intestinal tight junction permeability associated with industrial food additives explain the rising incidence of autoimmune disease. Autoimmunity Reviews. 2015;14(6):479-89.
125. Sander GR, Cummins AG, Powell BC. Rapid disruption of intestinal barrier function by gliadin involves altered expression of apical junctional proteins. FEBS Letters. 2005;579(21):4851-5.
126. Lammers KM, Lu R, Brownley J, Lu B, Gerard C, Thomas K, et al. Gliadin Induces an Increase in Intestinal Permeability and Zonulin Release by Binding to the Chemokine Receptor CXCR3. Gastroenterology. 2008;135(1):194-204.e3.
127. Laparra Llopis JM, Sanz Herranz Y. Gliadins induce TNFα production through cAMP-dependent protein kinase A activation in intestinal cells (Caco-2). Journal of Physiology and Biochemistry. 2010;66(2):153-9.
128. AFRC RF. Probiotics in man and animals. Journal of applied bacteriology. 1989;66(5):365-78.
129. Tuohy KM, Probert HM, Smejkal CW, Gibson GR. Using probiotics and prebiotics to improve gut health. Drug discovery today. 2003;8(15):692-700.
130. Tuomola EM, Salminen SJ. Adhesion of some probiotic and dairy Lactobacillus strains to Caco-2 cell cultures. International Journal of Food Microbiology. 1998;41(1):45-51.

131. Mattar A, Teitelbaum DH, Drongowski R, Yongyi F, Harmon C, Coran A. Probiotics up-regulate MUC-2 mucin gene expression in a Caco-2 cell-culture model. Pediatric surgery international. 2002;18(7):586-90.
132. Roselli M, Finamore A, Britti MS, Mengheri E. Probiotic bacteria Bifidobacterium animalis MB5 and Lactobacillus rhamnosus GG protect intestinal Caco-2 cells from the inflammation-associated response induced by enterotoxigenic Escherichia coli K88. British Journal of Nutrition. 2007;95(6):1177-84.
133. Koninkx JFJG, Tooten PCJ, Malago JJ. Probiotic bacteria induced improvement of the mucosal integrity of enterocyte-like Caco-2 cells after exposure to Salmonella enteritidis 857. Journal of Functional Foods. 2010;2(3):225-34.
134. Fernández de Palencia P, López P, Corbí AL, Peláez C, Requena T. Probiotic strains: survival under simulated gastrointestinal conditions, in vitro adhesion to Caco-2 cells and effect on cytokine secretion. European Food Research and Technology. 2008;227(5):1475-84.
135. Bengoa AA, Zavala L, Carasi P, Trejo SA, Bronsoms S, Serradell MdlÁ, et al. Simulated gastrointestinal conditions increase adhesion ability of Lactobacillus paracasei strains isolated from kefir to Caco-2 cells and mucin. Food Research International. 2018;103:462-7.
136. Bentley-Hewitt KL, Narbad A, Majsak-Newman G, Philo MR, Lund EK. Lactobacilli survival and adhesion to colonic epithelial cell lines is dependent on long chain fatty acid exposure. European Journal of Lipid Science and Technology. 2017;119(11).
137. Shim K-Y, Lee D, Han J, Nguyen N-T, Park S, Sung JH. Microfluidic gut-on-a-chip with three-dimensional villi structure. Biomedical microdevices. 2017;19(2):37.
138. Castro-Herrera VM, Rasmussen C, Wellejus A, Miles EA, Calder PC. In Vitro Effects of Live and Heat-Inactivated Bifidobacterium animalis Subsp. Lactis, BB-12 and Lactobacillus rhamnosus GG on Caco-2 Cells. Nutrients. 2020;12(6):1719.
139. Nallathambi R, Poulev A, Zuk JB, Raskin I. Proanthocyanidin-rich grape seed extract reduces inflammation and oxidative stress and restores tight junction barrier function in Caco-2 colon cells. Nutrients. 2020;12(6):1623.
140. Iaia N, Rossin D, Sottero B, Venezia I, Poli G, Biasi F. Efficacy of theobromine in preventing intestinal CaCo-2 cell damage induced by oxysterols. Archives of biochemistry and biophysics. 2020;694:108591.
141. Beisl J, Pahlke G, Abeln H, Ehling-Schulz M, Del Favero G, Varga E, et al. Combinatory effects of cereulide and deoxynivalenol on in vitro cell viability and inflammation of human Caco-2 cells. Archives of toxicology. 2020;94(3).

142. Capraro J, De Benedetti S, Di Dio M, Bona E, Abate A, Corsetto PA, et al. Characterization of Chenopodin Isoforms from Quinoa Seeds and Assessment of Their Potential Anti-Inflammatory Activity in Caco-2 Cells. Biomolecules. 2020;10(5):795.
143. Iglesias DE, Cremonini E, Fraga CG, Oteiza PI. Ellagic acid protects Caco-2 cell monolayers against inflammation-induced permeabilization. Free Radical Biology and Medicine. 2020;152:776-86.
144. Nie N, Bai C, Song S, Zhang Y, Wang B, Li Z. Bifidobacterium plays a protective role in TNF-α-induced inflammatory response in Caco-2 cell through NF-κB and p38MAPK pathways. Molecular and cellular biochemistry. 2020;464(1):83-91.
145. Martins IM, Macedo GA, Macedo JA. Biotransformed grape pomace as a potential source of anti-inflammatory polyphenolics: Effects in Caco-2 cells. Food Bioscience. 2020;35:100607.
146. Li W, Gao M, Han T. Lycium barbarum polysaccharides ameliorate intestinal barrier dysfunction and inflammation through the MLCK-MLC signaling pathway in Caco-2 cells. Food & function. 2020;11(4):3741-8.
147. Hasegawa T, Mizugaki A, Inoue Y, Kato H, Murakami H. Cystine reduces tight junction permeability and intestinal inflammation induced by oxidative stress in Caco-2 cells. Amino Acids. 2021:1-12.
148. Mayangsari Y, Okudaira M, Mano C, Tanaka Y, Ueda O, Sakuta T, et al. 5, 7-Dimethoxyflavone enhances barrier function by increasing occludin and reducing claudin-2 in human intestinal Caco-2 cells. Journal of Functional Foods. 2021;85:104641.
149. Dasilva G, Boller M, Medina I, Storch J. Relative levels of dietary EPA and DHA impact gastric oxidation and essential fatty acid uptake. The Journal of Nutritional Biochemistry. 2018;55:68-75.
150. Beguin P, Schneider A-C, Mignolet E, Schneider Y-J, Larondelle Y. Polyunsaturated fatty acid metabolism in enterocyte models: T84 cell line vs. Caco-2 cell line. In Vitro Cellular & Developmental Biology - Animal. 2014;50(2):111-20.
151. Tullberg C, Vegarud G, Undeland I, Scheers N. Effects of Marine Oils, Digested with Human Fluids, on Cellular Viability and Stress Protein Expression in Human Intestinal Caco-2 Cells. Nutrients. 2017;9(11):1213.
152. Renaville B, Mullen A, Moloney F, Larondelle Y, Schneider YJ, Roche HM. Eicosapentaenoic acid and 3,10 dithia stearic acid inhibit the desaturation of trans-vaccenic acid into cis-9, trans-11-conjugated linoleic acid through different pathways in Caco-2 and T84 cells. British Journal of Nutrition. 2006;95(4):688-95.

153. Willemsen LE, Koetsier MA, Balvers M, Beermann C, Stahl B, van Tol EA. Polyunsaturated fatty acids support epithelial barrier integrity and reduce IL-4 mediated permeability in vitro. European journal of nutrition. 2008;47(4):183-91.
154. Usami M, Muraki K, Iwamoto M, Ohata A, Matsushita E, Miki A. Effect of eicosapentaenoic acid (EPA) on tight junction permeability in intestinal monolayer cells. Clinical Nutrition. 2001;20(4):351-9.
155. Usami M, Komurasaki T, Hanada A, Kinoshita K, Ohata A. Effect of gamma-linolenic acid or docosahexaenoic acid on tight junction permeability in intestinal monolayer cells and their mechanism by protein kinase C activation and/or eicosanoid formation. Nutrition. 2003;19(2):150-6.
156. Rosella O, Sinclair A, Gibson PR. Polyunsaturated fatty acids reduce non-receptor-mediated transcellular permeation of protein across a model of intestinal epithelium in vitro. Journal of gastroenterology and hepatology. 2000;15(6):626-31.
157. Li Q, Zhang Q, Wang M, Zhao S, Xu G, Li J. n-3 polyunsaturated fatty acids prevent disruption of epithelial barrier function induced by proinflammatory cytokines. Molecular Immunology. 2008;45(5):1356-65.
158. Xiao K, Liu C, Qin Q, Zhang Y, Wang X, Zhang J, et al. EPA and DHA attenuate deoxynivalenol-induced intestinal porcine epithelial cell injury and protect barrier function integrity by inhibiting necroptosis signaling pathway. The FASEB Journal. 2019.
159. Xiao G, Tang L, Yuan F, Zhu W, Zhang S, Liu Z, et al. Eicosapentaenoic Acid Enhances Heat Stress-Impaired Intestinal Epithelial Barrier Function in Caco-2 Cells. PLOS ONE. 2013;8(9):e73571.
160. Beguin P, Errachid A, Larondelle Y, Schneider Y-J. Effect of polyunsaturated fatty acids on tight junctions in a model of the human intestinal epithelium under normal and inflammatory conditions. Food & Function. 2013;4(6):923-31.
161. Anbazhagan AN, Priyamvada S, Gujral T, Bhattacharyya S, Alrefai WA, Dudeja PK, et al. A novel anti-inflammatory role of GPR120 in intestinal epithelial cells. Am J Physiol Cell Physiol. 2016;310(7):C612-C21.
162. Ramakers JD, Mensink RP, Schaart G, Plat J. Arachidonic acid but not eicosapentaenoic acid (EPA) and oleic acid activates NF-kappa B and elevates ICAM-1 expression in Caco-2 cells. Lipids. 2007;42(8):687-98.
163. Bentley-Hewitt KL, De Guzman CE, Ansell J, Mandimika T, Narbad A, Lund EK. Polyunsaturated fatty acids modify expression of TGF-β in a co-culture model ultilising human colorectal cells and human peripheral blood mononuclear cells

exposed to Lactobacillus gasseri, Escherichia coli and Staphylococcus aureus. European journal of lipid science and technology. 2014;116(5):505-13.
164. Kimura R, Takahashi N, Lin S, Goto T, Murota K, Nakata R, et al. DHA attenuates postprandial hyperlipidemia via activating PPAR alpha in intestinal epithelial cells. Journal of Lipid Research. 2013;54(12):3258-68.
165. Hofmanová J, Vaculová A, Kozubík A. Polyunsaturated fatty acids sensitize human colon adenocarcinoma HT-29 cells to death receptor-mediated apoptosis. Cancer Letters. 2005;218(1):33-41.
166. Zhao L, Kwon M-J, Huang S, Lee JY, Fukase K, Inohara N, et al. Differential modulation of Nods signaling pathways by fatty acids in human colonic epithelial HCT116 cells. Journal of Biological Chemistry. 2007;282(16):11618-28.
167. Vincentini O, Quaranta MG, Viora M, Agostoni C, Silano M. Docosahexaenoic acid modulates in vitro the inflammation of celiac disease in intestinal epithelial cells via the inhibition of cPLA(2). Clinical Nutrition. 2011;30(4):541-6.
168. Marion-Letellier R, Butler M, Dechelotte P, Playford RJ, Ghosh S. Comparison of cytokine modulation by natural peroxisome proliferator-activated receptor gamma ligands with synthetic ligands in intestinal-like Caco-2 cells and human dendritic cells-potential for dietary modulation of peroxisome proliferator-activated receptor gamma in intestinal inflammation. American Journal of Clinical Nutrition. 2008;87(4):939-48.
169. Wijendran V, Brenna JT, Wang DH, Zhu W, Meng D, Ganguli K, et al. Long-chain polyunsaturated fatty acids attenuate the IL-1β-induced proinflammatory response in human fetal intestinal epithelial cells. Pediatric research. 2015;78(6):626.
170. Weylandt K-H. Docosapentaenoic acid derived metabolites and mediators – The new world of lipid mediator medicine in a nutshell. European Journal of Pharmacology. 2016;785(Supplement C):108-15.
171. Levine A, Boneh RS, Wine E. Evolving role of diet in the pathogenesis and treatment of inflammatory bowel diseases. Gut. 2018;67(9):1726-38.
172. Mozaffari H, Daneshzad E, Larijani B, Bellissimo N, Azadbakht L. Dietary intake of fish, n-3 polyunsaturated fatty acids, and risk of inflammatory bowel disease: a systematic review and meta-analysis of observational studies. European journal of nutrition. 2019:1-17.
173. Soderholm AT, Pedicord VA. Intestinal epithelial cells: at the interface of the microbiota and mucosal immunity. Immunology. 2019;158(4):267-80.

174. Iizuka M, Konno S. Wound healing of intestinal epithelial cells. World journal of gastroenterology: WJG. 2011;17(17):2161.
175. Bamias G, Corridoni D, Pizarro TT, Cominelli F. New insights into the dichotomous role of innate cytokines in gut homeostasis and inflammation. Cytokine. 2012;59(3):451-9.
176. McGuckin MA, Eri R, Simms LA, Florin THJ, Radford-Smith G. Intestinal Barrier Dysfunction in Inflammatory Bowel Diseases. Inflammatory Bowel Diseases. 2008;15(1):100-13.
177. Ghosh SS, Wang J, Yannie PJ, Ghosh S. Intestinal barrier dysfunction, LPS translocation, and disease development. Journal of the Endocrine Society. 2020;4(2):bvz039.
178. Pasparakis M. IKK/NF-κB signaling in intestinal epithelial cells controls immune homeostasis in the gut. Mucosal Immunology. 2008;1:S54.
179. Andrews C, McLean MH, Durum SK. Cytokine tuning of intestinal epithelial function. Frontiers in immunology. 2018;9:1270.
180. Simon-Assmann P, Turck N, Sidhoum-Jenny M, Gradwohl G, Kedinger M. In vitro models of intestinal epithelial cell differentiation. Cell biology and toxicology. 2007;23(4):241-56.
181. Markowska M, Oberle R, Juzwin S, Hsu C-P, Gryszkiewicz M, Streeter AJ. Optimizing Caco-2 cell monolayers to increase throughput in drug intestinal absorption analysis. Journal of Pharmacological and Toxicological Methods. 2001;46(1):51-5.
182. Rothen-Rutishauser B, Braun A, Günthert M, Wunderli-Allenspach H. Formation of Multilayers in the Caco-2 Cell Culture Model: A Confocal Laser Scanning Microscopy Study. Pharmaceutical Research. 2000;17(4):460-5.
183. Basson MD, Turowski G, Emenaker NJ. Regulation of human (Caco-2) intestinal epithelial cell differentiation by extracellular matrix proteins. Experimental cell research. 1996;225(2):301-5.
184. Zucco F, Batto A-F, Bises G, Chambaz J, Chiusolo A, Consalvo R, et al. An inter-laboratory study to evaluate the effects of medium composition on the differentiation and barrier function of Caco-2 cell lines. Alternatives to laboratory animals. 2005;33(6):603-18.
185. Biganzoli E, Cavenaghi LA, Rossi R, Brunati MC, Nolli ML. Use of a Caco-2 cell culture model for the characterization of intestinal absorption of antibiotics. Il Farmaco. 1999;54(9):594-9.

186. Lee SH. Intestinal permeability regulation by tight junction: implication on inflammatory bowel diseases. Intest Res. 2015;13(1):11-8.
187. Costantini TW, Deree J, Loomis W, Putnam JG, Choi S, Baird A, et al. Phosphodiesterase inhibition attenuates alterations to the tight junction proteins occludin and ZO-1 in immunostimulated Caco-2 intestinal monolayers. Life Sciences. 2009;84(1):18-22.
188. Ciana A, Meier K, Daum N, Gerbes S, Veith M, Lehr CM, et al. A dynamic ratio of the α+ and α− isoforms of the tight junction protein ZO-1 is characteristic of Caco-2 cells and correlates with their degree of differentiation. Cell biology international. 2010;34(6):669-78.
189. Schulzke J, Gitter A, Mankertz J, Spiegel S, Seidler U, Amasheh S, et al. Epithelial transport and barrier function in occludin-deficient mice. Biochimica et biophysica acta (BBA)-Biomembranes. 2005;1669(1):34-42.
190. Han X, Fink MP, Delude RL. Proinflammatory Cytokines Cause No··Dependent and -Independent Changes in Expression and Localization of Tight Junction Proteins in Intestinal Epithelial Cells. Shock. 2003;19(3):229-37.
191. Zhang Q, Li Q, Wang C, Liu X, Li N, Li J. Enteropathogenic Escherichia coli changes distribution of occludin and ZO-1 in tight junction membrane microdomains in vivo. Microbial pathogenesis. 2010;48(1):28-34.
192. Edelblum KL, Turner JR. The tight junction in inflammatory disease: communication breakdown. Current opinion in pharmacology. 2009;9(6):715-20.
193. Dokladny K, Zuhl MN, Moseley PL. Intestinal epithelial barrier function and tight junction proteins with heat and exercise. Journal of Applied Physiology. 2016;120(6):692-701.
194. Pearce SC, Al-Jawadi A, Kishida K, Yu S, Hu M, Fritzky LF, et al. Marked differences in tight junction composition and macromolecular permeability among different intestinal cell types. BMC biology. 2018;16(1):1-16.
195. Al-Sadi R, Khatib K, Guo S, Ye D, Youssef M, Ma T. Occludin regulates macromolecule flux across the intestinal epithelial tight junction barrier. American Journal of Physiology-Gastrointestinal and Liver Physiology. 2011;300(6):G1054-G64.
196. Lei-Leston AC, Murphy AG, Maloy KJ. Epithelial cell inflammasomes in intestinal immunity and inflammation. Frontiers in immunology. 2017;8:1168.
197. Ghosh S, Panaccione R. Anti-adhesion molecule therapy for inflammatory bowel disease. Therapeutic advances in gastroenterology. 2010;3(4):239-58.

198. Van Raemdonck K, Van den Steen PE, Liekens S, Van Damme J, Struyf S. CXCR3 ligands in disease and therapy. Cytokine & Growth Factor Reviews. 2015;26(3):311-27.
199. Marion R, Coëffier Ms, Gargala G, Ducrotté P, Déchelotte P. Glutamine and CXC chemokines IL-8, Mig, IP-10 and I-TAC in human intestinal epithelial cells. Clinical Nutrition. 2004;23(4):579-85.
200. Mudter J, Neurath MF. Il-6 signaling in inflammatory bowel disease: Pathophysiological role and clinical relevance. Inflammatory Bowel Diseases. 2007;13(8):1016-23.
201. Park JH, Peyrin-Biroulet L, Eisenhut M, Shin JI. IBD immunopathogenesis: A comprehensive review of inflammatory molecules. Autoimmunity Reviews. 2017;16(4):416-26.
202. Nowarski R, Jackson R, Gagliani N, de Zoete Marcel R, Palm Noah W, Bailis W, et al. Epithelial IL-18 Equilibrium Controls Barrier Function in Colitis. Cell. 2015;163(6):1444-56.
203. Suzuki T. Regulation of intestinal epithelial permeability by tight junctions. Cellular and Molecular Life Sciences. 2013;70(4):631-59.
204. De Souza HS, Fiocchi C. Immunopathogenesis of IBD: current state of the art. Nature reviews Gastroenterology & hepatology. 2016;13(1):13.
205. Mahida Y, Johal S. NF-κB may determine whether epithelial cell–microbial interactions in the intestine are hostile or friendly. Clinical and experimental immunology. 2001;123(3):347.
206. Russell F, Bürgin-Maunder C. Distinguishing health benefits of eicosapentaenoic and docosahexaenoic acids. Marine drugs. 2012;10(11):2535-59.
207. Lindoso L, Venkateswaran S, Kugathasan S. PUFAs and IBD: Is There a Relationship? Inflammatory Bowel Diseases. 2017;23(11):1905-7.
208. O'Connell TD, Mason RP, Budoff MJ, Navar AM, Shearer GC. Mechanistic insights into cardiovascular protection for omega-3 fatty acids and their bioactive lipid metabolites. European Heart Journal Supplements. 2020;22(Supplement_J):J3-J20.
209. Troesch B, Eggersdorfer M, Laviano A, Rolland Y, Smith AD, Warnke I, et al. Expert Opinion on Benefits of Long-Chain Omega-3 Fatty Acids (DHA and EPA) in Aging and Clinical Nutrition. Nutrients. 2020;12(9):2555.
210. Djuricic I, Calder PC. Beneficial Outcomes of Omega-6 and Omega-3 Polyunsaturated Fatty Acids on Human Health: An Update for 2021. Nutrients. 2021;13(7):2421.

211. Calder PC. Very long-chain n-3 fatty acids and human health: fact, fiction and the future. Proceedings of the Nutrition Society. 2017;77(1):52-72.
212. Spite M. Deciphering the role of n-3 polyunsaturated fatty acid-derived lipid mediators in health and disease. Proceedings of the Nutrition Society. 2013;72(4):441-50.
213. Drouin G, Rioux V, Legrand P. The n-3 docosapentaenoic acid (DPA): A new player in the n-3 long chain polyunsaturated fatty acid family. Biochimie. 2019;159:36-48.
214. Dalli J, Colas RA, Serhan CN. Novel n-3 immunoresolvents: structures and actions. Sci Rep. 2013;3(1):1-15.
215. Serhan CN, Dalli J, Colas RA, Winkler JW, Chiang N. Protectins and maresins: New pro-resolving families of mediators in acute inflammation and resolution bioactive metabolome. Biochimica et Biophysica Acta (BBA) - Molecular and Cell Biology of Lipids. 2015;1851(4):397-413.
216. Byelashov OA, Sinclair AJ, Kaur G. Dietary sources, current intakes, and nutritional role of omega-3 docosapentaenoic acid. Lipid Technology. 2015;27(4):79-82.
217. Sanders TA. DHA status of vegetarians. Prostaglandins, leukotrienes and essential fatty acids. 2009;81(2-3):137-41.
218. Burdge GC, Calder PC. Conversion of alpha-linolenic acid to longer-chain polyunsaturated fatty acids in human adults. Reproduction Nutrition Development. 2005;45(5):581-97.
219. Stark AH, Crawford MA, Reifen R. Update on alpha-linolenic acid. Nutrition reviews. 2008;66(6):326-32.
220. Walker CG, Jebb SA, Calder PC. Stearidonic acid as a supplemental source of ω-3 polyunsaturated fatty acids to enhance status for improved human health. Nutrition. 2013;29(2):363-9.
221. Prasad P, Anjali P, Sreedhar R. Plant-based stearidonic acid as sustainable source of omega-3 fatty acid with functional outcomes on human health. Critical Reviews in Food Science and Nutrition. 2021;61(10):1725-37.
222. Sherratt SCR, Dawoud H, Bhatt DL, Malinski T, Mason RP. Omega-3 and omega-6 fatty acids have distinct effects on endothelial fatty acid content and nitric oxide bioavailability. Prostaglandins, Leukotrienes and Essential Fatty Acids. 2021;173:102337.

223. Calder PC. The relationship between the fatty acid composition of immune cells and their function. Prostaglandins, Leukotrienes and Essential Fatty Acids. 2008;79(3):101-8.
224. Miller E, Kaur G, Larsen A, Loh SP, Linderborg K, Weisinger HS, et al. A short-term n-3 DPA supplementation study in humans. European journal of nutrition. 2013;52(3):895-904.
225. Kapourchali FR, Saedisomeolia A, Moghadam AM, Leili EK. The investigation of the effects of eicosapentaenoic acid and docosahexaenoic acid on cultured human airway epithelial cells. World Applied Sciences Journal. 2012;18(3):336-42.
226. Huang Y-S, Liu J-W, Koba K, Anderson SN. N-3 and n-6 fatty acid metabolism in undifferentiated and differentiated human intestine cell line (Caco-2). Molecular and cellular biochemistry. 1995;151(2):121-30.
227. Brenna JT. DHA retroconversion revisited: dietary DHA spares endogenous EPA. Oxford University Press; 2019.
228. Metherel AH, Irfan M, Klingel SL, Mutch DM, Bazinet RP. Compound-specific isotope analysis reveals no retroconversion of DHA to EPA but substantial conversion of EPA to DHA following supplementation: a randomized control trial. The American Journal of Clinical Nutrition. 2019;110(4):823-31.
229. Saini RK, Keum Y-S. Omega-3 and omega-6 polyunsaturated fatty acids: Dietary sources, metabolism, and significance — A review. Life Sciences. 2018;203:255-67.
230. Maki KC, Rains TM. Stearidonic Acid Raises Red Blood Cell Membrane Eicosapentaenoic Acid. The Journal of Nutrition. 2012;142(3):626S-9S.
231. Phipps JE. Effect of Dietary Treatment with Stearidonic Acid and Eicosapentaenoic Acid on Membrane Phospholipid Fatty Acid Composition and Glycogen-Elicited Peritoneal Neutrophil Survival in Absence or Presence of Bacterial Endotoxin. 2005.
232. Farré R, Fiorani M, Abdu Rahiman S, Matteoli G. Intestinal permeability, inflammation and the role of nutrients. Nutrients. 2020;12(4):1185.
233. Leech B, McIntyre E, Steel A, Sibbritt D. Risk factors associated with intestinal permeability in an adult population: A systematic review. International journal of clinical practice. 2019;73(10):e13385.
234. Khoshbin K, Camilleri M. Effects of dietary components on intestinal permeability in health and disease. American Journal of Physiology-Gastrointestinal and Liver Physiology. 2020;319(5):G589-G608.

235. Arrieta M-C, Bistritz L, Meddings J. Alterations in intestinal permeability. Gut. 2006;55(10):1512-20.
236. Cunningham KE, Turner JR. Myosin light chain kinase: pulling the strings of epithelial tight junction function. Annals of the New York Academy of Sciences. 2012;1258(1):34-42.
237. Wang J, Ghosh SS, Ghosh S. Curcumin improves intestinal barrier function: modulation of intracellular signaling, and organization of tight junctions. American Journal of Physiology-Cell Physiology. 2017;312(4):C438-C45.
238. Che S-y, Yuan J-w, Zhang L, Ruan Z, Sun X-m, Lu H. Puerarin prevents epithelial tight junction dysfunction induced by ethanol in Caco-2 cell model. Journal of Functional Foods. 2020;73:104079.
239. Miao W, Wu X, Wang K, Wang W, Wang Y, Li Z, et al. Sodium butyrate promotes reassembly of tight junctions in Caco-2 monolayers involving inhibition of MLCK/MLC2 pathway and phosphorylation of PKCβ2. International journal of molecular sciences. 2016;17(10):1696.
240. Lea T. Caco-2 cell line. The impact of food bioactives on health: Springer, Cham; 2015. p. 103-11.
241. Mokkala K, Laitinen K, Roytio H. Bifidobacterium lactis 420 and fish oil enhance intestinal epithelial integrity in Caco-2 cells. Nutrition Research. 2016;36(3):246-52.
242. Suzuki T. Regulation of the intestinal barrier by nutrients: The role of tight junctions. Animal Science Journal. 2020;91(1):e13357.
243. Lapointe TK, Buret AG. Interleukin-18 facilitates neutrophil transmigration via myosin light chain kinase-dependent disruption of occludin, without altering epithelial permeability. American Journal of Physiology-Gastrointestinal and Liver Physiology. 2012;302(3):G343-G51.
244. Wawrzyniak P, Noureddine N, Wawrzyniak M, Lucchinetti E, Krämer SD, Rogler G, et al. Nutritional Lipids and Mucosal Inflammation. Molecular Nutrition & Food Research. 2021;65(5):1901269.
245. Martin JB, Muccioli M, Herman K, Finnell RH, Plageman Jr TF. Folic acid modifies the shape of epithelial cells during morphogenesis via a Folr1 and MLCK dependent mechanism. Biology open. 2019;8(1):bio041160.
246. Li Q, Zhang Q, Zhang M, Wang C, Zhu Z, Li N, et al. Effect of n-3 polyunsaturated fatty acids on membrane microdomain localization of tight junction proteins in experimental colitis. The FEBS Journal. 2008;275(3):411-20.

247. Lindmark T, Kimura Y, Artursson P. Absorption enhancement through intracellular regulation of tight junction permeability by medium chain fatty acids in Caco-2 cells. Journal of Pharmacology and Experimental Therapeutics. 1998;284(1):362-9.
248. Shen L, Black ED, Witkowski ED, Lencer WI, Guerriero V, Schneeberger EE, et al. Myosin light chain phosphorylation regulates barrier function by remodeling tight junction structure. Journal of cell science. 2006;119(10):2095-106.
249. Lian P, Braber S, Garssen J, Wichers HJ, Folkerts G, Fink-Gremmels J, et al. Beyond heat stress: intestinal integrity disruption and mechanism-based intervention strategies. Nutrients. 2020;12(3):734.
250. Goto Y, Ivanov II. Intestinal epithelial cells as mediators of the commensal–host immune crosstalk. Immunology and cell biology. 2013;91(3):204-14.
251. Rimoldi M, Chieppa M, Salucci V, Avogadri F, Sonzogni A, Sampietro GM, et al. Intestinal immune homeostasis is regulated by the crosstalk between epithelial cells and dendritic cells. Nature immunology. 2005;6(5):507-14.
252. Stadnyk AW. Cytokine production by epithelial cells 1. The FASEB Journal. 1994;8(13):1041-7.
253. Schottelius A, Baldwin Jr A. A role for transcription factor NF-kB in intestinal inflammation. International journal of colorectal disease. 1999;14(1):18-28.
254. Christian F, Smith EL, Carmody RJ. The regulation of NF-κB subunits by phosphorylation. Cells. 2016;5(1):12.
255. Goua M, Mulgrew S, Frank J, Rees D, Sneddon A, Wahle K. Regulation of adhesion molecule expression in human endothelial and smooth muscle cells by omega-3 fatty acids and conjugated linoleic acids: involvement of the transcription factor NF-κB? Prostaglandins, leukotrienes and essential fatty acids. 2008;78(1):33-43.
256. Baker E, Miles E, Calder P. Comparing effects of polyunsaturated fatty acids derived from marine and plant sources on endothelial cell inflammation. The Proceedings of the Nutrition Society. 2020;79(OCE2).
257. Bui TM, Wiesolek HL, Sumagin R. ICAM-1: a master regulator of cellular responses in inflammation, injury resolution, and tumorigenesis. Journal of leukocyte biology. 2020;108(3):787-99.
258. Bulut K, Pennartz C, Felderbauer P, Meier JJ, Banasch M, Bulut D, et al. Glucagon like peptide-2 induces intestinal restitution through VEGF release from subepithelial myofibroblasts. European journal of pharmacology. 2008;578(2-3):279-85.

259. Boquoi A, Jover R, Chen T, Pennings M, Enders GH. Transgenic expression of VEGF in intestinal epithelium drives mesenchymal cell interactions and epithelial neoplasia. Gastroenterology. 2009;136(2):596-606. e4.
260. Hasan AU, Ohmori K, Konishi K, Igarashi J, Hashimoto T, Kamitori K, et al. Eicosapentaenoic acid upregulates VEGF-A through both GPR120 and PPARγ mediated pathways in 3T3-L1 adipocytes. Molecular and cellular endocrinology. 2015;406:10-8.
261. Ando N, Hara M, Shiga K, Yanagita T, Takasu K, Nakai N, et al. Eicosapentaenoic acid suppresses angiogenesis via reducing secretion of IL-6 and VEGF from colon cancer-associated fibroblasts. Oncology reports. 2019;42(1):339-49.
262. Calviello G, Di Nicuolo F, Gragnoli S, Piccioni E, Serini S, Maggiano N, et al. n-3 PUFAs reduce VEGF expression in human colon cancer cells modulating the COX-2/PGE 2 induced ERK-1 and -2 and HIF-1α induction pathway. Carcinogenesis. 2004;25(12):2303-10.
263. Bork CS, Baker EJ, Lundbye-Christensen S, Miles EA, Calder PC. Lowering the linoleic acid to alpha-linoleic acid ratio decreases the production of inflammatory mediators by cultured human endothelial cells. Prostaglandins, Leukotrienes and Essential Fatty Acids. 2019;141:1-8.
264. Shen J, Shen S, Das UN, Xu G. Effect of essential fatty acids on glucose-induced cytotoxicity to retinal vascular endothelial cells. Lipids in Health and Disease. 2012;11(1):1-10.
265. Węglarz L, Wawszczyk J, Orchel A, Jaworska-Kik M, Dzierżewicz Z. Phytic Acid Modulates In Vitro IL-8 and IL-6 Release from Colonic Epithelial Cells Stimulated with LPS and IL-1β. Digestive Diseases and Sciences. 2007;52(1):93-102.
266. Russo RC, Garcia CC, Teixeira MM, Amaral FA. The CXCL8/IL-8 chemokine family and its receptors in inflammatory diseases. Expert review of clinical immunology. 2014;10(5):593-619.
267. Honda KL, Lamon-Fava S, Matthan NR, Wu D, Lichtenstein AH. EPA and DHA exposure alters the inflammatory response but not the surface expression of Toll-like receptor 4 in macrophages. Lipids. 2015;50(2):121-9.
268. Erdinest N, Shmueli O, Grossman Y, Ovadia H, Solomon A. Anti-inflammatory effects of alpha linolenic acid on human corneal epithelial cells. Investigative ophthalmology & visual science. 2012;53(8):4396-406.
269. Baeuerle PA, Henkel T. Function and activation of NF-kappa B in the immune system. Annual review of immunology. 1994;12:141-79.

270. Horton MR, Boodoo S, Powell JD. NF-κB activation mediates the cross-talk between extracellular matrix and interferon-γ (IFN-γ) leading to enhanced monokine induced by IFN-γ (MIG) expression in macrophages. Journal of Biological Chemistry. 2002;277(46):43757-62.
271. Hoffmann A, Baltimore D. Circuitry of nuclear factor κB signaling. Immunological reviews. 2006;210(1):171-86.
272. Pei Z, Li H, Guo Y, Jin Y, Lin D. Sodium selenite inhibits the expression of VEGF, TGFβ1 and IL-6 induced by LPS in human PC3 cells via TLR4-NF-KB signaling blockage. International immunopharmacology. 2010;10(1):50-6.
273. Libermann TA, Baltimore D. Activation of interleukin-6 gene expression through the NF-kappa B transcription factor. Molecular and cellular biology. 1990;10(5):2327-34.
274. Fard SG, Cameron-Smith D, Sinclair AJ. n−3 Docosapentaenoic acid: The iceberg n−3 fatty acid. Current Opinion in Clinical Nutrition & Metabolic Care. 2021;24(2):134-8.
275. Tian Y, Katsuki A, Romanazzi D, Miller MR, Adams SL, Miyashita K, et al. Docosapentaenoic acid (22: 5n-3) downregulates mRNA expression of pro-inflammatory factors inLPS-activated murine macrophage like RAW264. 7 cells. Journal of Oleo Science. 2017:ess17111.
276. Liu B, Zhang Y, Yang Z, Liu M, Zhang C, Zhao Y, et al. ω-3 DPA Protected Neurons from Neuroinflammation by Balancing Microglia M1/M2 Polarizations through Inhibiting NF-κB/MAPK p38 Signaling and Activating Neuron-BDNF-PI3K/AKT Pathways. Marine Drugs. 2021;19(11):587.
277. Khaddaj-Mallat R, Morin C, Rousseau É. Novel n-3 PUFA monoacylglycerides of pharmacological and medicinal interest: Anti-inflammatory and anti-proliferative effects. European journal of pharmacology. 2016;792:70-7.
278. Sung J, Jeon H, Kim I-H, Jeong HS, Lee J. Anti-inflammatory effects of stearidonic acid mediated by suppression of NF-κB and MAP-kinase pathways in macrophages. Lipids. 2017;52(9):781-7.
279. Natoli M, Leoni BD, D'Agnano I, Zucco F, Felsani A. Good Caco-2 cell culture practices. Toxicology in vitro. 2012;26(8):1243-6.
280. Martínez C, González-Castro A, Vicario M, Santos J. Cellular and molecular basis of intestinal barrier dysfunction in the irritable bowel syndrome. Gut and liver. 2012;6(3):305.

281. Sergent T, Piront N, Meurice J, Toussaint O, Schneider Y-J. Anti-inflammatory effects of dietary phenolic compounds in an in vitro model of inflamed human intestinal epithelium. Chemico-Biological Interactions. 2010;188(3):659-67.
282. Kuhn KA, Manieri NA, Liu T-C, Stappenbeck TS. IL-6 stimulates intestinal epithelial proliferation and repair after injury. PloS one. 2014;9(12):e114195.
283. Kucharzik T, Hudson JT, Lügering A, Abbas JA, Bettini M, Lake JG, et al. Acute induction of human IL-8 production by intestinal epithelium triggers neutrophil infiltration without mucosal injury. Gut. 2005;54(11):1565-72.
284. Dinarello C, Novick D, Kim S, Kaplanski G. Interleukin-18 and IL-18 binding protein. Frontiers in immunology. 2013;4:289.
285. Dwinell MB, Lügering N, Eckmann L, Kagnoff MF. Regulated production of interferon-inducible T-cell chemoattractants by human intestinal epithelial cells. Gastroenterology. 2001;120(1):49-59.
286. Lee SH, eun Kwon J, Cho M-L. Immunological pathogenesis of inflammatory bowel disease. Intest Res. 2018;16(1):26.
287. Ajabnoor SM, Thorpe G, Abdelhamid A, Hooper L. Long-term effects of increasing omega-3, omega-6 and total polyunsaturated fats on inflammatory bowel disease and markers of inflammation: a systematic review and meta-analysis of randomized controlled trials. European Journal of Nutrition. 2021;60(5):2293-316.
288. Rusca A, Di Stefano AFD, Doig MV, Scarsi C, Perucca E. Relative bioavailability and pharmacokinetics of two oral formulations of docosahexaenoic acid/eicosapentaenoic acid after multiple-dose administration in healthy volunteers. European journal of clinical pharmacology. 2009;65(5):503-10.
289. Kris-Etherton PM, Grieger JA, Etherton TD. Dietary reference intakes for DHA and EPA. Prostaglandins, Leukotrienes and Essential Fatty Acids. 2009;81(2-3):99-104.
290. GOED. EPA+DHA Daily Intake Recommendations 2017 [Available from: https://goedomega3.com/storage/app/media/GOED%20Intake%20Recommendations.pdf.
291. Panchal SK, Brown L. Addressing the insufficient availability of EPA and DHA to meet current and future nutritional demands. Multidisciplinary Digital Publishing Institute; 2021. p. 2855.
292. Calder PC, Yaqoob P. Omega-3 polyunsaturated fatty acids and human health outcomes. Biofactors. 2009;35(3):266-72.

293. Cencič A, Langerholc T. Functional cell models of the gut and their applications in food microbiology — A review. International Journal of Food Microbiology. 2010;141:S4-S14.
294. Yazdi PG. A review of the biologic and pharmacologic role of docosapentaenoic acid n-3. F1000Research. 2013;2:256.
295. Gobbetti T, Dalli J, Colas RA, Canova DF, Aursnes M, Bonnet D, et al. Protectin D1n-3 DPA and resolvin D5n-3 DPA are effectors of intestinal protection. Proceedings of the National Academy of Sciences. 2017;114(15):3963-8.
296. Saini RK, Keum Y-S. Omega-3 and omega-6 polyunsaturated fatty acids: Dietary sources, metabolism, and significance—A review. Life sciences. 2018;203:255-67.
297. Harris WS. Stearidonic acid as a 'pro-eicosapentaenoic acid'. Current opinion in lipidology. 2012;23(1):30-4.
298. Yuan Q, Xie F, Huang W, Hu M, Yan Q, Chen Z, et al. The review of alpha-linolenic acid: Sources, metabolism, and pharmacology. Phytotherapy Research. 2022;36(1):164-88.
299. Brenna JT, Salem Jr N, Sinclair AJ, Cunnane SC. α-Linolenic acid supplementation and conversion to n-3 long-chain polyunsaturated fatty acids in humans. Prostaglandins, leukotrienes and essential fatty acids. 2009;80(2-3):85-91.
300. Jalili M, Hekmatdoost A. Dietary ω-3 fatty acids and their influence on inflammation via Toll-like receptor pathways. Nutrition. 2021;85:111070.
301. Mashukova A, Wald FA, Salas PJ. Tumor necrosis factor alpha and inflammation disrupt the polarity complex in intestinal epithelial cells by a posttranslational mechanism. Molecular and cellular biology. 2011;31(4):756-65.
302. Lin F-C, Young HA. The talented interferon-gamma. 2013.
303. Nava P, Koch S, Laukoetter MG, Lee WY, Kolegraff K, Capaldo CT, et al. Interferon-γ regulates intestinal epithelial homeostasis through converging β-catenin signaling pathways. Immunity. 2010;32(3):392-402.
304. Allaire JM, Crowley SM, Law HT, Chang S-Y, Ko H-J, Vallance BA. The intestinal epithelium: central coordinator of mucosal immunity. Trends in immunology. 2018;39(9):677-96.
305. Roig-Perez S, Cortadellas N, Moreto M, Ferrer R. Intracellular Mechanisms Involved in Docosahexaenoic Acid-Induced Increases in Tight Junction Permeability in Caco-2 Cell Monolayers. Journal of Nutrition. 2010;140(9):1557-63.

306. Turner J, Angle J, Black E, Joyal J, Sacks D, Madara J. PKC-dependent regulation of transepithelial resistance: roles of MLC and MLC kinase. American Journal of Physiology-Cell Physiology. 1999;277(3):C554-C62.
307. Ashammakhi N, Nasiri R, Barros NRd, Tebon P, Thakor J, Goudie M, et al. Gut-on-a-chip: Current progress and future opportunities. Biomaterials. 2020;255:120196.
308. Mariamenatu AH, Abdu EM. Overconsumption of Omega-6 Polyunsaturated Fatty Acids (PUFAs) versus deficiency of omega-3 PUFAs in modern-day diets: the disturbing factor for their "Balanced Antagonistic Metabolic Functions" in the human body. Journal of lipids. 2021;2021.
309. Punia S, Sandhu KS, Siroha AK, Dhull SB. Omega 3-metabolism, absorption, bioavailability and health benefits–A review. PharmaNutrition. 2019;10:100162.
310. Tocher DR, Betancor MB, Sprague M, Olsen RE, Napier JA. Omega-3 long-chain polyunsaturated fatty acids, EPA and DHA: bridging the gap between supply and demand. Nutrients. 2019;11(1):89.
311. Ohata A, Usami M, Miyoshi M. Short-chain fatty acids alter tight junction permeability in intestinal monolayer cells via lipoxygenase activation. Nutrition. 2005;21(7):838-47.